Fluorine and the Environment

Agrochemicals, Archaeology, Green Chemistry & Water

EDITED BY

Alain Tressaud

ADVANCES IN FLUORINE SCIENCE 2

Fluorine and the Environment

Agrochemicals, Archaeology, Green Chemistry & Water

ASSOCIATE EDITORS

Advances in Fluorine Science

Fluorine and the Environment

Agrochemicals, Archaeology, Green Chemistry & Water

Volume 2

Edited by

Alain Tressaud
Research Director CNRS,
ICMCB-CNRS
University of Bordeaux I
Pessac Cedex,
France

ELSEVIER

Amsterdam ● Boston ● Heidelberg ● London ● New York ● Oxford ● Paris
San Diego ● San Francisco ● Singapore ● Sydney ● Tokyo

Elsevier
Radarweg 29, PO Box 211, 1000 AE Amsterdam, The Netherlands
The Boulevard, Langford Lane, Kidlington, Oxford OX5 1GB, UK

First edition 2006

Library of Congress Cataloging in Publication Data
A catalogue record for this book is available from the Library of Congress.

British Library Cataloguing in Publication Data
A catalogue record for this book is available from the British Library.

ISBN-13: 978-0-444-52672-4
ISBN-10: 0-444-52672-2
ISSN: 1872-0358

Printed and bound in Italy

06 07 08 09 10 10 9 8 7 6 5 4 3 2 1

CONTENTS

This page intentionally left blank

Contributors

This page intentionally left blank

Preface

"*Advances in Fluorine Science*" is a new book series presenting critical multidisciplinary overviews on areas in which fluorine and fluoride compounds have a decisive impact. The individual volumes of *Advances in Fluorine Science* are thematic, addressing comprehensively both the science and applications on topics including the Environment, Green chemistry, Medicine, Health & Life Sciences, New Technologies & Materials Science, Energy and the Earth Sciences.

The first volume of the series, that is "*Fluorine and the Environment: Atmospheric Chemistry, Emissions & Lithosphere*" covered a wide scope of important issues about our atmospheric environment. The contributions, written by chemists and environmental scientists, mostly dealt with the effects of fluorine-based gases and emissions either from natural or anthropogenic origin. The present volume deals with other topics concerned by *Fluorine and the Environment*, including *Water, Agrochemicals, Green Chemistry, Analytical aspects and Archaeology*.

Fluorine constitutes 0.065% of the Earth's crust and is among the first fifteen elements in importance on Earth. This element is present in most parts of the geosphere: it is found as fluoride ion in more than 300 minerals, in volcanic magmas, large crystals, etc; also in oceans, lakes, rivers, and all other forms of natural water; in the bones, teeth, and blood of all mammals, in some plants, etc. Various fluorine-containing ores are used in advanced technologies, e.g. the metallurgy of aluminium which has been developed one century ago thanks to the flux properties of cryolite (Na_3AlF_6). We can quote also rare-earth elements, largely used in TV screens, which are extracted from fluorocarbonate minerals, and natural crystals of fluorite (*or fluorspar*) which are nowadays used as starting material for the growth of ultra pure single crystals of CaF_2: such an ultra-high quality material is required for use as windows for the development of 157 nm lithography ion microelectronics.

In the present volume, the key-position of fluoro-products in agriculture is reviewed, since a large percentage of agro-chemicals and pesticides contain at least one fluorine atom. However, improvements in the use of fluorine-based products in agrochemicals could not be developed without taking into consideration a safer environment, on both levels of greener synthesis routes and a reduction of the negative impact on plants and organisms. Green chemistry which

can be defined as ''*the utilization of a set of principles that reduces or eliminates the use or generation of hazardous substances in the design, manufacture and application of chemical products*'' tends to achieve the ultimate goal of zero-waste processes. Within this scope, fluorine has a very peculiar place, since its high reactivity yields several advantages, for instance in by-passing various polluting multi-step reactions. In quite different fields, fluorine-based materials could be used as efficient tools for protecting our cultural heritage, either for wood artefacts or stone conservation. Using up-to-date techniques such as ion beam analyses, this element could also help relative dating applications, ranging from burial durations of archaeological bones and teeth to the determination of exposure ages of meteorites on the Antarctic ice shield. This element has allowed indeed solving several archaeological enigmas.

However, the negative impact of fluorides on plants, animals and human beings—as already pointed out in the first volume—cannot be forgotten and pollution and illness mechanisms should be confined, in order to find adapted solutions. Although most pollution is coming through airborne particles, the amount of fluorine present in drinking water and food should be also strictly controlled, in order to stay within acceptable levels. An important excess of fluoride ions may cause endemic fluorosis, as found in rural areas of Western Africa, Ethiopia, Rajasthan, or in desertic zones of China. The regular use of defluoridation techniques of water, as presented here in two contributions, has become therefore an extremely important mean to solve acute health problems related to high fluoride concentrations.

Through the topics which are discussed within the present volume, we can be point out among the major issues of the volumes:

- an original approach of the complex relationships between chemistry and the environment, by collating complementary visions on a same important environmental issue relating with fluorine and fluoride products;
- a better awareness—through the example of fluoride products—that we are surrounded by [made with] chemistry and chemicals which are compulsory for our life conditions and for our future, insofar man gives himself the means to improve his environment.

We can anticipate that the forthcoming volumes of the series will deal with fluorine & fluoride products in medicine and health.

Alain Tressaud
Malmussou, May 2006

CHAPTER 1

Fluoride Removal from Water Using Adsorption Technique

Maurice S. Onyango,[1] and Hitoki Matsuda[2,*]

[1]*Centre for Process Engineering, Department of Process Engineering, University of Stellenbosch, Stellenbosch, Private Bag X1, Matieland, 7602, South Africa*
[2]*Department of Chemical Engineering, Nagoya University, Furo-cho, Chikusa-ku, Nagoya 468-8603, Japan*

Contents

*Corresponding author.;
E-mail: matsuda@nuce.nagoya-u.ac.jp

FLUORINE AND THE ENVIRONMENT, VOLUME 2
ISSN 1872-0358 DOI: 10.1016/S1872-0358(06)02001-X

Abstract

Management of contaminants such as fluoride is a major public issue. Fluoride of geogenic origin in groundwater used as a source of drinking water is a major concern because fluoride content above permissible levels is responsible for human dental and skeletal fluorosis. Consequently, water sources containing elevated levels of fluoride have to be treated. Coagulation/precipitation, electrochemical, electrodialysis, reverse osmosis, adsorption and hybrid processes combining adsorption and dialysis are widely used defluoridation techniques. Currently, however, the development of cost effective and clean processes due to economic constraints and stringent environmental policies is desired. Adsorption technique is arguably one of the most versatile of all the defluoridation techniques due to a number of reasons such as cost, diverse end-uses, socio-cultural acceptance, regulatory compliance, environmental benignity and simplicity. For this technique, activated alumina, bone char and clay adsorption media are the most developed. During the past two decades, extensive research has focused on a number of alternative adsorbents, some exhibiting improved fluoride sorption performances while at the same time do not alter the quality of treated water. Studies have also shifted toward systematic modeling to approximate adsorber design parameters. In view of these, this review opens with a description of paradigm shifts in drinking water sources and highlights the genesis and toxicological effects of fluoride in drinking water as a means of defining the existing problem. Next, potential and established techniques for defluoridation are revisited. This is closely followed with a review of defluoridation adsorbents recognized by the World Health Organization and those novel defluoridation adsorbents reported in literature over the last two decades, with special reference to drinking water. Emphasis is laid on their availability, fluoride sorption capacity and mechanisms. In recognizing surface-tailored zeolite as a novel sorbent, detailed analysis of fluoride adsorption behavior is provided for this sorbent. Finally, defluoridation adsorption unit configurations, and challenges to and prospects for their implementation are briefly discussed.

1. INTRODUCTION

Water is a finite and vulnerable natural resource and the bulk of it is stored as saltwater in the oceans [1]. For the saltwater to be used for industrial, agricultural or household purposes, an expensive conversion process would be required. Thus, freshwater, because of its purity, is generally used in human activities as opposed to saltwater. It is estimated that only 3% of the world's water supply is fresh water and of this, only a third is available as either surface water or groundwater. Over the years, the world population has been surging upward, while most economies have stagnated. The increase in population has exerted an enormous pressure on the world's limited freshwater supply. It is estimated that

water use has been growing at more than twice the rate of the population increase [2]. The end result has been overutilization and pollution of the existing water resources.

From time immemorial, surface water played a pivotal role to human life as a source of drinking water because of its easy access compared with any other water source. A few decades ago, the use of contaminated surface water sources was found to contribute to the transmission of waterborne bacterial diseases. Thus, a paradigm shift in water usage from surface to groundwater was inevitable.

Groundwater is one of the most valuable natural resources possessed by many developed and developing nations. It is reliable in dry seasons or droughts because of the large storage, is cheaper to develop, since, if unpolluted, it requires little or no treatment and it can often be tapped where it is needed, on a stage-by-stage basis. As a result, groundwater has become immensely important for human water supply in urban and rural areas in developed and developing nations alike. Countless large towns and many cities derive much of their domestic and industrial water supply from aquifers, both through municipal well fields and through many private bore holes. However, a gloom picture hangs over the use of groundwater in certain regions. Studies have shown that in certain regions, though groundwater has been perceived to be clean, contain contaminants that are deleterious to human health. Amongst the most notable of these contaminants is fluoride [3].

Fluoride in groundwater is mostly of geogenic origin arising from breakdown of rocks containing the fluoride ions. In addition, anthropogenic sources such as infiltration of chemical fertilizers in agricultural areas and liquid wastes from industrial entities also contribute to fluoride ions in groundwater. Over the years, fluoride in drinking water above permissible limits has attracted public health interest. At low concentrations fluoride can reduce the risk of dental cavities. Exposure to somewhat higher amounts of fluoride can cause dental fluorosis. In its mildest form this results in discoloration of teeth, while severe dental fluorosis includes pitting and alteration of tooth enamel. When water containing severely higher concentration of fluoride is ingested for a long period of time, changes to bone, a condition known as skeletal fluorosis, may result. This can cause joint pain, restriction of mobility and possibly increase the risk of some bone fractures.

Putting the above health effects into consideration, there are maximum contaminant levels (MCL) for fluoride in drinking water set by each country depending also partly on its economic and technological powers. For example, in 1974, Tanzania adopted a value of 8 mg/L [4] for rural water supply, in 1985 the USEPA raised the maximum allowable concentration to 4 mg/L, while Canada and the WHO recommend a permissible limit of 1.5 mgF/L. Waters containing fluoride ions above the preceding permissible levels have to be treated. There are several treatment techniques that have been developed or show potential for remedying fluoride-contaminated water. These techniques include: coagulation/precipitation,

the use of membranes, ion exchange, electrodialysis and adsorption, among others. The choice of a treatment technique for a given utility usually depends on the concentration of the ions, chemical species in source water, existing treatment processes, treatment costs, handling of residuals [5] and versatility of a given technique. Because of limitations in terms of cost, production of enormous waste and difficulty in end-use applications of some of the above treatment techniques, an environmentally benign, robust and low-cost technique has to be devised for remedying contaminated water. Proponents of adsorption technology argue that the technique is economical and efficient and produces high-quality water [6]. Thus, there have been a lot of studies on the removal of fluoride by use of various adsorbents [7–23]. More importantly, adsorption technique is versatile and can be used in large-scale central water treatment systems and in the development of a small-scale point-of-entry (POE) or point-of-use (POU) system.

Our main focus for this review is to briefly and critically describe some of the defluoridation techniques as a means of getting a basis to support the adsorption technique, to evaluate the defluoridation adsorbents now being utilized and those novel defluoridation adsorbents reported in literature over the last two decades, with special reference to drinking water. Emphasis is laid toward the adsorbents availability, fluoride sorption capacity and where applicable their kinetic adsorption characteristics and column performances are reported. Detailed characteristics of fluoride adsorption onto surface-tailored zeolite are provided. In addition, various adsorber configurations are reexamined and challenges to and prospects for their application to less developed countries (LDCs) are discussed.

2. TECHNOLOGIES AND POTENTIAL TECHNOLOGIES FOR REMOVING FLUORIDE FROM WATER

An extensive review of the literature has been performed to critically evaluate what technologies are presently being utilized, and what technologies may potentially be applicable to the removal of fluoride from drinking water. A summary of the technologies is presented in the succeeding subsections.

2.1. Non-treatment and blending techniques

In areas where several water sources are available, installation of multiple wells may provide an opportunity for obtaining water with low fluoride levels without necessarily treating the water. These methods ensure that the water entering the distribution network meets the maximum contaminant level, by blending the targeted source waters. Two other strategies are to recharge the aquifer and to treat a side-stream and subsequently blend the treated water with the untreated. This latter strategy reduces the amount of water to be treated and thus decreases

the design flow. One disadvantage of this method is that the MCL can only be achieved if the quality of the source waters is good.

2.2. Precipitation/coagulation

In this method, fluoride removal from water is mediated by calcite, $Mg(OH)_2$, $Al(OH)_3$ or $Fe(OH)_3$ floc formation. The principle involved in this technology is that the fluoride ions adsorb on the flocs and are then subsequently removed either simultaneous or in succeeding treatment units such as sedimentation, fixed bed or microfiltration unit. A lot of studies have been reported on the use of alum [24] (and hence $Al(OH)_3$) and lime [4,25]. In the 70 s, a co-precipitation technique, the so-called ''Nalgonda technique'', was introduced to the Indian population for fluoride removal from drinking water and also has been tested at pilot scale level in LDCs such as Kenya, Senegal and Tanzania. The method involves the addition of alum and lime into water followed by rapid mixing. After some time, the stirring intensity is reduced and this induces floc formation that is subsequently removed by simple settling. According to the report of the National Environmental Engineering Research Institute (NEERI) of Nagpur, India, the technique is applicable to different levels of water treatment. On a small scale (household), the chemicals are introduced in buckets or drums, while on a medium scale for a small community, a fill-and-draw plant is used. For large-scale operation, a process combining mixing, flocculation and sedimentation is used.

Although precipitation is an economical and a robust technique in the removal of fluoride from water, the technique has been found to suffer from excessive sludge generation and dewatering such sludge has proven to be difficult since the solid size and content are extremely small and low, respectively; instability of the sludge under adverse environmental conditions has too been reported and in most cases, achieving the maximum contaminant level has been found to be difficult. Considering the fact that chemical handling is involved in precipitation/coagulation technique, this technique may not be popular with many uneducated groups, especially in LDCs. Therefore, the technique is only suited to centralized water treatment system. In line with the above disadvantages, this technique has not been very attractive to many end users.

2.3. Membrane techniques

As the quality of drinking water sources gets worse, the methods of water treatment or the traditional water treatment systems need to be modernized. Pressure-driven membrane systems such as reverse osmosis (RO), nanofiltration (NF) and ultrafiltration (UF) and electric-driven membrane system such as

electrodialysis (ED) are considered as alternative innovative and efficient technology with great future prospects for the purification and reprocessing of water and sewage. Basic advantages arising from the application of membrane processes as compared with traditional water treatment systems are as follows: production of water of invariable quality, smaller quantity of added chemical substances, lower consumption of energy, compactness of the installation, possibility to effect full automation of the process, application in both small and larger scale treatment systems as POE and POU, and simultaneous removal of other dissolved species in water. Owing partly to the above wholesale advantages, several studies have recently been reported on the use of membranes, in particular NF and RO membranes. Pontié *et al*. [26,27] and Diawara *et al.* [28] have presented various aspects of application of NF to defluorinating water, while Arora *et al*. [29] have studied extensively on the use of RO for the treatment of water containing fluoride under various experimental conditions such as feed composition and pH (*see also their contribution in this book*). They found that up to 95% of fluoride could be removed from water. At present, the WHO and United States Environmental Protection Agency (USEPA) classify RO as one of the best demonstrated available technology (BDAT). A full-scale plant operation specifically constructed for fluoride removal is found at Fort Irwin. Interestingly, Lhassani *et al*. [30] have shown that by optimizing the pressure, selective desalination of fluorinated brackish water by NF is feasible and drinking water can be produced at much lower cost than by using RO.

Although membrane use has received universal acceptance, a number of limitations has slowed its use in some regions. Fouling arising from feed water characteristics is a major problem and due to high quantity of water rejection typically between 35% and 65%, it is not suitable to regions where water is scarce. Moreover, brine discharge from RO plant is highly concentrated and requires treatment. The technique also involves a high investment cost, requires high technology for operation and maintenance and therefore does not suit developing countries.

2.4. Ion exchange (IE)

Ion-exchange resins are most commonly used in water treatment processes to soften the water supply by exchanging sodium ions for ‘‘hardness’’ ions including calcium and magnesium. Ion-exchange filters exchange the major ions present in the water, removing fluoride and other ions in water. Selective fluoride removal can be performed using the calcium form of DOWEX G-26 (H) strong acid cation-exchange resin. The calcium forms an insoluble complex with the fluoride in water with low to high salt concentrations. Soluble anions such as sulfate, arsenic, selenium and nitrate and TDS can compete with fluoride and can affect the run

length ([31]). Thus, if systems contain high levels of suspended solids and precipitated iron that can cause clogging of the IE bed, then pre-treatment may be required. USEPA has proposed passage of water through a series of columns to improve removal and decrease regeneration frequency.

Some of the limitations to the use of ion exchange include the production of a highly concentrated waste by-product stream that poses a disposal problem (this problem can be reduced by brine recycling). Run length is affected by sulfate level. The technology is only recommended primarily for small groundwater systems with low sulfate and low TDS. Another limitation to its use is that it requires a high level of operator skill and therefore not popular with many end-users.

2.5. Electrochemical technique

Electrochemical technique (also electrocoagulation) is a simple and efficient method for the treatment of potable water. This process is characterized by a fast rate of contaminant removal, a compact size of the equipment, simplicity in operation and low capital and operating costs. Moreover, it is particularly more effective in treating wastewaters containing small and light suspended particles, such as oily restaurant wastewater, because of the accompanying electroflotation effect.

The electrochemical technique is in general at a developmental stage and therefore is not an established technology for defluoridation. Some researchers [32,33] have demonstrated that electrocoagulation (EC) using aluminum anodes is effective in defluoridation. In the EC cell, the aluminum electrodes first sacrifice themselves to form aluminum ions. Afterward, the aluminum ions are transformed into $Al(OH)_3$ before being polymerized to $Al_n(OH)_{3n}$. The $Al(OH)_3$ floc is believed to adsorb F^- strongly as shown by the following reaction:

$$Al(OH)_3 + xF^- \Leftrightarrow Al(OH)_{3-x}F_x + xOH^-. \quad (1)$$

At aluminum cathode, hydrogen gas is released according to the following reaction:

$$2H_2O + 2e^- \Rightarrow H_2 + 2OH^- \quad (2)$$

Unfortunately, up to date, no solid evidence was reported to support the hypothesis of the above adsorption mechanism. Moreover, the hydrogen gas produced at the EC cathode prevents the flocs from settling properly on leaving the electrolyzer [34]. In order to overcome this problem, an EC process followed by an electroflotation (EF) operation can be applied. In this combined process, the EC unit is primarily for the production of aluminum hydroxide flocs. The EF unit would undertake the responsibility of separating the formed flocs from water by floating them to the surface of the cell.

2.6. Adsorption technique

Adsorption in water treatment is a robust technique for removing water-soluble ions, especially when these ions exist in water at low concentrations. Coincidentally, fluoride ions exist in some groundwaters at low concentrations, which are above the permissible limits. The principle behind this technique is that a component (fluoride in our case) is transported by diffusion from the bulk phase to the solid surface where it is bound at the surface or interface between two phases by either chemical or physical forces [35]. Numerous investigations have focused on surface adsorption as a means of removing fluoride from water. As a result of these studies various water treatment plants using treatment media such as activated alumina or bone char have been constructed and are in use in several countries. One example is a water purification plant in Kansas that utilizes activated alumina [36]. Several other smaller fluoride treatment facilities are scattered all over India, Kenya and Tanzania, among other nations.

2.7. Fluoride removal technique screening

The treatment techniques mentioned above are those that are widely reported in literature. Their application in a specific geographical region depends on a number of factors. In discussing these factors, our argument will be biased toward application of the various techniques in LDCs because these regions bear the highest occurrence of fluoride contamination of drinking water. These factors are also the basis of a decision framework for helping utilities determine the most appropriate technique.

2.7.1. Cost

To understand how cost of a given technique is important, we need first to identify the countries that are most affected by fluoride contamination of drinking water. Among these countries are Kenya, Tanzania, Uganda, Ethiopia, India, Mexico, Argentina, Libya, Senegal, Pakistan, Srilanka, New Zealand and China. Most of these countries have low *per capita* incomes and therefore application of a given technique will depend on the cost of the technique. Moreover, the distribution of wealth in some of these countries is such that majority of people live below poverty line. In line with this, only low-cost options that perform adequately well may be applicable. Most literatures indicate that membrane techniques, ion exchange and electrochemical technique are medium to high cost, while adsorption and precipitation/coagulation techniques are low-cost fluoride treatment options.

2.7.2. Regulatory compliance

Currently, the WHO recommends a maximum value of 1.5 mgF/L in drinking water. Countries like India have lowered their permissible limits to 1.0 mg/L. The performance of the technologies considered in this review depends on the quality of the water to be treated. In general, most of these technologies will meet the WHO's maximum allowable concentration (MAC) values. However, precipitation/coagulation method has been found to rarely meet the safe levels of fluoride in drinking water. To achieve safe levels using this technique, a treatment train involving the addition of an adsorption unit or a membrane unit is required. The latter comes with additional cost.

2.7.3. Appropriateness of the technique

A given technology of choice should be tailor-made to suit the local conditions of the region in which it is intended. The local conditions include the fact that most of the contaminated water are obtained from tube wells, that the wells are scattered all over the region where in most cases there is no electricity, that the users are mainly women with no strong education and no sound incomes [37]. In considering these factors, ion exchange, membrane and electrochemical techniques are automatically disqualified, as they require medium- to high-level skills to operate. Moreover, they cannot be applied to areas where there is no supply of electricity.

2.7.4. Environmental burden

In the 21st century, the impetus to protect the environment is very strong. Consequently, the benefits arising from a given technology should not override the environmental load the technology imparts on the environment. Most technologies considered in this review increase environmental load to certain extent. For example, precipitation/coagulation is known to produce a large amount of sludge that has low content of solid and thus difficult to dewater. Adsorption on the other hand produces non-hazardous spent regeneration solution containing a high content of fluoride and thus an additional chemical handling facility would be required. Membrane processes on their part reject a large amount of water, while ion exchange produces highly concentrated brine. Based on these assessments, these technologies will all impact negatively on the environment. Adsorption technique, however, produces little amount of non-hazardous waste.

2.7.5. Public perception and acceptance

Public perception and acceptance is critical to the success of a given fluoride treatment technique. To make a technique popular, there must be an

understanding of local socio-cultural inclination. In general, all the techniques considered here have positive public perception. However, adsorption technique based on bone char adsorbent is known to be unacceptable to several religious groups. Also, some clique of people has mistakenly associated activated alumina (AA) with aluminum poisoning. Thus, they do not believe that water treated with AA is clean to drink.

Considering the above screening strategies as well as the summary in Table 1, it is observed that adsorption technique for fluoride removal from water is an established, low-cost, environmentally benign technique that has public acceptance. Thus, our discussion will henceforth concentrate on adsorptive removal of fluoride from drinking water.

3. DEVELOPMENT OF DEFLUORIDATION ADSORPTION UNIT: ALGORITHM

Most people in LDCs are affected by fluoride-contaminated drinking water supplied by the numerous scattered tube wells. The most feasible solution to this problem is to develop a cost-affective technique with diverse end-uses. As already mentioned in the previous sections, one robust technique is that based on adsorption. The development of an adsorption unit in general requires a number of stages. These are summarized in the Fig. 1 (Adsorption Research Inc. USA). According to the Adsorption Research Inc. (USA), the adsorption unit development stages frequently follow a pattern, with ideas being generated and data being collected, all focused on developing a full-scale process. As Fig. 1 suggests, the process idea in our case is to defluoridate drinking water. Since the technique to be adopted is known, i.e. adsorption, the next stage is to examine the adsorption media. Frequently, a few or even several adsorbent candidates are examined as potential choices. To this end, we have provided in Section 3.1 a description of some of the adsorption media reported in literature over the last two decades.

To evaluate the adsorbents, the relevant factors such as cost implication, availability, performance and regenerability are considered. The performance of an adsorption media for defluoridation is indicated as isotherms and rate data, while costs in general are determined by local availability, regenerability of the adsorption media, whether the media is synthetic or natural, needs further processing before use, among others. Using such factors as mentioned above, it is frequently possible to decide beforehand whether an adsorbent is suitable or not. In order to design an effective adsorption separation or purification unit using a chosen adsorption media, preliminary design information is required [38]. Often, these pieces of information are gathered through the performance of an extensive series of experiments that are time consuming and expensive. The aim of such a study is to predict *a priori* what will happen in a full-scale operation under

Table 1. Summary of fluoride removal technology screening

Screening strategy	Precipitation and coagulation	Membrane processes	Ion exchange	Electrochemical	Adsorption
Cost	Low	High	Medium	May be high	Low
Regulatory compliance	MCL not achievable	MCL achievable	MCL achievable	MCL achievable	MCL achievable
Appropriateness	Nalgonda method applicable to LDCs	Not appropriate to LDCs	Not appropriate to LDCs	Not appropriate to LDCs	Appropriate to LDCs and is versatile
Environmental burden	Difficult to dewater sludge	Water rejection high	Highly concentrated brine	At development stage	Non-hazardous waste
Public perception and acceptance	Acceptable	Acceptable	Acceptable	At development stage	Acceptable

Note: Non-treatment technique is not considered.

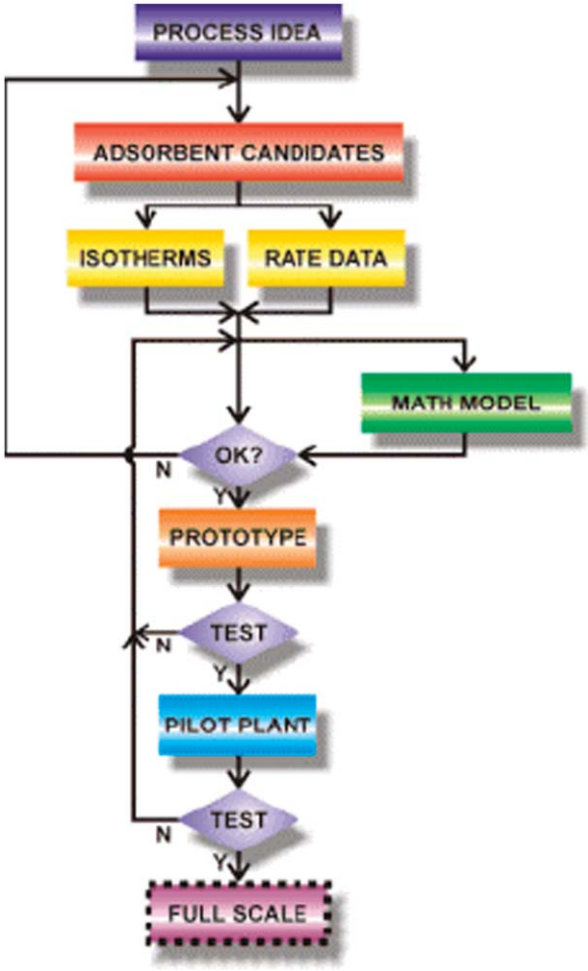

Fig. 1. Adsorption process development flow chart (Adsorption Research Inc., USA).

various design and operating parameters. Among the operating parameters and fluid features that are paramount for a good design are linear flow rate, initial concentration, bed height, size of adsorption media, type of adsorbent, pH and temperature of water. To reduce costs and to save time in doing unnecessarily too many experiments, mathematical models are used to predict the optimum conditions when the above parameters are varied. As an example, using surface-tailored zeolite as an efficient fluoride adsorption media, the modeling approach for batch equilibrium and kinetic data and column breakthrough curves are illustrated in Section 3.2. If factors such as cost, availability, performance and regenerability and/or mathematical model imply that the purification will be

successful, then a prototype system may be built. Otherwise, additional adsorbent candidates would be evaluated. If the prototype tests are successful, a larger pilot plant might be built, for on-site testing. During the on-site tests, field-based performance and acceptability are evaluated. In case the prototype tests are unsuccessful, it is necessary to revise the model conditions or parameters, or possibly to look at other adsorbent candidates. If the pilot plant tests are successful, a full-scale plant could be built. Conversely, it is necessary to revise the model conditions or parameters, or possibly to look at other adsorbent candidates again. Among the configurations (pilot/full-scale configurations, where applicable) that are considered in this review are ''tea bag'' POU, ''coffee filter'' POU, household POU, cartridge POU, community-based tube-well-attached defluoridator, household POE and centralized water treatment systems. By virtue of the nature of these configurations, some are extremely simple and their developments do not necessarily follow the algorithm illustrated in Fig. 1.

3.1. Established and potential adsorption media for fluoride

Adsorption technology is frequently used as a robust technique to remove water-soluble ions that are detrimental to human health from aqueous solutions, especially when these ions exist in low concentrations. Thus, a lot of studies have been reported in literature on the use of various adsorbents for fluoride removal from drinking water. The studies have mainly been motivated by the need to have alternative adsorbents that are low in cost, have local availability, require little processing and are superior in performance. Synthetic adsorbents have good capacities for fluoride but are always expensive, while natural materials that are available in large quantities or certain wastes from agricultural or industrial concerns may potentially be low-cost materials. An overview of some of the adsorbents that have been reported in literature over the last two decades are given below.

(a) *Activated alumina*. AA are commonly used as adsorbents, desiccants and catalysts and therefore the chemistry, size and structure of these aluminas are tailored to specific applications. Based on pH in water, four kinds of AA can be identified. These are: basic (pH 9.5 ± 0.5), neutral (pH 7.5 ± 0.5), weakly acidic (pH 6.0 ± 0.5) and acidic (pH 4.5 ± 0.5) AA. As an adsorbent, AA has been widely applied in the removal of contaminants from water. Removal of fluoride by AA is an established treatment technology and has been and is still practiced both by small- and large-scale water treatment enterprises. The WHO and USEPA classify AA adsorption as one of the best demonstrated available technology (BDAT) for fluoride removal. AA has high affinity for fluoride because in aqueous environment at pH values below its pH_{pzc} – the point of zero charge – it forms protonated ($\equiv$Al-OH_2^+) and neutral ($\equiv$Al-OH) aluminol sites, which are

responsible for binding fluoride ions by formation of inner-sphere complexes. Because of the good performance of AA, several researchers have studied its fluoride sorption behavior under varying conditions [36,39–46]. Interestingly, different researchers have obtained different adsorption capacities as shown in Table 2. Usually, the efficiency of the AA for adsorbing fluoride is generally poor on the first adsorption cycle unless the alumina is pre-treated. A pre-treatment that involves allowing a dilute aluminum sulfate solution ($\sim$29 g $Al_2(SO_4)_3$ $18H_2O$/L) to remain in contact with the alumina for 1 h is found to be particularly satisfactory. In another similar pre-treatment of AA to improve its performance, Wasay *et al*. [46] intensively studied the effect of impregnating AA with La (III) and Y (III) ions. They found that the capacity of AA after the impregnation increased twofold. Ku and Chiuo [44] using γ-activated alumina found optimal adsorption (capacity $=$ 16.3 mgF/g) of fluoride to take place in the pH range 4–6.

Although AA is a robust adsorbent for fluoride uptake, it is expensive and its performance is affected by the presence of co-ions in water such as silicates, sulfates, chlorides, bicarbonates and phosphates. The effect of bicarbonate ions on the performance of AA is particularly strong, i.e. the removal efficiency of fluoride by AA decreases significantly with an increase in bicarbonate content. This is partially due to the fact that bicarbonate ions buffer water pH at higher values thus reducing the number of active sites on AA available for binding fluoride. This brings us to another factor (pH) from solution chemistry that induces a negative effect on the performance of AA. The pH has an inhibiting effect of fluoride uptake since solution pH determines the speciation of fluoride, the number and the distribution of active sites on AA. In the acidic media (pH $<$ 7), the fluoride uptake by AA usually decreases with a decrease in pH due to the fact that

Table 2. Summary of adsorption capacities of AA

Source	Material	Capacity (mg F/g)	Mode of operation
Anonymous [36]	Al-pretreated AA	4.6	Column
Ghorai and Pant [39]	Locally (India) available AA	2.41	Batch
Coetzee *et al*. [45]	Type 504C, Fluka	0.5	Batch
Li *et al*. [17]	γ-Al_2O_3	3.70	Batch
Ku and Chiuo [44]	γ-activated alumina	16.34	Batch
Ramos *et al*. [11]	α-alumina	8.42	Batch
Wasay *et al*. [46]	AA	3.3	Batch
Wasay *et al*. [46]	La(III)-pretreated AA	6.3	Batch
Wasay *et al*. [46]	Y(III)-pretreated AA	6.1	Batch
Rubel [61]	AA	0.627–2.627	Pilot plant

HF is weakly ionized (pH < 3.2), and soluble alumino–fluoro complexes are formed resulting in the presence of aluminum ions in the treated water and lowering of the active sites. At near neutral pHs, the uptake of fluoride is maximum. Assuming that the pH_{pzc} of AA is about 8–9 as reported in several literatures, then at near neutral pHs the active sites consist of $=Al\text{-}OH_2^+$ (protonated) and $=Al\text{-}OH$ (non-protonated) aluminol sites. The interaction between fluoride and the protonated aluminol sites leads to the formation of inner-sphere complexes and elimination of water. The reaction can be represented by

$$=Al\text{-}OH_2^+ + F^- \Leftrightarrow =AlF + H_2O \tag{3}$$

The protonated aluminol sites are the most effective fluoride sorption sites and are usually responsible for the rapid kinetics due to coulombic attraction between the positively charged sites and the negatively charged fluoride species. The reaction with non-protonated sites involves ligand exchange, leads also to the formation of inner-sphere complexes, releases hydroxyl ions, is slow and characterized by a higher activation energy.

$$=Al\text{-}OH + F^- \Leftrightarrow =AlF + OH^- \tag{4}$$

Further increase in pH beyond pH_{pzc} is expected to enhance electrostatic shielding of the active sites and to reduce their number and activity. This argument explains why AA is reported to perform poorly at $pH > pH_{pzc}$.

The use of AA in water defluoridation has been limited to certain extent to countries with well-established economies. AA being synthetic is relatively expensive and may not be locally available in all fluoritic regions. India has an increasing incidence of fluorosis, both dental and skeletal, and with some 62 million people at risk. High-fluoride groundwaters are present especially in the hard rock areas south of the Ganges valley and in the arid northwestern part of the country. Owing to the robust performance of the Indian economy over the years, more and more AA-based tube-wells-attached columns are being used to defluoridate drinking water. Moreover, in recent times, an Indian company called Mytry De-Fluoridation Technologies (MDFFT) has produced and implemented AA-based defluoridation filters. The Mytry filter is a two-bucket system with the upper bucket containing the filter media. Murcott [47] reported that since 2004, the MDFFT had sold 9000 units and produced 50 units daily.

(b) *Bone char*. Bone char, a mixed adsorbent containing around 10% carbon and 90% calcium phosphate, is mainly produced by the carbonization of bones. Structurally, the calcium phosphate in bone char is in the hydroxyapatite form. Bone char has traditionally been used to decolorize sugar solutions in the sugar refining industry for many years. More than four decades ago, it was recognized as a potential medium for partial defluoridation of water. The defluoridation process was reportedly of the ion exchange in which carbonate radical of the apatite, $Ca(PO_4)_6.CaCO_3$, was replaced by fluoride to form an insoluble fluorapatite [48].

Bone char is therefore a well-established adsorbent for water defluoridation. Unfortunately, the treated water in some cases had bad taste. Moreover, socio-cultural acceptance in some communities was lacking, while at the same time cost and availability of raw materials were inhibiting. In 1988, however, the WHO recommended bone char for use in fluoride removal from drinking water in LDCs. Earlier, USEPA [49] reported that a full-scale defluoridation plant was operational in South Dakota, while Phanfumvanit and LeGeros [50] presented a robust bone char-based defluoridation units for individual households. Mwaniki [51] presented more interesting results of fluoride sorption characteristics of different grades of bovine bone char. They found that the 24 h-batch capacity of fluoride depended on the temperature of the heat-treatment of the bones. Black-grade bone char (heat-treated at 350°C) had a capacity of 11.4 mg/g, gray grade (heat-treated at 450°C) had a capacity of 2.4 mg/g, while white grade (heat-treated at 450°C) had a capacity <0.3 mg/g. Although black bone char (BBC) has high capacity for fluoride, Menda [52] reported from a Tanzanian experience that the water quality arising from the use of BBC was low due to bad smell and discolored water.

In a laboratory study, Abdel-Raouf and Daifullah [53] reported that the bone char derived by heating animal bone to 500–600°C could be used to remove fluoride from drinking water. Table 3 summarizes some of the capacities of bone char reported in literature.

Owing to enormous challenges facing Tanzania as most of her groundwaters have excess fluoride levels and most of the population is poor, a robust system of making bone char for water defluoridation has been devised in order to cut the cost of production. It involves charring raw fresh bones in an easy-to-use charcoal-fueled kiln at about 500–600°C. The charred bones are then pulverized into grains of sizes ranging between 0.5 and 2 mm and used in POU systems for treating cooking and drinking water only [4]. In Kenya where fluoride in drinking

Table 3. Summary of adsorption capacities of various grades of bone char

Source	Material	Capacity (mg F/g)	Mode of operation
USEPA [49]	Bone char	2.2	Full-scale plant operation
Mwaniki [51]	Black bone char	11.4	Batch
Mwaniki [51]	Gray bone char	2.4	Batch
Mwaniki [51]	White bone char	0.3	Batch
Abe *et al*. [19]	Bone char	>3	Batch
Mjengera and Mkongo [4]	Locally made bone char	7000 L/4 kg column	Column POU operation

water has also enormously attracted public health attention, the Catholic Diocese of Nakuru (CDN) has extensively researched and is in the implementation phase of a bone char-based household and community filters for water defluoridation. In the latter system, the bone char is either placed into a two-bucket POU system or into a large tank through which water contaminated with fluoride is passed [47].

(c) *Hydroxyapatite*. Hydroxyapatite is a highly crystallized material. One report by Fan *et al.* [16] gives its specific surface area as $0.052\,m^2/g$ and very close to that of calcite, quartz and fluorspar. The uptake of fluoride in hydroxyapatite is dominated by ion exchange. In water defluoridation, the fluoride ions firstly adsorb onto hydroxyapatite surfaces and the adsorbed fluoride is exchanged with OH group at the nearest surface of apatite particles, and then exchanged with the mobile OH group inside the hydroxyapatite particles, resulting in a much higher uptake of fluoride by hydroxyapatite. The exchange process can be represented by

$$Ca_{10}(PO_4)_6(OH)_2 + nF^- = Ca_{10}(PO_4)_6(OH)_{2-n}F_n + nOH^- \quad (5)$$

As a consequence of the above reaction, the capacity of hydroxyapatite for fluoride was found to be 4.54 [16].

(d) *Carbonaceous materials*. Carbon-based adsorbents have widely been used in adsorption processes for water treatment. Most of these adsorbents have very high internal surface area needed for adsorption. However, the affinity of anions by carbon is quite low. Thus, Ramos *et al.* [11] utilizing the high surface area of activated carbon, and the high affinity and capacity of aluminum toward fluoride ions, produced a novel sorbent, aluminum-impregnated carbon. In a batch study, they found that the aluminum-impregnated carbon had a 3–5 times higher capacity of fluoride than that of plain carbon. Just like with any other sorbent, the performance of aluminum-impregnated carbon was found to be dependent upon the pH of the impregnating solution, temperature of calcinations and solution pH of fluoride-containing water. In another study, Li *et al*. [54] used Al_2O_3-doped carbon nanotubes to remove fluoride from water. Carbon nanotubes are needle-like cylindrical tubules of concentric graphitic carbon capped by fullerene-like hemispheres. Since their discovery [55], great efforts have focused on their synthesis, characterization, theoretical investigation and their applications. Owing to their novel mechanical and electronic properties, large specific area and high thermal stability, they have a tremendous potential for future engineering applications, in such areas as hydrogen storage, field emission, catalyst supports and composite materials, among others. Application of carbon nanotubes as adsorbent in environmental pollution control is an emerging field. For this reason, Li *et al*. [17] prepared aligned carbon nanotubes (ACNTs) by catalytic decomposition of xylene using ferrocene as catalyst and tested the adsorbent in fluoride adsorption. They found a moderate capacity of ACNTs for fluoride. In explaining the mechanism of fluoride uptake by ACNT, they cited the availability of defects and

coats of amorphous carbon. These defects and amorphous carbon offered active sites for fluoride adsorption on the outer surfaces of the ACNTs. Additionally, the inner cavities and the micropores or mesopores composed by internanotube space between the densely ACNTs may have also contributed to the effective adsorption of fluoride. In a research using various carbonaceous materials such as charcoal, carbon black and activated carbons, Abe *et al*. [19] found the percentage of fluoride ion removal by the carbonaceous materials to increase with an increase in iodine-adsorption capacity. They explained that it meant that the adsorbability of the fluoride ions onto carbonaceous materials depended upon the specific surface area. Generally speaking, the amount of adsorbates adsorbed onto carbonaceous materials depends upon pore size distribution because adsorption occurs in pores, suggesting a physical adsorption.

Although a lot of research has been reported on the use of various carbonaceous materials in defluoridation, no known column or full-scale plant operation is easily available in open literature. One reason for this is that most carbonaceous materials show poor adsorption capacity (Table 4) for fluoride and therefore only laboratory-scale performances have so far been reported. Amorphous alumina supported on carbon nanotubes on the other hand show high capacity (28.7 mgF/g adsorbent) for fluoride and is therefore a promising material for drinking water defluoridation.

(e) *Geomaterials*. Geomaterials are low-cost adsorbent resources used in water and wastewater treatment. In addition, they are mostly locally available and require minimal processing, if any, before they are used. Moges *et al*. [56] intensively investigated both in batch and column operation modes, the fluoride adsorption ability of fired clay chips from a region in Ethiopia. They found that the clay had an appreciable fluoride adsorption capability and could lower the fluoride levels in drinking water to an acceptable value (Table 5).

Table 4. Summary of adsorption capacities of various carbonaceous materials

Source	Material	Capacity (mg F/g)	Mode of operation
Ramos *et al*. [11]	Plain carbon	0.49	Batch
Ramos *et al*. [11,82]	Al-impregnated carbon	1.07	Batch
Li *et al*. [54]	ACNTs	4.1	Batch
Li *et al*. [17]	Al_2O_3/CNT	28.7	Batch
Abe *et al*. [19]	Carbon black	0.2	Batch
Abe *et al*. [19]	Activated carbons	0.34 (coal based)	Batch
Abe *et al*. [19]	Charcoals	0.07	Batch

Table 5. Summary of adsorption capacities of selected geomaterials

Source	Material	Capacity (mg F/g)	Mode of operation
Moges *et al*. [56]	Fired clay	0.20	Batch
Moges *et al*. [56]	Fired clay	0.285	Column
Zevenbergen *et al*. [7]	Ando soil	5.51	Batch
Srimurali *et al*. [8]	Bentonite	1.15	Batch
Srimurali *et al*. [8]	Charfine	0.95	Batch
Wang and Reardon [57]	Tertiary soil	0.150	Column
Sugita *et al*. [58]	Kaolinite	≈0.667	Batch
Das *et al*. [59]	Titanium-rich bauxite	3.7–4.1	Batch

Zevenbergen *et al*. [7] attempted to make use of a locally available Kenyan soil derived from volcanic ash (i.e. Ando soils or soils with andic properties) as a fluoride adsorbent. The Ando soil contains in small quantities aluminum, iron and silica. It is probably these constituents that provide the active sites for fluoride ions. The ability of the Kenyan Ando soil to adsorb fluoride was determined experimentally. The batch capacity for fluoride adsorption was estimated at 5.51 mg/g, using the Langmuir isotherm model. These results were extended to possible technical application using a one-dimensional solute transport model. Based on the results it was concluded that the use of Ando soils appeared to be an economical and efficient method for defluoridation of drinking water on a small scale in rural areas of Kenya and other regions along the Rift Zone. Further research was warranted to evaluate its practical applications and social acceptance. In another study, Srimurali *et al*. [8] tested charfine, lignite, bentonite and kaolinite in fluoride sorption. At optimum conditions using a solution containing 5 mgF/L, the authors found that charfine and bentonite had an appreciable adsorption capacity of 38% and 46%, respectively. They explained, on the one hand, that the mechanism of uptake of fluoride by bentonite proceeded by adsorption onto the lattice structure and possibly by reaction with aluminum silicate, while on the other, fluoride adsorption on charfine proceeded by chemical interaction due to the surface heterogeneity and imperfections contained in charfine.

Limestone is another promising geomaterial for drinking water defluoridation. However, it has only been tested in wastewater containing high concentration of fluoride. In a research work by Reardon and Wang [60], limestone was used in a two-column continuous flow system (limestone reactor) to reduce fluoride concentrations from wastewaters to below the MCL of 4 mg/L for wastewater. Calcite was forced to dissolve and fluorite to precipitate in the first column. The degassing condition in the second column (did not serve to remove fluoride) caused the

precipitation of the calcite dissolved in the first column, thus returning the treated water to its approximate initial composition.

In a study by Wang and Reardon [57], heavily weathered tertiary soil from Xinzhou, China was used as a sorbent for defluoridation of high-fluoride drinking water. The soil was composed of quartz, feldspar, illite and goethite, with Fe oxide content of 6.75%. The authors found the soil's sorption capacity (150 μg/g) to be about a quarter of the low-end range of values reported by Rubel [61] for commercially available AA. The sorption of F^- ions was specific and involved ligand exchange between hydroxyl ions and fluoride ions according to the equation

$$\equiv FeOH + F^- \Leftrightarrow \equiv FeF + OH^- \quad (6)$$

The authors further explored the optimum heating temperature and found that heating the tertiary soil at 400–500°C enhanced the adsorbent's fluoride removal capacity. Moreover, a preliminary column experiment showed that 4.0 kg of 400°C heat-treated soil could treat more than 300 L of 5 mg/L fluoride feed water before the effluent fluoride concentration of 1.0 mg/L was reached. To minimize environmental impact of the used material, a cost-effective regeneration technique was devised and it involved rinsing the soil with sodium carbonate solution, followed with dilute HCl and finally twice with distilled water.

Using coal-based sorbents, Sivasamy *et al*. [62] evaluated their ability to remove fluoride from water. On equilibrium basis, Langmuir and Freundlich models were used to describe the data points, while the kinetic data points were interpreted in terms of reaction and mass transfer processes. Kaolinite, adioctahedral two-layered (silica and alumina) silicate (1:2 type), has also been tested in drinking water defluoridation. Recently, Sugita *et al*. [58] and earlier Kau *et al*. [63] and Weerasooriya *et al*. [10] presented fluoride adsorption results of kaolinite. The fluoride-binding sites in kaolinite consist of aluminol and silinol sites. The authors explained that the fluoride–kaolinite interaction led to the formations of both the inner- and outer-sphere complexes.

Bauxite ores, abundantly available in many parts of India, usually contain oxides/oxyhydroxides of Al, Fe and Si. The titania content in the bauxite ore depends upon the geological process that controlled the development of bauxite and usually varies in the range of 1–3 wt%. However, bauxite ore from several parts of central India (especially in the states of Jharkhand and Chattisgarh) mainly consists of oxides/oxyhydroxides of Ti and Al and small amounts of Fe and Si. Each of these oxides/oxyhydroxides possesses good adsorption capacity for fluoride as also seen in several recent investigations [9,16,64–66]. In an attempt to devise a simple and cost-effective fluoride removal process using locally available F sorbent (e.g., titanium-rich bauxite (TRB)), a study was designed to evaluate the adsorption capacity and to optimize the fluoride adsorption parameters using TRB so that a suitable adsorption process could be developed in future to abate fluoride from drinking water. The effect of pH, heat-treatment and

regeneration ability of the material were studied. Considering the pH profile and nature of oxides/oxyhydroxides present in TRB, the adsorption of fluoride is represented by the following two-step protonation/ligand-exchange mechanism:

$$\equiv SOH_{(s)} + H^{+}_{(aq)} \rightleftarrows \equiv SOH^{+}_{2(s)} \tag{7}$$

$$\equiv SOH^{+}_{2(s)} + F^{-}_{(aq)} \rightleftarrows \equiv SF_{(s)} + H_2O \tag{8}$$

which gives the net reaction

$$\equiv SOH_{(s)} + H^{+} + F^{-}_{(aq)} \rightleftarrows \equiv SF_{(s)} + H_2O \tag{9}$$

where $\equiv$S represents the surface of adsorbent. This two-step mechanism is favorable at pH $<$ 6. However, at pH $>$ 6, fluoride ion is pre-dominantly adsorbed by the following mechanism:

$$\equiv SOH_{(s)} + F^{-}_{(aq)} \rightleftarrows \equiv SF_{(s)} + OH^{-} \tag{10}$$

The progressive decrease of fluoride uptake at pH $>$ 6 is mainly due to two factors: the electrostatic repulsion of fluoride ion to the negatively charged surface of the TRB ($pH_{zpc} = 7.05$–7.5) and the competition for active sites by excessive amount of hydroxyl ions. The adsorption capacities of the geomaterials described above are summarized in Table 6.

(f) *Waste-derived adsorbents*. Waste-derived adsorbents are considered low-cost alternative defluoridation media. The ability of treated alum sludge to remove fluoride from aqueous solution was investigated by Sujana *et al*. [9]. Alum sludge is a waste product generated during the manufacture of alum from bauxite. This material mainly consists of aluminum and titanium with small amounts of undecomposed silicates. It is well known that these constituents have fluoride ions affinity. In using this material in fluoride adsorption, the authors argued that they solved two problems, fluoride contamination and waste disposal problems. The fluoride uptake was found to follow the Langmuir isotherm suggesting sorption on

Table 6. Summary of adsorption capacities of selected waste-derived materials

Source	Material	Capacity (mg F/g)	Mode of operation
Sujana *et al*. [9]	Alum sludge	5.39	Batch
Cengeloglu *et al*. [13]	Red mud	3.12	Batch
Cengeloglu *et al*. [13]	Activated red mud	6.29	Batch
Mahramanlioglu *et al*. [14]	SBE	7.75	Batch
Liao and Shi [67]	Zr(IV)-loaded collagen fiber	43.51	Batch

homogeneous sites, while kinetically the adsorption reaction was first order. Also from an environmental and economic standpoint, spent bleaching earth (SBE), a solid waste from edible oil-processing industry, was tested as a low-cost adsorbent for fluoride adsorption [14]. SBE has two components: residual oil not removed by filter pressing and montmorillonite clay. When not utilized as in this case, the material is normally disposed off directly to landfill either in a dry state or as wet slurry. The material was found to be most effective at pH 3.5 and the adsorption transient curves were best described by second-order kinetics.

Another waste material that has found fluoride adsorption application is the red mud. Just like the alum sludge, red mud (bauxite wastes of alumina manufacture) emerges as an unwanted by-product during the alkaline-leaching of bauxite in the Bayer process. Çengeloğlu *et al*. [13] reported that about 500,000 m^3 of strongly alkaline (pH ≈ 12–13) red mud water was dumped annually into specially constructed dams around Seydiğehir Aluminium Plant-Turkey. Since the plant began to operate, the red mud accumulated and posed severe environmental problem. Consequently, the authors investigated the possibility of utilizing the material in the original or activated form as an adsorbent for the removal of fluoride from aqueous solution. They explained that the uptake of fluoride involved ligand-exchange reaction as follows:

$$\mathrm{MOH} + \mathrm{H^+} \rightleftharpoons \mathrm{MOH_2^+} \tag{11}$$

$$\mathrm{MOH_2^+} + \mathrm{F^-} \rightleftharpoons \mathrm{MOH_2 - F(or\ MF + H_2O)} \tag{12}$$

$$2[\,\rangle\mathrm{MOH}\,] + 2\mathrm{F^-} \rightleftharpoons \begin{matrix}\rangle\mathrm{MOF} \\ | \\ \rangle\mathrm{MF}\end{matrix} + \mathrm{H_2O} \tag{13}$$

where M represents metal ion (Al, Fe or Si). The first reaction involves the protonation of the neutral sites, usually taking place at pH values below the pH_{pzc} of the adsorption media (red mud). According to the second reaction, fluoride ions interact with the positively charged sites to form either the outer-sphere complexes or inner-sphere complexes with elimination of water molecule. The third reaction involves interaction between fluoride and the neutral sites forming inner-sphere complex.

Collagen fiber, an abundant natural biomass, comes from the skin of animals and has been traditionally used as raw material in leather manufacturing. The collagen molecule is composed of three polypeptide chains with triple-helical structure, and they are aggregated through hydrogen bonds to form collagen fiber. Collagen fiber is water insoluble but is a hydrophilic material. According to the principles of leather manufacture, collagen fiber that has abundant functional groups is capable of chemically reacting with many kinds of metal ions, such as Cr(III), Al(III), Zr(IV). Thus, Liao and Shi [67] prepared a novel adsorbent by impregnating Zr(IV) on collagen fiber, and its adsorption behavior in removing

fluoride from water was investigated. The adsorption capacity was 43.51 mg/g (Table 6) at pH = 5.5. The adsorption isotherms were well fitted with the Langmuir equation. The adsorption capacity increased with an increase in temperature suggesting an endothermic adsorption. These facts imply that the mechanism of chemical adsorption might have been involved in the adsorption process of fluoride on the adsorbent and that fluoride ions formed a monolayer on the surface of the adsorbent. The adsorption kinetics of fluoride onto Zr(IV)-impregnated collagen fiber were described by Lagergren's pseudo-first-order rate model. In addition, results of desorption indicated that this adsorbent was easily regenerated by use of dilute NaOH solution.

In a similar study operated in a batch mode, Oguz [23] used gas concrete waste materials to remove F^- from aqueous solutions under varying experimental conditions such as solution pH and temperature. It was thought that the removal of fluoride by gas concrete took place both by adsorption and precipitation of Al^{3+} and Ca^{2+} salts. As a result of this study, it was concluded that wastes of gas concrete were an efficient adsorbent (about 96%) for the removal of fluoride ions from water.

(g) *Polymeric materials*. Chelating resins have been recognized for their promising metal-adsorption properties. Utilizing their ability to adsorb trivalent metals and their large internal matrices, several author have studied extensively the application of metal-loaded polymeric resins as potential adsorbents for anions: in particular, fluoride. La(III)-loaded PMA resin, Zr(IV)-loaded Amberlite XAD-7, La(III)-AFB resin, Pr(III)-AFB resin [68], Al(III)-AMPA resin [69], La(III)-impregnated silica gel, cross-linked pectic acid (CPA) gel, phosphorylated cross-linked orange juice (POJR) gel, La(III)-loaded 200CT resin, saponificated orange residue (SOJR) are some of the polymeric adsorbents that have been tested for fluoride uptake in acidic to near neutral pH range using a batch mode of operation. For these materials, their capacities are appreciable higher than those of other adsorbents. Because of the metal loading onto the adsorbents, the mechanism of fluoride removal from water is that due to ligand exchange between fluoride ions from water and hydroxyl ions from the resin. Not much is known about the large-scale operation of these adsorbents and nor is their long-term stability well defined from the scanty literature available. However, Fang *et al*. [70] presented column dynamics of fluoride removal from water using La(III)-loaded 200CT resin. They found that the adsorbent could only process 50-bed volumes before breakthrough was reached indicating that the high-batch capacities (Table 7) of these adsorbents are fallacious. Because these kinds of adsorbent are synthetic, they are expected to be relatively expensive.

(h) *Layered double hydroxides*. In nature layered double hydroxides (LDHs) are very rare; however, they can be synthesized in a laboratory by a co-precipitation method. The applications of LDHs as adsorbents to selectively remove anionic organic or inorganic pollutants from aqueous solutions have attracted considerable attention in the recent past [71–79] .The LDHs, also called hydrotalcite-like

Table 7. Summary of adsorption capacities of selected polymeric materials

Source	Material	Capacity (mg F/g) (BV: bed volume)	Mode of operation
Chikuma and Nishimura [68]	Pr(III)-AFB resin	0.5	Batch
Popat *et al*. [69]	Al(III)-AMPA resin	11.16	Batch
Popat *et al*. [69]	Al(III)-AMPA resin	86.7 BV	Column
Fang *et al*. [70]	200CT resin	5.39	Batch
Fang *et al*. [70]	200CT resin	50 BV at breakthrough	Column
Fang *et al*. [70]	IR124 resin	42.0	Batch
Fang *et al*. [70]	CPA gel	39.3	Batch
Fang *et al*. [70]	POJR gel	22.2	Batch
Fang *et al*. [70]	SOJR gel	16.15	Batch

compounds or anion clays, consist of brucite-like hydroxide sheets. Many cations can be incorporated in the brucite-like sheets. The general formula is

$$[M^{II}_{1-x}M^{III}_{x}(OH)_2]^{x+}[(A^{n^-})_{x/n} \cdot mH_2O]^{x-} \quad (14)$$

where M^{II} is divalent cation like Mg^{2+}, Zn^{2+}, Cu^{2+}, etc., M^{III} trivalent cations like Al^{3+}, Cr^{3+}, Fe^{3+}, etc. and A^{n-} anion [80]. Owing to the partial substitutions of M^{III} for M^{II}, the hydroxide sheets are positively charged and require intercalation of anions such as CO_3^{2-}, Cl^- or NO_3^- to remain electrically neutral. Studies have shown that LDHs can uptake some inorganic or organic anionic pollutants by exchange with interlayer anions [74,75], but the efficiency of uptake is affected considerably by the properties of interlayer anions. Generally, LDHs have greater affinities for multivalent anions such as CO_3^{2-} and PO_4^{3-} than for monovalent anions. In a recent study by Das *et al*. [18], calcined Zn/Al hydrotalcite-like compound (HTlc) was used to remove fluoride from aqueous solution. The maximum adsorption took place within 4 h at pH 6.0. The fluoride removal was exothermic in nature, the efficiency increased with an increase in the adsorbent dose, but decreased with an increase in the fluoride concentration. The maximum adsorption capacity was 16.2 mg/g at 30°C.

(i) *Zeolites*. Zeolites are aluminosilicates with a framework structure of $(SiAl)O_4$ tetrahedral containing pores filled with water molecules and exchangeable cations. The ions and molecules of water contained in the voids have a considerable freedom of movement that leads to ion exchange and reversible dehydration. Zeolites are abundantly available in both natural and synthetic form and among them are: Zeolite A, Zeolite X, Zeolite Y, Zeolite F9, Clinoptilolite, Mordenite, HSZ

300HUD, Erionite, Zeolite ZSM-5, Offretite, Type L and Omega. Over the years, zeolites have gained enormous applications especially in sorption processes as evidenced from researches by Song *et al*. [81], García-Sánchez *et al*. [82], Färm [83], Doula and Ioannou [84], Majdan *et al*. [85], Daković *et al*. [86], Dal Bosco *et al*. [87], Turan *et al*. [88] and Wingenfelder *et al*. [89]. Recent adsorption data of anions by surface-tailored zeolite suggests that this novel media has potential for water treatment [90–95].

By using the wet impregnation method, a novel adsorbent, aluminum-loaded Shirasu-zeolite P_1 (Al-SZP_1), was developed for the removal of fluoride ions from aqueous system [96]. The dependence of removal percentage upon aluminum concentration in the loading solution, pH, initial concentration and co-existing anions was investigated. The rate of adsorption of fluoride followed first-order kinetics, equilibrium data described by Freundlich isotherm, while the mechanism was supposedly an ion exchange process between fluoride and the hydroxide groups on the surface of A1-SZP_1. In another study, a new adsorbent, cerium(IV) oxide coated on SiMCM-41 ((Ce)SiMCM-41), was prepared by Xu *et al*. [97] for the removal of fluoride ions from water. Factors investigated were the number of impregnations, Ce/Si ratios, the concentration of F^- ions, pH values and calcination temperatures. The dynamics, isotherms and mechanism of adsorption of F^- ions were discussed. Using a similar impregnation method, Onyango *et al*. [98–100], have shown that low-silica zeolites can be charge-reversed and used in fluoride removal from water. Table 8 summarizes some of the reported zeolite capacities.

3.2. Characteristics of fluoride adsorption onto surface-tailored low-silica zeolite

In this section, detailed analysis of fluoride adsorption characteristics are provided. Zeolite-adsorption media is chosen for this purpose. Zeolites are well

Table 8. Summary of adsorption capacities of zeolites

Source	Material	Capacity (mg F/g)	Mode of operation
Xu *et al*. [97]	(Ce)SiMCM-41	114.4	Batch
Onyango *et al*. [98]	La-exchanged F9	54.3	Batch
Onyango *et al*. [98]	Al-exchanged F9	39.5	Batch
Onyango *et al*. [100]	Al-exchanged A4	41.4[a]	Batch
Onyango *et al*. [100]	Al-pretreated HUD	28.1[a]	Batch
Onyango *et al*. [100]	Na-Al-pretreated HUD	34.8[a]	Batch

[a] Indicates values are determined from Dubinin–Radushkevitch isotherm.

known for their ion-exchange phenomenon and are an emerging competitive adsorbent. Their role in the conversion of solid and liquid hazardous wastes into environmentally acceptable product is well documented. In water treatment, several zeolites, namely, clinoptilolite, chabazaite, Shirasu-zeolite SZP1, 13X and 5A have been identified as potential adsorption media. Synthetic zeolites are useful because of their controlled and known physicochemical properties relative to those for natural zeolites [95]. More importantly, low-silica synthetic zeolites provide relatively higher number of ion-exchange sites. This latter property was utilized to create a novel adsorbent for fluoride.

3.2.1. Surface modification of zeolite

One disadvantage of using zeolites in anions adsorption inheres in their negative zeta potential in solution over a wider pH range. The preceding factor (negative charge) results in coulombic repulsion between the zeolite surfaces and adsorbing anions. Thus, to effectively use zeolites in anions adsorption, their surfaces need to be tailored in such a manner as to create surface-active sites that are efficient and specific to target anions. By a wet impregnation method using Al^{3+} ions the net surface charge of zeolite can be altered as shown in Fig. 2 [98].

Figure 2 above shows a typical plot of changes in electrokinetic properties of zeolite F9 (Na-form, Si/Al ratio = 1.23) and its modified forms suspensions in 10 mM NaCl as a background electrolyte. Zeolite F9 contains sodium oxide, silicon oxide and aluminum oxide and therefore it is a mixed oxide adsorbent. It is shown in Fig. 2 that zeolite F9 is negatively charged over the whole pH range tested and therefore has no pH_{pzc}. By contrast, when Na^+ ions were exchanged for Al^{3+} ions, the zeolite particles were charge-reversed and the pH_{pzc} was found to be 8.15. At this pH, the positively charged aluminol sites (Zeo-$AlOH_2^+$) and those due to unexchanged sodium, if any, are basically equal to the negatively charged sites mainly from silica and hydroxylized aluminol sites. Also indicated in the figure is the field pH range (6.5–8.5) of drinking water over which defluoridation is desired.

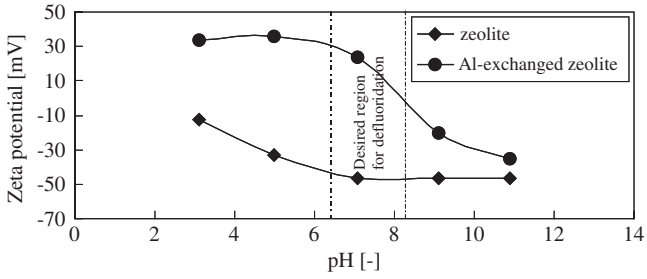

Fig. 2. Changes in electrokinetic properties of zeolite F9 and its modified form, Al^{3+}-exchanged zeolite.

Over this pH range, the number of active sites in Al-exchanged zeolite F9 is expected to reduce substantially as can be deduced from the fall in zeta potential. Using the surface-modified zeolite, batch equilibria and kinetics and column dynamic were studied.

3.2.2. Batch fluoride adsorption equilibrium

Figure 3 summarizes the typical equilibrium data for fluoride sorption on 0.150–0.300 mm surface-tailored zeolite F9. Only the low-concentration range was considered where the Henry's law is applicable. Co-incidentally, fluoride ions exist in natural systems, such as groundwater, at low concentrations. It is observed that the data fit well to the linear isotherm suggesting sorption onto sites with high capacity for fluoride. From Fig. 3, the linear isotherm constant, K ($= 2.337$ L/g), was obtained and coupled into the diffusion model, equation (16).

3.2.3. Prediction of mass transfer processes

Adsorption process involves the transfer of a species from the bulk solution to the adsorbent surface, then to the interior matrix of the adsorbent where the species is bound onto the active sites. Figure 4 shows the effect of varying initial fluoride concentration from 5 to 20 mgF/L. The quantities of fluoride removed from the solution increased with an increase in initial concentration. Diffusion is a passive transport process driven/governed by the concentration gradient at the solution/sorbent interface. At higher initial concentration, the driving force, which is the difference between the bulk-phase concentration and the sorbed-phase concentration, is expected to be higher. This leads to larger uptake in both the early and longer contact times, for higher initial concentration.

During transport, both external and intraparticle mass transfer resistances play a role to a varying degree. A first step in adsorber design is to predict or

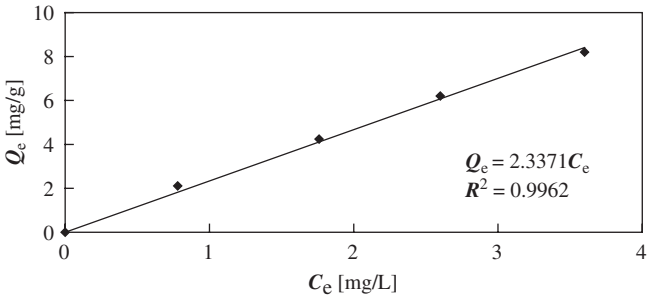

Fig. 3. Linear adsorption isotherm. Initial fluoride concentration ranged from 5–20 mg/L.

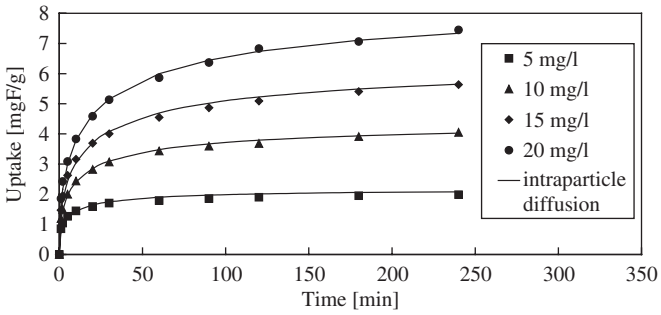

Fig. 4. Effect of initial concentration on fluoride uptake: particle size, 0.150–0.300 mm; sorbent dose, 2 g/L; agitation speed, 300 rpm and solution temperature, 295.1 K.

determine these resistances. Thus, a batch operation mode was adopted to determine the film and intraparticle diffusion coefficients under varying initial fluoride concentration (5–20 mg/L), as an example. The mass transfer values obtained from such study can then be used as first estimates in mechanistic modeling of columns. The evaluation of external resistance to mass transfer was done, by determining the film diffusion coefficients according to a simple method proposed by Mckay [101]. The method involves the calculation of the initial slope of the concentration against time curve and substituting the obtained value into Equation

$$\left.\frac{\mathrm{d}(C_t/C_o)}{\mathrm{d}t}\right|_{t=0} = -k_\mathrm{f} S_A \tag{15}$$

where k_f is the film diffusion coefficient (cm/s) and S_A the specific surface area of the zeolites (cm^{-1}). The specific surface area is expressed as

$$S_A = \frac{6m_\mathrm{s}}{\rho_\mathrm{p} d(1-\varepsilon_\mathrm{p})} \tag{16}$$

where m_s is the zeolite mass per unit volume ($\mathrm{g/cm}^3$), ρ_p the density of zeolite ($\mathrm{g/cm}^3$), d the average zeolite size (cm) and ε_p the porosity. The film diffusion coefficients determined according to equation (15) are summarized in Table 9. The magnitude of k_f values was in the range 2.07×10^{-2}–3.08×10^{-2} cm/s. This range of k_f values is high implying less external resistance to mass transfer. Moreover, they are comparable to those reported by Mahramanlioglu *et al*. [14] and Ghorai and Pant [39] for fluoride adsorption on SBE and AA, respectively, and indicate the rapidity with which fluoride ions were transported to the external surface of the zeolites.

In general, as an adsorbate is transported in the internal matrix of adsorbent, there is tendency of adsorbate–adsorbate interaction in the pores and hopping, from site to site, of adsorbed species along the wall of the adsorbent. These phenomena give rise to pore and surface diffusion resistances to intraparticle

Table 9. Summary of mass transfer parameters for batch fluoride adsorption

Initial concentration (mg/L)	Mass transfer parameters			
	K_f (cm/s)	D_e (cm^2/s)	$N_{Bi} = k_f\, r_o/D_e$ (−)	$\Delta q\%$
5	3.05×10^{-2}	1.11×10^{-9}	»100	4.66
10	2.07×10^{-2}	5.27×10^{-10}	»100	1.45
15	2.45×10^{-2}	3.22×10^{-10}	»100	2.16
20	3.08×10^{-2}	2.68×10^{-10}	»100	1.48

mass transfer. Thus, a parallel pore–surface diffusion model for a differential radial shell of zeolite adsorbent is given by

$$\varepsilon_p \frac{\partial c}{\partial t} + \rho_p(1-\varepsilon_p)\frac{\partial q}{\partial t} = D_p\varepsilon_p \frac{1}{r^2}\frac{\partial\left(r^2 \frac{\partial c}{\partial r}\right)}{\partial r} + \rho_p D_s \frac{1}{r^2}\frac{\partial\left(r^2 \frac{\partial q}{\partial r}\right)}{\partial r} \tag{17}$$

where c and q are the pore- and adsorbed-phase concentrations, respectively, D_p and D_s the pore and surface diffusion coefficients, ε_p the particle porosity, ρ_p the particle density, r the radial dimension and t the time. In this model it is assumed that a local equilibrium exists between the adsorbing fluoride ions and those in pore phase for $0 \le r \le r_o$ and that equilibrium is described by a linear isotherm as described in Section 3.2.2. Analytical solution of the above equation is given by Crank [102]:

$$Q_{av,t} = Q_e\left\{1 - \sum_{n-1}^{\infty} \frac{6\alpha(\alpha+1)\exp(-\beta_n^2 k' t)}{9 + 9\alpha + \beta_n^2\alpha^2}\right\} \tag{18}$$

where r_o is the mean particle radius, $Q_{av,t}$ is the average amount adsorbed in the pore and surface, Q_e the equilibrium concentration and β_ns are the positive non-zero roots of

$$\tan\ \beta_n = \frac{3\beta_n}{3 + \alpha\beta_n^2} \tag{19}$$

and $\alpha = 1/\rho K$ represents the sorbent load factor and $k' = D_e/r_o^2$ represents the intraparticle diffusional time constant, D_e (combines pore and surface diffusion coefficients) is the effective intraparticle diffusion coefficient and ρ equal to sorbent mass to particle-free volume. The intraparticle resistance to sorbate transport is determined by intraparticle diffusion coefficient, D_e· Thus, the D_e values were determined, by minimizing the normalized standard deviation ($\Delta q\%$) and are summarized in Table 9. As the initial concentrations were raised, the effective diffusion coefficients decreased in a non-linear fashion. McKay and Al-Duri [103] found a non-linear decrease in effective diffusivity with an increase in dyes concentration and attributed this to surface diffusion effects. To the contrary,

Ma *et al*. [104] attributed a decrease in diffusivity with an increase in initial concentration to pore diffusion effects. Because zeolites are bi-dispersed sorbents, both surface and pore diffusions may dominate different regions. In micropores, surface diffusion may be dominant, while pore diffusion may be dominant in macropores. This, therefore, supports the use of a lumped parameter (D_e). To explore further the relative importance of external mass transfer *vis-a-vis* internal diffusion, Biot number ($N_{Bi} = k_f\, r_o/D_e$) was considered. Table 9 summarizes the N_{Bi} values for the four initial concentrations. The N_{Bi} values are significantly larger than 100 indicating that film diffusion resistance was negligible.

3.2.4. Defluoridation in zeolite column

In liquid-phase adsorption separation and purification process, there are a number of configurations such as batch, fixed bed and fluidized bed that are applicable for a given utility. Among these, fixed bed is the most commonly used configuration in drinking water treatment. The advantages of using fixed-bed adsorbers in water treatment inhere in the high quality of drinking water produced, their simplicity, ease of operation and handling and regeneration capacity. Moreover, for such configuration, both POU system that can serve an individual household and POE system that can serve a small or large community are possible. Thus, a number of researchers have studied defluoridation of drinking water using various adsorption media in fixed-bed column. Rubel [61] and Ghorai and Pant [22] using AA and Mjengera and Mkongo [4] using bone char showed that fixed-bed configuration is a feasible defluoridation unit.

In order to design an effective adsorption separation or purification unit, preliminary design information is required [38]. Often, these pieces of information are gathered through the performance of an extensive series of pilot-plant experiments that are time consuming and expensive. The aim of such a study is to predict *a priori* what will happen in a full-scale column under various design and operating parameters. Among the operating parameters and fluid features that are paramount for a good design are: linear flow rate, initial concentrations, bed height, particle size, adsorbent types, pH and temperature, among others. To cut costs and to save time in doing unnecessarily too many experiments, Ko and coworkers [38] suggest that models should be used to predict the optimum conditions when the above parameters are varied. Models may broadly be divided into empirical, simplistic and mechanistic models. In mechanistic models for fixed-bed adsorber, all the fundamental mass transport mechanisms, including external film, pore and surface diffusions, axial dispersion and reaction kinetics have to be accounted for. Unfortunately, the solution of a number of differential equations involved often require numerical techniques and thus require high-level expertise. In addition, these solutions also require accurate correlations for mass transfer parameters to describe external film, internal pore diffusion and the

equilibrium relationship between sorbate and sorbent [38]. Because of the above limitations, several simplified design models such as the empty bed contact time (EBCT), the bed depth service time (BDST) and empirical design model such as the two-parameter model are some of the common approaches usually applied. These kinds of the so-called ''short-cut'' models ensure that pilot-plant testing is used largely for verification rather than information gathering, thus, saving time and money. In this communication, therefore, fluoride removal using fixed-bed column is undertaken at different bed heights and initial fluoride concentrations. The results are interpreted using EBCT approach, and BDST and two-parameter models.

(a) *The bed depth service time model*. The laboratory-scale fixed-bed column used in this study was 15 cm long with 2.1 cm internal diameter containing granular surface-tailored zeolite of 0.150–0.355 mm size. Fluoride-spiked solution was pumped to the column in an upward-flow mode. The effects of two variables, bed height and initial fluoride concentration, on breakthrough curves are reported.

The BDST model is based on the assumption that reaction kinetics plays a limiting role in adsorption. Therefore, the starting point in BDST modeling approach is to consider the reaction kinetics. As already mentioned, both the protonated and neutral aluminol surface sites are the fluoride-adsorption sites. These surface groups are located at the 0-plane. Fluoride ion being an inner-sphere complex-forming species, interacts with the active sites in the region bounded by the adsorbent surface (0-plane) and inner Helmholtz plane (IHP) of the Stern layer, as illustrated in Fig. 5.

Mechanistically, the interaction between fluoride and the active sites follows second-order kinetics. If we let S_t to be the total number of sites, SF the sites occupied by fluoride, and $S_t - SF$ the sites available for reaction, then the rate of reaction, r_s, is given by

$$r_s = \frac{d[SF]}{dt} = k_a[F^-][S_t - SF] - k_d[SF] \tag{20}$$

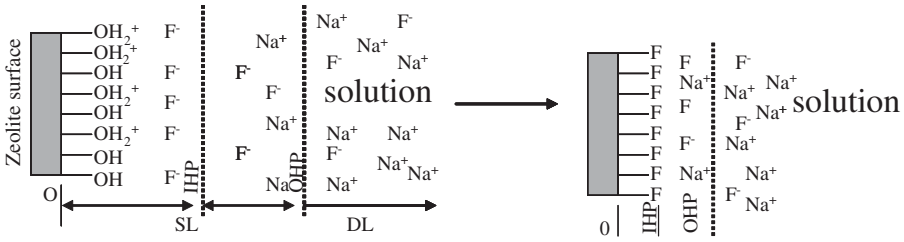

Fig. 5. Illustration of the scheme of surface-tailored zeolite–water interface with adsorbing fluoride ions found in the region bound between planes 0 and IHP. The interaction leads to the formation of inner-sphere complexes of surface-tailored zeolite/fluoride. Sodium ions do not penetrate the IHP.

or simply

$$\frac{dq}{dt} = k_a c(q_m - q) - k_d q \tag{21}$$

where $[SF] = q$, $[S_t] = q_m$, $[F^-] = c$, k_a is the forward rate constant and k_d the backward rate constant. If the zeolite–fluoride bonding is strong, then $k_a \gg k_d$. Moreover, Bohart and Adams [105] simplified the above expression for ion exchange as follows:

$$\frac{dq}{dt} = -k_a qc \tag{22}$$

In carrying out material balance over a small control volume of a fixed bed, it is considered that fluoride removal is solely by adsorption onto the zeolite particles. Additionally, the system is assumed to be isothermal, non-equilibrium and non-adiabatic single-component fixed-bed adsorption. For the control volume (Fig. 6), $A_x dz$, for a limiting situation $z \to 0$, the material balance is given by

$$\frac{\partial C_z}{\partial t} = D_L \frac{\partial^2 C_z}{\partial z^2} - u\frac{\partial C_z}{\partial z} - C_z \frac{\partial u}{\partial z} - \frac{(1-\varepsilon)}{\varepsilon}\rho_s \frac{\partial q}{\partial t} \tag{23}$$

where A_x is the cross-sectional area of the bed, z the axial dimension, D_L the axial dispersion coefficient, C_z the concentration, w (Fig. 6) the bed weight, u the linear velocity, ε the bed porosity and ρ_s the particle density. For mathematical expediency, axial dispersion is assumed negligible and for dilute solution u is assumed to be constant, and therefore a combination of equations (22) and (23) gives

$$\frac{\partial C_z}{\partial t} + u\frac{\partial C_z}{\partial z} = -k_a qc \tag{24}$$

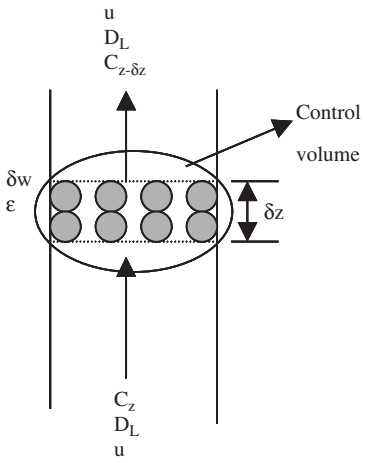

Fig. 6. Control volume of a fixed bed over which material balance is carried.

If the volumetric sorption is expressed by N_o (gF/L), then the solution of equation (24) over the bed length is given by a simplistic model, well known as the BDST, expressed as

$$\ln\left(\frac{C_o}{C_t}-1\right)=\ln\left(e^{k_aN_oZ/u}-1\right)-k_aC_ot \tag{25}$$

The linearized form of the above equation is given by

$$t=\frac{N_oZ}{C_ou}-\frac{1}{k_aC_o}\ln\left(\frac{C_o}{C_b}-1\right),\quad \text{for } C_t=C_b \text{ (breakthrough concentration)} \tag{26}$$

Application of the BDST model (equation (25)) to simulate breakthrough curves of fluoride adsorption onto zeolite in a fixed bed is shown in Fig. 7. The BDST model satisfactorily simulates the experimental data points. It is observed that as the bed height is raised, it takes longer time for a given concentration to exit due to increases in the number of active sites and possibly due to increase in contact time. The BDST model was further considered in the linearized form according to equation (26) and as shown in Fig. 8, in which the service time is correlated with the bed depth. A highly significant linear regression line was obtained. From the linear plot, for $C_b = 1.5$ mg/L (WHO permissible limit), the rate constant k_a was found to be 8.3×10^{-4} L/mg/min. The critical bed depth was also determined. The critical bed depth (Z_0) represents the theoretical depth of adsorbent necessary to prevent the sorbate concentration to exceed the limit concentration C_b. From equation (26) when $t = 0$, we have

$$Z_0=\frac{u}{k_aN_o}\ln\left(\frac{C_o}{C_b}-1\right) \tag{27}$$

The critical bed depth (Z_0) was found to be 0.8 cm. When the column capacity at breakthrough was compared with batch capacity at the same concentration, the

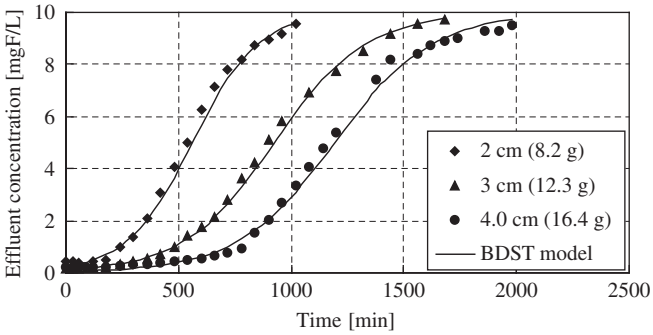

Fig. 7. Effect of bed height on fluoride removal from water. BDST model simulation is represented by continuous line. Initial concentration = 10 mg/L; flow rate ≈ 9.8 mL/min; particle size = 0.150–0.355 mm; and pH = 6.2–6.4.

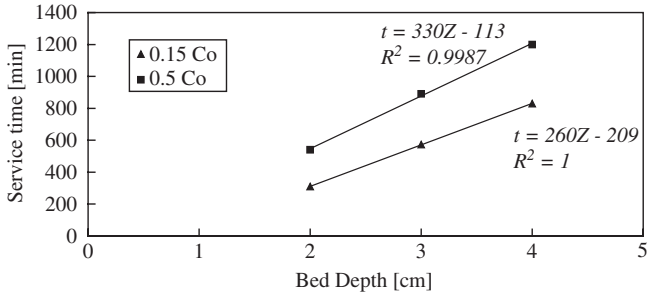

Fig. 8. BDST: fixed bed design.

former was found to be higher. This and other useful pieces of information are summarized in Table 10.

In another experimental run, the initial fluoride concentration was varied from 5 to 20 mg/L as shown in Fig. 9. It is observed that the higher the concentration, the steeper the slope of breakthrough curves, hence a reduction in zone spreading time. Also, the breakthrough curves shift towards the origin with increase in initial concentration. These observations are due to the fact that at higher concentration, the active sites are quickly filled up. From this figure and model simulation, the times required for the exit concentration to rise to breakthrough point ($C_b = 1.5$ mg/L) and 50% of initial concentration at the exit and column capacity were determined and are summarized in Table 10.

In optimizing fixed bed, it is important to know how the EBCT affect the adsorbent exhaustion rate (AER) (AER: mass of adsorbent per volume of water treated at breakthrough). Thus, AER was determined at various adsober heights and initial concentrations. On the one hand, it was found that an increase in bed height resulted in a decrease in AER, while on the other, an increase in initial concentration resulted in a corresponding increase in AER (Table 10). The former suggests that within the range of heights used in this study, a longer bed is preferred, while from the latter, it can be concluded that lower concentrations lead to processing of more bed volumes.

(b) *The two-parameter model*. A simple two-parameter model is an empirical expression for modeling breakthrough curves and it takes the form [106]

$$\frac{C_t}{C_o} = \frac{1}{2}\left(1 + \mathrm{erf}\left[\frac{(t - t_o)\exp\left(\sigma(t/t_0)\right)}{\sqrt{2}\sigma t_0}\right]\right) \tag{28}$$

where erf[x] is the error function of x, defined by

$$\mathrm{erf}[x] = \frac{2}{\sqrt{\Pi}}\int_0^x \exp(-\eta^2)\,\mathrm{d}\eta \tag{29}$$

where t is the column residence time, t_0 the time at which the effluent concentration is half the influent concentration and σ represents the standard deviation

Table 10. Summary of BDST and EBCT data

Variable	Lowest concentration (mg/L)	Time to breakthrough, C_b (min)	Time to 0.5 C_o (min)	Capacity at C_b (mg/g)	Batch capacity at C_b (mg/g)	EBCT (min)	AER (g/L)
Effect of Bed depth							
2 cm	0.42	310	540	3.72	3.49	0.69	2.70
3 cm	0.19	573	891	4.64	3.49	1.06	2.13
4 cm	0.21	830	1200	4.79	3.49	1.39	2.02
Effect of initial concentration							
5 mg/L	0.23	1211	1524.5	3.79	3.49	1.06	1.04
10 mg/L	0.19	573	891	4.64	3.49	1.06	2.13
20 mg/L	0.28	307.5	473	4.93	3.49	1.06	3.84

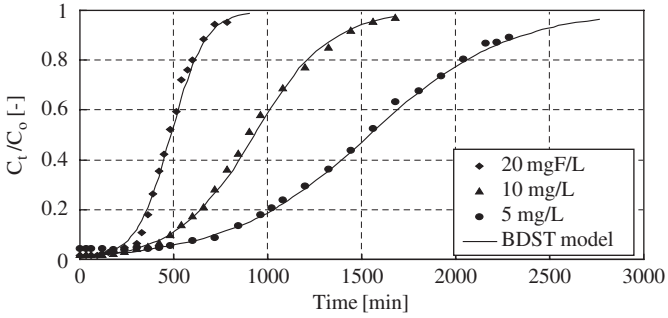

Fig. 9. Effect of initial concentration on fluoride removal from water. BDST model simulation is represented by continuous line. Bed height = 3 cm, flow rate- ≈9.8 mL/min; particle size = 0.150–0.355 mm; and pH = 6.2–6.4.

which is a measure of the slope of the breakthrough curve. Chu [106] further suggests that the use of simpler and more tractable models that avoid the need for numerical solution appears more suitable and logical and could have immediate practical benefits. In general, such a model is easier to use and more efficient from a computational point of view compared to the use of full mechanistic models which are much more complicated mathematically. For these reasons, we also explored the possibility of simulating the breakthrough curves using the two-parameter model (equation (28)), by considering the effects of bed height and initial fluoride ions concentration.

The model parameters σ and t_0 for the adsorption of fluoride onto surface-tailored zeolite were determined by matching equation (28) with experimental data. This was done by minimizing the objective function, ϕ, expressed as

$$\phi = \sum \frac{\left|C_{ecp} - C_{cal}\right|}{n} \tag{30}$$

where C_{exp} and C_{cal} are the experimental and calculated values of concentration at the column exit and n is the number of data points. In Figs. 10 and 11, the breakthrough curves determined using the best-fit values of σ and t_0 are represented by continuous lines. As was with the case of BDST model, the data points are well represented with the two-parameter model. When the height of the bed and the initial concentration were increased, σ decreased (Table 11). The parameter t_0 on the other hand increases with an increase in bed height and a decrease in initial concentration.

Although both the BDST and two-parameter models fit the experimental data points so well, care should be taken when they are being used in fixed-bed design. Consequently, Chu [106] in contradicting an early work of Ko *et al*. [38], suggests that these models should not be used to predict breakthrough *a priori*. The modeling approach presented here is thus for the purpose of illustration only.

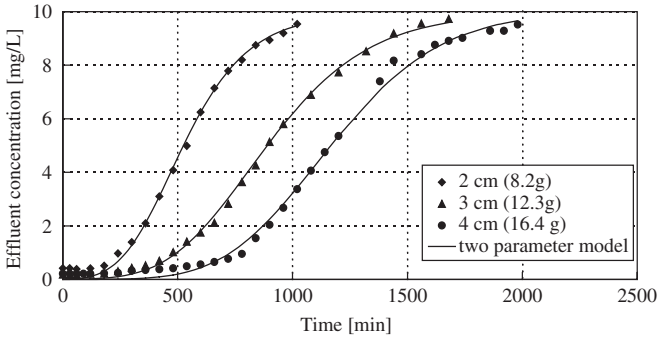

Fig. 10. Effect of bed height on fluoride removal from water. Two-parameter model simulation is represented by continuous line.

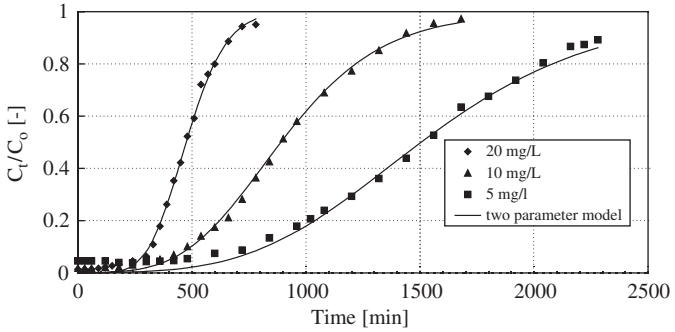

Fig. 11. Effect of initial fluoride concentration on fluoride removal from water. Two-parameter model simulation is represented by continuous line.

A better approach would be to correlate the model parameters with several process variables before the model can be used to design and scale-up the column.

3.3. Configurations and modes of operation of adsorbent-based defluoridation units

Once an adsorption media is chosen and where applicable, model simulations are satisfactory, the next step would be to consider various defluoridator configurations. There are several attractive water treatment configurations based on adsorption technique. These configurations are also principally applicable to water defluoridation. The choice of a given configuration will depend on the amount of water to be treated, the knowledge base of the general population of a given region where the configuration is to be applied, performance and costs of

Table 11. Summary of two-parameter model data

Bed height (cm)	Model parameters	
	σ (−)	t_0 (min)
2	0.315	525
3	0.293	890
4	0.250	1167
Initial concentration (mg/L)		
5	0.300	1505
10	0.293	890
20	0.230	473

adsorption media and of developing a given defluoridation unit. Established and potential defluoridation configurations and their modes of operation are described below.

3.3.1. ‘‘Tea bag’’ POU system

Fluoride-related health hazards are associated with the use of fluoride-contaminated water for drinking and cooking. This corresponds only to 2–4 L per capita per day. Fluoride removal in rural areas in LDCs, where centralized water treatment and distribution facilities are unavailable, should consequently be carried out at a household level and the system applied should be simple and affordable. In this regard, ‘‘tea bag’’ POU system becomes handy. Although this kind of system has not been specifically reported for water defluoridation, it has been tested for arsenic [37,107]. It is therefore a short-term potential technique worth considering. In this technique, adsorption medium is placed in a tea bag-like packet, which is subsequently placed in a bucket of water to be treated. To ensure faster defluoridation kinetics, the bag should be swirled inside the water. It therefore operates like a batch reactor and hence requires a relatively longer adsorption time to achieve the permissible levels. Since the swirling motion is supposed to be human-powered, the technique would require a material with very fast kinetics or very fine adsorption media.

3.3.2. ‘‘Coffee filter’’ POU system

This is also a simple and potential adsorbent-based technique that is worth considering as a short-term solution to fluorosis pandemic. Laboratory trials for the removal of arsenic from water have been reported [107]. Principally, the operation of this kind of defluoridation unit is similar to that of a coffee filter.

Accordingly, water to be treated is passed through adsorption media contained in a filter paper. In doing so, the adsorption media retains fluoride ions, while clean water passes through the filter. Thus, because of the dynamic nature of this process, the adsorption time is relatively shorter than that of the ''tea bag'' POU system. This kind of system may be handy when only a small amount of water for drinking and cooking is needed. One disadvantage of such a system is that the quality of treated water cannot be guaranteed since its performance depends on the ingenuity of the user.

3.3.3. Household defluoridation POU unit

The use of household defluoridation POU units has increased in recent times in several developing countries such as Kenya, Tanzania and India. As the name suggests, the units are mostly small and can only treat a small amount of water to serve a household. These units operate under the same principle as fixed beds; water to be defluoridated is passed in an upward or downward flow through a small column or bucket containing adsorption media. The designs, however, vary from region to region. The mostly reported adsorption media for this kind of defluoridator are AA and bone char. In India, for example, a Mytry defluoridation filter, which is a two-bucket system with the upper bucket containing AA has been developed and implemented. Murcott [47] reported that since 2004, the MDFFT had sold 9000 units and produces 50 units daily.

In the same country, UNICEF launched an AA household defluoridator unit shown in Fig. 12 [108]. The unit basically consists of two chambers, upper bucket containing adsorption media and lower chamber where the treated water is collected. The upper chamber is fitted with a simple flow control device (removable circular ring) at the bottom. The average flow is 10 L/h. The main component of this unit is a PVC casket containing 3 Kg of AA giving a bed depth of 17 cm. A perforated plate of either stainless steel or tin metal is placed on the top of AA bed to facilitate uniform distribution of raw water. The lower chamber of the defluoridator is fitted with a tap to draw the treated water. Since adsorption media efficiency reduces during operation, regeneration is required for economic and environmental impacts reasons. Thus, exhausted AA can be regenerated by dip-regeneration method. In this method, the casket containing exhausted AA is placed in a plastic bucket containing 8 L of 1% NaOH for 4 h. The casket is then transferred to a bucket containing water and is rinsed by occasional lifting. Thereafter, the casket is placed in a plastic bucket containing 8 L of 0.20% H_2SO_4 for 4 h. Other reports indicate that AA can be regenerated by aluminum sulfate solution [31]. Once regeneration is done, the AA is washed till the pH rises above 7.0 and is then ready for the next defluoridation cycle.

Aluminum oxide present in soil has been utilized to make brick pieces of 15–20 mm sizes that are effective in drinking water defluoridation. When the

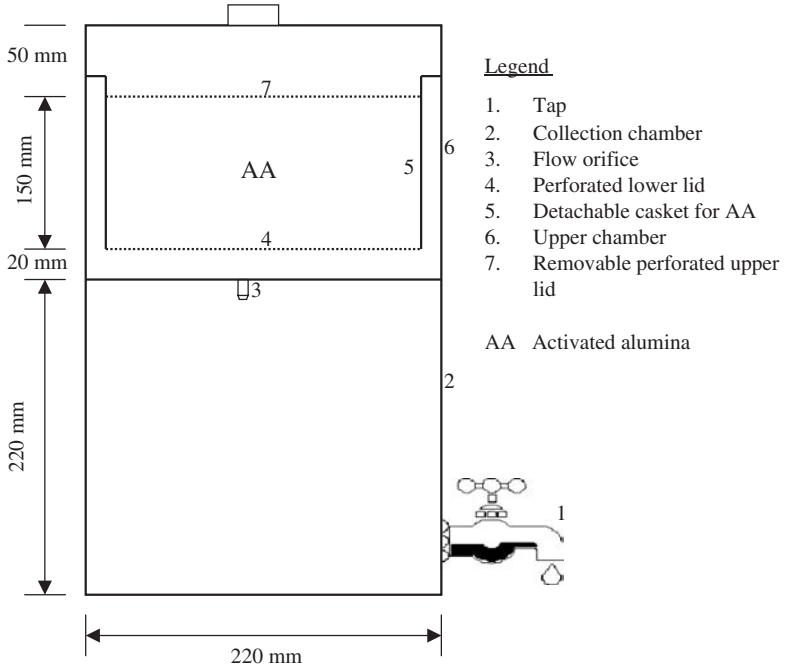

Fig. 12. Household-level AA filter [108].

bricks are burnt in a kiln, they become activated. A defluoridation unit using brick pieces has been developed. The unit consists of two PVC concentric pipes, the inner being 20 mm diameter serves as the raw water inlet, while the outer one has a diameter of 225 mm. The bricks are packed in the space between the inner and outer pipes and raw water is allowed to come in contact with the bricks from the bottom of the unit through a perforated plate. This unit is estimated to treat 16 L of water for drinking and cooking. Currently, the unit retails at an equivalent of USD 14 and can operate for 3 months before replacement of the media.

Moges *et al*. [56] and Agarwal *et al*. [109] have reported that ground-fired clay pot could effectively defluoridate drinking water. However, the process is extremely slow. The use of mud pots dates back to ancient times. When mud pots are fired, they become activated and have affinity for fluoride ions. The ability to remove the fluoride ions, however, depends on the alumina content of the soils used for molding the pots. These kinds of pots are cost effective and their use do not require any know-how. They are estimated to retail at USD 0.33/pot.

In Tanzania where fluorosis is also endemic, a household bone char filter column defluoridator has been developed [4]. This unit is slightly differently configured from those described above. It has two separate detached sections. The upper section holds water to be treated, while the lower section is column-like and contains the adsorption media. Water from the upper section is passed by gravity

to the bottom of the column and by upward flow the water is contacted with the adsorption media. Treated water is directly withdrawn from the top of the column.

The disadvantage of household water treatment systems relative to those of centralized water treatment systems is that it is difficult to monitor the performance of the units since they would be scattered in rural settings that are not easily accessible.

3.3.4. Cartridge POU system

Cartridge POU systems are common in regions with tap water. They are relatively expensive and are not common in developing countries. The cartridges are usually installed under the sink to treat water for cooking and drinking. The Environmental and Research Technology – India has however developed over and under the counter kitchen units that do not require any electricity to operate and can be easily moved from one place to another. The adsorption media used is AA packed in a 3″ × 9 3/4″ cartridge for optimum use. This cartridge can last for 6 months when used to treat water containing 10 ppm fluoride and 12 months when the fluoride content is 5 ppm, calculated on a daily consumption of 20 L of water per family. Recently also, an attempt has been made by Mavura *et al*. [110] to construct a cartridge to be used for the defluoridation of drinking water. This cartridge packed with bone char material can be fixed onto a domestic faucet as a flow-through defluoridation unit. The construction material was PVC of various sizes made from a 3/4″ pipe. The efficiency of fluoride removal was determined for the following parameters: cartridge length, flow rate of water, compactness of bone char material and particle size with the aim of determining the optimum conditions for a good cartridge.

3.3.5. Household POE systems

When a water system serves a few dozen homes or less, POE water treatment systems may provide a low-cost alternative to centralized water treatment. In POE systems, rather than treating all water at a central facility, treatment units are installed at the entry point to individual households or buildings. POE systems can save the cost of installing expensive new equipment in a central water treatment facility. Moreover, POE systems can also save the considerable costs of installing and maintaining water distribution mains when they are used in communities where homeowners have individual wells. Lahlou [111], however, reports that AA-based POE system may be relatively expensive in terms of initial operating and maintenance costs compared with other POE systems. Regulators often have significant objections to using POE devices. Concerns include the difficulty and cost of overseeing system operation and maintenance when

treatment is not centralized, and liability associated with entering customers' homes. These objections have merit, particularly as system size increases and the complexity of monitoring and servicing the devices increases. Using centralized water treatment should be the preferred option, and POE or POU treatment should be considered only if centralized treatment is not possible. In general, POE systems for drinking water defluoridation suit mainly developed countries or those countries in economic transition.

3.3.6. Community-based tube-well-attached defluoridator

Tube-well-attached defluoridator is increasingly becoming popular among the rural population in several LDCs and thus is a community-based water treatment solution. This kind of unit (Fig. 13) is used to treat water serving several households or institutions like schools. In India, a fluoride treatment plant using AA housed in a column operated in a down-flow mode is reported. The water from the tube-well hand pump enters the unit at the bottom and flows upward through the AA media onto which fluoride is adsorbed. Up-flow mode has also been reported by Daw [112]. The adsorption media requires regular monitoring, so that once the breakthrough point is exceeded, regeneration is effected. The frequency of regeneration depends on the raw water fluoride concentration and flow rate.

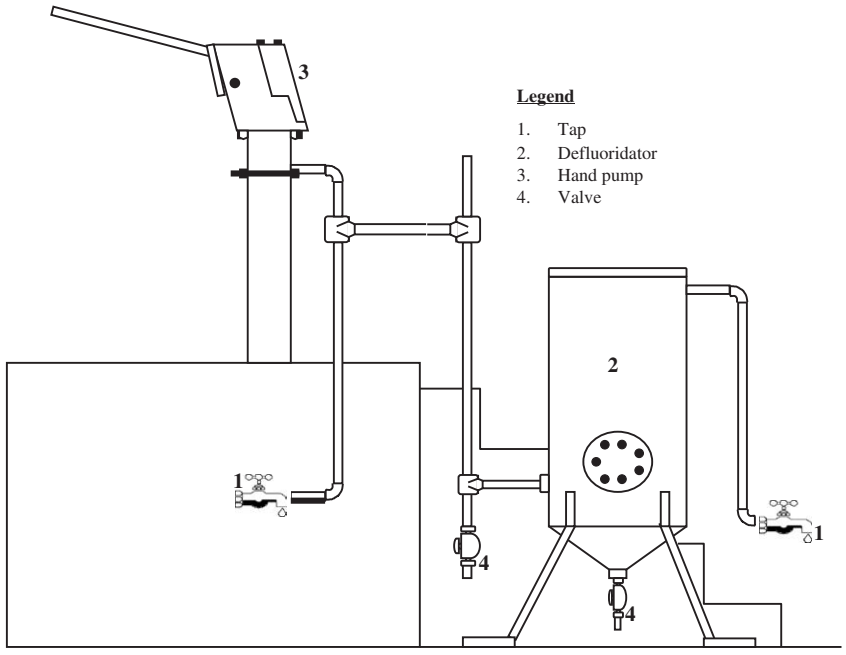

Fig. 13. Hand pump-attached defluoridation unit [112].

After exhaustion, the AA media is regenerated and restored with sulfuric acid and caustic soda. The process of regeneration and restoration requires skilled personnel, for which village-level volunteers can be trained.

3.3.7. Centralized water treatment

Fluoride can also be removed from a centralized water treatment point. This is common in developed or countries in economic transition and provides a long-term solution to fluoride problem in drinking water. A full-scale water purification plant based on AA-adsorption media was reported to be in operation in Kansas, USA. In this technique, all water to the distribution system is treated irrespective of its intended use. Thus, it is unrealistic way of defluoridating water since the main concern is usually fluoride ions contained in drinking water. From the technical point of view, however, centralized water treatment guarantees the quality of drinking water since the performance of the defluoridation plant can easily be monitored. Wider application of this technique for the sole purpose of removing fluoride from water is not widely reported in literature.

3.4. Implementation of defluoridation units: challenges and prospects

In most third world countries as opposed to the developed nations, most people live in the rural areas where water is scarce, the available sources are scattered, the areas are inaccessible and the locals are ill educated. Moreover, it is estimated that several hundreds of millions of people rely on unsafe drinking water containing contaminants such as fluoride. The contaminants are known to cause chronic poisoning. Efforts should thus be made to enlighten the rural population about the dangers of consuming fluoride-containing water. Also, effective technologies for community and household water treatment and storage, in combination with improved hygiene should be instituted [113]. Water technologies aim to make water clean, available, sustainable and economical. Several community and household configurations based on adsorption technique have been designed (Section 3.3) that can suit different geographical regions. Unfortunately, only three adsorbents are currently well recognized by WHO. These are AA, bone char and clay-based adsorbent. AA is relatively expensive and has low capacity for fluoride, while bone char has limited acceptance in certain regions due to religious reasons. Fortunately, indications are that some economies are growing up rapidly and several other good performing adsorbents (Section 3.1) are now available in abundant quantities and some at reduced cost since they are derived from waste materials. However, as indicated in the previous sections, not so much is known about their performance in the field since they have only been

tested under laboratory conditions. More work is thus required to ascertain their performances.

Experience has shown that community water treatment systems hardly pass the test of time. This is partly due to a lack of sense of ownership by the user communities, resulting in indifferent attitude toward the operation and maintenance of these plants [112]. Defluoridation plants are no exception. To succeed, a holistic participatory approach should be adopted in dealing with defluoridation plants/units. The local government, private sector, community-based organizations (CBOs) and the local water users should form a concerted effort in mitigating the fluoride problem and implementing treatment technologies. In this regard, the local government should devise a cost-sharing method in which, say, they provide maintenance personnel but impose some tariffs to water users. Additionally, public–private partnership should be encouraged. Women being the main users of fluoride treatment technologies in rural areas should not be isolated but should participate fully. Indian experience in arsenic treatment technologies has shown that technical solution alone will rarely lead to a sustainable solution [47]. Thus, local knowledge and ingenuity should be inputted into implementation phase to reach higher success rates because they address the problems or issues specific to the community.

4. CONCLUSIONS

This paper provided an overview of the defluoridation techniques with accompanying decision framework for helping utilities determine the most appropriate technique. We biased our discussions towards applications of these techniques to LDCs where fluoride occurrence and distribution is a major issue. Consequently, adsorption technique was vouched for its low cost in general, versatility and environmental benignity, and formed the main focus of our discussion. The emphasis was placed on established and potential adsorption media that are in use or those reported in literature over the last two decades. An attempt was made to critically evaluate the performances of selected adsorption media, interms of batch capacity, batch kinetics and column adsorption characteritics, where applicable. It was shown that several adsorption media are attractive for water defluoridation. However, there was paucity of information regarding field application of most adsorption media, the quality of treated water, the stability of the adsorption media and the long term availability. Moreover, the use of adsorption as a drinking water treatment technique faces major challenges such as dependeces of perfomance on solution pH, fast breakthrough by established adsorption media and accumulation of bacteria in the media. An emerging novel adsorbent, surface tailored zeolite, was discussed in more details using recent laboratory data.

The use of adsorbent based POU or POE system was described as an attractive defluoridation configuration that should be given more impetus in LDCs. Though a lot of challenges exist to implementation of defluoridators, it was suggested that a holistic participatory approach by all stakeholders be adopted in fluorotic areas in remedying fluoride contaminated drinking water.

APPENDIX: LIST OF ACRONYMS

POE	point-of-entry
POU	point-of-use
LDC	less developed countries
NEERI	National Environmental Engineering Research Institute
RO	reverse osmosis
NF	nanofiltration
UF	ultrafiltration
ED	electrodialysis
USEPA	United States Environmental Protection Agency
BDAT	best demonstrated available technology
IE	ion exchange
EF	electroflotation
AA	activated alumina
BBC	black bone char
ACNT	aligned carbon nanotubes
MCL	maximum contaminant level
TRB	titanium-rich bauxite
SBE	spent bleaching earth
LDH	layered double hydroxides
EBCT	empty bed contact time
BDST	bed depth service time
MDFFT	Mytry De-Fluoridation Filter Technologies

REFERENCES

[1] Earth Summit, Comprehensive Assessment of the Freshwater Resources of the World. Agenda 21, Chapter 18, paragraphs 18.6 and 18.8, as endorsed at the United Nations Conference on Environment and Development, Rio de Janeiro, June 1992.
[2] United Nations (UN), Comprehensive Assessment of the Freshwater Resources of the World, 1999, http://geocompendium.grid.unep.ch/reference_scheme/final_version/GEO/Geo-2-121.htm (Accessed October 2005).
[3] Unesco, Trace Elements in Water and Public Health, http://www.iah.org/briefings/Trace/trace.htm (Accessed October 2004).
[4] H. Mjengera, G. Mkongo, Phys. Chem. Earth 26 (2003) 1097.
[5] H. Chen, M.M. Frey, D. Clifford, S.L. McNeill, M. Edwards, J. AWWA 91 (1999) 74.
[6] K.K.H. Choy, J.F. Porter, G. McKay, Chem. Eng. Sci. 59 (2004) 501.
[7] C. Zevenbergen, L.P. van Reeuwijk, G. Frapporti, R.J. Louws, R.D. Schuiling, Sci. Total Env. 188 (1996) 225.

[8] M. Srimurali, A. Pragati, J. Karthikeyan, Environ. Poll. 99 (1998) 285.
[9] M.G. Sujana, R.S. Thakur, S.B. Rao, J. Colloid Interface Sci. 206 (1998) 94.
[10] H. Weerasooriya, H.U.S. Wickramarathne, H.A. Dharmagunawardhane, Colloid Surf. A: Physicochem. Eng. Aspects 144 (1998) 267.
[11] R.L. Ramos, J. Ovalle-Turrubiartes, M.A. Sanchez-Castillo, Carbon 37 (1999) 609.
[12] A.M. Raichur, M.J. Basu, Sep. Purif. Technol. 24 (2001) 121.
[13] Y. Cengeloglu, E. Kir, M. Ersoz, Sep. Purif. Technol. 28 (2002) 81.
[14] M. Mahramanlioglu, I. Kizilcikli, I.O. Bicer, J. Fluorine Chem. 115 (2002) 41.
[15] L. Ruixia, G. Jinlong, T. Hongxiao, J. Colloid Interface Sci. 248 (2002) 268.
[16] X. Fan, D.J. Parker, M.D. Smith, Water Res. 37 (2003) 4929.
[17] Y.-H. Li, S. Wang, X. Zhang, J. Wei, C. Xu, Z. Luan, D. Wu, Mater. Res. Bull. 38 (2003) 469.
[18] D.P. Das, J. Das, K. Parida, J. Colloid Interface Sci. 261 (2003) 213.
[19] I. Abe, S. Iwasaki, T. Tokimoto, N. Kawasaki, T. Nakamura, S. Tanada, J. Colloid Interface Sci. 275 (2004) 35.
[20] S. Annouar, M. Mountadar, A. Soufiane, A. Elmidaoui, M.A.M. Sahli, Desalination 165 (2004) 437.
[21] Y. Zhou, C. Yu, Y. Shan, Sep. Purif. Technol. 36 (2004) 89.
[22] S. Ghorai, K.K. Pant, Sep. Purif. Technol. 42 (2005) 265.
[23] E. Oguz, J. Hazard. Mater. 117 (2005) 227.
[24] A. Mekonen, P. Kumar, A. Kumar, Water Res. 35 (2001) 3127.
[25] F. Shen, X. Chen, P. Gao, G. Chen, Chem. Eng. Sci. 58 (2003) 987.
[26] M. Pontié, C.K. Diawara, M. Rumeau, Desalination 151 (2003) 267.
[27] M. Pontie, H. Buisson, C.K. Diawara, H. Essis-Tome, Desalination 157 (2003) 127.
[28] C.K. Diawara, S.M. Lô, M. Rumeau, M. Pontie, O. Sarr, J. Membr. Sci. 219 (2003) 103.
[29] M. Arora, R.C. Maheshwari, S.K. Jain, A. Gupta, Desalination 170 (2004) 105.
[30] A. Lhassani, M. Rumeau, D. Benjelloun, M. Pontie, Water Res. 35 (2001) 3260.
[31] Anonymous, Arsenic in Drinking Water: Treatment Technology: Removal, 1993, http://www.dainchi-consul.co.jp/ENGLISH/arsenic/treat1.html (Accessed March 2001).
[32] L.S. Cheng, Water Supply 3 (1985) 177.
[33] N. Mameri, A.R. Yeddou, H. Lounici, D. Belhocine, H. Grib, B. Bariou, Water Res. 32 (1998) 1604.
[34] F. Pouet, F. Persin, M. Rumeau, Water Res. 25 (1992) 247.
[35] S.D. Faust, O.M. Aly, Chemistry of Water Treatment, Ann Arbor Science, Ann Arbor, 1983, p. 723.
[36] Anonymous, Fluoride Removal by Activated Alumina, Available at http://www.tramfloc.com/tf78.html (Accessed October 2005).
[37] S. Murcott, Appropriate remediation technologies for arsenic-contaminated wells in Bangladesh, in Proc. Int. Conf. Arsenic in Ground Water in Bangladesh: Sources and Remedies, Wagner College, Staten Island, New York, February 27–28, 1999.
[38] D.C.K. Ko, J.K. Porter, G. McKay, Ind. Eng. Chem. Res. 38 (1999) 4868.
[39] S. Ghorai, K.K. Pant, Chem. Eng. J. 98 (2004) 165.
[40] H. Lounici, D. Belhocine, H. Grib, M. Drouiche, A. Pauss, N. Mameri, Desalination 161 (2004) 287.
[41] H. Lounici, L. Adour, D. Belhocine, A. Elmidaoui, B. Bariou, N. Mameri, Chem. Eng. J. 81 (2001) 153.
[42] C.-F. Chang, P.-H. Lin, W. Höll, Colloids and Surfaces A: Physicochemical and Engineering Aspects 280 (2006) 194.
[43] E.A. Savinelli, A.P. Black, J. AWWA 50 (1958) 33.
[44] Y. Ku, H.M. Chiuo, Water, Air, Soil Pollut. 133 (1–4) (2002) 349.
[45] P.P. Coetzee, L.L. Coetzee, R. Puka, S. Mubenga, Water SA 29 (2003) 33.
[46] S.A. Wasay, S. Tokunaga, S.W. Park, Sep. Sci. Technol. 31 (1996) 1501.
[47] S. Murcott, Arsenic and Fluoride Removal-New Household Approaches for Addressing Chemical Contamination, WHO International Network to Promote

Household Water Treatment and Safe Storage, B. Gordon (Ed.), Issue 2, May 2005, P. 8.
[48] Rao, C.R. Nagendra, Fluoride and environment-a review, in M.J. Bunch, V. Madha Suresh, T. Vasantha Kumaran (Eds.), Proc. Third Int. Conf. Environ. Health, Chennai, India, 15–17 December, 2003, Chennai: Department of geography, University of Madras and Faculty of Environmental Studies, York University, p. 386–389.
[49] US Environmental Protection Agency (USEPA), Technologies and costs for the removal of fluoride from potable water supplies, Science and Technology Branch Criteria and Standards Division, Office of Drinking water, Washington, DC, 1985, 29–32.
[50] P. Phanfumvanit, R.Z. Legeros, Fluoride 30 (1997) 207.
[51] D.L. Mwaniki, J. Dent. Res. 71 (1992) 1310.
[52] A. Menda, Tanzania: challenges and successes of water defluoridation, Available at http://www.scienceinafrica.co.za/2004/july/fluoride, (Accessed in September 2005).
[53] M.W. Abdel-Raouf, A.A. Daifullah, Adsorpt. Sci. Technol. 15 (1997) 539.
[54] Y.-H. Li, S. Wang, A. Cao, D. Zhao, X. Zhang, C. Xu, Z. Luan, D. Ruan, J. Liang, D. Wu, B. Wei, Chem. Phys. Lett. 350 (2001) 4.
[55] S. Iijima, Nature 354 (1991) 56.
[56] G. Moges, F. Zewge, M. Socher, J. Afr. Earth Sci. 22 (1996) 479.
[57] Y. Wang, E.J. Reardon, Appl. Geochem. 16 (2001) 531.
[58] H. Sugita, T. Komai, S. Okita, S. Tokunaga, I. Matsunaga, J. Mining Miner. Process. Inst. Jpn. 121 (2005) 416.
[59] N. Das, P. Pattanaik, R. Das, Colloid Interface Sci. 292 (2005) 1.
[60] E.J. Reardon, Y. Wang, Environ. Sci. Technol. 24 (2000) 3247.
[61] F. Rubel Jr., The removal of excess fluoride from drinking water by the activated alumina method, in: J.L. Shupe, H.B. Peterson, N.C. Leone (Eds.), Fluoride Effects on Vegetation, Animals and Humans, Paragon Press, Salt Lake city, 1983, pp. 345–349.
[62] A. Sivasamy, K.P. Singh, D. Mohan, M. Maruthamuthu, J. Chem. Technol. Biotechnol. 76 (2001) 717.
[63] P.M.H. Kau, D.W. Smith, P. Binning, Geoderma 84 (1998) 89.
[64] Y. Cengeloglu, E. Kir, M. Ersoz, Water Res. 37 (2003) 4929.
[65] D. Mohapatra, D. Mishra, S.P. Mishra, G.R. Choudhury, R.P. Das, J. Colloid Interface Sci. 275 (2004) 355.
[66] L. Ngee, T. Ishihara, S. Ueshima, H. Nishiguchi, Y. Takita, J. Colloid Interface Sci. 272 (2004) 299.
[67] X.P. Liao, B. Shi, Environ. Sci. Technol. 39 (2005) 4628.
[68] M. Chikuma, M. Nishimura, React. Polym. 13 (1990) 131.
[69] K.M. Popat, P.S. Anand, B.D. Dasare, React. Polym. 23 (1994) 23.
[70] L. Fang, K.N. Ghimire, M. Kuriyama, K. Inoue, K. Makino, J. Chem. Technol. Biotechnol. 78 (2003) 1038.
[71] M.A. Ulibarri, I. Pavlovic, M.C. Hermosín, J. Cornejo, Appl. Clay Sci. 10 (1995) 131.
[72] Y. You, G.F. Vance, H. Zhao, Appl. Clay Sci. 20 (2001) 13.
[73] E.L. Crepaldi, J. Tronto, L.P. Cardoso, J.B. Valim, Colloid Surf. A: Physicochem. Eng. Aspects 211 (2002) 103.
[74] T. Toraishi, S. Nagasaki, S. Tanaka, Appl. Clay Sci. 22 (2002) 17.
[75] J. Orthman, H.Y. Zhu, G.Q. Lu, Sep. Purif. Technol. 31 (2003) 53.
[76] N.N. Das, J. Konar, M.K. Mohanta, S.C. Srivastava, J. Colloid Interface Sci. 270 (2004) 1.
[77] R. Chitrakar, S. Tezuka, A. Sonoda, K. Sakane, K. Ooi, T. Hirotsu, J. Colloid Interface Sci. 290 (2005) 45.
[78] O.P. Ferreira, S. Gomes de Moraes, N. Durán, L. Cornejo, O.L. Alves, Chemosphere 62 (2006) 80.
[79] K. Kuzawa, Y.-J. Jung, Y. Kiso, T. Yamada, M. Nagai, T.-G. Lee, Chemosphere 62 (2006) 45.
[80] M.-X. Zhu, Y.-P. Li, M. Xie, H.-Z. Xin, J. Hazard. Mater. 120 (2005) 163.

[81] K.C. Song, H.K. Lee, H. Moon, K.J. Lee, Sep. Purif. Technol. 12 (1997) 215.
[82] A. García-Sánchez, A. Alastuey, X. Querol, Sci. Total Environ. 242 (1999) 179.
[83] C. Färm, Sci. Total Environ. 298 (2002) 17.
[84] M.K. Doula, A. Ioannou, A. Microporous Mesoporous Mater. 58 (2003) 115.
[85] M. Majdan, S. Pikus, M. Kowalska-Ternes, A. Gladysz-Plaska, P. Staszczuk, L. Fuks, H. Skrzypek, J. Colloid Interface Sci. 262 (2003) 321.
[86] A. Daković, M. Tomašević-Čanović, V. Dondur, G.E. Rottinghaus, V. Medaković, S. Zarić, Colloid Surf. B: Biointerfaces 46 (2005) 20.
[87] S.M. Dal Bosco, R.S. Jimenez, W.A. Carvalho, J. Colloid Interface Sci. 281 (2005) 424.
[88] M. Turan, U. Mart, B. Yüksel, M.S. Çelik, Chemosphere 60 (2005) 1487.
[89] U. Wingenfelder, B. Nowack, G. Furrer, R. Schulin, Water Res. 39 (2005) 3287.
[90] M.P. Elizalde-González, J. Mattusch, R. Wennrich, P. Morgenstern, Microporous Mesoporous Mater. 46 (2001) 277.
[91] M.P. Elizalde-González, J. Mattusch, W.-D. Einicke, R. Wennrich, Chem. Eng. J. 81 (2001) 187.
[92] Y.-H. Xu, Tsunenori Nakajima, A. Ohki, J. Hazard. Mater. 92 (2002) 275.
[93] M.S. Onyango, H. Matsuda, T. Ogada, J. Chem. Eng. Jpn. 36 (2003) 477.
[94] M.S. Onyango, Y. Kojima, H. Matsuda, A. Ochieng, J. Chem. Eng. Jpn. 36 (2003) 1516.
[95] S. Shevade, R.G. Ford, Water Res. 38 (2004) 3197.
[96] Y.-H. Xu, A. Ohki, S. Maeda, Toxicol. Environ. Chem. 76 (2000) 111.
[97] Y.-M. Xu, A.-R. Ning, J. Zhao, J. Colloid Interface Sci. 235 (2001) 66.
[98] M.S. Onyango, Y. Kojima, O. Aoyi, E.C. Bernardo, H. Matsuda, J. Colloid Interface Sci. 279 (2004) 341.
[99] M.S. Onyango, Y. Kojima, D. Kuchar, S.O. Osembo, H. Matsuda, J. Chem. Eng. Jpn. 38 (2005) 701.
[100] M.S. Onyango, Y. Kojima, D. Kuchar, M. Kubota, H. Matsuda, Sep. Sci. Technol. 41 (2006) 683.
[101] G. McKay, Chem. Eng. J. 27 (1983) 187.
[102] J. Crank, The Mathematics of Diffusion, Clarendon Press, Oxford, U.K., 1975.
[103] G. McKay, B. Al-Duri, J. Chem. Tech. Biotechnol. 48 (1990) 269.
[104] Z. Ma, R.D. Whitley, N.-H.L. Wang, AICHE J. 42 (1996) 1245.
[105] G.S. Bohart, E.Q. Adams, J. Chem. Soc. 42 (1920) 523.
[106] K.H. Chu, Chem. Eng. J. 97 (2004) 233.
[107] B. Petrusevski, J. Boere, S.M. Shahidullah, S.K. Sharma, J.C. Schippers, Water SRT – Aqua 51 (2002) 135.
[108] P. Mariappan, T. Vasudenvan, (2005) Domestic defluoridation techniques and sector approach for fluoris mitigation, http://www.twadboard.com/photos/nletjune02_01.pdf (Accessed October 2005).
[109] M. Agarwal, K. Rai, R. Shrivastav, S. Dass, J. Cleaner Prod. 11 (2003) 439.
[110] W.J. Mavura, F.T. Mwanyika, G. Wrensford, B. Chem. Soc. Ethiopia 18 (2004) 1.
[111] Z.M. Lahlou, Point of use/point of entry systems, A National Drinking Water ClearingHouse Fact Sheet, Available at http://www.nesc.wvu.edu/ndwc/pdf/OT/TB/TB_Sp03_point.pdf (Accessed October 2005).
[112] R.K. Daw, People-centred approaches to water and environmental sanitation: Experiences with domestic defluoridation in India, Paper presented at the 30th WEDC International Conference, Vientiane, Lao PDR, 2004.
[113] IRC Report, Household water treatment, IRC International Water and Sanitation Centre, The Netherlands, http://www.irc.nl/page/8028 (Accessed October 2005).

Note from the Editor

See also in this series the chapter by M. Pontié *et al*. on nanofiltration processes.

CHAPTER 2

Water Defluoridation Processes: A Review. Application: Nanofiltration (NF) for Future Large-Scale Pilot Plants

M. Pontié,[1,*] C. Diawara,[2] A. Lhassani,[3] H. Dach,[1,3] M. Rumeau,[4] H. Buisson,[5] and J.C. Schrotter[5]

[1]*Group analysis and processes (GAP), University of Angers, 2, Bd. Lavoisier, 49045 Angers cedex 01, France*
[2]*Chemistry Dept., University Cheikh Anta Diop, LaChimia, Dakar Fann, Senegal*
[3]*Faculty of Science and Technology, Laboratory of Applied Chemistry, P.O. Box 2202, Fez, Morocco*
[4]*24 Quai du commandant Méric, 34300 Le Grau d'Agde, France*
[5]*Veolia Water, Anjou Recherche, Chemin de la Digue, BP 76, 78603 Maisons-Laffitte, France*

Contents

*Corresponding author. Tel.: +33-2-41-73-52-07; Fax.: +33-2-41-73-53-52;
E-mail: maxime.pontie@univ-angers.fr

FLUORINE AND THE ENVIRONMENT, VOLUME 2
ISSN 1872-0358 DOI: 10.1016/S1872-0358(06)02002-1

Abstract

Defluoridation of waters using clays as substrates has become popular in many countries to solve problems related to high fluoride concentrations in drinking water in rural areas. But this treatment is limited to low fresh water production. In this work, F^- elimination using a nanofiltration (NF) operation will solve problems for-large-scale pilot plants in the future. Results obtained in these fields help-users to facilitate the selection between reverse osmosis (RO) and NF membranes of the most cost-effective membrane for desalination of high fluorinated water. Two sorts of characterization have been developed: (i) physico-chemicals, in terms of hydrophobicity/hydrophilicity, morphology and topography aspects and (ii) mass transfer in terms of pure water and saline solution permeabilities, charged solute rejections and molecular weight cut-off (MWCO). A model inspired by the phenomenological approach proposed by Kedem and Katchalsky (KK) will help to quantify both parts of the mass transfer occurring in NF and RO, i.e. the pure convection and the pure diffusion, separately. This new and original approach will be applied to three membranes, 2 NF and 1 LPRO (low-polarization reverse osmosis), respectively. The study will be limited to low concentration polarization by using diluted solutions (10^{-3}–10^{-1} M) and high tangential flow rate (4 m s^{-1}) under low conversion ratio (5%), operational conditions. Different tools such as contact angle measurements, topography and roughness measurements using atomic force microscopy (AFM), hydraulic permeability and salt solution permeability, will be used to characterize the three membranes. This analytical approach will be coupled with the Spiegler, Kedem and Katchalsky (SKK) phenomenological mass transfer model in order to determine the mass transfer parameters σ and P_s for synthetic chloride and sulphate solutions.

This novel integer approach makes it possible to determine today an NF most efficient membrane for the elimination of excess F^- in a Senegalese water sample taken from the endemic region of Fatick. This membrane denoted NF90 works very well due to its diffusional behaviour for fluoride rejection, its high hydraulic permeability and sufficient observed rejection for F^- in comparison to RO.

1. INTRODUCTION

Fluorosis caused by high fluoride (F^-) intake predominantly through drinking water containing F^- concentrations higher than $1\,mg\,L^{-1}$, is a chronic disease manifested by mottling of teeth in mild cases (dental fluorosis) and changes in bone structure (skeletal fluorosis), ossification of tendons and ligaments, and neurological damage in more severe cases [1–3].

Today an increasing concern is being expressed that these adverse effects of fluorosis are irreversible, in particular for African, Indian and Chinese populations living in rural areas in which drinking water is supplied from wells and boreholes with high F^- concentrations. The development of a long-term solution to the defluoridation of F^- contaminated groundwaters is thus of critical importance. This would require appropriate water treatment procedures. Appropriate technology must be technically simple, cost effective, easily transferable, using local resources and accessible to the rural community.

The removal of fluoride from water using defluoridation techniques is a common practice worldwide, both domestically and industrially. Current methods of fluoride removal from water include adsorption onto activated alumina, bone char and clay,[1] precipitation with lime, dolomite and aluminium sulphate, the Nalgonda technique [4], ion exchange [5] and membrane processes such as reverse osmosis (RO), electrodialysis and very recently NF [6–9].

This chapter is organized into two parts: (i) the first part is dedicated to a review on the defluoridation processes of drinking waters (see Table 1) and (ii) the second part is based on the presentation of original results concerning a comparison study of NF and RO for a selective defluoridation of a highly fluorinated brackish water from the endemic region of Fatick (Senegal).

2. BACKGROUND

2.1. The origin and distribution of fluoride in groundwaters

High F^- concentrations in groundwater are found in many countries around the world, notably in Africa, Asia and USA [21,22]. The most severe problems associated with high F^- waters occur in China [23], India [24] and the Rift Valley countries in Africa [25]. Groundwaters with high fluoride contents have been studied in detail in Africa, in particular, Kenya and Tanzania [12,26–28]. The abundance of F^- in Rift Valley groundwaters is due to the weathering of alkaline volcanic rocks rich in F^-. Typical fluoride concentrations of towns in the Rift Valley are between 1 and $33\,mg\,L^{-1}$. High fluoride groundwater is also found in

[1] Note of the Editor: See also in this series the chapter by M. Onyango and H. Matsuda *et al.* on adsorption processes.

Table 1. Materials and methods of defluoridation

Process	Reference
Coprecipitation (Nalgonda technique) aluminium salts	Dahi [10]
Precipitation calcium and phosphate compounds	Larsen [11]
Adsorption/ion exchange	Moges [12] and Veressinina [13]
Activated alumina	Hao [14] and Schoeman [15,16]
Fly ash	Chaturvedi [17]
Clays	Srimurali [64]
Soils	Omueti and Jones [18]
Sulphonated carbonaceous materials	Mohan Rao [5]
Membrane processes	
RO	
	Elmidaoui [19]
Electrodialysis	Pontié [6,7,20]
	Lhassani [8]
NF	Diawara [9]

the East Upper Region of Ghana [29]. The concentration of fluoride was found to be between 0.11 and 4.60 mg L^{-1}. The hydrogeology and hydrochemistry of ground waters in Senegal have been thoroughly studied by Y. Travi [30]. In France, two major basins are concerned, the Aquitan Basin and Parisian Basin with F^- concentrations between 0.6 and 4.2 mg L^{-1}.

2.2. Fluorosis

Fluoride has certain physiological properties [31,32] of great importance to human health. The role of fluoride in the process of mineralization of certain tissues is important. At low concentrations fluoride stabilizes the skeletal system by increasing the size of apatite crystals and reducing their solubility [12]. Although beneficial effects can be demonstrated at low concentrations, it has detrimental effects when concentrations exceed the threshold [33].

The relationship between fluoride and dental caries was first noted in the early part of the 20th century when it was observed that residents of certain areas of USA developed brown stains on their teeth. In the 1930s, it was observed that the prevalence and severity of this type of mottled enamel was directly related to high amounts of ingested fluoride [34].

Endemic fluorosis is known to be global in scope, occurring in all continents and affecting many millions of people. Cases of skeletal fluorosis have been

reported all over the world [35]. According to a report from UNICEF [36], fluorosis is endemic in at least 25 countries across the globe. The fluorosis problem is most severe in the most populous countries in the world, China and India [37–39]. For example, in China some 38 million people are reported to suffer from dental fluorosis and 1.7 million from the more severe skeletal fluorosis. In India fluorosis is endemic in 15 states, with over six million people seriously afflicted [40].

The drinking water standards for fluoride ion stipulated by WHO authorities are between 0.8 and 1.5 mg L^{-1}, the average suggested in USA by US Public Health is 0.7–1.2 mg L^{-1} and 0.7–1.5 mg L^{-1} in UE.

2.3. Symptoms of fluorosis

Fluoroapatite is a less soluble order of magnitude than hydroxyapatite, the principal mineral constituent of bone. The F^- ion substitutes for the OH^- ion, leading to a buildup of F^- in bone tissue which may eventually lead to skeletal fluorosis. Early in the development of fluorotic changes in the skeleton, the patient often complains of a vague discomfort in the limbs and the trunk. Pain and stiffness in the back appear next, especially in the lumbar region. In severe fluorosis, in addition to joint problems, some victims can experience deformation of their bones (Fig. 1). The stage at which skeletal fluorosis becomes crippling usually occurs between 30 and 50 years of age in endemic regions. The factors which govern the development of skeletal fluorosis are (a) the prevalence of high levels in fluoride intake, (b) continual exposure to fluoride, (c) strenuous manual labour, (d) poor nutrition and (e) impaired renal function due to disease [41].

Human beings throughout history have suffered from dental fluorosis, but until the 20th century the cause of the condition was unknown. Given the common incidence of high F^- groundwaters in the East African Rift Valley [43], it is evident that ancient people could have suffered from dental fluorosis. The mottling of teeth is one of the earliest and most easily recognized symptoms [44]. It is the permanent teeth that are most affected. They lose their normal creamy white translucent colour and become rough, opaque and chalky white. Dental fluorosis is a developmental disturbance which increases with time. Therefore primary teeth are less severely affected than the permanent teeth, and those teeth which erupted first (the incisors and first permanent molars) are less affected than those erupting later, the premolars and other permanent molars [45].

The first signs of dental fluorosis (moderate dental fluorosis) are thin white lines running across the entire enamel surface and which can only be seen after drying the tooth surface [46]. With more fluorosis these thin lines become broader, merge and may be clear without the need for drying. At slightly greater severity the tooth surface shows distinct, irregular, opaque or cloudy white areas, caused by increasing porosity of the tooth enamel. Dental fluorosis has been studied in several parts of South Africa [47–49] and in West Africa in Senegal, especially for

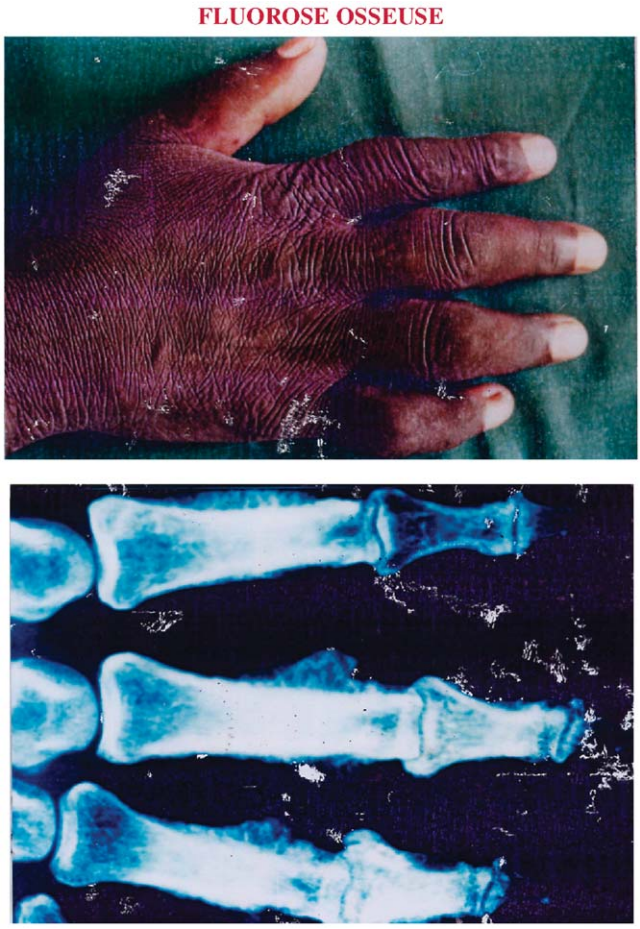

Fig. 1. Illustration of a hand attained by osseous fluorosis in Senegal after regular ingestion of drinking water with F^- level higher than 4 mg/L for 30 years of exposition in an endemic region [42].

the endemic region of Fatick. In this area, waters with high level of fluoride are circulating below a phosphated eocene roof; As shown in Fig. 2, the fluoride level drastically decreases with the disappearance of the phosphated roof [30]. The findings by Mothusi [48] indicated that in the North West province of South Africa, dental fluorosis has resulted in cases of psychological trauma, particularly among adolescents. In areas with fluoride levels of drinking water exceeding 3 mg L^{-1}, a high demand of local inhabitants for extracting teeth and replacing them with dentures is noticed. Dental fluorosis was also investigated in areas surrounding the Pilanesberg complex [50]. It was reported in this study that severe dental fluorosis occurred in 28% of the population, while 41% had moderate dental fluorosis. The same results were reported in the study by Du Plessis [25]. He

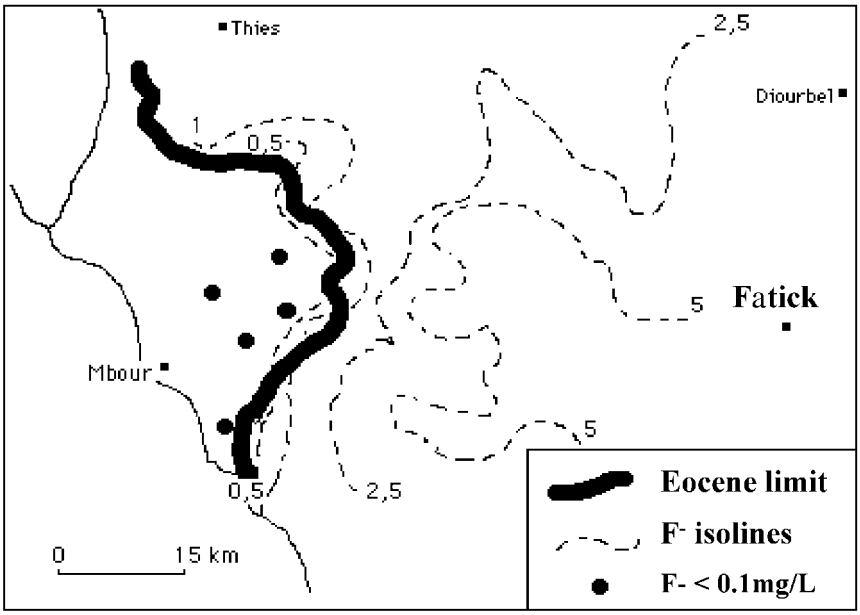

Fig. 2. Scheme showing F^- concentrations in groundwaters at the limits of the endemic region of Fatick (Senegal, west Africa). (Bold line includes border of the phosphated eocene "roof"; dotted lines indicates fluoride iso-concentrations ($mg\,L^{-1}$)) [30].

found that 39% of pupils in the Bloemfontein area had clearly dental fluorosis. The spatial variations of dental fluorosis in seven villages was studied by Zietsman [51]. Furthermore the concentration of fluoride in drinking water was recently shown by Steiner [52] to be inversely correlated with the incidence of dental caries and cancer. It is proposed that dental caries, cancer and possibly other diseases are the result of a nutritional deficiency in fluoride.

2.4. Ways of solving the problem: defluoridation techniques

The prevention of fluorosis through treatment of drinking water in rural areas is a difficult task because of economical and technological restrictions. Defluoridation of water is the only measure to prevent fluorosis and many different defluoridation techniques have been developed [17]. However, many cannot be easily implemented in areas where the problems occur. This section gives a brief overview of defluoridation methods (see Table 1).

Defluoridation processes can be classified into four main groups: *Adsorption methods*, in these methods sorbents such as bone charcoal, activated alumina and clay are used in column or batch systems. *Ion-exchange methods*, these methods require expensive commercial ion-exchange resins. *Coprecipitation and*

contact precipitation methods, these methods coprecipitate F^- with, for example, aluminium sulphate and lime (Nalgonda technique) or precipitate F^-, for example, with calcium and phosphate compounds. *Membrane processes*, these include RO, electrodialysis and NF methods. The last one is very promising for large-scale pilots plants in the future.

Taking into account the realities of the problem as outlined in this short review, the provision of an affordable and technologically simple solution must obviously lie in empowering the local communities to construct viable defluoridation systems from local and readily available materials. There is thus a need for developing low cost methods to remove fluoride from water. The removal of fluoride using locally available clays has been studied in many countries where the problem occurs and the development of laboratory scale defluoridation columns to study the efficiency of fluoride removal using different sorbents is recommended for local communities.

3. DEFLUORIDATION PROCESSES

3.1. Precipitation methods

Precipitation methods can be divided into two categories, those based on co-precipitation of adsorbed F^- and those based on the precipitation of insoluble fluoride compounds.

3.1.1. Methods based on coprecipitation

Coprecipitation (e.g. the Nalgonda technique) is the process by which aluminium salts (aluminium chloride and aluminium sulphate) are added to F^- contaminated drinking waters [53,54].

This process is used in three ways: A bucket system designed to be used on household scale; Fill and draw plants to be used on a community scale; A waterworks flow system developed for larger communities.

(i) Bucket system. The bucket defluoridation system was first practised for domestic use in Tanzania [27]. The two chemicals (aluminium chloride and aluminium sulphate) are added simultaneously to the raw water bucket and stirred with a wooden paddle. Lime is added to adjust the pH of water to about 6.7. After addition of the chemicals it is left to settle for about 1 h. This process is suitable for a daily routine, where one bucket of water is treated for one day's water supply of about 20 L. The process produces water with residual F-between 1 and 1.5 mg L^{-1} [10].

(ii) Fill and draw system. This system is also used in Tanzania for the defluoridation of drinking water [27]). It consists of a cylindrical vessel equipped with

a hand-operated stirring mechanism. The vessel is filled with raw water and a defluoridation procedure similar to the one using the bucket system is performed. Raw water is pumped onto the tank and the required amounts of alum, lime and bleaching powder are added. The contents are stirred slowly for 10 min and allowed to settle for 2 h. The defluoridated supernatant water is withdrawn and supplied through stand posts. The settled sludge is discarded.

(iii) Waterworks flow system. A bigger defluoridation system is used for larger communities. This system involves the combined use of alum and lime for the defluoridation process [10]. It consists of several components, namely, reactors a sump well, sludge drying beds, elevated service reservoir, electric room and chemical storehouse. The raw water from the source is pumped to the reaction-cum-sedimentation tank, which is referred to as a reactor. A sludge pipe with a sluice valve is provided to withdraw the settled sludge once a day.

The Nalgonda technique has been introduced in many countries, e.g. India, Kenya, Senegal and Tanzania. However, the method has a number of disadvantages. These include: the treatment efficiency is about 70%, which means the process cannot be used in cases of high fluoride contamination; a large amount of aluminium sulphate, up to 700–1200 mg L^{-1} may be needed; the adverse health effects of dissolved aluminium species in the treated water.

3.1.2. Methods based on F^- precipitation with calcium and phosphate compounds

Many methods for the precipitation of fluorides with salts of calcium, aluminium and iron are reported in the literature (46–48). Precipitation processes are governed by the solubility of a forming salt [55]. The most common method of treatment is the precipitation of calcium fluoride using calcium from either lime or calcium chloride. The fundamental problem that exists using lime arises from the low solubility of the calcium hydroxide. It therefore requires excess of reagent to complete precipitation. The relatively high solubility of the calcium fluoride does not allow a complete removal of F^-. An additional difficulty with lime precipitation is the poor settling characteristics of the precipitate. The lime-based fluoride removal can be improved by using $CaCl_2$-lime mixture. The highly soluble $CaCl_2$ provides more calcium than lime without increasing pH. Fluoride removal by lime and $CaCl_2$-lime costs about the same.

3.2. Adsorption methods

Fluoride can be removed by adsorption onto many adsorbent materials. The criteria for the selection of suitable sorbents are cost of the medium and running costs, ease of operation, adsorption capacity, potential for reuse, number of

useful cycles and the possibility of regeneration. Some of the most frequently encountered sorbents are reviewed in this section.

3.2.1. Activated alumina

Activated alumina is a granular form of aluminium oxide (Al_2O_3) with very high internal surface area, typically in the range of 200–300 $m^2\,g^{-1}$. This high surface area gives rise to a very large number of sites in the material on which adsorption can occur. It has been widely used for removal of F- from drinking water [14,16]. The mechanism of F^- removal from water is similar to those of a weak base ion-exchange resin. Fluoride removal efficiency is excellent (typically $>95\%$), and is dependent on pH. Fluoride removal capacity is best in the narrow range of pH 5.5–6. Fine (28–48 mesh) particles of activated alumina are typically used for removal. The adsorption sites of activated alumina are also attractive for a number of anions different from F^-. The selectivity sequence [56] of activated alumina in the pH range of 5.5–8.5 is

$$OH^- > H_2A_sO_4^- > Si(OH)_3O^- > HSeO_3^- > F^- > SO_4^{2-} > CrO_4^{2-} \gg HCO_3^- > Cl^- > NO_3^- > Br^- > I^-$$

Activated alumina can be regenerated by flushing with a solution of 4% sodium hydroxide which displaces F^- from the alumina surface (p. 51). This procedure is followed by flushing with acid to re-establish a positive charge on the surface of the alumina.

3.2.2. Clays and soils

The first comprehensive study of fluoride adsorption onto minerals and soils was published in 1967 [57]. Since that time, several workers have investigated the adsorption of fluoride on various substrates. These studies include the use of Ando soils of Kenya [58], Illinois soils of USA [59], Alberta soil Luther [60], illite–goethite soils in China [2] clay pottery [61,62], fired clay [63], fired clay chips in Ethiopia [12], kaolinite [64], bentonite and kaolinite [65,66] and fly ash [17].

3.2.3. Other sorbents

In addition to activated alumina, clays and soils, other materials such as spent bleaching earth, spent catalyst, rare earth oxides, bone charcoal and activated carbon were studied as sorbents for F^-. Mahramanlioglu [67] investigated the adsorption of F^- using spent bleaching earth. They found that the removal of F^- depends on the contact time, pH and adsorbent concentration. Lai and Liu [68] studied the F^- removal from water with spent catalyst. Their findings showed that spent catalysts could be utilized as adsorbent for F^- removal. Its adsorption capacity was comparable to that of activated alumina. Raichur and Basu [69] studied the great potential for F^- removal from water using rare earth oxides. Rare earth oxides showed. Lu [70] investigated the removal of F^- using red mud,

which was found to be 82%. For a sustainable development of such processes, adsorbent reuse should be engaged and waste water treated.

3.3. Ion-exchange resins

Ion-exchange resins are effective in removing F^- from water. Mohan Rao and Bhaskaran [71] studied the removal of F^- using ion-exchange materials such as sulphonated material from coconut shell, Carbion, Tulsion and Zeocarb 225. From the results, it was evident that Zeocarb 225 had the highest F^- removal capacity and sulphonated material of coconut shell has the lowest one. It was also indicated that the ion- exchange material could be regenerated by aluminium sulphate solution (2–4%). Castel *et al*. [72] studied the removal of F^- by a two-way ion-exchange cyclic process. This system used two anion-exchange columns. The results show that this process can effectively remove fluoride from water. The use of anion-exchange resins for F^- removal is not current because of their relatively high costs. The presence of other anions such as chloride and sulphate also presents a major problem when using ion-exchange resins for F^- removal. Because F^- removal is accompanied by sorption of other anions, the sorption capacity is limited to 0.5 mg L^{-1} of F^-concentration level in the bulk [13].

3.4. Electrochemical technique

Electrochemical technique (also electrocoagulation) is a simple and efficient method for the treatment of drinkable water. Recent results reported by Parthasarathy and Yang [54,55] have demonstrated that electrocoagulation (EC) using aluminium anodes is effective in defluoridation. In the EC cell, the aluminium electrodes sacrifice themselves to form aluminium ions first. Afterwards the aluminium ions are transformed into $Al(OH)_3$ before being polymerized to $Al_n(OH)_{3n}$. The $Al(OH)_3$ floc is believed to adsorb F^- strongly as illustrated by the equation.

$$Al(OH)_3 + xF^- = A(OH)_{3-x}F_x + xOH^-$$

Usually the EC operation is completed by an electroflottation (EF) in order to separate the formed floc from water by floating them to the surface cell [73–75].

3.5. Membrane processes

Membrane processes such as RO, NF, dialysis and electrodialysis have become recently developed methods for F^- removal from drinking waters [6,8,15,76–78] and brackish waters [7,9,79]. The second part of this chapter is dedicated to the presentation of recent results obtained from the comparison of RO and NF membranes processes for a selective defluoridation of a Senegalese brackish water from the endemic region of Fatick.

4. COMPARISON BETWEEN NANOFILTRATION AND REVERSE OSMOSIS OPERATIONS

The NF membrane is a type of pressure-driven membrane which properties are situated between RO and ultrafiltration (UF) membranes. NF offers several advantages such as low operation pressure, high flux, high retention of multivalent anion salts and organics compounds with molecular weight above 300 Da, relatively low investment and low operation/maintenance costs. Because of these advantages, the applications of NF worldwide have increased. The history of NF dates back to the 1970s when RO membranes with a reasonable water flux operating at relatively low pressures were developed. Hence, the high pressures traditionally used in RO resulted in a considerable energy cost. Thus, membranes with lower rejections of dissolved components, but with higher water permeability, appeared be a great improvement for separation technology. Such low-pressure RO membranes became known as NF membranes. By the second half of the 1980s, the interest for NF had become established, and the first applications were reported as detailed in a recent review [80]. Today 10% of brackish waters market in the world is dedicated to NF membranes [81]. While NF is a relatively new membrane process, it is already widely used for water treatment in different parts of Europe, Israel and the US. Striving towards improved quality, efficiency and applicability, research is continuing in an attempt to understand and model the varying parameters involved during NF. A technique that is often used for the evaluation of membranes is the flux and rejection behaviour of uncharged and charged solutes [82]. However, many membranes have to be screened before finding a suitable one.

NF is used when high molecular weight solutes have to be separated from a solvent. It is effective in the production of drinking water, especially in the case of water softening. Compared to RO, a lower retention is found for monovalent ions. But very recently [9], it has been found that NF separates the ions of the same valency for a selective defluorination of brackish water. RO and UF have shown, respectively, solution-diffusion and convection mass transfers. In NF, a synergism between both can be observed but strongly depends on the operational conditions (pH, ionic strength, flow rate, transmembrane pressure) and on the membrane material used.

The aim of the present chapter is to establish a systematic approach in the characterization of commercial NF and low-pressure RO membranes in order to help the user to the better choice between NF and RO operations.

The first part is dedicated to the characterizations of two NF membranes, denoted NF270, NF90 and one low-pressure RO membrane, denoted BW30. We will give two sorts of characterizations: (i) a physico-chemical one, involving hydrophobicity, morphology and topography experiments and (ii) a mass transfer one occurring *via* water and synthetic salt solution permeability measurements (denoted L_p and L_p', respectively), charged solutes rejections and diffusive fluxes for NaCl and Na_2SO_4 solutions.

Furthermore, these characterizations will be completed in determining mass transfer parameters σ and P_s, C_{conv} and J_{diff} , respectively, the reflection coefficient and the solute permeability of the membranes, the part of solute mass transfer dedicated to convection and J_{diff} the part of mass transfer dedicated to hydration-diffusion, for two synthetic chlorides and sulphates sodium salts solutions under different concentrations, 10^{-3} and 10^{-1} M.

In a second part, recent results dedicated to the comparison of NF and RO membranes for the defluoridation of a Senegalese water sample from the endemic region of Fatick, Senegal will be presented and illustrated with a semi-industrial pilot plant.

4.1. Theory

The transport of solutes through a membrane can be described by using the principles of irreversible thermodynamics (IT) to correlate the fluxes with the forces through phenomenological coefficients. For a two-components system, consisting of water and a solute, the IT approach leads to two basic equations [83].

$$J_v = P_w\left[\frac{dP}{dx} - \sigma\frac{d\pi}{dx}\right] \tag{1}$$

$$J_s = -P_s\frac{dc_s}{dx} + (1-\sigma)J_v c_s \tag{2}$$

where $\underline{J_v}$ and J_s are, respectively, the solvent flux and the solute flux, and dP/dx and $d\Pi/dx$ define, respectively, the pressure and osmotic gradients inside the membrane; P_w is the filtration coefficient ($m^2\,s^{-1}\,Pa^{-1}$) or specific hydraulic permeability constant, σ the local reflection coefficient, P_M the local solute permeability coefficient ($m^2\,s^{-1}$) and c_s the local solute concentration in the membrane at a distance x from the membrane surface ($mol\,m^{-3}$).

With constant fluxes and constant transport parameters (P_S and σ), the integration of equation (2) on the membrane thickness yields, in term of the real salt rejection.

$$R = \frac{\sigma(1-F)}{1-\sigma F} \tag{3}$$

with $F = e^{-(1-\sigma/P_s)\delta_m J_v} = e^{-(1-\sigma/P_M)J_v} = e^{-Pe}$

where $P_M = P_s/\delta_m$ is the overall permeability coefficient and $Pe = 1-\sigma/P_M J_v$ is the Peclet number [84].

From equation (3), it appears that the retention increases with increasing water flux and reaches a limiting value σ at an infinitely high water flux. As the diffusive flux of the solute can be neglected in the range of the higher water flux, the reflection coefficient σ is a characteristic of the convective transport of the solute. A σ value of 100% means that the convective solute transport is totally hindered or that no transport by convection takes place at all. This is the case for ideal RO

membranes in which the membranes have dense structure and no pores are available for convective transport. Equation (3) however only relates the membrane surface concentration to the permeate concentration. It needs to be combined with concentration polarization if the permeate concentration is to be related to the bulk feed concentration which results in the combined film theory – Spiegler–Kedem [85].

According to the film theory, the relation between the observed rejection rate and the true rejection rate may be expressed as

$$\ln\left(\frac{1-R_{obs}}{R_{obs}}\right) = \ln\left(\frac{1-R}{R}\right) + \frac{J_v}{K} \tag{4}$$

where K is the mass transfer coefficient.

Substitution of equation (3) into equation (4) and rearranging results in the following equation [85]:

$$R_{obs} = \frac{1}{\frac{1-\sigma}{\sigma\left(1-e^{-\left(\frac{1-\sigma}{P_M}\right)J_v}\right)}e^{J_v/K} + 1} \tag{5}$$

By using a non-linear parameter estimation method by supplying the data of R_{obs} *vs.* J_v taken at different pressures but at constant feed rate and constant feed concentration for each set, equation (5) may be used to estimate the membrane parameters σ and P_M and the mass transfer coefficient, K, simultaneously [84]. A wide variation of transmembrane pressure at a constant feed flow rate is required to prevent poor regression due to too many unknowns (σ, P_s and K) compared to the experimentally available variables (J_v and R_{obs}). Even in this case, poor regression might still be obtained for high values of K. In this particular case, the inequality $K \gg J_v$ holds at most values of J_v. This point prevents to obtain K with a high level of confidence because R_{obs} equals R (equation (5) reduces to equation (3) for any value of $K \gg J_v$). To the authors opinion, the best way to determine σ and P_s values is to work under experimental conditions so that $K \gg J_v$ (high tangential rate and low pressure). This allows to obtain directly the true rejection and then σ and P_s using a non-linear least squares estimation procedure that make equation (3) fit the data as closely as possible.

Another way to quantify the convective and diffusive parts is to express equation (2) as

$$J_s\,dx = -P_s dc_s + (1-\sigma)J_v c_s\,dx$$

with constant fluxes and constant transport parameters (P_w and σ), the integration of this equation on the membrane thickness (δ_m) yields

$$J_v C_p \delta_m = -P_s \Delta c_s + (1-\sigma)J_v \int_{\delta_m} c_s dx$$

or

$$J_v C_p = -P_M \Delta c_s + (1 - \sigma) J_v C_{int} \quad (6)$$

where $C_{int} = 1/\delta_m \int_{\delta_m} c_s \, dx$ is the mean solute concentration inside the membrane.

Note that this equation is identical to the Kedem–Katchalsky model and does not imply a linear concentration gradient as it is frequently reported. It may be expressed as well as [7,8]

$$J_{diff} + J_v C_{conv} = C_P J_v$$

where J_{diff} is the solute flux due to diffusion, and C_{conv} is the solute concentration due to convection [$= (1-\sigma) C_{int}$].

Then the concentration in the permeate becomes

$$C_P = \frac{J_{diff}}{J_v} + C_{conv} \quad (7)$$

By following C_p *vs.* the reverse of the permeate flux, it is possible to quantify separately both part of the solute mass transfer occurring in NF: convection and solvation (hydration)/diffusion as developed recently [9]. The results are expected to be valid only in some limited domains of operating conditions (J_{diff} and $C_{conv} = C$tes) but may be useful for the comparison of the behaviour of different membranes.

Since NF membranes have pores, a reflection coefficient below 100% will be found if the solutes are small enough to enter the membrane pores. During our experiments we have limited the concentration polarization by using dilute solutions and high flow rate. In fact, the SKK model was developed first for uncharged membranes such as RO membranes while most NF membranes are charged, negatively or positively, depending upon the physico-chemical conditions (pH, ionic strength) and the kind of used material. The membrane charge has been neglected in the present study because the membranes employed appear to have an RO behaviour.

4.2. Experiments

4.2.1. Membrane materials

The membranes under study are thin-film composite membranes composed of two layers as illustrated in Fig. 3; a thin polyamide film as active layer and a large mesoporous polysulphone as the support layer. The three studied membranes are 2 NF membranes, noted NF90, NF270 and a low-polarization reverse osmosis (LPRO) membrane , noted BW30. All membranes were purchased from Filmtec (DOW, USA); the specifications of the membranes are given in Table 2. The chemical structures of the support and active layer materials are reported in Fig. 4 [86]. Polyamide material is the more used but some authors have reported results

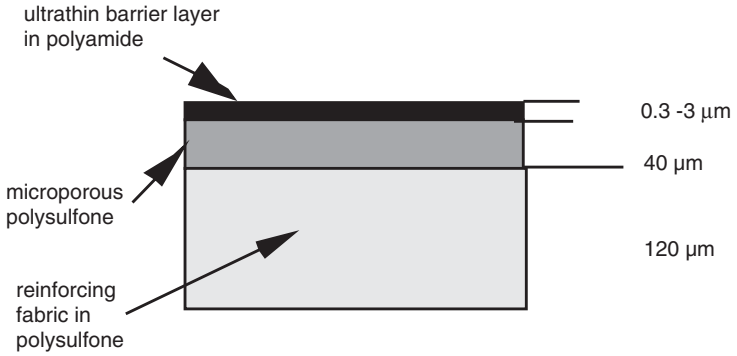

Fig. 3. Schematic diagram of thin film composite membranes.

Table 2. NF and LPRO membrane characteristics from Filmtec (DOW)

	NF270	NF90	BW30
Maximum temperature (°C)	45	35	45
Pressure range (bar)	17	25	41
pH range	3–10	3–9	2–11
NaCl rejection (%)	40–60	85–95	99.5
Product name	NF270-400	NF90-400	BW30-400
Material	Polyamide	Polyamide	Polyamide

with cellulosic membranes [87]. Before use, the membranes were rinsed with UP MilliQ water (Millipore system, France) until the conductivity of the permeate remains below UP water conductivity ($3\,\mu S\,cm^{-1}$). The effective surface membrane area was $472\,cm^2$. All the salts used (NaCl, Na_2SO_4) were of analytical grade from Aldrich (France) and used as received. All solutions were prepared from a MilliQ water with a purity water presenting a conductivity lower than $3\,\mu S\,cm^{-1}$ and $pH = 6.7$. The salts analyses were carried out by a conductimeter after standardization for each salt and concentration were deduced for single salt solutions.

4.2.2. Bench scale pilot plant

The NF/LPRO pilot plant was supplied by Sepratech (Separation Technoloy, INC, US), and consisted of a feed tank, a pump and planar module, as detailed in Fig. 5. All studies were done using a low conversion rate (5%) and a high tangential flow rate ($\sim 4\,m\,s^{-1}$) in order to minimize the polarization concentration effects. The applied transmembrane pressures were in the range of 0–25 bar. The temperature was maintained at 25°C.

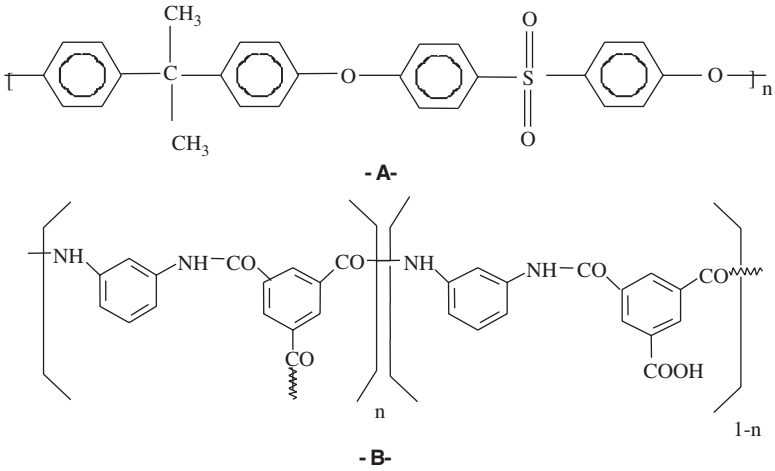

Fig. 4. Chemical structures of the support (A) and active layers (B) of the NF(NF90, NF270) and LPRO (BW30) membranes.

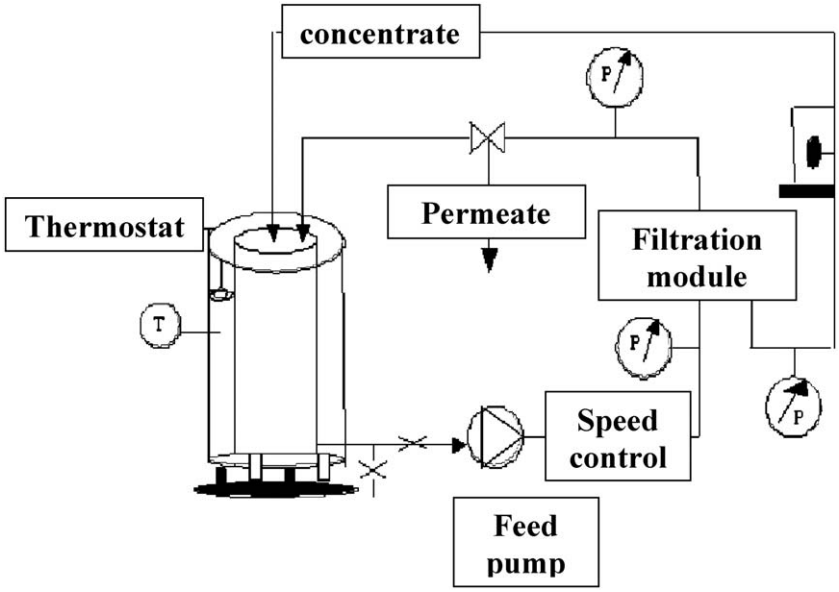

Fig. 5. Flow diagram of the NF/LPRO plant (lab-scale experiments, January–March 2005).

Permeated solutions were recycled during the runs except for samples withdrawn for the calculation of observed retention denoted R_{obs} according to

$$R_{obs} = 1 - \frac{C_p}{C_o} \tag{8}$$

where C_p and C_o are the concentrations in the permeate and feed solutions, respectively. But, under hydraulic conditions we can consider that $R_{obs} = R_{real}$.

Pure water flux through a membrane can be described by-Darcy's law

$$J_v = L_p \Delta P \tag{9}$$

with L_p the hydraulic permeability of the membrane usually given in $L\,h^{-1}\,m^{-2}\,bar^{-1}$.

4.2.3. Contact angle measurements

The contact angle measurements were carried out by the sessile drop technique. The different membranes were primarily washed twice with deionized water for a period of 24 h and then dried at room temperature over silica gel in a dessicator. A droplet of UP milliQ water solution (a volume of 1–2 μL) was deposited onto the surface with a microsyringe and contact angles of the droplet with the surface were measured with a KRUSS G10 contact angle meter. Reported values correspond to the average of the contact angles (right and left) of 5 droplets. During the short time of measurement (less than 1 min), no change in contact angle was observed. Contact angles do not give absolute values but allow a comparison between each material. A variation of 2° in the angle is needed to differentiate each kind of materials with the low roughness NF membranes studied.

4.2.4. AFM experiments

Atomic force microscopy (AFM) studies contribute also to the improvement of the NF membranes, especially for desalination of brackish water. AFM characterization of a series of commercial NF and RO membranes of different polymer types for brackish water desalination had not been attempted, so far. Thus, as reported by Hilal [79], it is imperative to study the properties of these membranes and to show that the characteristics obtained from AFM correlate to the process behaviour. This is expected to provide substantial new insights into the influence of NF/RO membrane properties on performance, providing a database for the selection of NF membranes to account for the complexities of brackish water.

The AFM equipments used were conducted with a Nanoscope III device from VEECO (USA). The membrane morphologies were imaged in contact mode in air with a scan rate of 1 Hz and 400 × 400-pixel resolution. The cantilevers used for such imaging were from Veeco, with a specified spring constant between 0.44 and 0.63 $N\,m^{-1}$ and a resonant frequency of 17–20 kHz. The mean roughness (denoted *Ra*) is the mean value of surface relative to the centre plane. The plane for which the volume enclosed by the image above and below this plane are equal and is calculated as

$$Ra = \frac{1}{L_x L_y} \int_0^{L_y} \int_0^{L_x} \left| z(x,y) \right| \, dx \, dy \tag{10}$$

where $z(x,y)$ is the surface relative to the centre plane and L_x and L_y are the dimensions of the surface analysed.

4.3. Results and discussion

4.3.1. Pure water permeabilities of the membranes

The flux solvent evolution of pure water with the transmembrane pressure across NF/LPRO membranes are reported in Fig. 6. The linear dependence of fluxes with the transmembrane pressure shows that Darcy's law is verified. As expected, the hydraulic permeabilities determined from the slopes (Table 3) show higher values for NF than LPRO membranes, due to their larger pore size. The NF90 membrane shows the higher hydraulic permeability with $L_p = 14.8\,L\,h^{-1}\,m^{-2}\,bar^{-1}$.

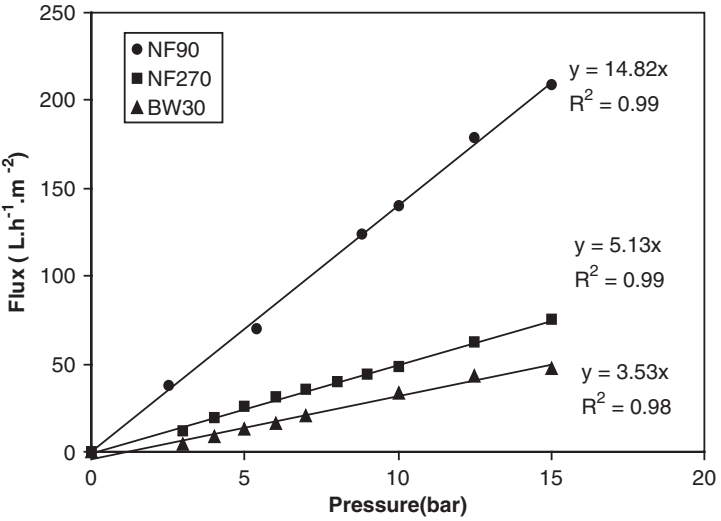

Fig. 6. Pure water flux (y) as a function of the transmembrane pressure (x) (ΔP) for NF membranes (NF270, NF90) and low-pressure RO membrane (BW30) at $T = 25\,^{\circ}C$, R being the linear regression coefficient.

Table 3. Pure water and saline solution (NaCl 0,1 M) permeabilities, contact angles and critical pressures of NF and LPRO membranes

Membrane	L_p (± 0.7) ($L\,h^{-1}\,m^{-2}\,bar^{-1}$)	L_p' (± 0.3) ($L\,h^{-1}\,m^{-2}\,bar^{-1}$)	θ ($^{\circ}$) (± 7)	P_c (bar) (± 0.1)
NF270	5.1	2.9	38	0.8
NF90	14.8	5.0	64	1.6
BW30	3.5	1.5	76	3.8

4.3.2. Saline aqueous solution permeabilities of the membranes

The interest in knowing the permeability of the membranes for a salty solution is to predict the fluxes which could be obtained for a real brackish water (total salinity near $6\,g\,L^{-1}$) without fouling. This parameter is not given by the membrane suppliers.

In the Fig. 7, we have reported the flux as function of the transmembrane pressure (ΔP) for a NaCl solution at a concentration of $10^{-1}\,mol\,L^{-1}$ ($6\,g\,L^{-1}$) which is typical of a synthetic brackish water. The linearity observed suggests that this salty solution follows the Kedem–Katchalscky model (i.e. Spiegler–Kedem model, with pressure and osmotic linear gradients). For linear gradients, equation (1) amounts to

$$J_v = P_w\left[\frac{\Delta P}{\Delta x} - \sigma\frac{\Delta\pi}{\Delta x}\right] = P_w\left[\frac{\Delta P}{\delta_m} - \sigma\frac{\Delta\pi}{\delta_m}\right]$$

or

$$J_v = L_p'[\Delta P - \sigma\Delta\pi] \tag{11}$$

with

$L_p' = P_w'/\delta_m$: membrane permeability to salty solution ($m\,s^{-1}\,kPa^{-1}$) or usually explained in $L\,h^{-1}\,m^{-2}\,bar^{-1}$ and $P_c = \sigma\Delta\pi$: critical pressure (kPa)

The critical pressures (P_c) obtained with this model are reported in- Table 3. The P_c values show that the flux through the RO membrane (BW 30) starts under

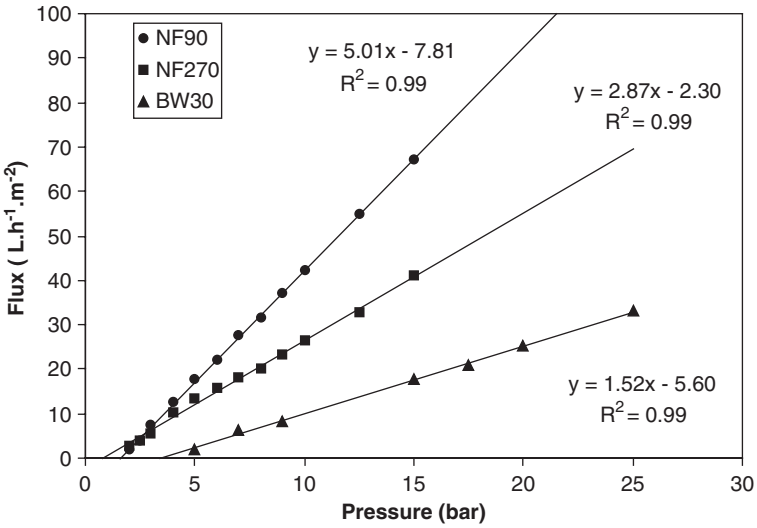

Fig. 7. Water flux of NaCl solution at 10^{-1} M as a function of the transmembrane pressure for NF membranes (NF270, NF90) and low-pressure RO membrane (BW30).

the theoretical osmosis pressure (around 4.5 bar for a solution of NaCl 0.1 M) suggesting that this RO membrane is more open than usual.

For the NF membranes (NF90 and NF270), the critical pressure is only slightly under 2 bars. The accumulation of NaCl on the membrane surface is limited by the high flow rate and the imposed low conversion ratio. Owing to more open pores in NF membranes than in RO membranes, the osmosis pressure is lower in the formers and then NF is less limited by osmosis pressure than LPRO for which the theoretical value of the osmosis pressure is mass transfer limiting. Finally, the interest in NF in presence of salt is due to its higher hydraulic permeability and also to its lower critical pressure. Furthermore the NF90 membrane shows the higher hydraulic permeability to the NaCl 0.1 M solution with $L_p' = 5.0\,\mathrm{L\,h^{-1}\,m^{-2}\,bar^{-1}}$.

4.3.3. Roughness of the membranes

AFM characterizations have been performed to determine the morphology and the topography of the studied membranes. The results obtained for one scan of $1 \times 1\,\mu m^2$ of the three membranes studied are reported in Fig. 8.

The resulting roughness for two scans ($50 \times 50\,\mu m^2$ and $1 \times 1\,\mu m^2$), are reported in Table 4. It may be seen that *Ra* is higher for the NF90 membrane which has more open pores. But, the more interesting result is that the NF270 present a lower roughness than the LPRO BW30 membrane. As usually observed, the average roughness decreases as the nominal molecular weight cut-off (MWCO) decreases.

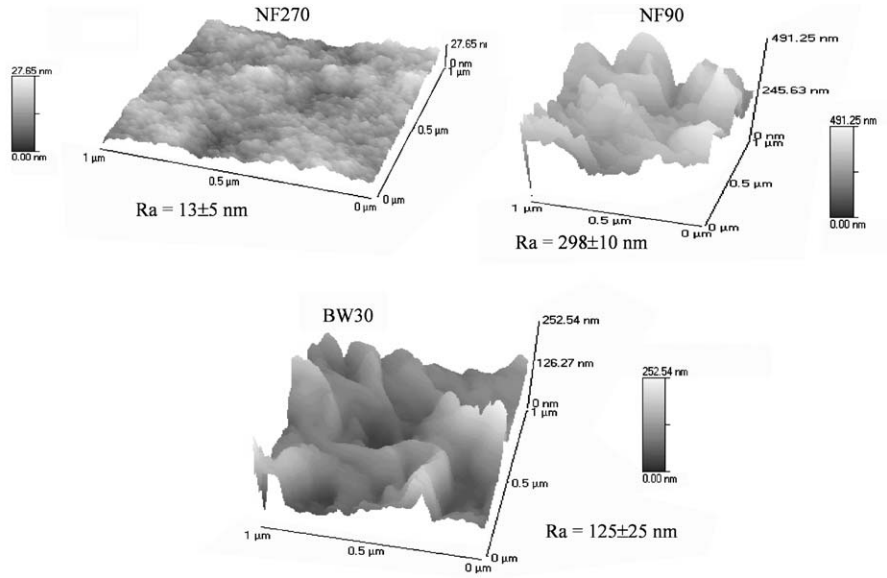

Fig. 8. 3D images of the NF270 (a), NF90 (b) and BW30(c).

Table 4. Average roughness of NF90, NF270 and BW30 membranes

Membrane	NF270		NF90		BW30	
Field analysed	$50 \times 50\,\mu m^2$	$1 \times 1\,\mu m^2$	$50 \times 50\,\mu m^2$	$1 \times 1\,\mu m^2$	$50 \times 50\,\mu m^2$	$1 \times 1\,\mu m^2$
Ra (nm)	45 ± 5	13 ± 5	390 ± 20	298 ± 10	290 ± 10	125 ± 25

4.3.4. Contact angle measurements

In Table 3, are reported the results of contact angle measurements determined by the sessile drop method and conducted on dry samples. Usually, the lower the contact angle the more hydrophilic is the material. Then, it appeared clearly that the more hydrophilic membrane surface is NF270. For NF90 and BW30 membranes it is more difficult to conclude because contact angle measurements can be highly influenced by their high roughness.

4.3.5. Determination of salt retention

Usually, to compare the selectivity of different membranes, the graph of the observed retention, denoted R_{obs}, as function of the transmembrane pressure (ΔP) is used (see Fig. 9a). For the three studied membranes the data obtained at $\Delta P = 5$ and 15 bar are reported in Table 5.

4.3.6. Hydrodynamical approach

The originality of the present approach is to build with the same results as in graph 9a, representing C_p as function of $1/J_v$, as illustrated in Fig. 9b. Then, the permeate concentration as a function of the reverse permeate flow ($1/J_v$) revealed a linear evolution in conformity to the equation (8) for the membranes studied. For $1/J_v \rightarrow 0$, the convective part of the solute mass transport, C_{conv}, is obtained and from the slope we got J_{diff}, the diffusion part of the mass transfer. All values of C_{conv} and $J_{diff.}$ obtained for the NF270, NF90 and BW30 membranes are reported in Table 6. From $C_{conv.}$ values, we can conclude that the NF270 membrane is more convective than NF90 and BW30 membranes, for both studied salts: NaCl and Na_2SO_4. The slopes obtained confirm also that the NF90 has a more diffusionnal behaviour than the NF270. A recent study has demonstrated that diffusional NF membranes are recommended for high fluoride rejection (p. 9), then the NF90 should be the best membrane for a selective defluoridation of drinking waters.

Furthermore, from C_{conv} values it is possible to calculate the MWCO of the three membranes, with [88]

$$C_{conv} = C_0 \left[1 - \left(\frac{M}{S_c} \right)^{1/3} \right]^2 \tag{12}$$

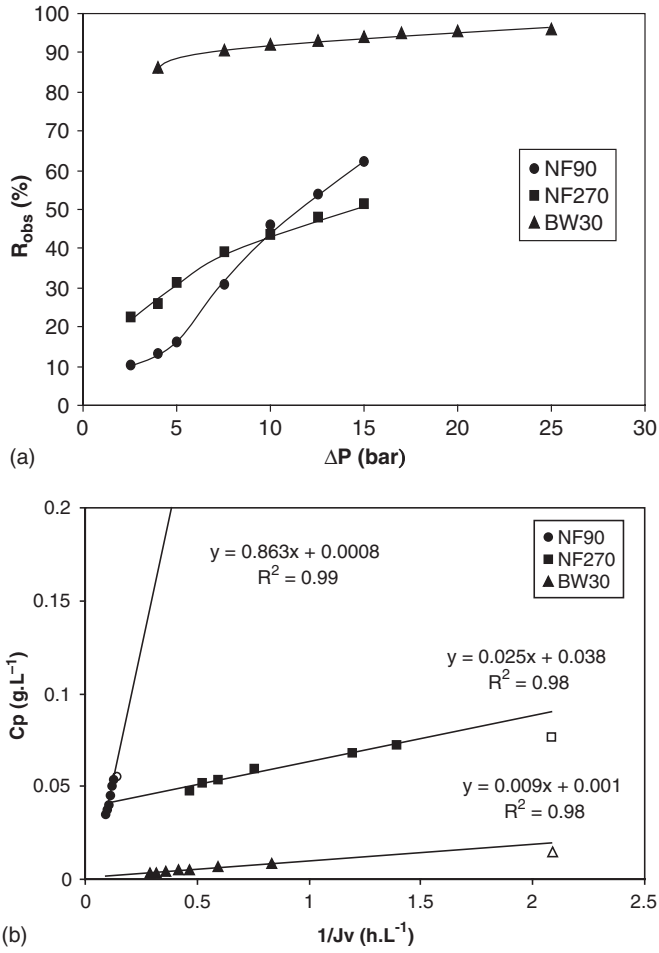

Fig. 9. (a) Observed retention (R_{obs}) *vs.* the transmembrane pressure (ΔP) (NaCl 0.001 M, pH = 6.5). (b) Permeate concentration (C_p) *vs.* the ratio $1/J_v$ (NaCl 0.001 M, pH = 6.5).

with M, molecular weight of a solute, S_c, MWCO of the membrane and C_0, initial concentration of the solute in the feed. The results of calculated MWCO are reported in Table 7. The results obtained show that the best conditions to determine NF MWCO is under diluted solution (10^{-3} M) using a divalent salt such as Na_2SO_4. We observed that the sequence BW30 < NF90 < NF270, is in good correlation with the convective properties of those membranes which is very low for the LPRO and highest for the NF270. This method is a very simple way to determine quickly the MWCO of a microporous membrane as recently reported [91].

Table 5. R_{obs} values determined for NF90, NF270 and BW30 membranes with different transmembrane pressure applied and two different salts (NaCl and Na_2SO_4)

		R_{obs} (%) ($P = 15$ bar)			
	Concentration ($mol\,L^{-1}$)	0.001		0.1	
		$P = 5$ bar	$P = 15$ bar	$P = 5$ bar	$P = 15$ bar
NaCl	NF270	34	59	11	20
	NF90	15	62	5	50
	BW30	—	94	—	93
			$P = 15$ bar		
Na_2SO_4	NF270	93		60	
	NF90	99		98	
	BW30	99		98	

Table 6. C_{conv}, J_{diff} values obtained from simplified SKK model

		C_{conv} ($g\,L^{-1}$)	J_{diff} ($mol\,m^{-2}\,s^{-1}$)	C_{conv} ($g\,L^{-1}$)	J_{diff} ($mol\,m^{-2}\,s^{-1}$)
	Concentration ($mol\,L^{-1}$)	10^{-3}		10^{-1}	
NaCl	NF270	0.0380	2.5×10^{-6} ($\pm 9 \times 10^{-7}$)	2.95	2.5×10^{-5} ($\pm 1 \times 10^{-5}$)
	NF90	0.0008	0.8×10^{-4} ($\pm 8 \times 10^{-6}$)	0.11	2.3×10^{-3} ($\pm 3 \times 10^{-4}$)
	BW30	0.0010	0.9×10^{-6} ($\pm 0.2 \times 10^{-6}$)	0.01	3.5×10^{-5} ($\pm 1 \times 10^{-5}$)
Na_2SO_4	NF270	0.0084	3.7×10^{-7} ($\pm 0.6 \times 10^{-7}$)	4.15	4.2×10^{-5} ($\pm 0.9 \times 10^{-5}$)
	NF90	0.0024	7.4×10^{-7} ($\pm 0.5 \times 10^{-7}$)	0.03	6.2×10^{-6} ($\pm 0.9 \times 10^{-6}$)
	BW30	0.0016	1.0×10^{-7} ($\pm 0.1 \times 10^{-7}$)	0.01	3.7×10^{-6} ($\pm 0.7 \times 10^{-6}$)

Table 7. Molecular weight cut-off determined from equation (12) from C_{conv} experimental results

	MWCO(Da) calculated		MWCO[a]
Concentration Na_2SO_4 ($mol\,L^{-1}$)	$10^{-3}(\pm 20)$	$10^{-1}(\pm 15)$	(± 7) (Da)
NF270	308	2000	120
NF90	213	190	250
BW30	187	159	96

[a] Determined from the molecular weight cut-off of a NF70 membrane and its hydraulic permeability. *Source*: From Pontie [20].

Table 8. Phenomenological σ and P_S parameters relating to sodium salts (NaCl and Na_2SO_4)

Concentration ($mol\,L^{-1}$)		NF270 10^{-3}	NF270 10^{-1}	NF90 10^{-3}	NF90 10^{-1}	BW30 10^{-3}	BW30 10^{-1}
NaCl	$\sigma(\pm 0.02)$	0.43	0.26	nd	nd	0.98	0.99
	P_s ($L\,h^{-1}$) (± 0.01)	1.01	1.32	nd	nd	0.11	0.13
Na_2SO_4	$\sigma(\pm 0.02)$	0.96	0.51	0.98	0.98	0.99	0.99
	P_s($L\,h^{-1}$) (± 0.01)	0.04	0.34	0.06	0.03	0.00	0.01

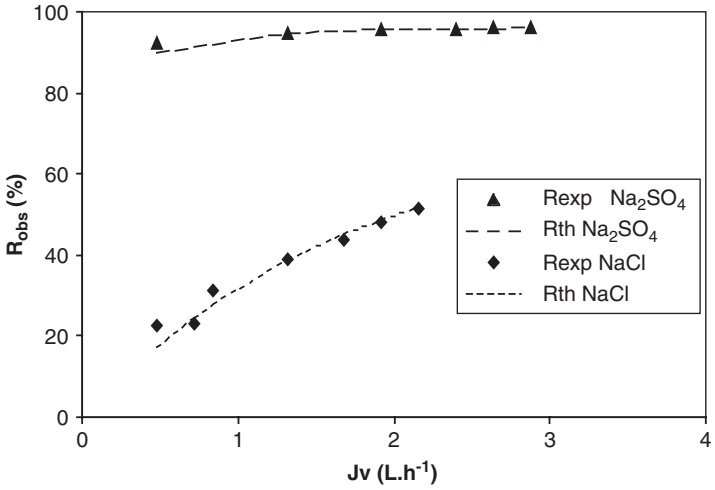

Fig. 10. Evolution of R_{obs} *vs.* J_v for NF270 membrane (salts concentrations 0.001 M, pH = 6.5).

4.3.7. Phenomenological approach

σ and P_M values from equation (5) which experimentally fit the data as closely as possible are reported in Table 8. In most cases, equation (5) adequately describe the data (see, e.g. Fig. 10). As expected the highest σ values where obtained for the BW30 membrane, independently of the electrolyte solution. For the NF270 the σ values decreased when the ionic strength change due to the decrease of the retention. For the NF90 membrane equation (5) does not fit the data obtained with NaCl solutions. We can assume that this membrane bears charges, as recently reported [20,89,90]. The limitation of our model is that it does not take into account the charge of the membrane. Indeed, the Donnan effect should play a non-negligible role and the effect of electrostatic forces can be noticeable and can facilitate the increase in the distribution coefficient by electric affinity, increasing subsequently the diffusion part of the mass transfer. For the P_M values,

if we compare the values obtained for Na_2SO_4, we can observe the following order at low ionic strength:

$$NF90 > NF270 > BW30$$

We observed a modification between both NF membranes at high ionic strength, with the following order:

$$NF270 > NF90 > BW30$$

We can attribute this modification to a decrease in the diffuse layer thickness under ionic strength variations. It seems also that the NF90 membrane is less sensitive to ionic strength modifications in comparison to NF270.

4.3.8. Results from the Fatick area

A sample of water (40 L) has been filtrated from the endemic region of Senegal (Fatick) with the three membranes previously described, under industrial conditions. Water analysis (see Table 9) show higher F^- and Cl^- concentrations than the WHO standards. All the results are reported in Fig. 11. The evolution of the fluoride contents in the permeate increase with the following order: NF270 > NF90 > BW30.

Table 9. Fatick's water analysis (Senegal)

	F^- (mg L^{-1})	Cl^- (mg L^{-1})	Turbidity (NTU)	pH	Total salinity (mg L^{-1})
Feed water	3.76	670	0.6	8.15	2361
WHO standards	1.5	200	1	6.5–9	500

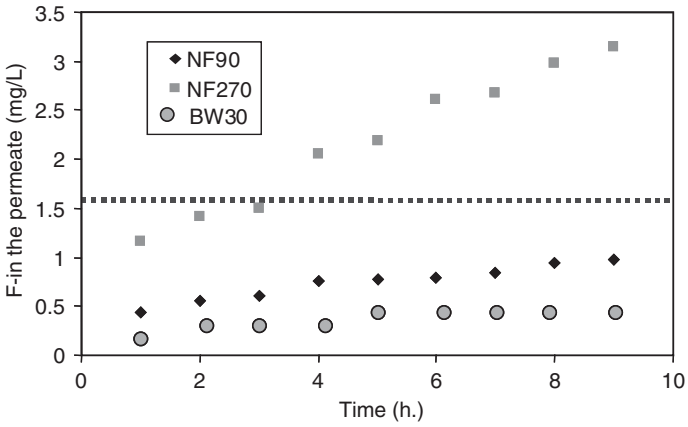

Fig. 11. F^- concentrations in the permeate *vs.* time during the filtration of the Fatick water on NF90, NF270 and BW30 membranes (Feed composition: see Table 9; operation conditions: Transmembrane pressure 7.5 bars; conversion ratio 0.87).

It can be concluded that the best NF tested membrane is NF90. Furthermore with this membrane the F^- amount exhibits a good level in terms of prophylactic effect. On the other hands with NF270 and BW30 membranes the F^- concentration are respectively too high and too low in comparison to the NF90.

Furthermore, we determined the Silt density Index (denoted SDI) of the water and obtained a value of 3.1. The parameter SDI has become the accepted standard for assessing the suitability of membrane processes, particularly for RO. The SDI value is merely a measure of the decline in filtration rate of a membrane filter under standard test conditions. The test is indeed an indirect ''measurement'' of all suspended solids, bacterial and colloidal matter in the water to be treated through an attempt to sacrificially plug a microporous cellulose ester membrane filter. The value obtained means that Fatick water has a low fouling properties for microporous membranes. This result permit to counter-balance the high roughness obtained for the NF90 membrane because a high roughness is usually associated to a high fouling properties of the membrane material. Those results confirm to a large scale experiments the interest in NF for water defluoridation as previously reported [1].

5. CONCLUSIONS

This article is a review of all the processes reported for drinking water defluoridation for fresh water preparation on both domestic- and industrial scales. Recent results are also reported on new NF membranes for a more selective defluoridation of drinking waters in Senegal. This original result permit to check that the commercialized NF90 membrane is more efficient due to its diffusional behaviour for salts, its high hydraulic permeability and its intermediate rejection of F^-. Further experiments are now being conducted in order to classify all commercial NF membranes. Operating conditions (transmembrane pressure, membrane material, conversion ratio, feed composition and membrane morphology) are the keys to selectivity for a better predictive NF operation in the future.

It is well known that the application of defluoridation techniques constitutes a big challenge in third world countries. Unfortunately, of the 25 countries in the world with severe fluoride problems, most have low economies. Then, two complementary approaches will have to be developed in the future depending on the local conditions: (i) defluoridation using clay for rural areas and (ii) defluoridation using NF for urban areas supported by private funds, for drinking water for all.

APPENDIX: LIST OF SYMBOLS AND ACRONYMS

C_{conv} solute concentration due to convection ($g\,L^{-1}$)
C_p solute concentration in the permeate ($g\,L^{-1}$)
C_0 solute concentration in feed ($g\,L^{-1}$)

J_{diff} solute flux due to diffusion (mol $m^{-2} s^{-1}$)
P_S solute permeability *vs.* membrane (L $h^{-1} m^{-2} bar^{-1}$)
J_v solvent flux (L h^{-1})
J_s solute flux (L h^{-1})
L_p pure water permeability (L $h^{-1} m^{-2} bar^{-1}$)
L_p' saline solution permeability (L $h^{-1} m^{-2} bar^{-1}$)
ΔP transmembrane pressure (bar)
$\Delta\Pi$ osmotic pressure difference across membrane (bar)
R_{obs} observed retention (%)
σ reflection coefficient
Ra membrane roughness (nm)
ΔC_s the concentration difference between each side of the membrane (mol L^{-1})
NF nanofiltration
RO reverse osmosis
UF Ultrafiltration
LPRO low-polarization reverse osmosis
MWCOmolecular weight cut-off
KK Kedem and Katchalsky
SKK Spiegler, Kedem and Katchalsky
EC electrocoagulation
AFM atomic force microscopy
SDI silt density index
WHO World Health Organization

REFERENCES

[1] M. Pontie, M. Rumeau, M. Ndiaye, C. Mart Diop, Sur le problè me de la fluorose au Sé né gal: bilan des connaissances et pré sentation d'une nouvelle mé thode de dé fluoruration des eaux de boisson, Cahiers Santé 6 (1) (1996) 27–36.
[2] Y. Wang, E.J. Reardon, Activation and regeneration of a soil sorbent for defluoridation of drinking water, App. Geochem. 16 (2001) 531–539.
[3] S.Ghorai, K.K. Pant, Investigations on the column performance of fluoride adsorption by activated alumina in a fixed bed. Report, Indian Institute of Technology Kharagpur, 2002.
[4] M. Srimurali, A. Pragathi, J. Karthikeyan, A study on removal of fluorides from drinking water by adsorption onto low-cost materials, Environ. Pollut. 99 (1998) 285–289.
[5] N.V.R. Mohan Rao, C.S. Bhaskaran, Studies on defluoridation of water, J. of Fluorine Chem. 41 (1988) 17–24.
[6] M. Pontie, Electrokinetics phenomena and ionics transfer across microporous membranes, PhD Thesis, University of Tours, France, 1996.
[7] M. Pontie, H. Buisson, C.K. Diawara, H. Essis-Tome, Studies of halide ions mass transfer in nanofiltration – application to selective defluorination of brackish water, Desalination 157 (2003) 127–134.
[8] A. Lhassani, M. Rumeau, D. Benjelloun, M. Pontie, Selective demineralisation of water by nanofiltration application to the defluoridation of brackish water, Water Res. 35 (2001) 3260–3264.
[9] C.K. Diawara, S.M. Lô, M. Rumeau, M. Pontié, O. Sarr, A phenomenological mass transfer approch in nanofiltration of halide ions for a selective defluorination of brackish drinking water, J. Membr. Sci. 219 (2003) 103–112.

[10] E. Dahi, F. Mtalo, B. Njalo, H. Bregnhj, Defluoridation using the Nalgonda technique in Tanzania, 22nd WEDC Conference, 1996.
[11] M.J. Larsen, E.I. Pearce, S.J. Jensen, Defluoridation of water at high pH with use of brushite, calcium hydroxite, and bone char, J. Dent. Res. 72 (11) (1993) 1519–1525.
[12] G. Moges, F. Zewge, M. Socher, Preliminary investigations on the defluoridation of water using fired clay chips, J. Afr. Earth Sci. 21 (4) (1996) 479–482.
[13] Y. Veressinina, M. Trapido, V. Ahelik, R. Munter, Fluoride in drinking water: the problem and its possible solutions, Proc. Estonian Acad. Sci. Chem. 50 (2) (2001) 81–88.
[14] O.J. Hao, A.M. Asce, C.P. Huang, M. Asce, Adsorption characteristics of fluoride onto hydrous alumina, J. Environ. Eng. 112 (6) (1986) 1054–1069.
[15] J.J. Schoeman, G.W. Leach, An investigation of the performance of two newly installed defluoridation plants in South Africa and some factors affecting their performance, Water Sci. Technol. 19 (1986) 953–965.
[16] J.J. Schoeman, H. Macleod, The effect of particle size and interfering ions on fluoride removal by activated alumina, Water SA 13 (4) (1987) 229–234.
[17] A.K. Chaturvedi, K.P. Yadava, K.C. Pathak, V.N. Singh, Defluoridation of water by adsorption on fly ash, Water, Air Soil Pollut. 49 (1990) 51–60.
[18] J.A.I. Omueti, R.L. Jones, Fluoride adsorption by Illinois soils, J. Soil Sci. 28 (1977) 546–572.
[19] A. Elmidaoui, F. Elhanouni, M. Taky, L. Chay, M.A.M. Sahli, L. Echihabi, M. Hafsi, Optimization of nitrate removal operation from ground water by electrodialysis, Sep. Purif. Technol. 29 (2002) 235–244.
[20] M. Pontie, C.K. Diawara, M. Rumeau, Streaming effect of single electrolyte mass transfer in nanofiltration: potential application for the selective defluorination of brackish drinking waters, Desalination 151 (2002) 267–274.
[21] W. Czarnowski, K. Wrzesniowska, J. Krechniak, Fluoride in drinking water and human urine in Northern and Central Poland, Sci. Total Environ. 191 (1996) 177–184.
[22] N. Azbar, A. Turkman, Defluoridation in drinking waters, Water Sci. Technol. 42 (1–2) (2000) 403–407.
[23] W. Wang, R. Li, J. Tan, K. Luo, L. Yang, H. Li, Y. Li, Adsorption and leaching of fluoride in soils of China, Fluoride 35 (2) (2002) 122–129.
[24] M. Agarwal, K. Rai, R. Shrivastav, S. Dass, Defluoridation of water using amended clay, J. Cleaner. Products 11 (2003) 439–444.
[25] J. B. Du Plessis, What would be the maximum concentration of fluoride in water that would not cause dental fluorosis? Fluoride and fluorosis, The Status of S. Afr. Res., North West Province, 4, 1995.
[26] T. Chernet, Y. Trafi, V. Valles, Mechanism of degradation of the quality of natural water in the lakes region of the Ethiopian rift valley, Water Res. 35 (12) (2002) 2819–2832.
[27] H. Mjengera, G. Mkongo, Appropriate defluoridation technology for use in fluorotic areas in Tanzania, 3rd WaterNet Symp., Water Demand Management for Sustainable Development, 2002.
[28] W.K.N. Moturi, M.P. Tole, T.C. Davies, The contribution of drinking water towards dental fluorosis: a case study of Njoro division, Nakuru district, Kenya, Environ. Geochem. Health 24 (2002) 123–130.
[29] W.B. Apambire, D.R. Boyle, F.A. Michel, Geochemistry, genesis and health implications of fluoriferous groundwaters in the upper regions of Ghana, Environ. Geol. 33 (1997) 13–24.
[30] Y. Travi, Hydrogéologie et hydrologie isotopique des aquifères fluorés du bassin du Sénégal, PhD Thesis, University of Paris-Sud, Orsay (1988); Mémoire No. 95, CNRS, ISSN 0302-2684, 1993.
[31] W.J. Muller, R.G.M. Heath, M.H. Villet, Finding the optimum: fluoridation of potable water in South Africa, Water SA 24 (1) (1998) 21–27.

[32] G. Notcutt, F. Davies, Biomonitoring of volcanogenic fluoride, Furnas Caldera, Sao Miguel, Azores, J. Volcan. Geoth. Res. 92 (1999) 209–214.
[33] Y.H. Li, S. Wang, A. Cao, D. Zhao, X. Zhang, C. Xu, Z. Luan, D. Ruan, J. Liang, D. Wu, B. Wei, Adsorption of fluoride from water by amorphous alumina supported on carbon nanotubes, Chem. Phys. Lett. 38 (3) (2001) 469–476.
[34] H.T. Dean, Classification of mottled enamel diagnosis, J. Am. Dent. Assoc. 211 (1934) 421–1426.
[35] S. Hillier, C. Cooper, S. Kellingray, G. Russell, H. Hughes, D. Coggon, Fluoride in drinking water and risk of hip fracture in the UK: a case-control study, The Lancet 335 (2000) 265–269.
[36] A.K. Susheela, Sound planning and implementation of fluoride and fluorosis mitigation programme in an endemic village, International Workshop on Fluoride in Drinking Water, 2001.
[37] J. Cao, Y. Zhao, J. Liu, Brick tea consumption as the cause of dental fluorosis among children from Mongol, Kazal and Yugu populations in China, Food Chem. Toxicol. 35 (1997) 827–833.
[38] K.F. Fung, Z.Q. Zhang, J.W.C. Wong, M.H. Wong, Fluoride contents in tea and soil from tea plantation and the release of fluoride into tea liquor during infusion, Environ. Pollut. 104 (1999) 197–205.
[39] A. Mekonen, P. Kumar, A. Kumar, Integrated biological and physicochemical treatment process for nitrate and fluoride removal, Water Res. 35 (13) (2002) 3127–3136.
[40] C.A. Kailash, S.K. Gupta, A.B. Gupta, Development of new low cost defluoridation technology (KRASS), Water Sci. Technol. 40 (2) (1999) 167–173.
[41] A. Nicolay, P. Bertocchio, E. Bargas, F. Coudore, G.L. Chahin, J.P. Reynier, Hyperkalemia risks in hemodialysed patients consuming fluoride-rich water, Clin. Chim. Acta 281 (1999) 29–36.
[42] M.H. Sy, P. Sene, S. Diouf, Fluorose osseuse au niveau de la main, Société d'Edition de l'association d'enseignement médical des hopitaux de Paris, 15 (2) (1996) 109–115.
[43] S.V. Walvekar, B.A. Qureshi, Endemic fluorosis and partial defluoridation of water supplies – a public health concern in Kenya, Comm. Dent. Oral Epidemiol. 10 (3) (1982) 156–160.
[44] W. Choi, Y. Chen, The removal of fluoride from waters by adsorption, J. AWWA, Water Technol. (1979) 562–570.
[45] A.C. Pereira, B.H.W. Moreira, Analysis of three dental fluorosis indexes used in epidemiologic trials, Braz. Dent. J. 10 (1) (1999) 1–60.
[46] H.T. Dean, F.H. Arnold, E. Elvove, Domestic water and dental caries, Publ. Health Report 57 (1942) 1115–1179.
[47] I.L. Carstens, A.J. Louw, E. Kruger, Dental status of rural school children in a suboptimal fluoride area, J. Dent. S. Afr. 50 (9) (1995) 405–411.
[48] B. Mothusi, Psychological effects of dental fluorosis. Fluoride and fluorosis, The Status of S. Afr. Res., Pilanesberg National Park, North West Province, 7, 1995.
[49] A.J. Louw, U.M.E. Chikte, Fluoride and fluorosis. The status of research in South Africa, Tygerberg, South Africa. 2nd International Workshop on Fluorosis and Defluoridation of Water, Int. Soc. Fluoride Res., 1997.
[50] M.J. Rudolph, M. Molefe, U.M.E. Chikte, Dental fluorosis with varying levels of fluoride in drinking water. Fluoride and fluorosis, The Status of S. Afr. Res., North West Province, 5, 1995.
[51] S. Zietsman, The relationship between the geological variation, the F^- of the water and the spatial variation in the occurrence of dental fluorosis in an endemic area, J. S. Afr. Geol. 71 (1987) 102–108.
[52] D.M. Steiner, G. Steiner, Fluoride as essential element in the prevention of disease, Med. Hypotheses 62 (2004) 710–717.

[53] M. Yang, T. Hashimoto, N. Hoshi, H. Myoga, Fluoride removal in a fixed bed packed with granular calcite, Water Res. 33 (16) (1999) 3395–3402.
[54] C.L. Yang, R. Dluhy, Electrochemical generation of aluminium sorbent for fluoride adsorption, J. Hazard. Mater. 94 (3) (2002) 239–252.
[55] N. Parthasarathy, J. Buffle, W. Haerdi, Combined use of calcium salts and polymeric aluminium hydroxide for defluoridation of waste waters, Water Res. 20 (4) (1986) 443–448.
[56] R. Johnston, H. Heijnen, Safe water technology for arsenic removal. Report, World Health Organization (WHO), 2002.
[57] C.A. Bower, J.T. Hatcher, Adsorption of fluoride by soils and minerals, J. Soil Sci. 3 (103) (1967) 151–154.
[58] C. Zevenbergen, L.P. Van Reeuwijk, G. Frapporti, R.J. Louws, R.D. Schuiling, A simple method for defluoridation of drinking water at village level by adsorption on Ando soils in Kenya, Sci. Total Environ. 188 (1996) 225–232.
[59] J. Omueti, R.L. Jones, Fluoride adsorption by Illinois soils, J. of Soil Sci. 28 (1977) 546–572.
[60] S.M. Luther, L. Poulsen, M.J. Dudas, P.M. Rutherford, Fluoride sorption and mineral stability in an Alberta soil interacting with phosphogypsum leachate, Can. J. Soil Sci. 76 (1996) 83–91.
[61] A.K. Chaturvedi, K.C. Pathak, V.N. Singh, Fluoride removal from water by adsorption on China clay, Appl. Clay Sci. 3 (1988) 337–346.
[62] S. Hauge, R. Österberg, K. Bjorvatn, K.A. Selvig, Defluoridation of drinking water with pottery: effect of firing temperature, Scand. J. Dent. Res. 102 (1994) 329–333.
[63] K. Bjorvatn, A. Bardsen, R. Tekle-Haimanot, Defluoridation of drinking water by use of clay/soil, Bergen, 2nd International Workshop on Fluorosis and Defluoridation of Water, Publ. Int. Soc. Fluoride Res. 1997.
[64] M.P. Motalane, C.A. Strydom, Potential groundwater contamination by fluoride from two South African phosphogypsums, Water SA 30 (4) (2004) 465–468.
[65] M. Srimurali, A. Pragathi, J. Karthikeyan, A study on removal of fluorides from drinking water by adsorption onto low-cost materials, Environ. Pollut. 99 (1998) 285–289.
[66] P.M.H. Kau, D.W. Smith, P. Binning, Experimental sorption of fluoride by kaolinite and bentonite, Geoderma 84 (1998) 89–108.
[67] M. Mahramanlioglu, I. Kizilcikli, I.O. Biccer, Adsorption of fluoride from aqueous solution by acid treated spent bleaching earth, J. Fluorine Chem. 115 (1) (2002) 41–47.
[68] Y.D. Lai, J.C. Liu, Fluoride removal from water with spent catalyst, Sep. Sci. Technol. 31 (20) (1996) 2791–2803.
[69] A.M. Raichur, M. JyotiBasu, Adsorption of fluoride onto mixed rare earth oxides, Sep. Purif. Technol. 24 (1–2) (2001) 121–127.
[70] Y.C. Lu, K. Esengul, M. Ersoz, Removal of fluoride form aqueous solution by using red mud, Sep. Purif. Technol. 28 (1) (2002) 81–86.
[71] N.V.R. Mohan Rao, C.S. Bhaskaran, Studies on defluoridation of water, J. Fluorine Chem. 41 (1988) 17–24.
[72] C. Castel, M. Schweizer, M.O. Simonnot, M. Sardin, Selective removal of fluoride ions by a two-way ion-exchange cyclic process, Chem. Eng. Sci. 55 (17) (2000) 3341–3352.
[73] L.S. Cheng, Electrochemical method to remove fluorine from drinking water, Water Supply 3 (1985) 177–186.
[74] N. Mameri, A.R. Yeddou, H. Lounci, D. Belhocine, H. Grib, B. Bariou, Defluoridation of septentrional Sahara water of North Africa by electrocoagulation process using bipolar aluminium electrodes, Water Res. 32 (5) (1998) 1604–1612.
[75] F. Pouet, F. Persin, M. Rumeau, Intensive treatment by electrocoagulation – flotation – tangential flow microfiltration in areas of high seasonal population, Water Res. 25 (1992) 247–253.

[76] H. Garmes, F. Persin, J. Sadeaur, G. Pourcelly, M. Mountadar, Defluoridation of groundwater by a hybrid process combining adsorption and Donnan dialysis, Desalination 145 (2002) 287–291.
[77] L. Durand-Bourlier,J. M. Laine, Proc. Membrane Technology Conf., New Orleans, 1997, pp. 1–16.
[78] M. Hichour, F. Persin, J. Sandeaux, C. Gavach, Fluoride removal from waters by Donnan dialysis, Sep. Purif. Technol. 18 (2000) 1–11.
[79] Z. Amor, B. Bariou, N. Mameri, M. Taky, S. Nicolas, A. Elmidaoui, Fluoride removal from brackish water by electrodialysis, Desalination 133 (2001) 215–223.
[80] N. Hilal, H. Al-Zoubi, A. Mohammad, A. Abu-Arabi, A comprehensive review of nanofiltration membranes: treatment, pretreatment, modelling and atomic force microscopy, Desalination 170 (2004) 281–308.
[81] J. M. Rovel, State and behaviour of seawater desalination in the future, Proc. CHEMRAWNXV, 21–23 June 2004, Paris, pp. 22–28.
[82] H.M. Krieg, S.J. Modise, K. Keizer, H.W.J.P. Neomagus, Salt rejection in nanofiltration for single and binary salt mixtures in view of sulphate removal, Desalination 171 (2004) 205–215.
[83] K.S. Spiegler, O. Kedem, Thermodynamics of hyperfiltration (reverse osmosis): criteria for efficient membranes, Desalination 1 (1966) 311–326.
[84] S. Jain, S.K. Gupta, Analysis of modified surface pore flow model with concentration polarization and comparison with Spiegler–Kedem model in reverse osmosis system, J. Membr. Sci. 232 (2004) 45–61.
[85] Z.V.P. Murphy, S.K. Gupta, Estimation of mass transfer coefficient using a combined nonlinear membrane transport and film theory model, Desalination 109 (1997) 39–49.
[86] R.J. Petersen, Composite membranes, J. Membr. Sci. 83 (1993) 81–93.
[87] A. Maurel, Dessalement de l'eau de mer et des eaux saumâtres, Tech et Doc, 2001.
[88] A. Lhassani, M. Rumeau, d. Benjelloun, Essais d'interprétation des mécanismes de transfert des sels en nanofiltration, Tribune de l'eau 1–3 (2000) 100–107.
[89] M. Manttari, T. Pekuri, M. Nystrom, NF270 a new membrane having promising characteristics and being suitable for treatment of dilute effluents from the paper industry, J. Membr. Sci. 242 (2004) 107–116.
[90] D. Violleau, H. Essis-Tome, H. Habarou, J.P. Croue, M. Pontie, fouling studies of a polyamide nanofiltration membrane by selected natural organic matter: an analytical approach, Desalination 173 (2005) 223–238.
[91] H. Dach, J. Leparc, H. Suty, C. Diawara, A. Jadas-Hecart, A. Lhassani, M. Pontie, Innovative approach for characterization of nanofiltration (NF) and low pressure reverse osmosis (LPRO) membranes for brackish water desalination, Desalination, 2006 (submitted).

CHAPTER 3

Calixpyrrole–Fluoride Interactions: From Fundamental Research to Applications in the Environmental Field

Angela F. Danil de Namor,* and Ismail Abbas

Laboratory of Thermochemistry, Chemistry Division, School of Biomedical and Molecular Sciences, University of Surrey, Guildford, Surrey GU2 7XH, UK

Contents

Abstract

Synthetic macrocycles such as calixpyrroles are capable of complexing anions and discriminating between them most effectively. This chapter is concerned with calixpyrrole and derivatives with selective properties towards the fluoride anion as demonstrated through the use of spectrometric, electrochemical and thermal (calorimetry) data. Selectivity is one of the main features in supramolecular chemistry. As such the importance of thermodynamics in assessing quantitatively selectivity is emphasised. An account is given about the steps undertaken for the thermodynamic characterisation of the binding process involving calixpyrroles and the fluoride anion in different media. Thus based on stability constant data, selectivity factors are calculated to illustrate the anion, receptor and medium effects on the selective binding of calixpyroles with the fluoride anion. Representative examples are given to demonstrate the role of solvation on the complexation process.

*Corresponding author.;
E-mail: A.Danil-De-Namor@surrey.ac.uk

FLUORINE AND THE ENVIRONMENT, VOLUME 2
ISSN 1872-0358 DOI: 10.1016/S1872-0358(06)02003-3

The applications of calixpyrroles in the design of sensors and new materials with potential use as decontaminant agents for the removal of fluorides from water are discussed.

1. FLUORIDE DILEMMA

Fluorine is a non-metal, characterised by its reactivity and electronegativity [1]. As such it combines with most elements (except oxygen and noble gases) to form fluorides (inorganic and organic). In the environment, inorganic fluorides predominate over organic fluorides [2]. During last century environmental concern about fluorides was focused on inorganic compounds although there are about 30 naturally occurring as well as manufactured organo-fluorides that are released into the environment [2]. Identified World reserves of fluorite (natural mineral form of calcium fluoride) are around the order of 500 million tonnes [2]. There is a wide range sources of fluorides which can be classified under two headings.

(i) Naturally occurring fluoride, for which the main source results from the weathering of fluoride minerals while the second major source are volcanoes through their release of gases containing hydrogen fluoride into the atmosphere with annual emissions of inorganic fluorides of the order of 60–6000 ktonnes. The third major natural source is provided by marine aerosols (20 ktonnes of inorganic fluorides per year) [3].
(ii) Fluoride resulting from human activities. Representative examples of these activities are aluminium smelting, phosphate processing operations, combustion of coal, manufacture of steel, brick, tile, clay and glass products, domestic sewage, etc. Consequently fluorides are found in water, air and soil, as well as in plants and animals and therefore these are part of the food chain consumed by humans. While fluoride air pollution occurs mainly in the vicinity of industrial areas, fluoride is released into the environment by a wide range of sources [4,5]. It is also likely that some of the fluorides emitted into the air are eventually carried into surface water through precipitation. Levels of fluoride in surface waters vary according to the location and the proximity to emission sources. The concentration of fluoride in unpolluted fresh and seawater generally ranges from 0.03 to 0.3 ppm for the former and 1.2 to 1.5 ppm for the latter [6].

Air pollution can lead to a substantial increase in fluoride content in soils through

(i) Particulate fluoride
(ii) Absorption of gaseous fluoride from rain or snow and
(iii) Fluoride-containing water used in irrigation. It has been reported [7] that more than 90% of the natural fluoride content in soils is practically insoluble or

tightly bound to soil particles. The fluoride content appears to be lower near the surface than in the inside particles indicating that its soluble fraction may be easily removed from the soil surface by water seeping into the ground. It appears therefore that under normal conditions the amount of fluoride available to plants may be relatively small even from rich-fluoride soils.

At this stage it seems relevant to describe some of the implications related to fluoride contamination in ecosystems. There is plenty of evidence in the literature [7,8] on the transformation that many environmental contaminants can undergo by the action of living organisms. In some cases, the resulting substance (metabolite) is characterised by a higher degree of toxicity than the pollutant in its original form. A typical example is the methylation of mercury by bacteria [9]. There is evidence that some plants are able to synthesise organic fluoride compounds, mainly fluoroacetate and fluorocitrate from inorganic fluorides. In fact, fluoroacetates and their related compounds are among the most poisonous substances known [10]. Indeed, their toxicity is much higher than that of inorganic fluorides.

Environmental contamination by fluorides and fluoride exposure *via* drinking water, foodstuffs and dental products has been the subjects of many scientific papers and review articles [11,12]. The fluoride ion is a direct cellular poison with the ability to bind calcium and therefore to interfere with the activity of proteolytic and glycolytic enzymes such as phosphatases, hexokinase, enolase, succinic dehydrogenase and pyruvic oxidase. It is well established that oxygen consumption and blood clotting are inhibited by fluoride and erythrocyte glycolysis is substantially induced by this anion [13]. Hydrogen fluoride inhalation leads to extreme irritation of the respiratory tract. Thus, its contact with skin and eyes results in coughing and choking. Irritation caused by the liquid or vapour may result in severe burns and long term or permanent visual defects. For detailed information regarding the implications associated with environmental contamination by fluorides, readers are referred to excellent papers and review articles available in the literature [14,15].

Given the implications involved in fluoride contamination in the environment, the development of

(i) New technological approaches for the removal of fluorides from contaminated sources and
(ii) Analytical tools for monitoring fluorides in water are issues of priority concern. Given that this chapter aims to highlight the scope of supramolecular chemistry in the environmental field and in particular, calix[4]pyrroles, the following section discusses some of the main concepts involved in supramolecular chemistry and the potential applications offered by calix[4]pyrroles due to their selective behaviour for fluorides over other environmentally relevant anions.

2. SUPRAMOLECULAR CHEMISTRY

As the field expands the definition of this subject gains complexity. Based on Lehn's statement [16], supramolecular chemistry is concerned with the interaction of two or more chemical species held together by intermolecular forces. Thus, the interaction between a receptor (host) and a substrate (guest) forms a supermolecule. This complex commonly consists of a macrocyclic ligand as the host for an ionic or neutral guest. Non-covalent interactions include ion–dipole, dipole–dipole, hydrogen binding and van der Waals forces [17]. Key features of supramolecular chemistry involve firstly recognition, where the host shows selectivity towards one substrate over another. Secondly, there is a chemical transformation in the nature of the guest upon complexation with the host, allowing for translocation of the guest through media it would not normally be able to pass through by itself. It is this complex formation that is thought to be responsible for the transport of hydrophilic ions across lipophilic membranes. However, there are other important factors to be considered and these have been discussed in details by Danil de Namor and co-workers [18]. Generally speaking, the supermolecule can be viewed as a protective casing which effectively masks the ion from the hydrophobic media, thus allowing it to pass through.

The earliest recognised examples of synthetic supramolecular structures were the complexes formed from crown ethers and metal cations [19]. Since then numerous macrocycles have been synthesised. Representative examples are the cryptands [20]. These differ from crown ethers in that the former contains a tridimensional cavity while the latter are characterised by a hole. Similarly, calix[4]arenes are compounds with a 'cup'-like structure that through lower rim functionalisation gives rise to a hydrophilic and a hydrophobic cavity, thus allowing the reception of ionic species in the former and neutral species in the latter. Most of the above mentioned macrocycles are known for their capability to serve as cation receptors.

However, anion receptors remain less well developed for a number of reasons which have clearly stated in a review article published by Dietrich [21].

Among these are

(i) as compared with isoelectronic cations, anions are considerably larger. Therefore the charge/size ratio is lower than that for cations. As a result highly flexible receptors are required.
(ii) Anions have different geometries and the design of receptors needs to take into account an appropriate orientation for a given anion.
(iii) Anions are characterised by higher hydration energies than cations of similar size. Therefore the competition between solvent and receptor for the anion is greater.
(iv) Receptor–anion interactions are usually weaker than those involving cations.

Calixpyrroles, a more recent addition to the assortment of macrocycles are able to recognise anions selectively and these are discussed in the next section.

3. CALIX[4]PYRROLES

Figure 1 shows the general structure of calixpyrroles. The basic ring structure resembles that of porphyrin. In the past, four pyrrole rings linked by methylene groups to form colourless macrocycles (that feature in the biosynthetic pathways to pyrrole pigments) were referred to as porphyrinogens [22]. The term calix[4]pyrrole was later ascribed to these macrocycles and their synthetic derivatives because of their relation to calix[4]arenes [23].

One of the advantages of calix[4]pyrroles for practical and commercial applications is that they are relatively easy to synthesise and functionalise. Indeed, the methyl substituted calix[4]pyrrole ($R_1 = R_2 = CH_3$) is obtained from the condensation reaction of pyrrole and acetone and its synthesis was first carried out by Baeyer [24] in 1886, although he did not quite realise it. It was 30 years later that the correct structure for the product was proposed and over the years the synthesis of this compound has been optimised and numerous derivatives were produced [25]. After lying virtually dormant in the literature for nearly a century, their anion recognition properties were first reported by Sessler *et al.* in 1996 [26]. The discovery that the NH arrays present in these macrocycles serve as binding sites for anions [26] has provoked great interest in the scientific community. Thus, a variety of derivatives has been prepared with the aim of enhancing the anion binding characteristics of the parent compound [27,28]. This aim has been fulfilled and the enhancement in binding abilities and selectivity have been successfully achieved [29,30]. The following section discusses calix[4]pyrrole, its

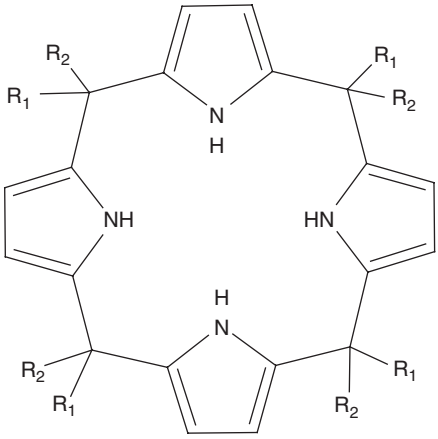

Fig. 1. Molecular structure of Calix[4]pyrrole.

derivatives and their interaction with the fluoride anion as assessed from spectrometric (^{1}H NMR, fluorescence spectroscopy), electrochemical (conductometry and cyclic voltammetry) and thermal (titration calorimetry) techniques.

4. SELECTIVE INTERACTION OF CALIX[4]PYRROLES WITH THE FLUORIDE ANION

The task of designing anion receptors is much more complex than that involving cations due to the chemical and physico-chemical characteristics of anions such as their size, geometry and often their pH dependence.

Selectivity is one of the main features in supramolecular chemistry and the search for receptors able to discriminate between one substrate from another has greatly motivated the synthetic developments in this area. A quantitative evaluation of the selective behaviour of a receptor for one species (ionic or neutral) over another can be obtained from the ratio of their thermodynamic stability constants in a given solvent and a given temperature.

Therefore, thermodynamics plays a fundamental role in supramolecular chemistry. However, thermodynamics is rigorous and as such, a great deal of ancillary information is required prior to the formulation of an equation representative of the process taking place in solution, such as, the composition of the complex and the nature of the speciation in solution. For the latter and when electrolytes are involved, knowledge of the ion-pair formation of the free and complex salts in the appropriate solvent is required particularly in non-aqueous solvents. This information would allow the establishment of the concentrations at which particular ions are the predominant species in solution. Similar considerations must be taken into account when neutral receptors are involved, given that in dipolar aprotic or inert solvents, monomeric species are not always predominant in solution. In addition, awareness of the scope and limitations of the methodology used for the derivation of thermodynamic data for the complexation process is needed and this aspect has been addressed elsewhere [18].

Unfortunately, these issues have not been often considered and have led to some controversy in the anion complexation data involving calixpyrroles. The following sections will discuss ^{1}H NMR, conductometric and thermodynamics studies involving calixpyrrole, its derivatives and their interactions with the fluoride anion in different media.

In the molecular recognition arena, the design and development of receptors that will bind selectively a single guest from a collection of putative guest species is an important goal. The calixpyrrole anion receptors (**1–21**) that show high selectivity for the fluoride anion are given here. Among the anion receptors, colorimetric and fluorescent chemosensors (**22–31**) are discussed later in the chapter.

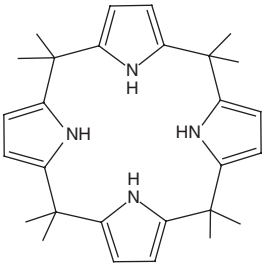

1

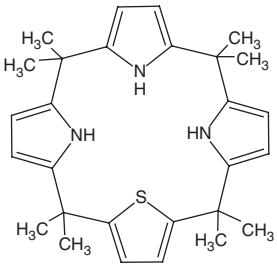

2

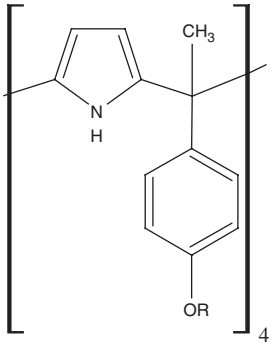

3- R = H ; **4**- R = Me
5- R = CH2COOEt;**6**- R = COMe
7- R = CH2CH2NHCONHC6H5

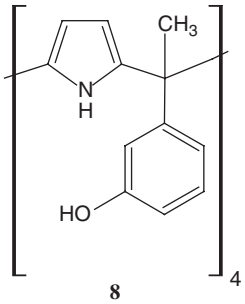

8

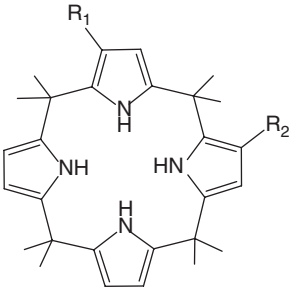

9- R1 = CH2CO2Et; R2= H
10- R1 = R2 = CH2CO2Et

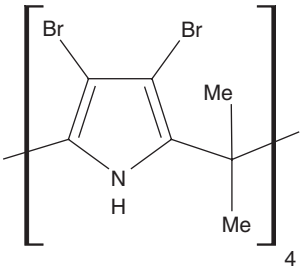

11

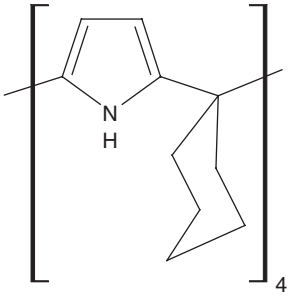

12

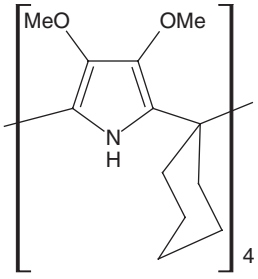

13

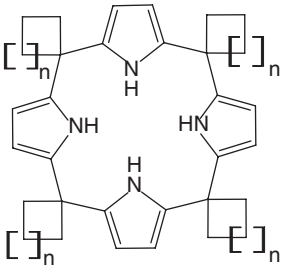

14- n = 2
15- n = 1

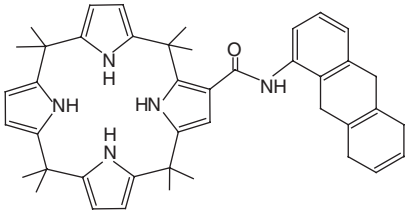

16

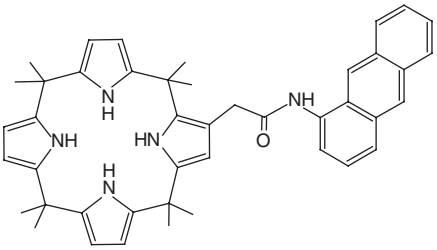

17

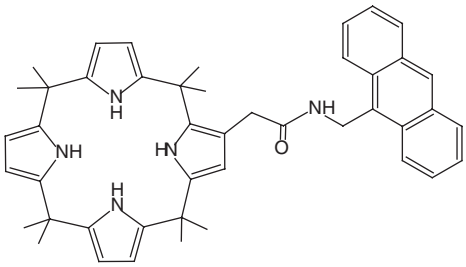

18

5. ^{1}H NMR STUDIES

^{1}H NMR studies have been carried out with the aim of

(i) Establishing the sites of interaction of the receptor with the anion.
(ii) Determining the composition of the anionic complex.
(iii) Calculating the complex stability constant.

Solvents selected are acetonitrile-d_3, dimethyl sulphoxide-d_6 and dichloromethane-d_2. The choice of these solvents was based on the following facts:

(i) The ligands are soluble in these media (unless otherwise indicated).
(ii) In acetonitrile and dimethyl sulphoxide, anion salts are predominantly in their ionic forms at low concentrations. Dichloromethane offers a low permittivity medium and therefore ion-pair formation of the free or anionic complex salts may occur. Therefore, our discussion will be limited to the former two solvents as far as ^{1}H NMR studies are concerned.

Thus, Table 1 reports chemical shift changes found by the addition of anion salts to calix[4]pyrrole and its derivatives relative to those for the free ligand in acetonitrile-d_3 and dimethyl sulphoxide-d_6 at 298 K. These data reveal that the

Table 1. ^{1}H NMR chemical shifts changes ($\Delta\delta$ (ppm)) of (a) 1, 2, 3, 8 and 19 in acetonitrile and (b) 1 and 2 in d_6-DMSO upon complexation with halide anions at 298 K

(a) Acetonitrile

	$\Delta\delta$ (ppm)									
	1		**2**		**3-**$\alpha\alpha\alpha\alpha$	**8-**$\alpha\alpha\beta\beta$		**8-**$\alpha\beta\alpha\beta$		**19**
Anion	NH	Pyrrole-H	H_{N1} (H_{N2})	$H_{Pyrrole\ 1}$ ($H_{Pyrrole\ 2}$)	OH	H_{N1} (H_{N2})	OH	NH	OH	NH
F^-	5.18	−0.28	—	−0.26	0.47	0.09	—	5.48	0.22	3.47
			(3.82)	(−0.15)		(−0.31)				
Cl^-	3.61	−0.26	2.92	−0.23	−0.04	0.08	1.89	2.08	0.69	1.93
			(2.25)	(−0.13)		(−0.33)				
Br^-	3.16	−0.24	0.75	−0.22	−0.02	0.12	0.77	1.00	0.12	1.65
			(0.67)	(−0.06)		(−0.25)				
I^-	0.06	0.02	0.05	−0.01	0.00	—	—	0.10	0.00	—
			(0.09)	(0.00)						

(b) Dimethyl sulphoxide

	$\Delta\delta$ (ppm)			
	1		**2**	
Anion	NH	Pyrrole-H	H_{N1}(H_{N2})	$H_{Pyrrole\ 1}$ ($H_{Pyrrole\ 2}$)
F^-	3.597	−0.283	—	−0.140
			(3.290)	(−0.105)
Cl^-	2.090	−0.025	0.070	−0.017
			(0.040)	(−0.007)
Br^-	0.304	−0.057	0.010	−0.007
			(0.004)	(−0.002)
I^-	0.003	−0.008	0.005	−0.002
			(0.003)	(−0.001)

receptors are not only effective anion binding agents in solution but they are also able to recognise anions selectively with a marked preference for the fluoride ion relative to other spherical (chloride, bromide and iodide) and non-spherical (dihydrogen phosphate) anions. The most substantial changes are observed for the pyrrole NH and β-CH protons, indicating that these provide the sites of interaction between these ligands and anions in solution. Thus, significant downfield shifts are observed in the NH protons of calixpyrrole derivatives (**1**, **2**, **8**-$\alpha\beta\alpha\beta$ and **19**) upon the addition of halides in acetonitrile-d_3 [31–34], although ligands **1** and **2** exhibit similar pyrrole β-CH chemical shift changes upon the addition of an excess amount of anion salt.

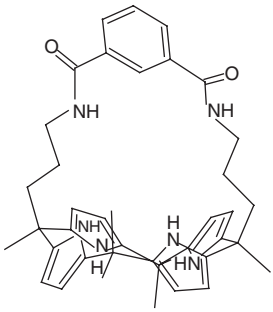

19

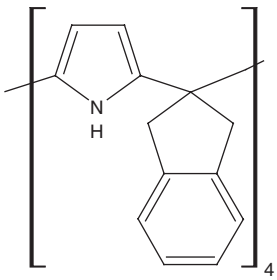

20

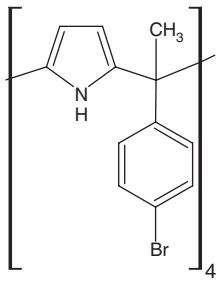

21

On the other hand, the pyrrole-NH protons of **1** show a greater downfield chemical shift change for fluoride ($\Delta\delta = 5.18$ ppm) than those for **2** ($\Delta\delta = 3.82$ ppm). Undoubtedly, the replacement of a pyrrole unit in **1** by a thiophene ring, **2** reduces the affinity of **2** for fluoride relative to **1** in this solvent.

As far as **3**-$\alpha\alpha\alpha\alpha$ is concerned, the low solubility of this ligand in acetonitrile-d_3 has led to difficulties in the location of NH signal in the spectrum due to its broadness. At high [F^-]/**3**-$\alpha\alpha\alpha\alpha$ ratios, a second-binding process, involving presumably the interaction between the fluoride anion and the phenolic OH residues was observed [35]. Thus, chemical shift changes exhibited by the OH protons are reported in Table 1. A clear picture emerging from the ^{1}H NMR data is that as far as the halide ions are concerned, there is a definite size effect in moving down the group. In fact, linear relationships are found in most cases when the $\Delta\delta$ values for the NH protons are plotted against the anion radii [17]. Representative examples are given in Fig. 2.

^{1}H NMR data in dimethyl sulphoxide-d_6 are also shown in Table 1. For the interaction of **1** and **2** with the halide ions, $\Delta\delta$ values in this solvent relative to acetonitrile-d_3 reflect the medium effect on the complexation process. The data reveal that in moving from acetonitrile-d_3 to dimethyl sulphoxide-d_6, there is a substantial decrease in the strength of complexation of these ligands with these anions, although the selectivity trend remains unaltered.

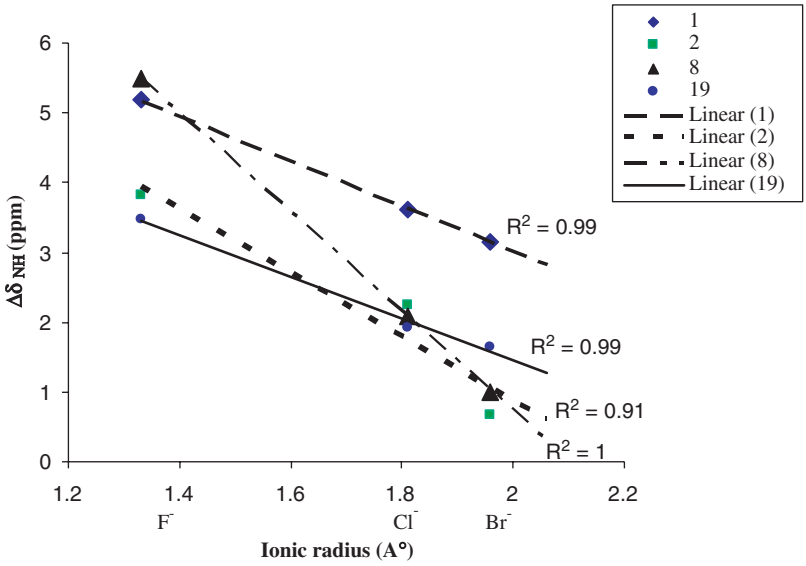

Fig. 2. Relationship between ionic radii (A^0) of halide anions and $\Delta\delta$ (ppm).

Although, in some cases the composition of the anion complex could be obtained from ^{1}H NMR data, this is not universally found. Therefore, the composition of the anion complex and the nature of speciation in solution are often established through conductance measurements and some representative examples on the systems investigated are discussed in the next section.

6. CONDUCTOMETRIC MEASUREMENTS

Conductance measurements have proved to be particularly useful for

(i) Establishing the concentration range over which the free and complex electrolytes are predominantly as ionic species in solution.
(ii) The determination of the composition of the anion complex. For these purposes two separate sets of experiments are required.

The former requires very accurate measurements of conductance carried out at different ionic strengths of the electrolyte under study. Molar conductances are then plotted against the square root of the ionic strength of the electrolyte, $I^{1/2}$. A representative example is shown in Fig. 3, where the molar conductance of the fluoride salt (tetra-*n*-butylammonium as counter ion) is plotted against the square root of the ionic strength of the electrolyte. It should be noted that for a 1:1 electrolyte and provided that this is the only species in solution, ionic strength, is

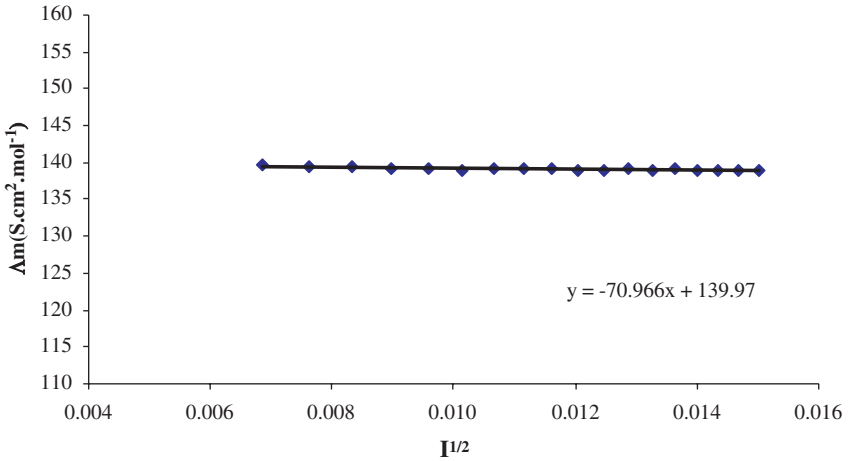

Fig. 3. Molar conductance (in units of S cm^2 mol^{-1}) of Bu_4NF as a function of the square root of molar concentrations in acetonitrile at 298.15 K.

equal to the molar concentration. This plot shows that the behaviour of these salts is typical of that expected for strong electrolytes [36,37].

As far as the determination of the composition of the complex is concerned, this can be obtained from the variation of electrical conductance of an ionic solution titrated with a solution of the neutral receptor as a result of the different mobilities of the species in solution. Plots of molar conductances, Λ_m, against the ratio of the concentrations of the receptor and anion can provide useful information regarding the strength of anion–receptor interaction. In fact, several conclusions can be drawn from the shape of the conductometric titration curves.

Generally speaking, plots with a small slope, showing no change in the gradient indicate that little or no complexation has occurred. A noticeable change indicates moderate complexation. If a sharp break is observed, this implies the formation of a highly stable complex. Illustrative examples of curves showing the molar conductance as a function of the ligand:anion ratio are given in Fig. 4. This figure unambiguously demonstrates the selective behaviour of **1** for the fluoride anion relative to chloride and bromide anions in acetonitrile. Indeed, the conductometric titration curve of fluoride with **1** shows two straight lines intersecting at the 1:1 stoichiometry of the complex demonstrating the formation of a highly stable complex relative to chloride (noticeable change in curvature, moderate complexation) or bromide (plot with small slope, weak complex).

The slope of the conductometric titration curve gives a measure of not only the strength of complexation but also its solvation. If an increase in conductance is observed on complex formation, this may indicate that the anions are highly solvated and therefore less mobile than the complex ion. This behaviour is uncommon but has been previously observed for systems involving lithium and

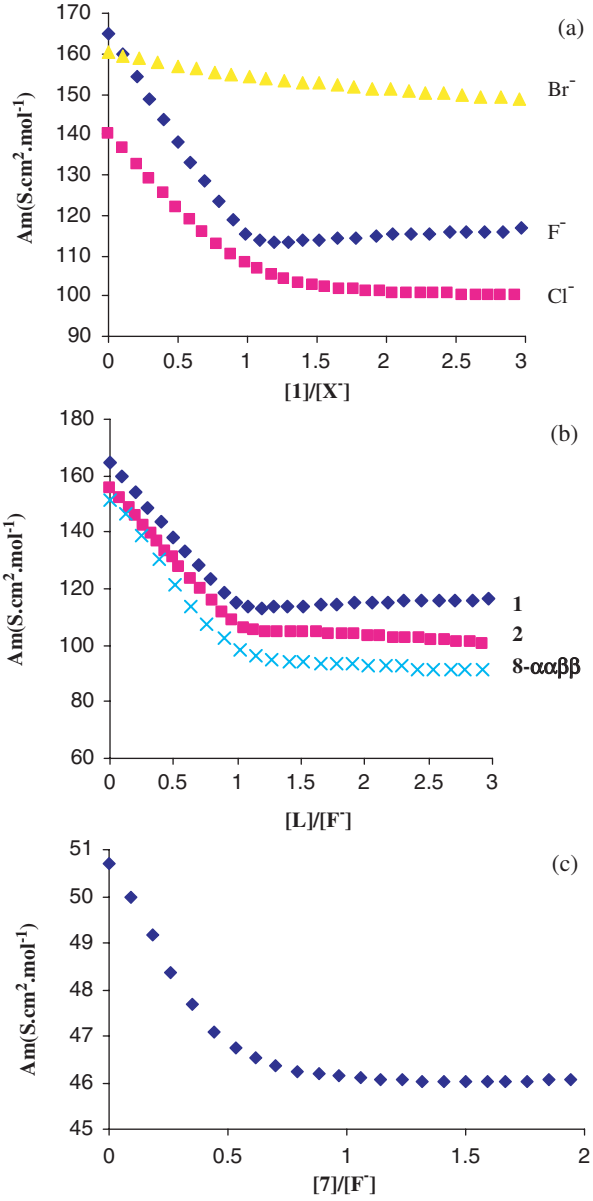

Fig. 4. Conductometric titrations of (a) F^-, Cl^- and Br^- by 1 in acetonitrile, (b) F^- by 1, 2 and 8 in acetonitrile and (c) F^- by 7 in *N*,*N*-dimethylformamide at 289.15 K.

some crown ethers [38]. In solvents of low permittivity such as dichloromethane, an increase in Λ_m values is often observed. This is attributed to the fact that the free salt is not fully dissociated and therefore ion pairs are also present in solution. The addition of the ligand leads to the formation of a complex electrolyte, which is more dissociated than the uncomplexed salt. The conductance behaviour observed for titrations involving fluoride and other halide anions follows the expected pattern with a decrease in Λ_m value upon complex formation. This is frequently attributed to the increase in the size of the fluoride anion in moving from the free to the complex state, which results in a lower mobility and consequently a decrease in conductivity.

The affinity of the various calix[4]pyrrole receptors (**1**, **2**, **8**-$\alpha\alpha\beta\beta$) for the fluoride anion in acetonitrile at 298.15 K is reflected in the conductometric titration curves of fluoride against the ligand/anion ratio. The data shown in Fig. 4b are in accord with ^{1}H NMR studies which show (Table 1) that the most significant chemical shift changes in the resonances of pyrrole NH and β-CH protons of receptors **1** and **2** were observed upon complexation with the fluoride anion in acetonitrile.

Like calix[4]arenes, calix[4]pyrroles are versatile ligands to the extent that the composition of the anion: receptor complex is solvent dependent. A representative example is that involving **8** and the fluoride anion. As shown in Fig. 4b, the well-defined change in curvature observed at 1:1 ligand:fluoride mole ratio indicates that in acetonitrile one fluoride anion interacts per unit of receptor **8**. However, in moving from acetonitrile to *N*,*N*-dimethylformamide, the noticeable changes in curvature observed at a ligand/anion mole ratio of 0.5 and 1, indicate respectively the formation of a 1:2 and 1:1 anion complexes, respectively, in this solvent.

The enhancement in the receptor capacity to host anions has been successfully achieved by the design of double-cavity ligands. This is reflected in the conductometric titration curve (Fig. 4c) for the fluoride anion when titrated with receptor **7**. In fact, in *N*,*N*-dimethylformamide, this receptor takes up two anions per unit of ligand while discriminating against other spherical (chloride, bromide and iodide) and non-spherical (hydrogen sulphate, perchlorate, nitrate and trifluoromethane sulphonate) anions except $H_2PO_4^-$. With this anion only the formation of a 1:1 complex was observed.

From the above discussion it is concluded that

(i) **1** and **2** are able to discriminate among the halide anions following the sequence

$$F^- > Cl^- > Br^- > I^-$$

(ii) The hosting capacity of **7** is greater for the fluoride anion relative to the dihydrogen phosphate anion in *N*,*N*-dimethylformamide.

(iii) The two calix[4]pyrrole isomers, **8**-$\alpha\alpha\beta\beta$ and **8**-$\alpha\beta\alpha\beta$ can discriminate between anions in acetonitrile. Thus, while **8**-$\alpha\alpha\beta\beta$ isomer is able to host two dihydrogen phosphate anions in acetonitrile relative to fluoride and other anions (1:1 complexes), **8**-$\alpha\alpha\beta\beta$ can still complex two dihydrogen phosphate as well as two fluoride anions relative to chloride.

7. THERMODYNAMICS OF COMPLEXATION

We have already discussed the relevant information required for the formation of an equation representative of the process taking place in solution. This is an essential requirement in the derivation of thermodynamic data, given that these must be referred to a well-defined process. In this section, the thermodynamics of complexation of calix[4]pyrroles and the fluoride anion is discussed. Only for comparative purposes and mainly for the calculation of the selectivity factor, data for other ions are included. Thus, Table 2 reports the stability constants and derived standard Gibbs energies, enthalpies and entropies of complexation of calix[4]pyrrole and its derivatives in a wide-range solvents [acetonitrile (MeCN), *N*,*N*-dimethylformamide (DMF), dichloromethane (DCM), dimethyl sulphoxide (DMSO) and propylene carbonate (PC)] at 298.15 K (unless otherwise indicated). The methodology used for the determination of the stability constant (expressed as $\log_{10} K_s$) and the enthalpy of complexation, $\Delta_c H$ is indicated at the footnote of Table 2. The standard Gibbs energy of complexation, $\Delta_c G^0$ is calculated from the relationship shown below

$$\Delta_c G^0 = -RT \ln K_s \tag{1}$$

In this equation R and T are the gas constant and the temperature (K), respectively. The data are referred to the standard state where the activity of reactants and product is equal to 1 mol dm^{-3}.

Standard entropies of complexation are calculated from

$$\Delta_c G^0 = \Delta_c H - T\Delta_c S^0 \tag{2}$$

Thermodynamic data reported in Table 2 reflect the affinity of these calix[4]pyrrole derivatives for the fluoride relative to other anions. Among the halides the selectivity trend follows the sequence

$$F^- > Cl^- > Br^- > I^-$$

However, the fact that fluorides are (i) associated with the application of some phosphate fertilisers that many leach into surface waters and shallow ground water and (ii) by-product of the phosphate fertiliser industry which are the primary sources of fluoride pollution call upon the need of receptors that are able to interact with both anions. Calix[4]pyrrole and most of the derivatives have

Table 2. Thermodynamic parameters of complexation of calixpyrrole receptors with halides and dihydrogen phosphate anions (tetra-*n*-butylammonium as counterion) in acetonitrile, dichloromethane, *N*,*N*-dimethylformamide, dimethyl sulphoxide and propylene carbonate

Receptor	Anion	L:X^-	T (K)	log K_s	$\Delta_c G^0$ (kJ mol^{-1})	$\Delta_c H^0$ (kJ mol^{-1})	$\Delta_c S^0$ (J mol^{-1} K^{-1})	Ref.
1	F^-		298	6.21 ± 0.03[a]	-35.4 ± 0.2	-43.5 ± 0.3	-27	[31]
			303	5.18[c]	-30.04	-34.52	-14	[62]
			298	6.32[e]				[61]
	Cl^-		298	4.70 ± 0.07	-26.8 ± 0.4	-44.7 ± 0.9	-60	[31]
			303	4.98[d]	-28.87	-36.86	-26	[62]
			298	4.72[e]				[61]
	Br^-		298	3.65 ± 0.06	-20.8 ± 0.3	-30.7 ± 0.9	-33	[31]
			303	3.44	-19.96	-34.89	-49	[62]
	$H_2PO_4^-$		298	5.00 ± 0.08[b]	-28.5 ± 0.5	-48.1 ± 0.1	-66	[31]
			303	4.18	-24.22	-48.5	-80	[62]
			295	3.11[e]				[35]
2	F^-		298	5.25 ± 0.01	-29.9 ± 0.1	-31.5 ± 0.1	-5	
	Cl^-		298	4.15 ± 0.07	-23.7 ± 0.4	-51.7 ± 0.5	-95	
	Br^-		298	3.46 ± 0.02	-19.7 ± 0.1	-34.6 ± 0.1	-49	[32]
	$H_2PO_4^-$	(1:1)	298	3.97 ± 0.10[b]	-22.7 ± 0.1	-43.7 ± 0.4	-70	
		(2:1)		3.72 ± 0.10[b]	-21.2 ± 0.2	-17.8 ± 0.1	11	
3-$\alpha\alpha\alpha\alpha$	F^-		295	>4[e]				
	Cl^-		295	2.51[e]				[35,40]
	$H_2PO_4^-$		295	2.70[e]				
3-$\alpha\alpha\alpha\beta$	F^-		295	3.69[e]				
	Cl^-		295	2.41[e]				
	$H_2PO_4^-$		295	2.36[e]				

Table 2. Continued

Receptor	Anion	L:X$^-$	T (K)	log K_s	$\Delta_c G^0$ (kJ mol^{-1})	$\Delta_c H^0$ (kJ mol^{-1})	$\Delta_c S^0$ (J mol^{-1} K^{-1})	Ref.
3-$\alpha\alpha\beta\beta$	F^-		295	>4[e]				
	Cl^-		295	3.15[e]				[35,40]
	$H_2PO_4^-$		295	2.71[e]				
4-$\alpha\alpha\alpha\alpha$	F^-		295	>4[e]				
	Cl^-		295	2.45[e]				[35,40]
	$H_2PO_4^-$		295	< 2				
4-$\alpha\alpha\alpha\beta$	F^-		295	3.04[e]				
	Cl^-		295	2.34[e]				[35,40]
			295	< 1.9				
4-$\alpha\alpha\beta\beta$	F^-		295	3.66[e]				
	Cl^-		295	< 2[e]				[35,40]
	$H_2PO_4^-$		295	< 2				
8-$\alpha\alpha\beta\beta$	F^-		298	3.08 ± 0.02[b]	-17.6 ± 0.1	-97.1 ± 0.8	-267	
	Cl^-		298	2.59 ± 0.04[b]	-14.8 ± 0.2	-55.46 ± 0.04	-136	
	$H_2PO_4^-$	(1:1)	298	3.60 ± 0.02[b]	-20.54 ± 0.04	-24.55 ± 0.06	-13	[33]
		(1:2)		2.50 ± 0.03[b]	-14.43 ± 0.04	-22.63 ± 0.06	-28	
8-$\alpha\beta\alpha\beta$	F^-	(1:1)	298	5.00 ± 0.04[b]	-28.5 ± 0.2	-31.4 ± 0.3	-10	[33]
		(1:2)		4.72 ± 0.01[b]	-27.0 ± 0.1	-61.5 ± 0.3	-116	
	Cl^-		298	2.36 ± 0.03[b]	-13.5 ± 0.1	-86.3 ± 0.3	-244	
	$H_2PO_4^-$	(1:1)	298	4.80 ± 0.02[b]	-27.4 ± 0.3	-20.2 ± 0.1	25	
		(1:2)		2.66 ± 0.10[b]	-15.2 ± 0.5	-29.9 ± 0.6	-50	
16	F^-		298	5.17[f]				[40]
	Cl^-		295	>4[e]				
			298	4.86[f]				

Table 2. Continued

Receptor	Anion	L:X$^-$	T (K)	log K_s	Δ_cG^0 (kJ mol^{-1})	Δ_cH^0 (kJ mol^{-1})	Δ_cS^0 (J mol^{-1} K^{-1})	Ref.
	Br^-		295	3.59[e]				
			298	3.98[f]				
	$H_2PO_4^-$		298	>4[f]				
	HSO_4^-		295	2.77[e]				
			298	4.26[f]				
17	F^-		298	4.69[f]				[40]
	Cl^-		295	>4[e]				
			298	3.81[f]				
	Br^-		295	3.00[e]				
			298	2.86[f]				
	$H_2PO_4^-$		295	3.50[e]				
			298	3.90[f]				
18	F^-		298	4.69[f]				[40]
	Cl^-		295	>4[e]				
			298	3.71[f]				
	Br^-		298	2.63[f]				
	$H_2PO_4^-$		298	3.08[f]				
20	F^-		298	5.39[e]				[61]
	Cl^-		298	5.1[e]				
21-$\alpha\alpha\beta\beta$	F^-		295	>4				[40]
	Cl^-		295	3.30				
	$H_2PO_4^-$		295	2.95				
21-$\alpha\alpha\alpha\beta$	F^-		295	>4				[40]
	Cl^-		295	3.32				

Table 2. Continued

Receptor	Anion	L:X$^-$	T (K)	log K_s	$\Delta_c G^0$ (kJ mol^{-1})	$\Delta_c H^0$ (kJ mol^{-1})	$\Delta_c S^0$ (J mol^{-1} K^{-1})	Ref.
	$H_2PO_4^-$		295	2.95				
22	F^-			5.34[f]				[46]
	Cl^-			4.02[f]				
	$H_2PO_4^-$			5.22[f]				
23	F^-			>6[f]				[46]
	Cl^-			4.26[f]				
	$H_2PO_4^-$			5.65				
24[h]	F^-			>5.30[f]				[46]
	Cl^-			<4[f]				
	$H_2PO_4^-$			5.83[f]				
					Dichloromethane			
1	F^-		298	4.23[e]				[26,40]
	Cl^-		298	2.54[e]				
	Br^-		298	1[e]				
	I^-		298	<1[e]				
	$H_2PO_4^-$		298	1.99[e]				
	HSO_4^-		298	<1[e]				
9	F^-		298	3.04[e]				[28]
	Cl^-		298	1.67[e]				
	$H_2PO_4^-$		298	<1				
11	F^-		298	4.43[e]				[28,40]
	Cl^-		298	3.63[e]				
	$H_2PO_4^-$		298	2.81[e]				

Table 2. Continued

Receptor	Anion	L:X$^-$	T (K)	log K_s	$\Delta_c G^0$ (kJ mol^{-1})	$\Delta_c H^0$ (kJ mol^{-1})	$\Delta_c S^0$ (J mol^{-1} K^{-1})	Ref.
			295	2.81[e]				
12	F^-		295	3.56[e]				[26,40]
	Cl^-		295	2.07[e]				
	$H_2PO_4^-$		295	< 1				
13	F^-		295	3.24[e]				[40]
	Cl^-		295	< 1.3[e]				
14	F^-		295	3.48[e]				[40]
	Cl^-		295	2[e]				
15	F^-		295	3.36[e]				[40]
	Cl^-		295	< 2[e]				
16	F^-		298	4.94[f]				[40,47]
	Cl^-		298	3.69[f]				
	Br^-		298	3.01[f]				
	$H_2PO_4^-$		298	4.20[f]				
17	F_-		298	4.52[f]				[47]
	Cl_-		298	2.96[f]				
	$H_2PO_4^-$		298	3.56[f]				
18	F^-		298	4.49[f]				[47]
	Cl^-		298	2.79[f]				
				N,*N*-dimethylformamide				
1	F^-		298	6.8 ± 0.3[a]	-39.0 ± 0.5	-26.2 ± 0.5	43	[31]
	Cl^-		298	4.2 ± 0.1	-24.0 ± 0.6	-14.5 ± 0.1	32	
	Br^-		298	3.4 ± 0.1	-19.1 ± 0.7	-9.2 ± 0.9	33	
	$H_2PO_4^-$		298	4.8 ± 0.1[b]	-27.4 ± 0.6	-18.8 ± 0.3	29	

Table 2. Continued

Receptor	Anion	L:X$^-$	T (K)	log K_s	$\Delta_c G^0$ (kJ mol^{-1})	$\Delta_c H^0$ (kJ mol^{-1})	$\Delta_c S^0$ (J mol^{-1} K^{-1})	Ref.
2	F^-		298	3.71 ± 0.02	−21.3 ± 0.1	−9.2 ± 0.4	40	[32]
	Cl^-		298	3.48 ± 0.04	−19.8 ± 0.2	−21.3 ± 0.9	−5	
7	F^-	(1:1)	298	4.3 ± 0.2[b]	−24.6 ± 0.8	−21.1 ± 0.2	12	[43]
		(1:2)	298	2.8 ± 0.3[b]	−15.7 ± 0.2	−6.4 ± 0.4	32	
	$H_2PO_4^-$		298	4.11 ± 0.03[b]	−23.4 ± 0.2	−22.74 ± 0.02	3	
8-$\alpha\alpha\beta\beta$	F^-	(1:1)	298	3.4 ± 0.1[b]	−19.2 ± 0.8	−13.6 ± 0.3	19	[33]
		(1:2)	298	3.2 ± 0.2[b]	−18.2 ± 1.1	−7.6 ± 0.2	35	
				Dimethyl sulphoxide				
1	F^-		295	>4[e]				[41]
	Cl^-		295	2.99[e]				
	$H_2PO_4^-$		295	3.75[e]				
2	F^-		298	2.12 ± 0.02	−12.1 ± 0.4	−24.5 ± 0.3	−42	[32]
6	F^-		298	1.86[e]				[42]
26	F^-		295	>6[g]				[41]
	Cl^-		295	2.76[g]				
	$H_2PO_4^-$		295	3.66[g]				
27	F^-		295	>6[g]				[41]
	Cl^-		295	2.81[g]				
	$H_2PO_4^-$		295	3.91				
28	F^-		295	>6[g]				[41]
	Cl^-		295	3.45[g]				
	$H_2PO_4^-$		295	5.20[g]				

Table 2. Continued

Receptor	Anion	L:X$^-$	T (K)	log K_s	$\Delta_c G^0$ (kJ mol^{-1})	$\Delta_c H^0$ (kJ mol^{-1})	$\Delta_c S^0$ (J mol^{-1} K^{-1})	Ref.
				Propylene carbonate				
2	F^-		298	4.37 ± 0.02	−24.9 ± 0.1	−13.5 ± 0.1	38	[32]
	Cl^-		298	4.00 ± 0.10	−22.8 ± 0.6	−18.1 ± 0.2	16	
	Br^-		298	3.77 ± 0.10	−21.6 ± 0.5	−7.7 ± 0.4	46	
	$H_2PO_4^-$		298	4.22 ± 0.20	−24.1 ± 0.3	−21.7 ± 0.2	8	

[a] From competitive calorimetry.
[b] Microcalorimetry (TAM).
[c] Calorimetry at 303.15 K using Kcryptand222$^+$ as counter ion.
[d] Tetraethyl ammonium as counterion.
[e] H NMR titration.
[f] Fluorescence spectroscopy.
[g] UV–visible spectroscopy.
[h] Stability constant determined in acetonitrile–water (96:4, pH 7).

potential applications for the removal of both species from contaminated sources, although these are selective for fluorides.

Data in Table 2 reveal that with a few exceptions, the stability of the complexes is enthalpy controlled and entropy destabilised. As previously stated, the variations observed in the thermodynamics of complexation of these systems as a result of the medium effect are the result of the solvation changes that the reactants (anion and receptor) and the product (complex anion) undergo in moving from one medium to another. This issue will be carefully addressed in the next section.

Given that selectivity is one of the main features in supramolecular chemistry, this is now discussed under three main leadings.

(i) Selectivity of calix[4]pyrrole for fluoride over other anions.

A quantitative assessment of selectivity requires accurate stability constant data. Whenever possible, different techniques should be used to derive stability constant data. In doing so, the scope and limitations of the methodology employed to derive the data must be carefully considered.

Availability of stability constant data allows the calculation of the selectivity factor, S, which is calculated from the ratio of stability constants of two ions and a given receptor in a given solvent and temperature as shown below

$$S_{X_1/X_2} = \frac{K_s^{\theta}(X_1)(s_1)}{K_s^{\theta}(X_2)(s_1)} \tag{3}$$

In equation (3), K_s^{θ} is the thermodynamic stability constant, as defined elsewhere [31]. Inspection of Table 3 shows that all the calix[4]pyrrole receptors (except **8**-$\alpha\alpha\beta\beta$, **22** and **24**) in non-aqueous solvents at a given temperature are more selective for the fluoride anion relative to other anions ($X^- = Cl^-$, Br^-, I^-, HSO_4^- and $H_2PO_4^-$).

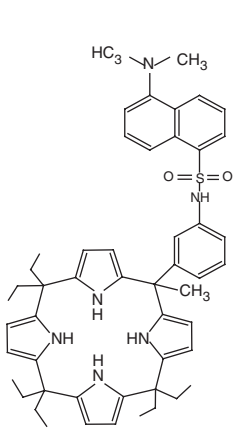

22

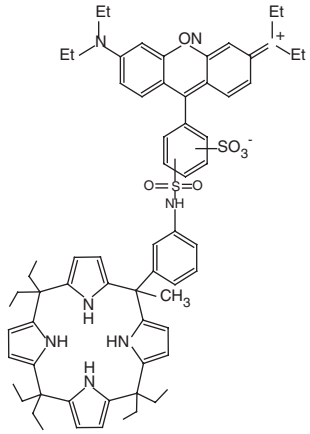

23

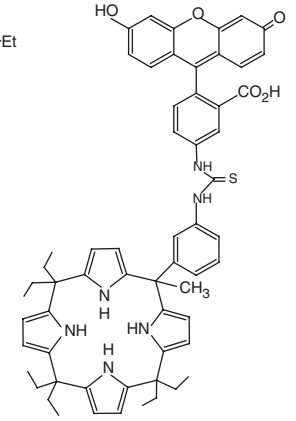

24

Table 3. Selectivity factor S_{F^-/X_2} of calix[4]pyrrole ligands for fluoride anion relative to other anions ($X_2 = Cl^-$, Br^-, I^- and $H_2PO_4^-$) in acetonitrile (MeCN), dichloromethane (DCM), *N*,*N*-dimethylformamide (DMF), dimethyl sulphoxide (DMSO) and propylene carbonate (PC)

			S_{F^-/X_2}				
Receptor	T (K)	X_2	MeCN	DCM	DMF	DMSO	PC
1	298	Cl^-	32	49	398	>10[a]	
		Br^-	363	1698	2512		
		I^-	45,684	<1698			
		$H_2PO_4^-$	16	174	100	>2[a]	
2	298	Cl^-	13		2		2
		Br^-	62				4
		$H_2PO_4^-$	19				1
3-$\alpha\alpha\alpha\alpha$	295	Cl^-	>31				
		$H_2PO_4^-$	>20				
3-$\alpha\alpha\alpha\beta$	295	Cl^-	19				
		$H_2PO_4^-$	21				
3-$\alpha\alpha\beta\beta$	295	Cl^-	>7				
		$H_2PO_4^-$	>19				
4-$\alpha\alpha\alpha\alpha$	295	Cl^-	>35				
		$H_2PO_4^-$	>100				
4-$\alpha\alpha\alpha\beta$	295	Cl^-	5				
		$H_2PO_4^-$	>14				
4-$\alpha\alpha\beta\beta$	295	Cl^-	>46				
		$H_2PO_4^-$	>46				
7	298	$H_2PO_4^-$			2[b]		
8-$\alpha\alpha\beta\beta$		Cl^-	3				
		$H_2PO_4^-$	0.3[b]				
8-$\alpha\beta\alpha\beta$		Cl^-	436				
		$H_2PO_4^-$	2[b]				
9	298	Cl^-		23			
		$H_2PO_4^-$		>110			
11	298	Cl^-		6			
		$H_2PO_4^-$		42			
12	298	Cl^-		31			
		$H_2PO_4^-$		>363			
13	295	Cl^-		>88			
14	295	Cl^-		30			
15	295	Cl^-		>23			
16	298	Cl^-	2	18			
		Br^-	15	85			

Table 3. Continued

Receptor	T (K)	X_2	S_{F^-/X_2} MeCN	DCM	DMF	DMSO	PC
		$H_2PO_4^-$	>15	5			
		HSO_4^-	8				
17	298	Cl^-	8	36			
		Br^-	68				
		$H_2PO_4^-$	6	9			
18	298	Cl^-	10	50			
		Br^-	115				
		$H_2PO_4^-$	41				
20	298	Cl^-	2				
21-$\alpha\alpha\alpha\beta$	295	Cl^-	>5				
		$H_2PO_4^-$	>11				
21-$\alpha\alpha\beta\beta$	295	Cl^-	>5				
		$H_2PO_4^-$	>11				
22		Cl^-	21				
		$H_2PO_4^-$	1				
23		Cl^-	>55				
		$H_2PO_4^-$	>2				
24		Cl^-	>20				
		$H_2PO_4^-$	>0.3				
26	295	Cl^-				>1738	
		$H_2PO_4^-$				>219	
27	295	Cl^-				>1549	
		$H_2PO_4^-$				>123	
28	295	Cl^-				>355	
		$H_2PO_4^-$				>6	

[a] $T = 295$ K.
[b] K_{s_1} of complexation process was considered in calculation.

As an illustrative example, receptor **1** is more selective for fluoride relative to chloride, bromide, iodide and dihydrogen phosphate by factors of 32, 363, 45,684 and 16, respectively. In acetonitrile receptors **8**-$\alpha\alpha\beta\beta$, **22** and **24** show a higher or similar selectivity to dihydrogen phosphate relative to fluoride. On the other hand, the calixpyrrole derivative **2** exhibits a similar selectivity towards dihydrogen phosphate as for fluoride anion [$S = (K_s(F^-)/K_s(H_2PO_4^-)) = 1$].

(ii) Selectivity of calix[4]pyrrole for the fluoride anion in one solvent, s_1, relative to another, s_2. This is defined as the stability constant ratio of a given calix[4]pyrrole with the fluoride anion in one solvent (s_1) relative to

another (s_2) (medium effect). Thus, the selectivity factor S_{s_1,s_2} is shown in equation (4).

$$S_{S_1,S_2} = \frac{K_s^{\theta}(\mathrm{F}^-)(s_1)}{K_s^{\theta}(\mathrm{F}^-)(s_2)} \tag{4}$$

Thus, fluoride and calixpyrrole receptors (**1**, **16**, and **18**) are more stable in acetonitrile than in dichloromethane (Table 4). The stability of the fluoride anion and **2** is greater in acetonitrile than in dimethyl sulphoxide and propylene carbonate by factors of 1349 and 8, respectively. The same analysis carried out for fluoride anion and receptors **1**, **2** and **8**-$\alpha\alpha\beta\beta$ shows that the stability of this anion and these receptors is greater in *N*,*N*-dimethylformamide than in acetonitrile (Table 4).

(iii) Selectivity of calix[4]pyrroles (R_1 and R_2) for fluoride in a given medium (Receptor Effect). The selectivity factor, S_{R_1,R_2} is defined as ratio of stability constants involving two receptors (R_1 and R_2) and the fluoride anion in a given solvent as shown in here.

$$S_{R_1,R_2} = \frac{K_s^{\theta}(R_1)}{K_s^{\theta}(R_2)} \tag{5}$$

As can be inferred from an inspection of Table 5, calix[4]pyrrole **1** is more selective for the fluoride anion than other receptors (**2**, **8**, **16**, **17**, **18**, and **20**) in acetonitrile at 298 K. Similar calculations in dichloromethane show that receptor **16** has the greater selectivity for the fluoride anion as compared with other receptors (**1**, **9**, **11**, **17** and **18**) at 298 K. On the other hand, the selectivity of **1** for the fluoride anion in *N*,*N*-dimethylformamide at 298 K exceeds those of **2**, **7** and **8**-$\alpha\alpha\beta\beta$ by factors of 1230, 316 and 2512, respectively.

Inspection of Table 2 suggests that the anion binding properties of calix[4]pyrroles can be tuned by

Table 4. Selectivity factor $S_{\mathrm{acetonitrile}/s_2}$ of calix[4]pyrrole receptors for fluoride anion in acetonitrile(s_1) relative to other solvents (s_2 = dichloromethane (DCM), *N*,*N*-dimethylformamide (DMF), dimethyl sulphoxide (DMSO) and propylene carbonate (PC)) at 298 K

	$S_{\mathrm{acetonitrile}/s_2}$			
Receptor	DCM	DMF	DMSO	PC
1	95	2.6×10^{-1}		
2		3.6×10^{-1}	1349	8
8-$\alpha\alpha\beta\beta$		5.0×10^{-1}		
16	2			
17	1			
18	2			

Table 5. Selectivity factor S_{R_1/R_2} of calix[4]pyrrole receptor R_1 for fluoride anion relative to another receptor R_2 in acetonitrile (MeCN), dichloromethane (DCM), *N*,*N*-dimethylformamide (DMF) at 298 K

	S_{R_1/R_2}		
R_2	MeCN ($R_1 = 1$)	DCM ($R_1 = 16$)	DMF ($R_1 = 1$)
1	1	5	1
2	9		1230
7	81(1:1)[a]		316
8-$\alpha\alpha\beta\beta$	1349		2512
8-$\alpha\beta\alpha\beta$	16		
9		79	
11		3	
16	11	1	
17	33	3	
18	33	3	
20	7		

[a] Enhanced Capacity.

(i) Appending different groups to the C-rim of these receptors (**9**, **11**, **13**)[39,40].
(ii) Functionalisation with chromophores (**29–31**) [41].
(iii) Synthesising receptors with extended (**3–6** and **8**) [33,35,40,42] and double cavities (**7**) [43].

Some of the factors contributing to the stability of these complexes are now highlighted. Thus, the lower stability constants of **13** for fluoride and chloride relative to **12** [26,40] in dichloromethane may be attributed to the electron-donating ability of the eight C-rim methoxy groups which reduces the acidity of the pyrrole NH protons and hence its anion binding ability. The possibility of ion-pair formation in this solvent (low permittivity) cannot be excluded.

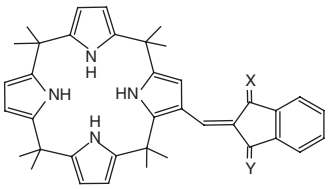

25- X= H2, Y = $C(CN)_2$
26- X = Y = O
27- X = O, Y = $C(CN)_2$
28- X = Y = $C(CN)_2$

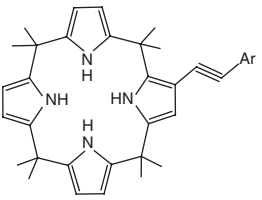

Ar:

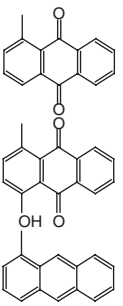

29
30
31

Likewise, **9** shows lower stability constants than **1** in dichloromethane. This reduction in the anion-binding strength may result from the unfavourable interactions between the bound anion and the lone pair electrons of the oxygen atoms of the C-rim ester group or again ion pair formation in this solvent.

However, the anion-binding properties of **29–31** receptors [41] seem to be stronger than those involving **1**. This may be attributed to the electron-withdrawing nature of the dicyanomethylidene, which enhances the ability of the pyrrole NH protons and hence increase their anion binding abilities of these ligands.

The orientation of the phenol group in **8**-$\alpha\alpha\beta\beta$ [33] turned the affinity of this isomer towards the tetrahedral dihydrogen phosphate (1:2, ligand:anion ratio) over the remaining spherical anions (1:1, ligand:anion ratio). Both isomers of **8** show a similar trend in terms of selectivity except that the **8**-$\alpha\beta\alpha\beta$ receptor shows an enhanced selectivity and capacity to interact with the fluoride anion in acetonitrile. Thus, the interaction of 8-$\alpha\beta\alpha\beta$ with fluoride is greater than that for the dihydrogen phosphate anion. The most distinctive feature of the data in Table 2 is that the stability of anion-**1** complexes is greater than for **2** in acetonitrile and *N*,*N*-dimethylformamide. This is attributed to the replacement of one pyrrole unit in **1** by a thiophene unit in **2** that led to a decrease in the complex stability of **2** relative to **1**.

Attempts to correlate stability constant data for **1** and **2** in acetonitrile with the chemical shift changes, $\Delta\delta$, of the pyrrole proton led to straight lines (Fig. 5). These findings clearly demonstrate the selective behaviour of these receptors for the fluoride anion.

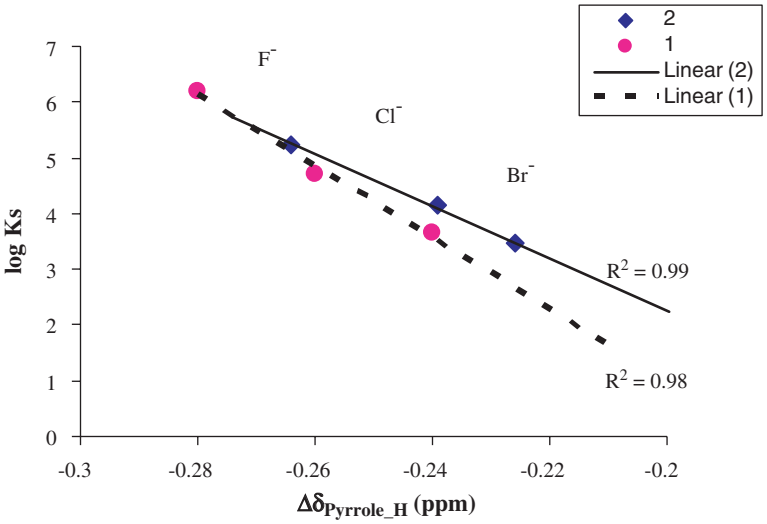

Fig. 5. Linear relationship between log K_s of 1 and 2 and $\Delta\delta$ values for the pyrrole proton in acetonitrile at 298 K.

8. SOLUTION THERMODYNAMICS OF REACTANTS AND PRODUCTS

Thermodynamics parameters of solution ($\Delta_s P^0$; $P = G$, H, S) of reactants (anion salt, MX and receptor, L) and product (complex salt, MLX) combined with corresponding data for the anion complexation process, $\Delta_c P^0$, in a given solvent, s_1, have been extensively used by us with the aim of deriving the thermodynamics referred to the coordination process, $\Delta_{coord} P^0$, where reactants and products are in their pure physical state

$$\Delta_{coord} P^0 = \Delta_s P^0(\mathrm{MX})(s_1) + \Delta_s P^0(L)(s_1) + \Delta_c P^0(s_1) - \Delta_s P^0(\mathrm{MLX})(s_1) \quad (6)$$

These data provide a useful mean of checking the reliability of the thermodynamic parameters associated with the solution and complexation processes. Indeed, coordination data should be the same (within the experimental error) independently of the solvent used in the solution process. This statement is now corroborated by representative examples involving the fluoride anion and **1**. Thus in fulfilling the requirements of equation (6), the enthalpies of solution of the reactants (Bu_4NF and **1**) and product (Bu_4N1F) are combined with the enthalpies of complexation of the fluoride anion and **1** in acetonitrile (MeCN) (equation (7)) and *N*,*N*- dimethylformamide (DMF) (equation (8)) to derive the enthalpy of coordination for this system in the solid state.

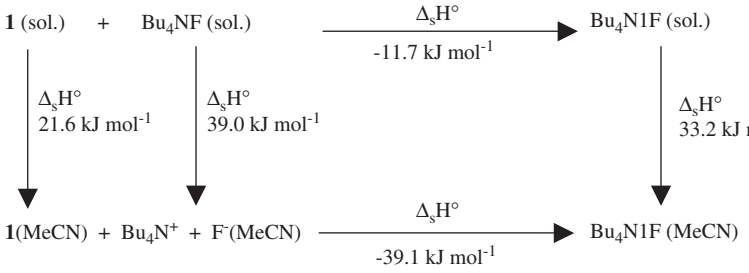

(7)

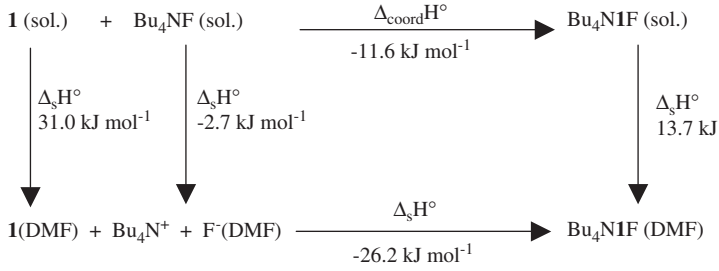

(8)

It can be concluded that for the fluoride-**1** system, both $\Delta_{coord}H^0$ values (equations (7) and (8)) derived from acetonitrile ($\Delta_{coord}H^0 = -11.7\,kJ\,mol^{-1}$) and *N*,*N*-dimethylformamide ($\Delta_{coord}H^0 = -11.6\,kJ\,mol^{-1}$) are in good agreement. For further details regarding the applicability of coordination data readers are referred to literature [18,44].

9. THE MEDIUM EFFECT OF THE COMPLEXATION OF CALIX[4]PYRROLE AND ITS DERIVATIVES WITH THE FLUORIDE ANION

The variations observed in the thermodynamics of complexation of calix[4]pyrrole and its derivatives with the fluoride anion (Table 2) as a result of the medium effect are controlled by the solvation changes that reactants and product undergo in moving from one solvent to another. These differences in solvation are reflected in the thermodynamic parameters of transfer, Δ_tP^0 for the reactants (fluoride and receptor) and the product (the anion complex) from a reference solvent, s_1 to another solvent, s_2. The relationship between these parameters and the thermodynamics of complexation, Δ_cP^0, in these solvents is shown in Equation (9).

$$\Delta_cP^0(s_1) - \Delta_cP^0(s_2) = \Delta_tP^0(L)(s_1 \rightarrow s_2) + \Delta_tP^0(F^-)(s_1 \rightarrow s_2) - \Delta_tP^0(LF^-)(s_1 \rightarrow s_2) \quad (9)$$

Equation (9) implies that complexation is favoured in a medium which is a good solvater for the product and poor for the reactants.

As far as fluoride is concerned, the determination of the standard Gibbs energy of the fluoride salts is by no means a trivial task. Indeed, the salts often undergo solvation when exposed to a saturated atmosphere of a non-aqueous solvent. The calculation of the solution Gibbs energy requires the same composition of the solid in equilibrium with the saturated solution. Therefore, it is not always possible to derive transfer Gibbs energy data for the fluoride salt in non-aqueous media. However, the medium effect can be easily assessed in terms of enthalpy data. Availability of Δ_tH^0 values from acetonitrile to *N*,*N*-dimethylformamide for *L* (*L* = **1**, **2** and **8**), the fluoride anion (based on Ph_4AsPh_4B convention [45]) and the Δ_cH^0 values in acetonitrile and DMF (Table 2), allows the calculation *via* the cycle of Δ_tH^0 values for the fluoride complex. The latter is also based on the Ph_4AsPh_4B convention [45]. By inserting the appropriate equations in the thermodynamic cycles (equations (10)–(12)), it follows that, as far as receptors **1** and **2** are concerned, the higher enthalpic stability for the complexation process in acetonitrile relative to *N*,*N*-dimethylformamide is entirely due to the favourable contribution of the free anion overcoming those for the ligand and its complex since these contribute unfavourably to complexation in acetonitrile.

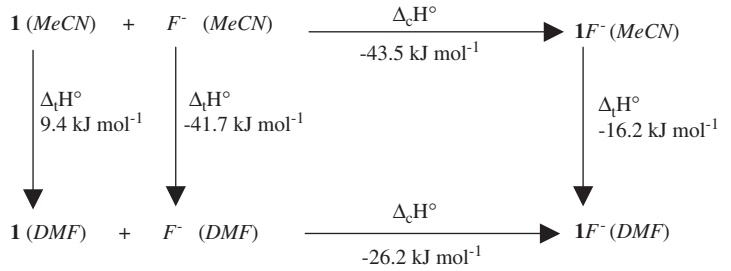

(10)

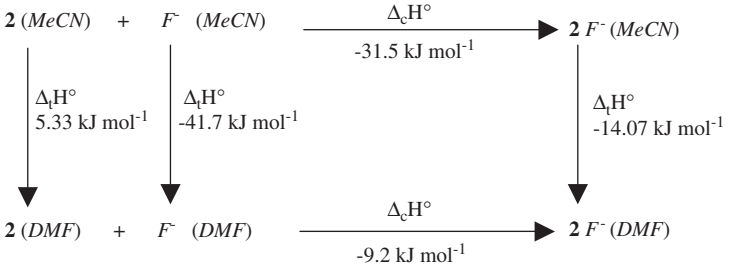

(11)

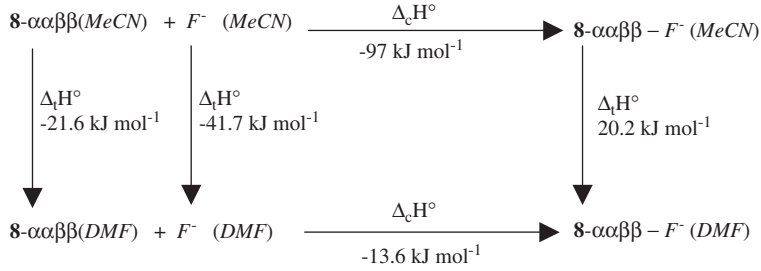

(12)

Another interesting aspect of the data is the decrease in enthalpic stability of the complex relative to the free anion in moving from acetonitrile to *N*,*N*-dimethylformamide. This observation could be explained in terms of the partial shielding of the anion by the ligand in the complex.

Acetonitrile offers the optimal conditions for the complexation of **8**-$\alpha\alpha\beta\beta$ and the fluoride anion (equation (12)) in that both, reactants and product favourably contribute to complex formation in this solvent. Indeed, on the one hand, acetonitrile interacts weakly with the reactants while these undergo strong interaction with *N*,*N*-dimethylformamide to an extent that both, fluoride and receptor are reluctant to interact strongly between themselves. On the other hand, acetonitrile is a better solvating medium for the anion complex than *N*,*N*-dimethylformamide. As a result, the enthalpic stability for the complexation of fluoride and 8-$\alpha\alpha\beta\beta$ in acetonitrile is quite high in contrast with the relatively low $\Delta_c H^0$ value observed for this system in *N*,*N*-dimethylformamide.

The above discussion highlights the importance of the effect of the medium on the complexation of calix[4]pyrroles and fluoride. Indeed, these data are a

reflection of the inherent nature of the solvent and the highly significant involvement in the solvation of reactants and product which control the strength of interaction between anion and receptor in one medium relative to another.

It is quite clear from Table 2 that there is a great deal to be investigated on the thermodynamics of fluoride–receptor interactions in different media.

10. CALIX[4]PYRROLES AND THEIR APPLICATIONS

The following section discusses some of the applications of calixpyrrole derivatives in aspects related to fluoride chemistry, which are relevant to environmental issues.

From the environmental point of view, calix[4]pyrrole and its derivatives show considerable promise in two main areas.

(i) The development of optical-based sensor systems which enable *in situ*, rapid detection of fluorides in water.
(ii) New materials for the removal of fluorides from contaminated sources. These can be achieved by their incorporation into solid support polymeric frameworks. These calixpyrrole-based materials are likely to play a significant contribution in the development of new technological approaches for the removal of fluorides from water. Some of the progress made so far on calixpyrrole anion sensors is now briefly described.

10.1. Calix[4]pyrrole sensors for fluoride

Optical sensors result from the combination of a receptor (able to recognise the substrate and a reporter (chromophore). Thus, changes in the absorption or emission properties resulting from the receptor-substrate binding process allow the detection of the substrate. Most of the contributions on calix[4]pyrrole-based anion sensors have been made by Sessler and co-workers [40,46,47]. These authors have developed anion sensors by linking either a fluorescent report group to calixpyrrole or through the use of *p*-nitrophenolate anions taking part in a displacement reaction. Anthracene derivatives (**16–18**) were used as signalling devices while **1** was the receptor. The fluorescence of these receptors quenched significantly in the presence of anions. Quenching data were used to calculate the stability constants of these receptors in their interaction with the halide and dihydrogen phosphate anions. It was stated by Sessler and co-workers [40,46] that the most efficient quenching was observed after the addition of fluoride anion, although to a lesser extent, quenching was also observed with other anions. Sensors based on receptors **22–24** also reported by Sessler [47] appear to be remarkably selective for fluoride relative to other halide and phosphate anions. It

seems that the presence of an additional binding site involving amide or thiourea moieties in the receptors has certainly enhanced their selective behaviour for dihydrogen phosphate relative to chloride.

Another interesting development in anion sensing is that reported by Nishiyabu and Anzenbacher [41]. These authors by the condensation reaction involving 2-formyl-octamethylcalix[4]pyrrole and 1,3-indanedione derivatives obtained sensors with push–pull chromophores able to display strong intramolecular charge transfer. Thus, an increase in signal output and significant changes in anion selectivity were observed relative to that involving the parent calix[4]pyrrole. Thus, the presence of anions, in particular fluoride led to dramatic colour changes before and after addition of fluoride-containing salts. However, the addition of chloride, bromide and nitrates led to weak or no colour changes [41]. Anion affinities of these sensors follow the sequence **26** > **27** > **28** in dimethyl sulphoxide at 295 K (Table 2).

More recently, a new class of covalent-linked calix[4]pyrrole–anthraquinone compounds (**29–31**) have been introduced by Sessler's group [48]. These are considered to be powerful naked eye sensors for fluoride, chloride and dihydrogen phosphate ions in dichloromethane. The most pronounced colour change was observed upon the addition of the fluoride anion into a solution of the receptor **30** in dichloromethane. The addition of bromide, iodide or nitrate anions did not lead to significant colour changes.

The complexation of a calixpyrrole dimer with the *p*-nitrophenolate anion [49] has been used as a colorimeter sensor by displacing the chromogen anion upon the addition of targeted anions. In this case anions, such as fluoride, displace the *p*-nitrophenolate anion from the complex thus enhancing the absorbance of the *p*-nitrophenolate anion. This was observed as a colourless to yellow colour change.

Sessler, Gale and co-workers [50] have produced ion selective electrodes (ISEs) containing calix[4]pyrrole moieties.

From the environmental viewpoint, the design of ISEs particularly for the '*in situ*' monitoring pollutants in water is important mainly in the Developing World where the most sophisticated analytical instrumentation is not always available and water contamination by toxic ions is on the increase. For supramolecular chemists, ISEs could offer a convenient tool for characterisation of the ion-binding properties of the receptor under interfacial organic-aqueous conditions rather than in water. In the latter medium, either due to low solubility of the receptor or weak receptor–ion interaction, the affinity involved between receptor and host cannot be assessed. It is well established that the sensitivity and selectivity obtained for a given neutral carrier depend significantly on the membrane composition and on the properties of mediator employed as well as the PVC/plasticiser ratio used. The PVC-membrane solutions in Sessler's work were prepared by mixing the ionophore **1**, the plasticiser [2-nitrophynel octyl ether (o-NPOE)] and PVC, both, in presence and absence of a lipophilic additive

[tridodecylmethylammonium chloride (TDDMA)]. The influence of pH on the sensitivity and linear range of the membrane was investigated, where the pH was adjusted with sodium hydroxide and sulphuric acid solutions. At low pH values (3.5 and 5.5), PVC ion selective electrode containing **1** displayed strong anionic responses towards halide and dihydrogen phosphate anions. However, at high pH = 9.0 the ISEs derived from **1** deviate from the Hofmeister selectivity series ($Br^- < Cl^- < OH^- \approx F^- < HPO_4^{2-}$). Consequently, the potentiometric selectivity of ISEs based on **1** is pH dependent.

10.2. Calix[4]pyrrole-based materials

The attachment of macrocycles to solid supports *via* covalent bonding has been the subject of many investigations [51,52]. Low yields generally obtained in the synthetic work and the wide range of applications of these compounds encouraged researchers to find economical ways to use these receptors. The natural choice was to incorporate macrocyclic ligands into polymeric supports or silica so these can be recycled. Blasius and co-workers [53–55] carried out pioneering work in this area. Indeed, these authors have prepared a considerable number of polymeric macrocyclic compounds *via* a polymerisation of crown ethers (dibenzo-18-crown-6 and others) or a cryptand with formaldehyde in formic acid. The properties and applications of these polymers have been extensively discussed by Blasius's group. These materials have been mostly used for cation extraction processes. Blasius's approach has been extended to calixpyrroles by Kaledkowski and Trochimczuk [56] and by the authors [57]. In fact, the former workers have used two strategic approaches to obtain calixpyrrole-based chelating resins. One of them consisted in anchoring meso-tetramethyltetrakis(*p*-hydroxylphenyl) calix[4]pyrrole, **3**, to the vinylbenzyl chloride (VBC)/divinyl benzene (DVB) co-polymer *via* the OH moieties. The second approach is based on Blasius's method using the same calix[4]pyrrole derivative. Preliminary investigations carried out on the anion extraction properties of these materials appear to indicate that while the modified co-polymer is able to remove 44% of fluoride, the percentage of the fluoride anion extracted by the condensation resin was 88% from 10^{-3} molar solutions of fluorides in acetonitrile. Quite clearly these results demonstrate the higher degree of efficiency of the latter resins relative to that of the modified co-polymer. These percentages of extraction are likely to be substantially reduced if water instead of acetonitrile was the source of fluoride. This is due to the competitive effect between the former solvent and the resin for the anion. There is still a great deal of research required to establish the relevant parameters (temperature, ionic strength, maximum loading capacity of the material, interfering ions) for optimising the extraction process. However, the use of these materials as decontaminating agents for the removal of fluoride from water seems to be promising.

Silica gel supports containing amidocalix[4]pyrrole groups (Gel M and Gel B) have been reported by Sessler *et al*. [58] for use in HPLC for anion separation. Several anions including fluoride were retained by these materials.

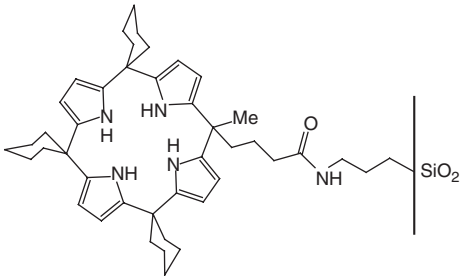

Ge l M

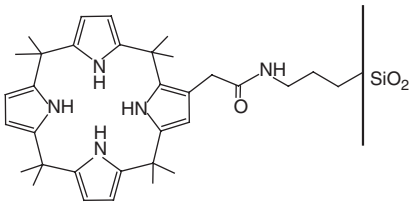

Ge l B

11. FINAL CONCLUSIONS

Calix[4]pyrrole and derivatives involved in this chapter are those receptors which are able to recognise selectively the fluoride anion in solution. It is shown that the fluoride anion binding ability of these receptors can be tuned.

a. By appending different groups to the carbon or C-rim of the calixpyrrole (**9**,**11** and **13**).
b. Functionalisation with chromophores (**29–31**).
c. Synthesising receptors with extended (**3–6** and **8**) and double cavities (**7**). However, calix[4]pyrrole **1** is more selective for the fluoride anion than other receptors (**2**, **8**, **16**, **17**, **18** and **20**) in acetonitrile.

When information was available, calix[4]pyrrole–fluoride interactions were discussed on the basis of ^{1}H NMR, conductometry, titration calorimetry, UV–Visible and fluorescence spectroscopy.

Calix[4]pyrroles are versatile ligands to the extent that the composition of the anion:receptor complex is solvent dependent. This chapter has been concerned with the affinity of calix[4]pyrrole for the fluoride anion. It was therefore considered of relevant to focus attention on the steps required for the derivation of reliable thermodynamic data. It is indeed the ratio between stability constants which defines quantitatively the selectivity factor. Thus, representative examples are given to demonstrate selectivity in terms of anion, receptor and solvent. The key role played by solvation in the complexation of these receptors with the fluoride anion is unambiguously demonstrated in the variations observed in the stability constants, enthalpies and entropies of complexation of these systems in the various solvents (Table 2). One convenient measure to assess solvation is through the thermodynamics of transfer of product and reactants from one

medium to another. Thus, illustrative examples for various systems are given using enthalpy data. Unfortunately, fluoride salts undergo extensive solvation when exposed to saturated atmosphere of a non-aqueous solvents and therefore it is not possible to determine their transfer Gibbs energies in moving from one to another solvent.

We have included in this chapter stability constants for these systems in dichloromethane, although this is a low permittivity medium and therefore the reliability of these data may be reduced by the formation of ion pairs. However, these data may be useful in solvent extraction processes due to the immiscibility of this solvent with water which allows the direct partition of electrolytes in the dichloromethane solvent system [59,60].

Results illustrating the thermodynamics of calixpyrroles and derivatives with fluoride collected in Table 2 show that there is a great deal to be done in this area. In addition, we are not aware of any data available on heat capacities involving these systems. This particular aspect of thermodynamics remains dormant.

Although, the main emphasis of this chapter lies on the fundamental aspects of calixpyrrole–fluoride complexation reactions, with the major part being devoted to the thermodynamic properties of these systems, calixpyrrole receptors seem to be promising for the development of chemical sensors and for the removal of fluorides from water. They also show promise for the separation of anion substrates.

As far as chemical sensors are concerned, colorimetric chemosensors for anions based on calix[4]pyrrole (**16–18**, **22–31**) showed strong binding to the fluoride anion. Receptors (**29–31**) are the first naked-eye detectable chemosensors that are able to discriminate between different anionic substrates as a result of detectable colour changes. On the other hand, the fluorescence of the receptors (**16–18**, **22–28**) is quenched significantly in the presence of anionic guests.

Among the anion carriers, calixpyrrole receptors have found applications as components in anion-selective membrane electrodes. The potentiometric selectivity for membranes ISEs based on calix[4]pyrrole, **1** towards a range of anions, namely fluoride, chloride, bromide and dihydrogen phosphate was found to be pH-dependent.

As far as calix[4]pyrrole-based materials are concerned, particular emphasis should be placed on the production of chelating resins. Those obtained by the condensation reaction of calix[4]pyrrole and formaldehyde in the presence of formic acid offer potential for their use as extracting agents for fluoride removal from water. Their advantage relies on the fact that a single-step procedure is required for polymerisation. However, research in this area is in a preliminary stage. Much work needs to be done to establish the full capacity of these materials to take up fluoride from water, the kinetics of the process, and the optimum experimental conditions for fluoride extraction. Although, their ability to extract fluoride reaches a value of 88% from solutions of tetra-*n*-butylammonium fluoride

in acetonitrile, it is expected that much lower percentages are to be extracted from water. Indeed, their scope as water decontaminating agents requires experimental work taking into account ionic species likely to be present in water. Among these, the counter-ion effect may be significant but can be closely predicted from available data on the transfer Gibbs energies of cations from water to non-aqueous medium [45]. For commercial applications, the recycling of these materials need to be investigated.

Undoubtedly, the future will bring further progress in this area and more developments on the synthesis of calix[4]pyrrole anion receptors. However, the design of anion receptors is still a challenging task.

REFERENCES

[1] N.N. Greenwood, A. Earnshaw, Chemistry of the Elements, Pergamon Press, Toronto, 1984.
[2] H.L. Weinstein, Fluorides in the Environment: Effects on Plants and Animals, CABI, Cambridge, MA, USA, 2004.
[3] R.B. Symonds, W.I. Rose, M.H. Reed, Nature 334 (1988) 415–418.
[4] R.L. Roy, P.G.C. Campbell, S. Prémont, J. Labrie, Toxicol. Chem. 19 (2000) 2457–2466.
[5] J.A. Camargo, J.V. Ward, K.L. Martin, Arch. Environ. Contam. Toxicol. 22 (1992) 107–113.
[6] D.K. Datta, L.P. Gupta, V. Subramanian, Bangladesh Environ. Geol. 39 (2000) 1163–1168.
[7] J.A. Camargo, Chemosphere 50 (2003) 251–264.
[8] S. Klein, H. Woggon, R. Macholz, Nahrung 23 (12) (1985) 59.
[9] J.T. Trevors, J. Basic Microbiol. 26 (8) (1986) 499–504.
[10] R.J. Hall, Fluoride 1 (1) (1968) 9–14.
[11] M. Grimaldo, V. Borja-Aburto, A. Ramirez, M. Rosas, F. Diaz-Barriga, Environ. Res. 68 (1995) 25–30.
[12] M. Alarcon-Herrera, I. Martin-Dominguez, R. Trejo-Vazquez, S. Rodriguez-Dozal, Fluoride 34 (2001) 138.
[13] M. Kessabi, Rev. Méd. Vét. 135 (1984) 497–510.
[14] G. Aydin, E. Çiçek, M. Akdoğan, O. Gökalp, J. Appl. Toxicol. 23 (2003) 437–446.
[15] N.J. Chinoy, Indian J. Environ. Toxicol. 1 (1991) 17–32.
[16] J.-M. Lehn, Supramolecular Chemistry: Concepts and Perspectives, VCH, New York, 1995.
[17] J.W. Steed, J.L. Atwood, Supramolecular Chemistry, Wiley, Chichester, UK, 2000.
[18] A.F. Danil de Namor, R.M. Cleverley, M.L. Zapata-Ormachea, Chem. Rev. 98 (1998) 2495–2525.
[19] B. Dietrich, Cryptands: coordination chemistry of alkali, alkaline-earth and toxic cations, Met. Ions Biol. Med. Proc. Int. Symp. 1 (1990) 447–451.
[20] J.M. Lehn, Pure Appl. Chem. 50 (9–10) (1978) 871–892.
[21] B. Dietrich, Pure Appl. Chem. 65 (7) (1993) 1457–1461.
[22] P.G. Sammes, Comprehensive Organic Chemistry. The Synthesis and Reactions of Organic Compounds: Heterocyclic Compounds 4, Pergamon Press.
[23] P.A. Gale, J.L. Sessler, V. Karl, J. Chem. Soc. Chem. Comm. 1 (1998) 1–8.
[24] A. Baeyer, Ber. Dtsch. Chem. Ges. 19 (1886) 2184.
[25] W.H. Brown, W.N. French, Can. J. Chem. 36 (1958) 371.

[26] P.A. Gale, J.L. Sessler, V. Kral, V. Lynch, J. Am. Chem. Soc. 118 (21) (1996) 5140–5141.
[27] C. Bucher, R.S. Zimmerman, V. Lynch, J.L. Sessler, J. Am. Chem. Soc. 123 (2001) 9716–9717.
[28] P.A. Gale, J.L. Sessler, W.E. Allen, N.A. Tvermoes, V. Lynch, J. Chem. Soc. Chem. Comm. 7 (1997) 665–666.
[29] H. Miyaji, J.L. Sessler, Supramol. Chem. 13 (2001) 661–669.
[30] W. Sato, H. Miyaji, J.L. Sessler, Tetrahedron Lett. 41 (2000) 6731–6736.
[31] A.F. Danil de Namor, M. Shehab, J. Phys. Chem. B 107 (2003) 6462–6468.
[32] A.F. Danil de Namor, I. Abbas, H. Hammud, J. Phys. Chem. B 110 (2006) 2142–2149.
[33] A.F. Danil de Namor, M. Shehab, I. Abbas, M.V. Withams, J. Phys. Chem. 110 (2006) 126653–126659.
[34] C.H. Lee, J.S. Lee, H.K. Na, D.W. Yoon, H. Miyaji, W.S. Cho, J.L. Sessler, J. Org. Chem. 70 (2005) 2067–2074.
[35] P. Anzenbacher Jr., K. Jursikova, V.M. Lynch, P.A. Gale, J.L. Sessler, J. Am. Chem. Soc. 121 (1999) 11020–11021.
[36] C. Drucker, Z. Physik. Chem. 105 (1923) 472–475.
[37] R. Lorenz, Z. Anorg. Allgem. Chem. 118 (1921) 209–222.
[38] A.F. Danil de Namor, C.Y.Ng. Joe, M. Llosa Tonco, M. Salomon, J. Phys. Chem. 100 (1996) 14485–14491.
[39] P.A. Gale, J.L. Sessler, W.J. Genge, V. Kral, M.A. Mckervey, J.L. Sessler, A. Walker, Tetrahedron Lett. 38 (49) (1997) 8443–8444.
[40] J.L. Sessler, P. Anzenbacher Jr., H. Miyaji, K. Jursíková, E.R. Bleasdale, P.A. Gale, Ind. Eng. Chem. Res. 39 (2000) 3471–3478.
[41] R. Nishiyabu, P. Anzenbacher Jr., Org. Lett. 8 (2006) 359–362.
[42] C.J. Woods, S. Camiolo, M.E. Light, S.J. Coles, M.B. Hursthouse, M.A. King, P.A. Gale, J.W. Essex, J. Am. Chem. Soc. 124 (2002) 8644–8652.
[43] A.F. Danil de Namor, M. Shehab, J. Phys. Chem. B 109 (2005) 17440–17444.
[44] A.F. Danil de Namor, Calixarenes 2001, Z. Asfari, V. Böhmer, J. Harrowfield, J. Vicens (Eds.), Kluwer Academic Publishers, Dordrecht, 2001, Chapter 19, p. 346.
[45] B.G. Cox, G.R. Hedwig, A.J. Parker, D.W. Watts, Aust. J. Chem. 27 (1974) 477–501.
[46] P. Anzenbacher Jr., K. Jursikova, J.L. Sessler, J. Am. Chem. Soc. 122 (2000) 9350–9351.
[47] H. Miyaji, P. Anzenbacher Jr., J.L. Sessler, E.R. Bleasdale, P.A. Gale, J. Chem. Soc. Chem. Comm. 17 (1999) 1723–1724.
[48] H. Miyaji, W. Sato, J.L. Sessler, Angew. Chem. Int. Ed. 39 (10) (2000) 1777–1780.
[49] P.A. Gale, L.J. Twyman, C.I. Handlin, J.L. Sessler, J. Chem. Soc. Chem. Comm. 18 (1999) 1851–1852.
[50] V. Kral, J.L. Sessler, T.V. Shishkanova, P.A. Gale, R. Volf, J. Am. Chem. Soc. 121 (1999) 8771–8775.
[51] A. Katz, P.D. Costa, A.C.P. Lam, J.M. Notestein, Chem. Mater. 14 (2002) 3364–3368.
[52] P.D. Barata, A.I. Costa, P. Granja, J.V. Prata, React. Funct. Polym. 61 (2004) 147–151.
[53] E. Blasius, K.P. Janzen, M. Keller, H. Lander, T. Nguyen-Tien, G. Scholtien, Talanta 27 (2) (1980) 107–126.
[54] E. Blasius, K.P. Janzen, W. Adrian, W. Klein, H. Klotz, H. Luxenburger, E. Mernke, V.B. Nguyen, T. Nguyen-Tien, R. Rausch, J. Stockemer, A. Toussaint, Talanta 27 (20) (1980) 127–141.
[55] E. Blasius, K.P. Janzen, H. Luxenburger, V.B. Nguyen, H. Klotz, J. Stockemer, J. Chromatogr. 167 (1978) 307–320.
[56] A. Kaledkowski, A. Trochimczuk, XIX-th Ars Separatoria- Złoty Potok, Poland, 2004, 89–92.

[57] M. Shehab, PhD Thesis, University of Surrey, 2005.
[58] J.L. Sessler, P.A. Gale, J.W. Genge, Chem. Eur. J. 4 (1998) 1095–1099.
[59] A.F. Danil de Namor, M. Shehab, J. Phys. Chem. A 108 (2004) 7324–7330.
[60] A.F. Danil de Namor, A. Pugliese, A.R. Casal, M. Barrios-Lereno, P.J. Aymonino, F.J. Sueros Velarde, Phys. Chem. Chem. Phys. 2 (2000) 4355–4360.
[61] X.K. Ji, D.S. Black, S.B. Colbran, D.C. Craig, K.M. Edbey, J.B. Harper, G.D. Willett, Tetrahedron 61 (2005) 10705–10712.
[62] F.P. Schmidtchen, Org. Lett. 3 (2002) 431–434.

This page intentionally left blank

CHAPTER 4

Fluorine-Containing Agrochemicals: An Overview of Recent Developments

George Theodoridis*

FMC Corporation, P.O. Box 8, Agricultural Products Group, Princeton, NJ, USA

Contents

Abstract

The dramatic effect of fluorine on the biological activity of agrochemicals such as herbicides, insecticides, fungicides, and plant growth regulators has earned fluorine a unique place in the toolbox of the agrochemical chemist. Introduction of fluorine into a biologically active molecule during the structure–activity optimization process can dramatically modify its biological activity by affecting any of a number of parameters, such as binding to a target receptor or enzyme, transporting the bioactive molecule from the point of application to the target site, and blocking metabolic deactivation. This enhanced role of fluorine in the

*Corresponding author. Tel: +1-609-951-3522, Fax: +1-609-951-3603;
E-mail: george_theodoridisg@fmc.com

FLUORINE AND THE ENVIRONMENT, VOLUME 2
ISSN 1872-0358 DOI: 10.1016/S1872-0358(06)02004-5

discovery of new agrochemicals is reflected in more than three-fold increase in the number of fluorine-containing agrochemicals in the past three decades. In this review, we discuss recent developments and challenges in the field of fluorine-containing agrochemicals and place them in the context of work done in the past five decades.

1. INTRODUCTION

According to the U.S. Census Bureau, world population reached six billion in June of 1999. It predicts that another billion will be added by 2013. With the world population constantly expanding, and the available farmland steadily diminishing, continued improvements in the production of food crops and fiber present a persistent challenge. Agrochemicals continue to play a key role in crop protection, while at the same time meeting the requirements for products that are safe for the environment. In addition to ensuring a safe and cheap supply of food and fiber, agrochemicals are essential tools in the public health sector in their control of disease-carrying urban pests such as cockroaches, mosquitoes, and rodents. They also find non-crop use in the protection of homes against termites and ants.

With each passing decade, newer, more efficacious agrochemicals, with more environmentally favorable physico-chemical properties, are introduced. The increased biological activity of these newer molecules requires lower application rates, which in turn translates into less environmental impact. These newer materials are slowly replacing older molecules, which required higher application doses or had become pest-resistant. For example, the introduction of the safe and highly active pyrethroid insecticides eventually displaced a number of highly chlorinated and persistent insecticides. Another example was the introduction of the sulfonylurea herbicides in the 1980s, whose very low application rates revolutionized the industry. In this landscape of the ever-present need to develop safer, more environmentally friendly, cost-effective agrochemicals, fluorine will continue to play a major role.

The dramatic effect of fluorine on the biological activity of numerous herbicides, insecticides, and fungicides has earned fluorine a unique place in the toolbox of the agrochemical chemist. These improvements in biological activity are dramatic enough to often, though not always, justify the added costs of incorporating fluorine into the molecule. In addition, the increased biological potency of the new fluorine-containing agrochemicals has resulted in both improved efficacy under field application with less material and significantly less impact on the environment. It is the balance between biological efficacy and cost of production that determines the success of a new agrochemical active ingredient.

A clear indication of the key role that fluorine plays in the development of new agrochemicals is the dramatic increase – more than triple – in the number of fluorinated agrochemicals in the past three decades: from 23 out of 543 (4%) listed in the 1977 edition of the *Pesticide Manual* [1], to the 126 (14%) out of

858 in the latest edition of the *Pesticide Manual* [2], of which 45% are herbicides, 33% are insecticides, and 18% are fungicides. The most common fluorine-containing groups of agrochemicals are aromatic fluorine, 37%, and aromatic trifluoromethyl, 32%.

The improved processes for the introduction of fluorine into biologically active molecules have resulted in the availability of more cost-effective fluorine-containing raw materials and intermediates. With an emphasis on biological efficacy, performance, and cost, this work attempts to review fluorine-containing agrochemicals of commercial potential that have been assigned an ISO name, and it is divided into two parts. The first part, Section 2, encompasses compounds introduced prior to 2001, and the second part, Section 3, covers developments after 2001. Within each part, the review is organized by grouping together all herbicides, insecticides, fungicides, plant growth regulators, and rodenticides, respectively, according to the kind of fluorine group present, for instance, aromatic trifluoromethyl-containing herbicides or aromatic fluorine. Classifying the agrochemicals this way more readily points up both the synthesis and the unique properties of each fluorinated group.

Fluorine-containing agrochemicals have been previously reviewed [3–7]. The earliest review that specifically covers the subject of fluorinated agrochemicals is that by Geoffrey Newbold [3], in which he discusses the various chemical classes of fluorinated agrochemicals. More recent reviews [4,6,7] discuss the unique properties that result from introducing fluorine into biologically active molecules.

The design of new agrochemicals involves the systematic structure–activity optimization of a biologically active molecule [8]. Most industrial research labs come upon these biologically active molecules, or hits, *via* the screening of compounds through a battery of biological tests. Structure–activity optimization of biologically active molecules is a complex process that attempts to optimize a variety of parameters, such as binding to a target receptor or enzyme, transporting the bioactive molecule from the point of application to the target site, and blocking metabolic deactivation. Introduction of fluorine into a biologically active molecule during the optimization process can dramatically modify its biological activity by affecting any of the parameters previously mentioned.

A number of general reviews discuss the synthesis of fluorine-containing organic molecules [9,10]. In general, introducing fluorine into a molecule results in considerable increase in costs. Yet the costs must be weighed against the unique properties that fluorine gives to biologically active molecules. Primary among those properties are:

- *Lipophilicity*. In general, the replacement of hydrogen by fluorine in a molecule increases its lipophilicity, particularly with groups such as CF_3 and OCF_3. Lipophilicity plays a key role in the transport of molecules through plant and insect cuticles. In addition to lipophilicity, increasing the number of fluorine atoms in a

molecule also increases its volatility, an important property in agrochemicals, particularly insecticides.

- *Steric effects*. As the second smallest substituent, fluorine closely resembles hydrogen's steric requirement for binding to an active site. This makes replacement of hydrogen by fluorine a common bioisosteric replacement [11].
- *Electronic effects*. The high electronegativity of fluorine (4.0 as compared to 2.1 for H) often changes the electronic properties of the molecule, resulting in modified physical properties and chemical reactivity.
- *Stability*. The C–F bond is much stronger than the C–H bond (485 kJ mol^{-1} compared with 416 kJ mol^{-1} for the C–H bond), resulting in increased oxidative and thermal stability of the molecule.

Finally, the future prominence of fluorine's role in agrochemicals will depend upon improved chemical processes for the industrial production of a wide array of fluorine-containing starting materials and intermediates. In addition to ensuring lowered costs and increased selection of raw materials, improvement in fluorine processes should also take into consideration the use of greener chemistry.

2. FLUORINE-CONTAINING AGROCHEMICALS: DEVELOPMENTS PRIOR TO 2001

2.1. Fluorinated alkyl aromatic and heteroaromatic agrochemicals

2.1.1. Trifluoromethyl aromatic agrochemicals

The trifluoromethyl functional group is among the most commonly found fluorine-containing group in agrochemicals, particularly when directly attached to an aromatic ring, and represents 32% of all fluorinated agrochemicals found in the *Pesticide Manual* [2]. Though there are a number of approaches to the preparation of the trifluoromethylbenzene group, the most common industrial approach involves the conversion of trichloromethylbenzene, obtained from free radical chlorination of toluene, to trifluoromethylbenzene with anhydrous hydrogen fluoride [12] (Fig. 1). Trichloromethyl groups attached to aromatic systems are exchanged with greater ease than those attached to aliphatic groups. In a similar manner 1,2-dichloro-4-trifluorobenzene, an important starting material for the preparation of 2-chloro-4-trifluorophenol, is obtained from the corresponding 4-chlorotoluene.

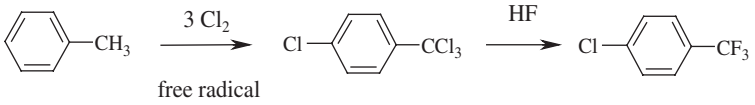

Fig. 1. Synthesis of aromatic trifluoromethyl group.

The preparation of complex trifluoromethylbenzene-containing agrochemicals is based on the derivatization of several key-starting materials, such as trifluoromethylbenzene. Trifluoromethylbenzene is prepared in large volumes, and is the basis for the synthesis of 3-aminobenzotrifluoride. Treatment of trifluoromethylbenzene with a solution of concentrated nitric and sulfuric acids at low temperatures results in a mixture of ortho-, meta-, and para-isomers in a 6/91/3 ratio (Fig. 2). Catalytic hydrogenation of 3-nitro trifluoromethylbenzene, followed by distillation, produces the desired 3-aminobenzotrifluoride [13–15].

2.1.1.1. Herbicides

The first significant commercial impact of fluorine in agriculture occurred with the introduction several decades ago of an aromatic trifluoromethyl group in several classes of herbicides, such as dinitroaniline, diphenyl ether, and bleaching herbicides. These early classes of herbicides continue to be used today, though their sales are steadily declining as newer, more effective materials are replacing them.

Dinitroaniline herbicides. Trifluralin (Treflan®), a 4-trifluoromethyl substituted 2,6-dinitroaniline derivative, was the first main fluorine-containing herbicide to be marketed, with 18,000 tons sold in 1982 in the United States alone [16]. Trifluralin, which was introduced in 1960 by Eli Lilly, is a pre-emergence herbicide used in soybean for the control of a variety of grass and broadleaf weeds [17]. It is prepared from the nitration of 4-chlorobenzotrifluoride, followed by nucleophilic displacement of chlorine with di-*n*-propyl amine (Fig. 3). Following the success of trifluralin, a number of related *N*,*N*-dialkyl 4-trifluoromethyl 2,6-dinitroaniline herbicides were later introduced [18].

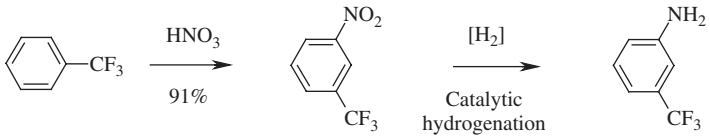

Fig. 2. Preparation of 3-aminobenzotrifluoride.

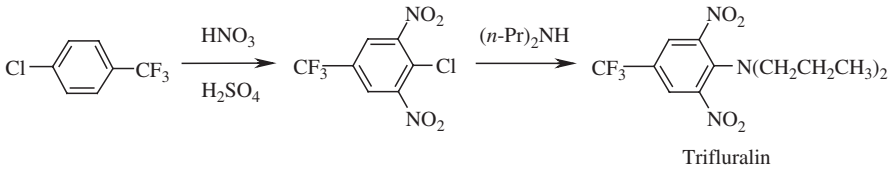

Fig. 3. Synthesis of the herbicide trifluralin.

Urea herbicides. Phenyl urea chemistry represents one of the earliest classes of herbicides. Replacement of the aromatic chlorines of diuron with a trifluoromethyl group resulted in improved crop selectivity. Fluometuron (Cotoran®) and parafluron are both selective urea herbicides, fluometuron developed for the control of grass and broadleaf weeds in cotton. It was prepared from the corresponding 3-trifluoromethyl anilines. A number of other phenyl urea herbicides were introduced later, including trimefluor, 3-chloro-4-trifluoromethoxyphenyl-*N,N*-dimethyl urea [19].

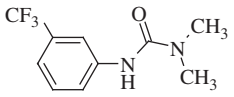

Fluometuron

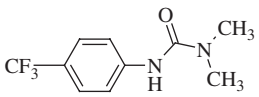

Parafluron

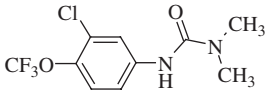

Trimefluor

Diphenyl ether herbicides. The diphenyl ether class of herbicides belongs to a broader area of herbicides known as protoporphyrinogen oxidase (Protox) herbicides [20,21]. Diphenyl ether herbicides were initially introduced over four decades ago in the 1960s with the discovery of nitrofen by Rohm and Haas (now Dow AgroSciences) [22] and bifenox by Mobil [23]. These early diphenyl ether herbicides did not attain a significant role in the control of weeds in commercial crops until the 1970s, with the introduction of the trifluoromethyl compounds oxyfluorfen [24] and acifluorfen–sodium [25]. Replacement of the chlorine with a trifluoromethyl group resulted in a dramatic increase in the herbicidal properties of these compounds, in terms of both potency and the spectrum of weeds controlled.

Nitrofen R = H
Bifenox R = CO_2CH_3

Oxyfluorfen R = OEt
Acifluorfen-sodium R = CO_2Na

Later, it was found that replacement of the carboxylic sodium salt group of acifluorfen–sodium with a methyl sulfonamide group to give fomesafen [26,27] provided good soybean safety when applied postemergently. Other trifluoromethyl-containing diphenyl ethers with further derivatized carboxylic groups include fluoroglycofen–ethyl and lactofen. Diphenyl ethers can be prepared in a variety of ways [28], the most common approach involving the nucleophilic displacement of a halogen with an appropriate phenolate salt, followed by nitration to give acifluorfen–sodium (Fig. 4) [29].

Phytoene desaturase bleaching herbicides. Bleaching herbicides inhibit the synthesis of carotenoids in plants [30,31]. A number of phytoene desaturase herbicides such as norflurazon (Solicam®, Zorial®), flurochloridone (Racer®), fluridone (Sonar®), and diflufenican (Fenican®, Legacy®) have been commercialized.

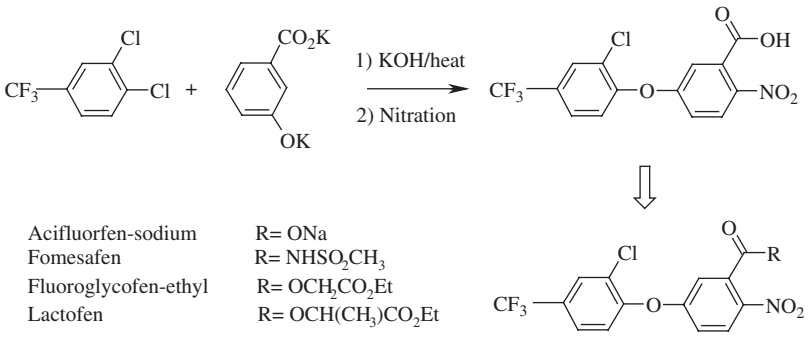

Fig. 4. Synthesis of diphenyl ether carboxylic acid intermediate.

They are generally used in cotton for the pre-emergence control of weeds. An exception is flurochloridone [32,33], which is used in sunflowers, and the more recently introduced diflufenican [34], which is used in cereal crops. In all cases, these herbicides have a trifluoromethyl group in the meta position of the aromatic ring.

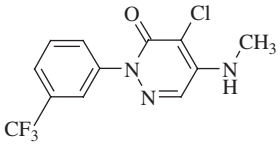

Norflurazon

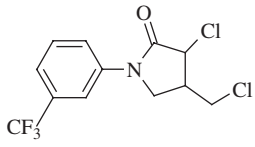

Flurochloridone

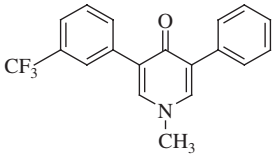

Fluridone

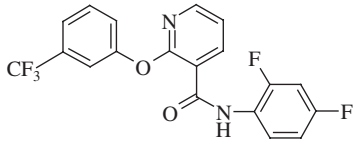

Diflufenican

3-Trifluoromethylaniline, directly or indirectly, is the starting material for the synthesis of all four of the herbicides norflurazon, flurochloridone, fluridone, and diflufenican. Norflurazon is prepared from 3-trifluoromethylphenyl hydrazine, which is obtained from the diazotization and reduction of 3-trifluoromethylaniline [35]. Diflufenican is prepared from the reaction of 3-trifluoromethylphenol and 2-chloro-3-carboxylic acid pyridine, with 3-trifluoromethylphenol also being obtained from the diazotization of 3-trifluoromethylaniline (Fig. 5).

A number of carotenoid biosynthesis inhibitors that came later include flurtamone [36,37], introduced in 1997, which is used as a pre-emergence and preplant incorporated herbicide. Flurtamone can be prepared in several steps from 3-(trifluoromethylphenyl)acetonitrile and ethyl phenylacetate (Fig. 6).

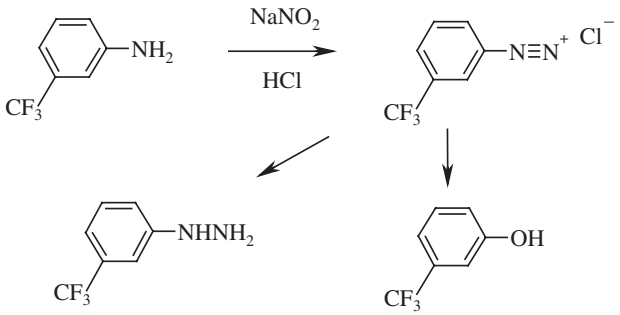

Fig. 5. Synthesis of 3-trifluoromethylphenyl hydrazine and 3-trifluoromethylphenol.

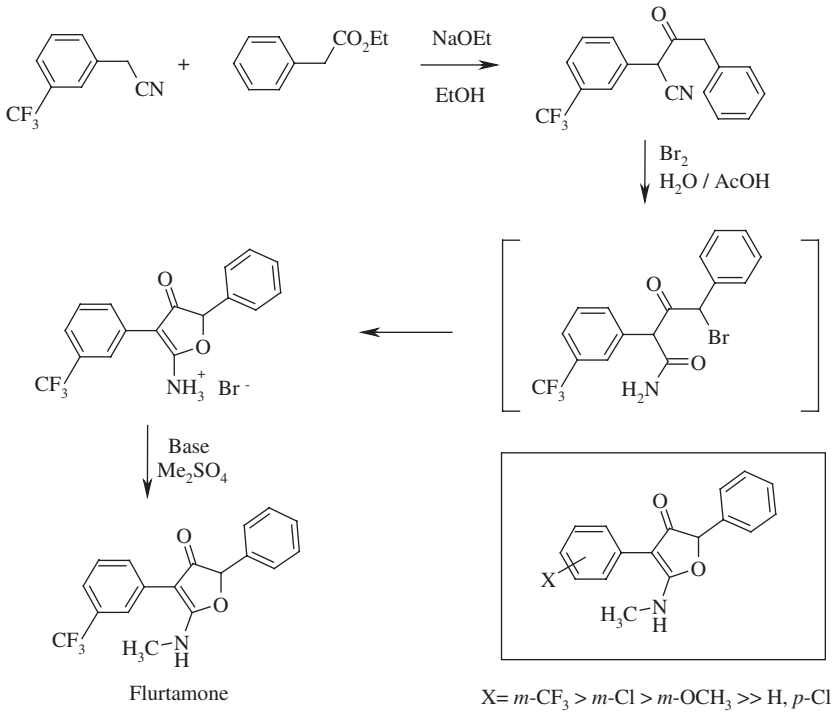

Flurtamone

Fig. 6. Synthesis and structure–activity of the herbicide flurtamone.

Structure–activity studies have shown the crucial role of the trifluoromethyl group in optimum biological activity of bleaching herbicides [38]. Isoxaflutole (Balance®, Merlin®) is a root or foliar uptake systemic herbicide with broad-spectrum control in corn and sugarcane of both grass and broadleaf weeds [39]. Isoxaflutole is rapidly converted in plants and in soil to the diketonitrile form, which is the biologically active species (Fig. 7) [40].

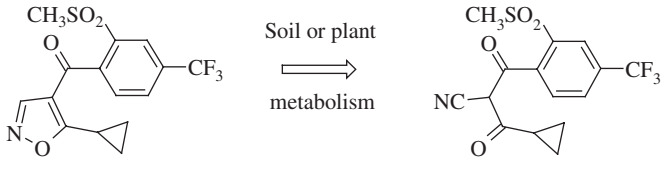

Fig. 7. Metabolic conversion of the herbicide isoxaflutole to its active form.

2.1.1.2. Insecticides

GABA insecticides. The *N*-phenylpyrazole insecticide fipronil, launched in 1993 by Rhone-Poulenc [41], is among the most successful insecticides introduced in over a decade.[1] A highly versatile insecticide, it is effective against a broad spectrum of insect pests that are detrimental to crops, animals, and public health. Fipronil acts at the gamma-aminobutyric acid (GABA) receptor to block the chloride channel [42]. The product is sold as Terminator® for termite control, and as Frontline® for flea and tick treatment in dogs and cats. According to the 2002 Phillips McDougall report, sales of Frontline® in 2001 were $358 million.

One approach to the introduction of the trifluoromethylsulfinyl group in fipronil involves the reaction of 5-amino-3-cyano-1-(2,6-dichloro-4-trifluoromethylphenyl)pyrazole and trifluoromethylsulfinyl chloride in toluene (Fig. 8) [43]. Exposure of fipronil to sunlight results in the extrusion of sulfur oxide, to give a 4-trifluoromethylpyrazole photoproduct derivative [44].

Insect growth regulators. Initially discovered in the mid-1970s, insect growth regulators (IGRs) act by inhibiting chitin synthesis in insects [45,46]. This interesting class of insecticides offers an alternative to known neurotoxic insecticides. It was originally discovered by serendipity by Dutch researchers at Philips-Duphar in the 1970s, while they were working with the herbicides diuron and dichlobenil. Initial attempts to create a new herbicide by combining the structural features of these two herbicides failed, with the end hybrid product, shown in Fig. 9, not effective as a herbicide. Instead, the benzoyl urea turned out to have insecticide activity and exhibited unique insect symptomology [47].

A number of representatives in this class of insecticides have a *N*-benzoyl-*N*′-phenyl urea group, where the benzoyl ring has halogens in the 2 and 6 positions, and substitution in the phenyl ring varies widely from molecule to molecule. One, flufenoxuron (Cascade®, Europe®, Sigona®) [48], commercialized in 1993, controls insect and mite pests in vegetables, vines, citrus, cotton, and other crops. Another, bistrifluron (Hanaro®) [49], is an experimental insecticide with controlling activity against lepidopterous and whiteflies in fruits.

[1] [*Note of the Editor: A recent article by A. Lattes and B. Sillion on the effects of Fipronil appeared in "Actualité Chimique" 294, pp. 6–10, 2006*].

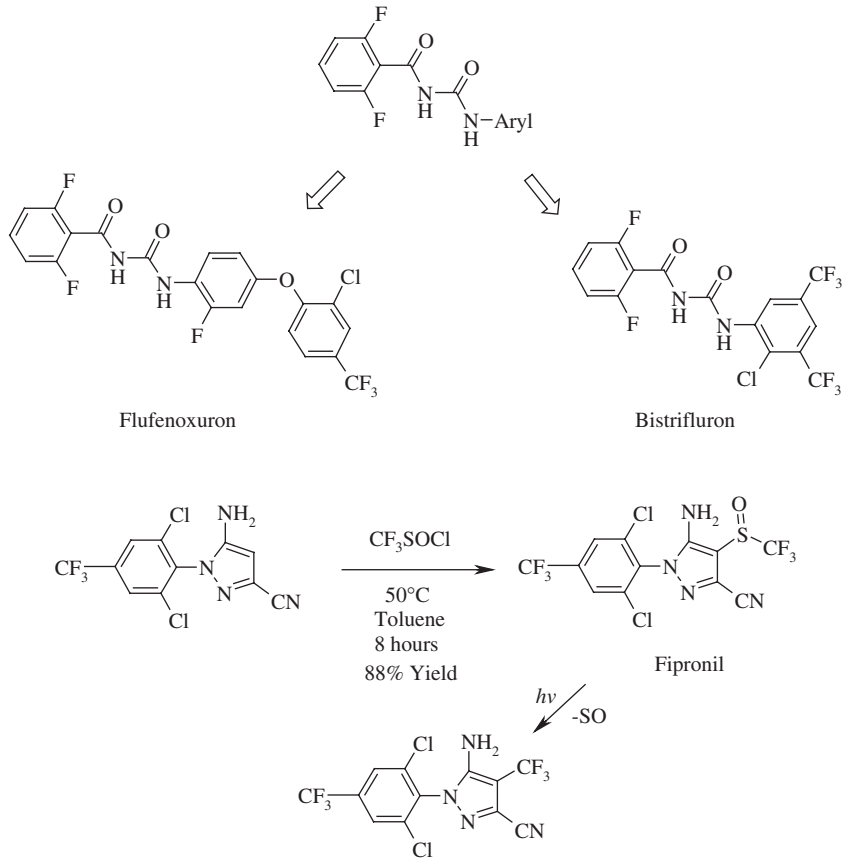

Fig. 8. Trifluoromethylsulfinylation of pyrazole to prepare fipronil, and elimination of sulfur oxide from under sunlight conditions.

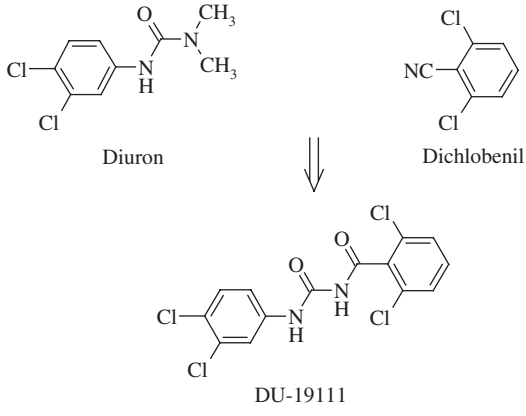

Fig. 9. Discovery of IGRs.

Pyrethroid insecticides. The natural pyrethrins, which act on the voltage-gated sodium channel, are highly potent insecticides obtained from flowers of the chrysanthemum plant. Though the pyrethrins are highly active insecticides, they are not stable enough for commercial use. However, a number of structural modifications of the early pyrethrin molecule resulted in a wide range of stable commercially useful pyrethroid insectides.

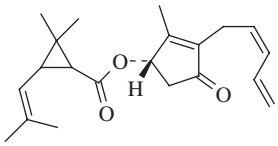

Pyrethrin

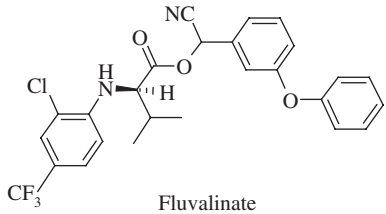

Fluvalinate

A large number of synthetic pyrethroids with a variety of aromatic and aliphatic fluorine substituents have been commercialized, and will be discussed in the sections on fluorinated ether, aromatic fluorine, and fluorinated aliphatic groups, respectively. Fluvalinate (Mavrik®) [50] is a trifluoromethylphenyl pyrethroid, initially introduced by Zoecon (later Zandos Ag) and later replaced by tau-fluvalinate, which contains two of the four isomers of fluvalinate. Tau-fluvalinate (Apistan®) is a synthetic pyrethroid used for the topical treatment of honeybees against the parasitic mite *Varroa jacobsoni*. Mite resistance to tau-fluvalinate has been reported [51].

2.1.1.3. Fungicides

β-Methoxyacrylates. This is an important class of commercial fungicides based on a group of natural products, the strobilurins (see Fig. 10), such as strobilurin A and oudemansin A. Strobilurins act by inhibition of mitochondrial respiration. In 1996, the first representatives of this class of fungicide were launched, including azoxystrobin [52]. In 1999, the first fluorine-containing strobilurin, trifloxystrobin (Flint®) [53], was launched by Syngenta and later acquired by Bayer for $760 million.

Sterol biosynthesis inhibiting insecticides. The earliest examples of sterol biosynthesis inhibitors were triadimefon, imazalil, and triarimol. These compounds act by blocking the C14 alpha demethylation step in ergosterol biosynthesis [54]. Further work in this area has resulted in numerous fungicides, a number of them containing aromatic fluorine, perfluoroalkyl ethers, and the trifluoromethylphenyl group (Fig. 11). In this section, we will discuss the trifluoromethylphenyl sterol biosynthesis inhibitors, such as triflumizole and fluotrimazole.

Triflumizole (Trifmine®, Procure®) [55] was obtained in several steps from 4-chloro-2-trifluoromethyl acetanilide, which was prepared from the reaction of 4-chloro-2-trifluoromethylaniline and propyloxyacetyl chloride. Conversion of the

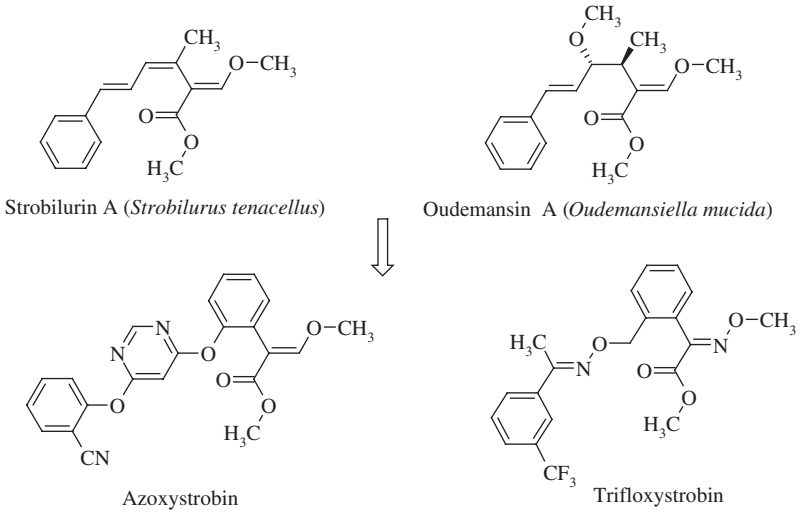

Fig. 10. Evolution of strobilurin fungicides from their natural products precursors.

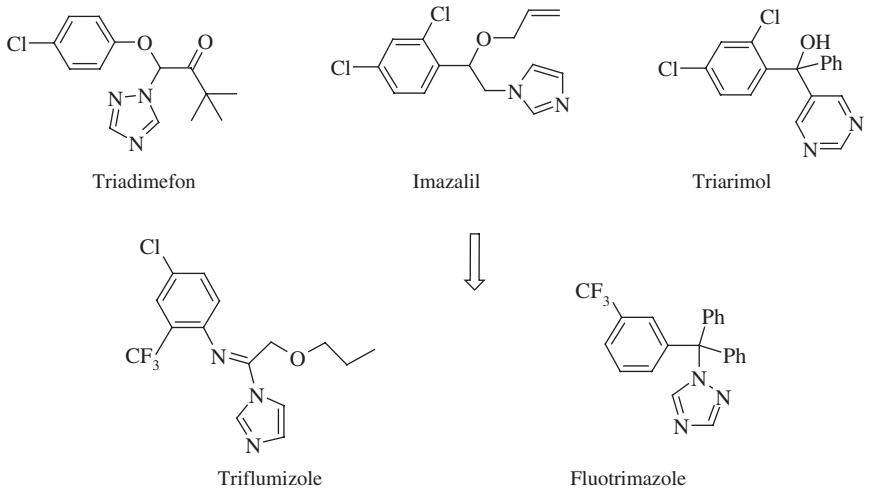

Fig. 11. Trifluoromethyl-containing generation of sterol biosynthesis inhibitors.

intermediate acetanilide to imidoyl chloride, followed by reaction with imidazole, gave triflumizole (Fig. 12) [56].

Fluotrimazole (Persulon®) was obtained from the reaction of 1-(chlorodiphenylmethyl)-3-(trifluoromethyl)benzene and triazole (Fig. 13). The 1-(chlorodiphenylmethyl)-3-(trifluoromethyl)benzene was prepared in what appears to be an inefficient sequence of steps involving chlorination of meta-xylene to give 1,3-bis(trichloromethyl)benzene, followed by halogen exchange with fluorine, to give

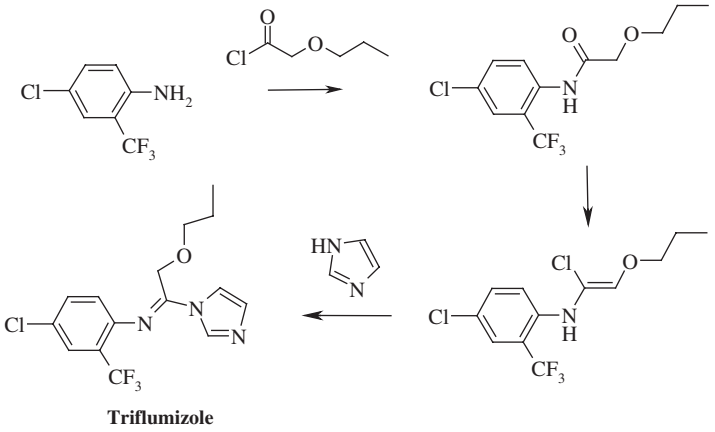

Fig. 12. Synthesis of the fungicide triflumizole.

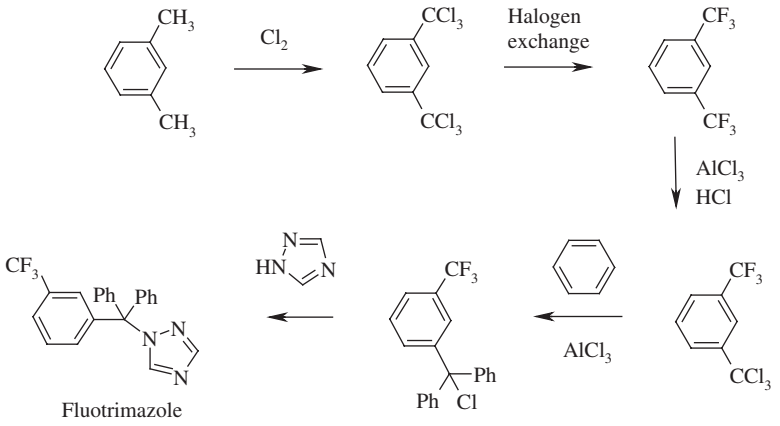

Fig. 13. Synthesis of the fungicide fluotrimazole.

the corresponding 1,3-bis(trifluoromethyl)benzene. In the next step, a second halogen exchange converts one trifluoromethyl group back to trichloromethyl. Thus, treatment of bis(trifluoromethyl)benzene with aluminum trichloride and hydrochloric acid gives 1-(trichloromethyl)-3-(trifluoromethyl)benzene, which when reacted with benzene and aluminum trichloride gives 1-(chlorodiphenylmethyl)-3-(trifluoromethyl)benzene [57].

2.1.1.4. Plant growth regulators

The limited amount of research invested by the agrochemical industry into this class of chemicals is reflected in the fact that there are only a handful of fluorine-containing plant growth regulators, or PGRs as they are more commonly known.

As their name implies, plant growth regulators are used by farmers to modify the growth of a plant in a particularly advantageous way. The best example of a trifluoromethyl-containing plant growth regulator is flumetralin, which is used to control suckers in tobacco [58]. Flumetralin (Prime®) is readily synthesized from 2-chloro-1,3-dinitro-5-(trifluoromethyl)benzene and 2-chloro-6-fluoro-*N*-ethylbenzylamine (Fig. 14) [59].

2.1.1.5. Rodenticides

Flocoumafen (Storm®) and bromethalin are two examples of aromatic trifluoromethylbenzene-containing rodenticides. Flocoumafen is a second-generation anticoagulant. It acts by inhibiting the metabolism of vitamin K_1, which results in depletion of vitamin K_1-dependent clotting factors in plasma. Flocoumafen is effective against rodents, which have become resistant to other anticoagulant rodenticides. As shown in Fig. 15, flocoumafen is prepared from the benzylation of the corresponding phenol intermediate and 4-trifluoromethylbenzyl chloride [60].

Though the mode of action of bromethalin [61] is not known, it has been determined that it is not an anticoagulant as flocoumafen is. The presence of four bulky groups ortho to the tertiary nitrogen makes its synthesis challenging. Bromethalin synthesis involves introducing one or more of the ortho bulky groups after the formation of diphenylamine (Fig. 16) [62].

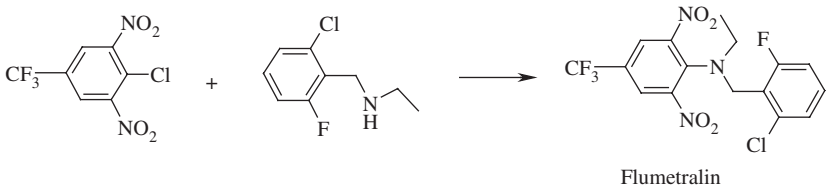

Fig. 14. Synthesis of the plant growth regulator flumetralin.

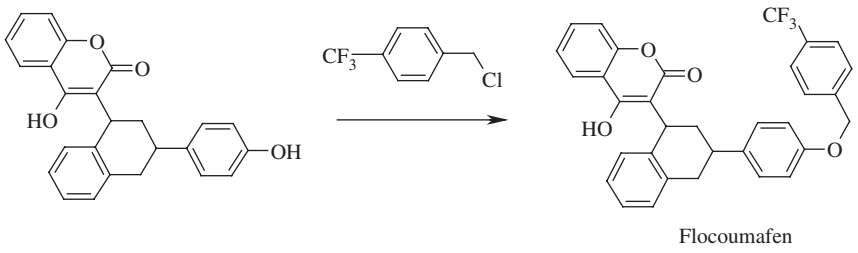

Fig. 15. Synthesis of the rodenticide flocoumafen.

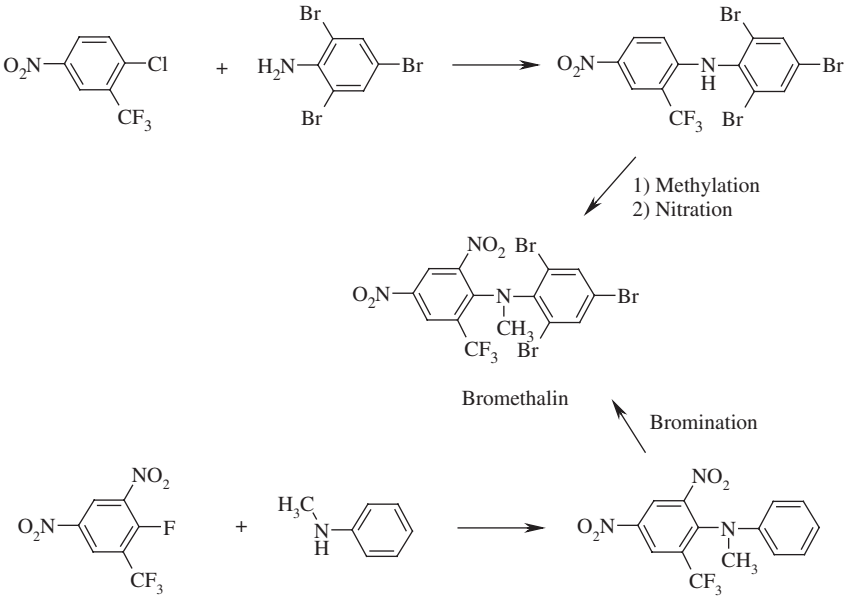

Fig. 16. Synthesis of the rodenticide bromethalin.

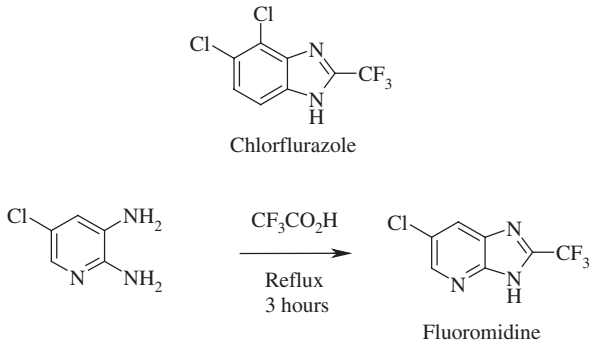

Fig. 17. Synthesis of 2-trifluoromethylimidazopyridine heterocycle ring.

2.1.2. Trifluoromethyl heterocyclic agrochemicals

2.1.2.1. Herbicides

A number of 2-trifluoromethylbezimidazole herbicides were developed in the 1960s, but they have since being replaced by newer, more effective herbicides. Examples of 2-trifluoromethylbezimidazole herbicides are chlorflurazole [63,64] and fluoromidine [65]. The 2-trifluoromethylimidazopyridine heterocycle ring in fluoromidine is prepared from the reaction of trifluoroacetic acid and the corresponding 5-chloro-2,3-diaminopyridine (Fig. 17) [66]. The mode of action of

2-trifluoromethylbezimidazole herbicides is known: they act as uncouplers of the oxidative phosphorylation process [67,68].

More recent examples of trifluoromethyl heteroaryl-containing herbicides include the trifluoromethyl uracil and pyridazine classes of Protox herbicides [69]. Benzfendizone is a postemergence herbicide that provides good control of grass and broadleaf weeds in tree fruits and vines, as a cotton defoliant, and in total vegetation control. The 6-trifluoromethyl group in the uracil ring is essential for biological activity; replacing it with methyl results in complete loss of activity [70].

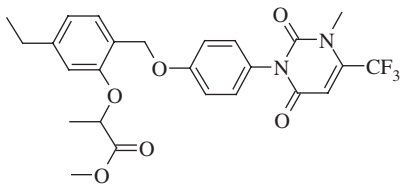

Benzfendizone

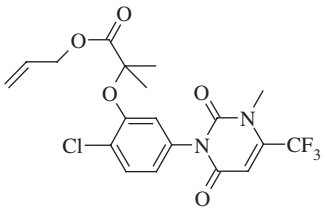

Butafenacil

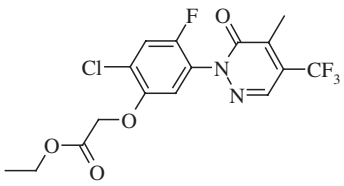

Flufenpyr-ethyl

The uracil heterocycles are readily prepared in high yields from the corresponding arylisocyanates and from ethyl trifluoromethylaminocrotonate in the presence of a base [71]. The uracil heterocycle is then directly *N*-methylated with methyl iodide in a one-pot reaction (Fig. 18).

A number of trifluoromethylpyridine-containing agrochemicals have found their way into commercial use. The grass herbicide fluazifop-*P*-butyl (Fusilade®), which is prepared from 2-chloro-5-trifluoromethylpyridine (Fig. 19), is one such product.

Another example of a trifluoromethyl heteroaryl-containing herbicide is dithiopyr (Dimension®) [72]. Structure–activity studies have demonstrated that a fluorinated alkyl group is required for optimum activity at the 2 and/or 6 positions of the pyridine ring [73]. Thiazopyr (Mandate®, Visor®), a herbicide related to dithiopyr, was introduced by Monsanto in 1992 and later sold to Rohm and Haas. It is used for the pre-emergence control of annual grass and a few broadleaf weeds in tree fruit, vines, sugar cane, and other crops.

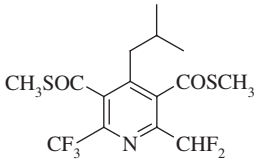

Dithiopyr

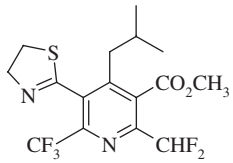

Thiazopyr

Flufenacet (Cadou®, Drago®), the 5-trifluoromethyl-1,3,4-thiadiazol-2-yloxy acetanilide herbicide developed by Bayer CropScience, belongs to the oxyacetamide class of herbicides. Flufenacet is effective in controlling a broad spectrum of annual grass, hedges, and small broadleaf weeds [74].

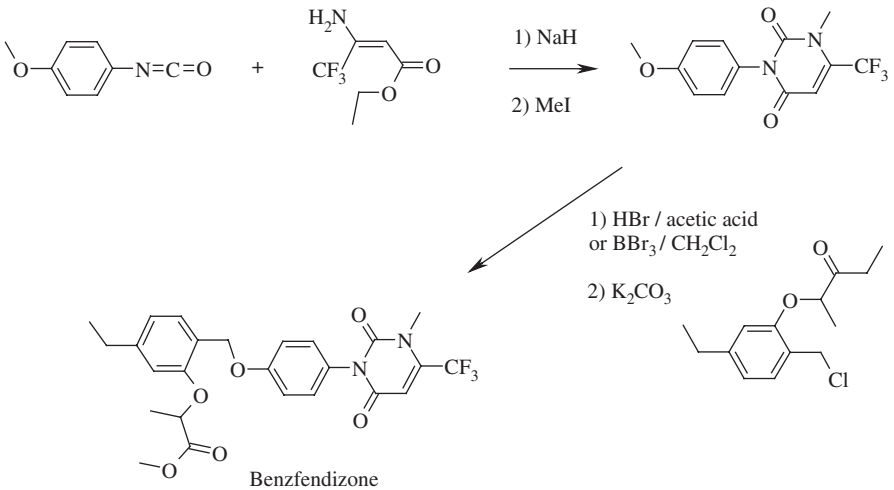

Fig. 18. Synthesis of the trifluoromethyl uracil ring of benzfendizone.

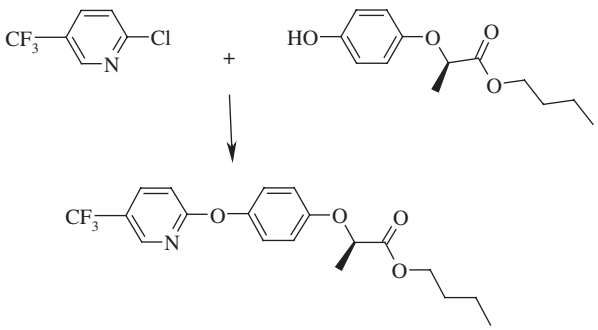

Fluazifop-P-butyl

Fig. 19. Synthesis of the herbicide fluazifop-*P*-butyl.

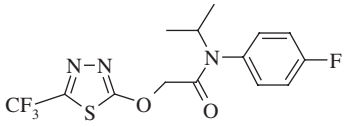

Flufenacet

The sulfonylurea herbicides represents a class of novel, highly selective, and very potent herbicides introduced by DuPont in the 1980s, when it revolutionized the herbicide industry by reducing application rates, generally below 100 g /ha, levels previously not thought possible [75]. The mode of action of the sulfonylurea herbicides is by inhibition of the acetolactate synthase (ALS) enzyme, a key enzyme in the biosynthesis of branched amino acids, such as leucine, isoleucine, and valine [76]. A large number of sulfonylurea molecules were developed by various companies; the general structure of the first compounds in this class is shown in Fig. 20. Replacement of the phenyl ring with trifluoromethylpyridine resulted in 1997 in two new herbicides, flazasulfuron (Katana®, Parandul®), from Ishihara Sangyo Kaisha [77], and flupyrsulfuron-methyl (Lexus®), from DuPont [78].

2.1.2.2. Insecticides

IGRs. Chlorfluazuron (Atabron®) [79] belongs to the *N*-benzoyl *N*′-phenyl IGR family of insecticides. These compounds act by inhibition of chitin formation in the insect.

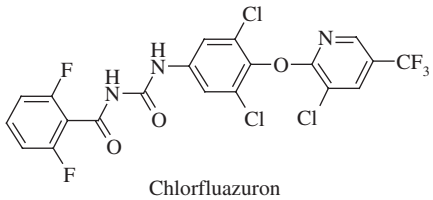

Chlorfluazuron

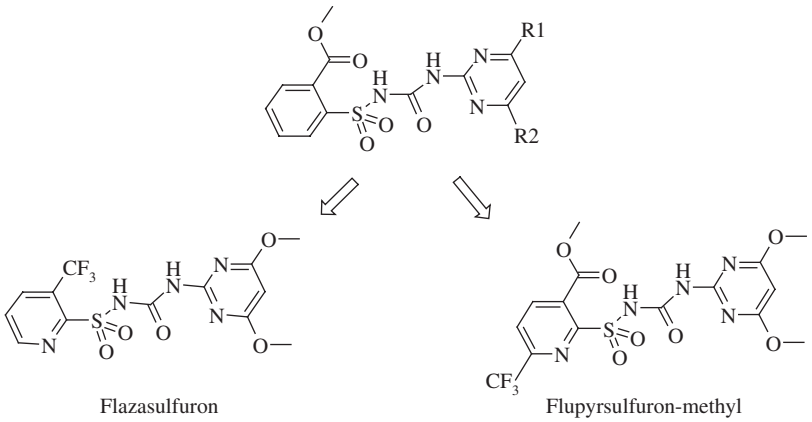

Flazasulfuron Flupyrsulfuron-methyl

Fig. 20. Trifluoromethylpyridine-containing sulfonylurea herbicides.

Chlorfenapyr (Phantom®), a trifluoromethyl-containing pyrrole ring insecticide, belongs to a new class of uncouplers of oxidative phosphorylation [80]. The original insecticidal lead that resulted in chlorfenapyr was the fermentation product dioxapyrrolomycin, isolated from a *Streptomyces* strain [81]. The presence of the trifluoromethyl group is essential for a broad spectrum of insecticide and acaricide activity.

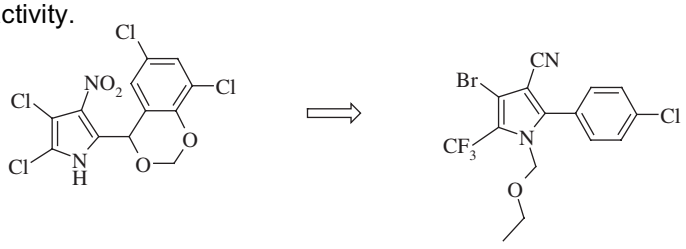

Dioxapyrrolomycin Chlorfenapyr

Chlorfenapyr can be prepared in several steps from the corresponding amino acid derivatives and trifluoroacetic anhydride (Fig. 21) [82].

2.1.2.3. Fungicides

β-Methoxyacrylates. As discussed earlier, in 1996 the first representatives of this class of fungicides were launched, including azoxystrobin [83]. Another entry in this class of fungicides is the trifluoromethyl pyridalyl-containing molecule picoxystrobin (Acanto®) [84].

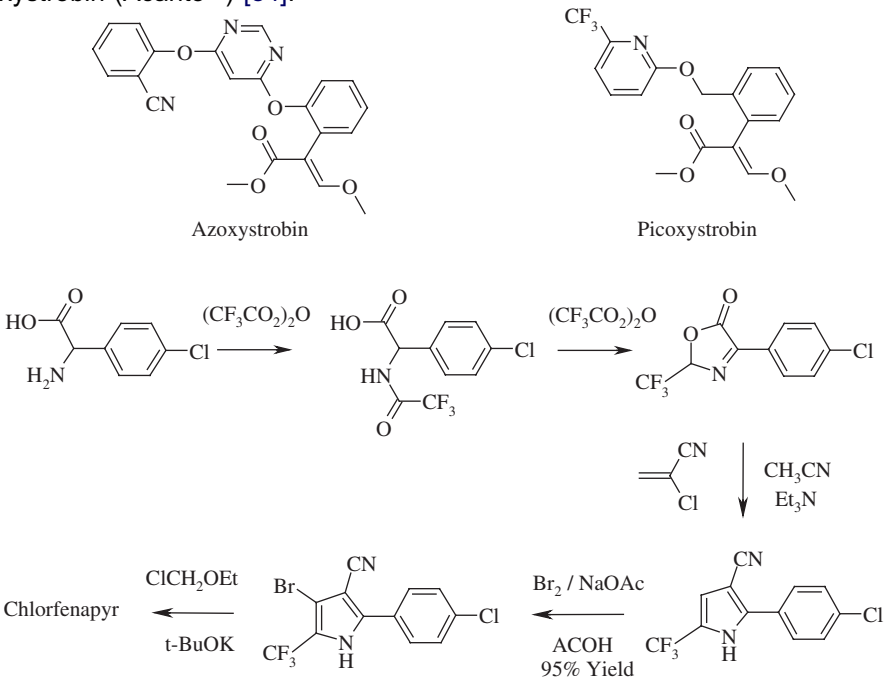

Fig. 21. Preparation of the insecticide chlorfenapyr.

Interestingly, replacement of the 6-trifluoromethyl-2-pyridyloxy ring of picoxystrobin with 2-isopropyloxy-6-trifluoromethyl-4-pyrimidyloxy results in a shift from fungicide to acaricide activity in the resulting compound, fluacrypim (Titaron®) [85]. Thifluzamide (Baton®, Greatam®, Greatum®, Pulsor®) [86], 2′,6′-dibromo-2-methyl-4′-trifluoromethoxy-4-trifluoromethyl-1,3-thiazole-5-carboxanilide, is a fungicide that acts by inhibition of succinate dehydrogenase in the tricarboxylic acid cycle. Thifluzamide can be applied foliarly or as a seed treatment in a variety of crops for the control of a number of basidomycete diseases. Thifluzamide is rapidly absorbed by roots and leaves and translocated throughout the plant.

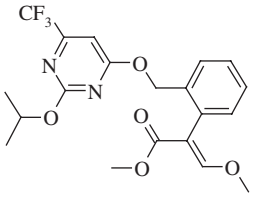

Fluacrypim

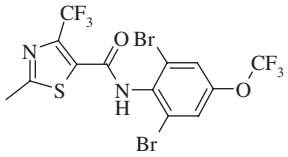

Thifluzamide

2.2. Fluorinated alkyl groups attached to heteroatoms

2.2.1. Trifluoromethoxy group

The trifluoromethyl and trifluoromethoxy groups of aromatic agrochemicals are often interchangeable, with availability of synthesis starting materials and cost as the determining factors. The synthesis of the trifluoromethoxybenzene derivatives involves a somewhat similar synthetic pathway to that used to prepare trifluoromethylbenzene. Chlorination of the methyl group under free radical conditions gives trichloromethoxybenzene in good yields; this is followed by displacement of the chlorines with anhydrous hydrogen fluoride (Fig. 22).

The electronic properties of the trifluoromethoxy group closely resemble those of halogens, such as chlorine and bromine. For instance, nitration studies have shown that trifluoromethoxy benzene nitrates several times slower than benzene, the trifluoromethyl group deactivating the aromatic ring *via* an inductive electron-withdrawing effect. This inductive electron-withdrawing effect is somewhat balanced by the ability of the oxygen of the trifluoromethoxy group to act as an electron donor *via* resonance, with nitration occurring only at the ortho- and para-positions of the aromatic ring [6].

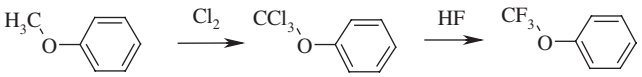

Fig. 22. Two-step synthesis of the trifluoromethoxy group.

2.2.1.1. Herbicides

The trifluoromethoxybenzene group is not commonly found in herbicides. One exception is the herbicide trimefluor, which is prepared from methyl 4-methoxy benzoate in four steps (Fig. 23) [19]. Trimefluor is a selective pre- and post-emergence herbicide for use in cotton.

Another example found in herbicides is the ALS inhibitor flucarbazone–sodium (Everest®) [87]. This postemergence wheat herbicide controls grass weeds, as well as a number of broadleaf weeds of commercial significance.

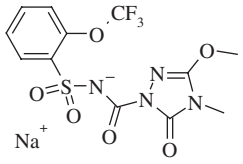

Flucarbazone-sodium

2.2.1.2. Insecticides

Indoxacarb (Steward®, Avaunt®) [88] is an insecticide commercialized by Dupont in 2000, with broad-spectrum control of lepidopteran insects. Of the two possible optical isomers, only one is biologically active, the (*S*)-enantiomer [89]. Indoxacarb is a proinsecticide: it is not toxic to insects until it goes through an activation process by the insect's metabolic system, which cleaves the *N*-carbomethoxy group to the NH insect active form. Indoxacarb acts by blocking the sodium channel, at a site different from that of the pyrethroids. Because indoxacarb binds to a different site, no cross-resistance with pyrethroids has been observed. Structure–activity studies of oxadiazine insecticide analogs of indoxacarb against *Spodoptera frugiperda* showed that the trifluoromethoxy substituent in the para position provided the best biological activity [90].

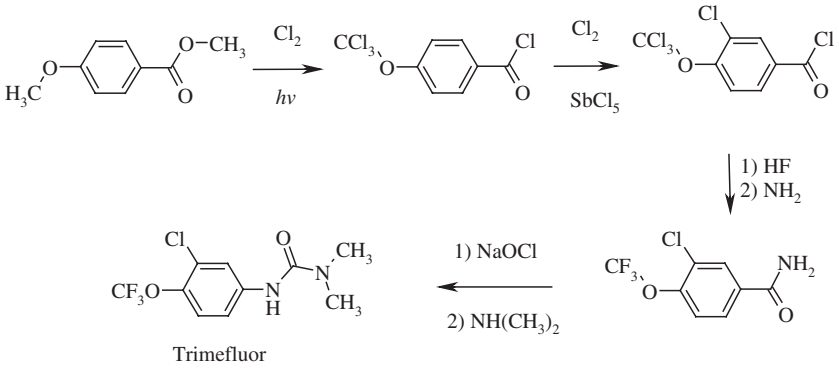

Trimefluor

Fig. 23. Synthesis of the herbicide trimefluor.

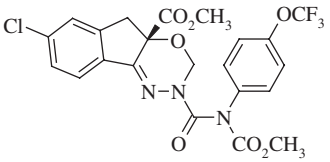

Indoxacarb

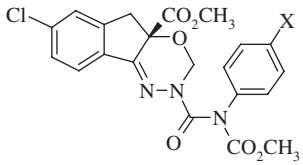

X = OCF_3 > CF_3 > Br, $OCHF_2$, > Cl > F

Triflumuron (Alsystin®, Baycidal®) [91,92], an *N*-benzoyl-*N*′-phenyl urea chitin synthase inhibitor commercialized by Bayer CropScience, is a broad spectrum insecticide that is active against chewing insects, as well as fleas and cockroaches.

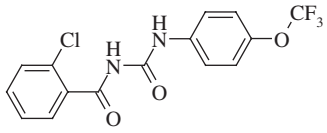

Triflumuron

2.2.1.3. Fungicides

Thifluzamide, previously discussed in Section 2.1.2.3 on trifluoromethyl heteroaryl-containing fungicides, is a fungicide that can be applied foliarly or as a seed treatment in a variety of crops for the control of a number of basidomycete diseases. Thifluzamide is prepared from the condensation of 2-methyl-4-trifluoromethyl-5-chlorocarbonylthiazole and 2,6-dibromo-4-trifluoromethoxyaniline. The 2-methyl-4-trifluoromethyl-chlorocarbonylthiazole heterocyclic ring was synthesized from the reaction of $CF_3COCHClCO_2Et$ and thioacetamide in refluxing DMF (Fig. 24) [93].

2.2.1.4. Plant growth regulators

The plant growth regulator flurprimidol (Cutless®) [94], though it chemically resembles fungicides that inhibit sterol biosynthesis, acts by interfering with gibberellin biosynthesis [95]. Flurprimidol can be prepared in several steps from 4-methoxybenzoyl chloride, free radical chlorination of which gives the corresponding 4-trichloromethoxybenzoyl chloride. Halogen exchange gives 4-trifluoromethoxybenzoyl fluoride [96], which is then converted to the nitrile. Reaction of 4-trifluoromethoxy benzonitrile with isopropyl Grignard results in the corresponding ketone, which then can react with pyrimidin-5-yl lithium to give flurprimidol (Fig. 25) [97].

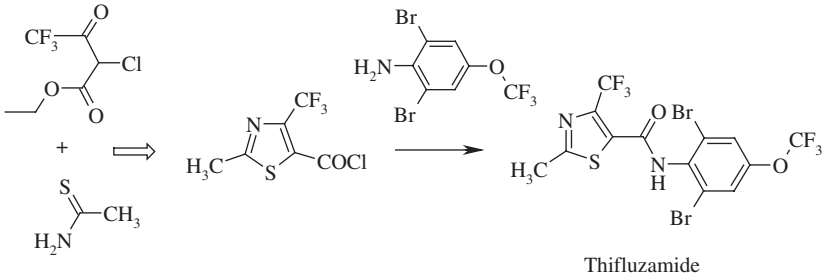

Fig. 24. Synthesis of the fungicide thifluzamide.

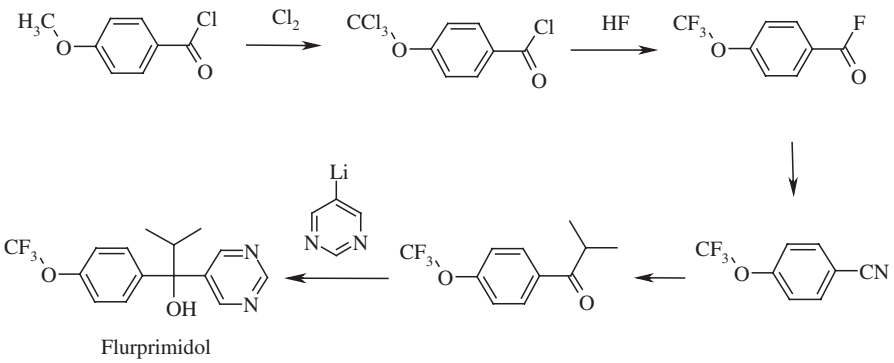

Fig. 25. Synthesis of the plant growth regulator flurprimidol.

2.2.2. Trifluoromethylthio derivatives

2.2.2.1. Herbicides

In the 1970s, it was discovered that a number of trifluoromethanesulfonalides exhibited herbicidal and plant growth regulator activity [98,99]. Perfluidone, fluoridamid, and mefluidide are three representatives of this class of herbicides. Perfluidone [100] is a selective pre-emergent herbicide introduced for the control of *Cyperus esculentus* and of many varieties of grass and selected broadleaf weeds in cotton, turf, rice, sugar cane, and other crops. Fluoridamid was followed by mefluidide (Embark®), which is far more effective.

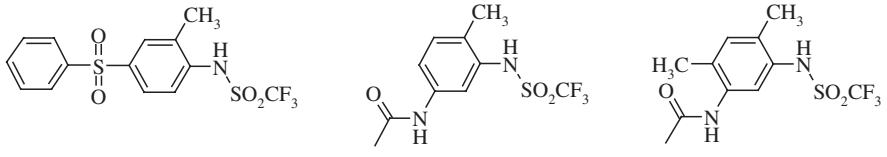

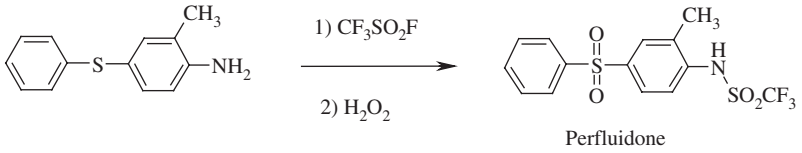

Fig. 26. Synthesis of the herbicide perfluidone.

They are prepared from trifluoromethylsulfonyl fluoride and the corresponding aniline. The trifluoromethylsulfonyl fluoride group was prepared by Simons electrochemical fluorination of methanesulfonyl fluoride (Fig. 26) [101].

2.2.2.2. Insecticides

The highly fluorinated *N*-ethyl perfluorooctane sulfonamide insecticide sulfluramid (Finitron®) [102] is used for the control of ants and cockroaches in households, and the control of red imported fire ants, *Solenopsis richteri* and *S. invicta*, in a number of other field situations. Sulfluramid is an uncoupler of oxidative phosphorylation [103]. Replacement of the fluorines by hydrogens resulted in the loss of all biological activity. The presence of the perfluorooctyl group makes sulfluramid a highly lipophilic and relatively stable molecule. Metabolism studies in animals have shown that sulfluramid is biotransformed by *N*-de-ethylation to give perfluorooctane sulfonamide, a toxic and insecticidally active metabolite [104].

$$CF_3(CF_2)_7SO_2NHCH_2CH_3 \text{ Sulfluramid}$$

The *N*-phenylpyrazole insecticide fipronil, already discussed in Section 2.1.1.2, contains the unusual trifluoromethylsulfinyl substituent, not often seen in agrochemical chemistry. Following the introduction of fipronil, several chemistries related to fipronil were launched, including acetoprole [105], an insecticide with acaricidal and nematicidal activity, and ethiprole [106], a systemic insecticide for the control of a broad spectrum of insects, both from Bayer CropScience.

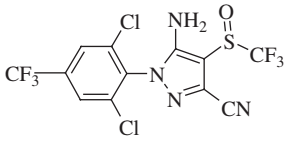

Fipronil

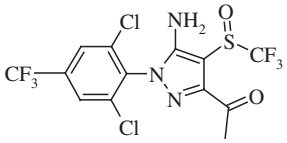

Acetoprole

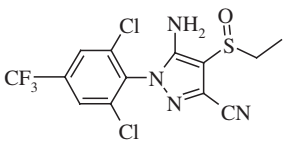

Ethiprole

2.2.3. Difluoromethoxy group

In fluorinated agrochemicals, the difluoromethoxy group is less commonly encountered than the trifluoromethoxy group. The difluoromethoxy group is readily available from the reaction of a phenoxy group and difluorocarbene, generated from chlorodifluoromethane and a base (Fig. 27) [6,107–109].

2.2.3.1. Herbicides

The difluoromethoxy group is widely used in a variety of herbicides, such as the ALS enzyme inhibitor primisulfuron-methyl (Beacon®) [110]. It is believed that introduction of the difluoromethoxy group in primisulfuron-methyl is responsible for its selective control of grass weeds in corn. It has been shown that corn can deactivate primisulfuron-methyl by hydroxylation of the aromatic rings [111].

Synthesis of the 4,6-difluoromethoxypyrimidin-2-yl amino portion of primisulfuron-methyl involves the reaction of the dihydroxy pyrimidine with difluorocarbene, which is generated *in situ* from chlorodifluoromethane and a base such as sodium hydroxide (Fig. 28) [112,113].

Pyraflufen-ethyl (Ecopart®) [114] is a broadleaf weed postemergence herbicide for use in cotton and cereals. Pyraflufen belongs to the family of herbicides that inhibit the Protox enzyme.

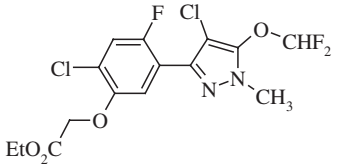

Pyraflufen-ethyl

2.2.3.2. Insecticides

We have earlier discussed the pyrethroid area of insecticides. A number of ester and non-ester pyrethroid insecticides have incorporated the difluoromethoxy group as a means of widening their biological activity to the control of mites [115]. Flucythrinate (Cybolt®, Cythrin®, Pay-Off®) [116] provides control of a variety of sucking insects, beetles, and lepidoptera in cotton and pome fruits. Later, a close analog, flubrocythrinate, was commercialized [117].

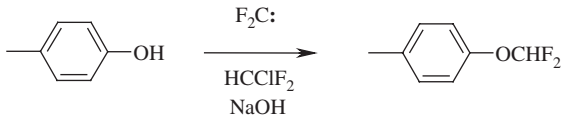

Fig. 27. Difluoromethylation of phenol derivatives.

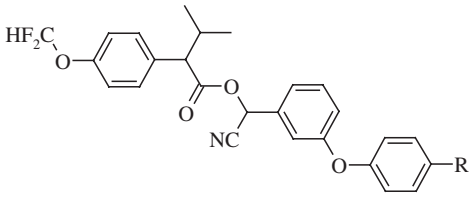

R = H Flucythrinate
R = Br Flubrocythrinate

In some instances, chlorine is successfully replaced with a difluoromethoxy group while retaining desirable properties. Flucythrinate was introduced after fenvalerate by two different companies; the only difference was the replacement of the 4-chloro group of fenvalerate with a difluoromethoxy group in flucythrinate. These two molecules have similar insecticidal properties, and though the chemical groups chlorine and difluoromethoxy are chemically different, their Hammet electronic values σ and their hydrophobic parameters π lie relatively close to each other in parameter space (Fig. 29) [118].

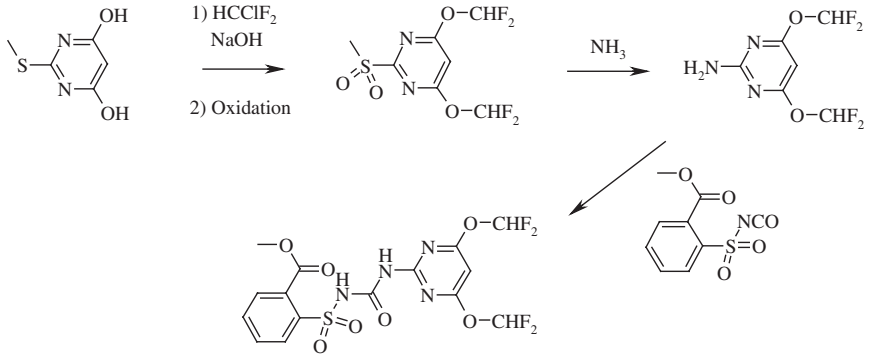

Primisulfuron-methyl

Fig. 28. Synthesis of the herbicide primisulfuron-methyl.

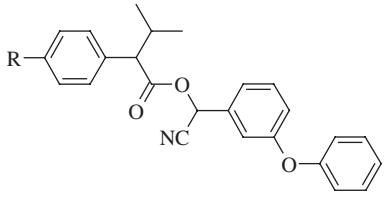

R substituents	sigma	pi	0.1 MR	
Cl	0.23	0.71	0.60	Fenvalerate
$OCHF_2$	0.18	0.31	0.79	Flucythrinate

Fig. 29. Comparison of physico-chemical parameters of chlorine and difluoromethoxy chemical groups in fenvalerate and flucythrinate.

2.2.3.3. Fungicides

Diflumetorim (Piricat®, Pyricut®) [119] is a non-systemic fungicide for use in cereals and ornamentals. Diflumetorim inhibits the germination of powdery mildew and rust.

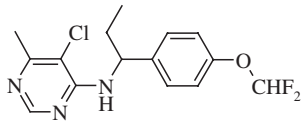

Diflumetorim

2.2.4. Miscellaneous fluoroalkyl groups attached to oxygen and nitrogen

2.2.4.1. Miscellaneous fluoroalkyl groups attached to oxygen

Insecticides. There are a number of agrochemicals with fluoroalkyl groups attached to oxygen with varying lengths of the carbon chain and differences in fluorine content. One such example is the pyrethroid insecticide acrinathrin (Rufast®, Ardent®) [120], where the halogens of cypermethrin have been replaced with a polyfluorinated ester group.

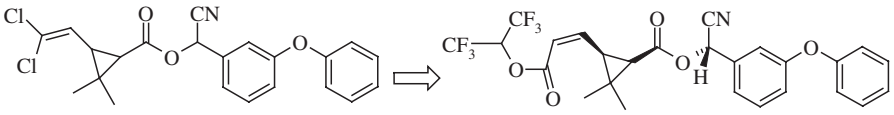

Cypermethrin Acrinathrin

Several *N*-benzoyl-*N*′-phenyl urea IGRs have a variety of polyfluorinated ethers. As mentioned earlier, these compounds act by inhibition of chitin synthesis in insects at the larval stage. They act mainly by ingestion, but in some cases they inhibit fecundity, exhibiting both ovicidal and contact toxicity [121]. Following the success of diflubenzuron, the first IGR compound to be commercialized, an intense search for more potent acylureas resulted in the development of newer molecules, such as hexaflumuron, lufenuron, novaluron, and noviflumuron. Changing the *N*-aryl portion of the molecule, while the 2,6-difluorophenyl acyl urea remained constant, resulted in molecules with different potencies and insect spectrum control. For instance, novaluron, a novel molecule in this class of insecticides, acts both by ingestion and contact, and is far more effective on eggs of larvae of *B. tabaci*, and suppressing developing stages of the leafminer *Liriomyza huidobrensis*, than teflubenzuron and chlorfluazuron, which are discussed in more detail in Section 2.3.2 [122].

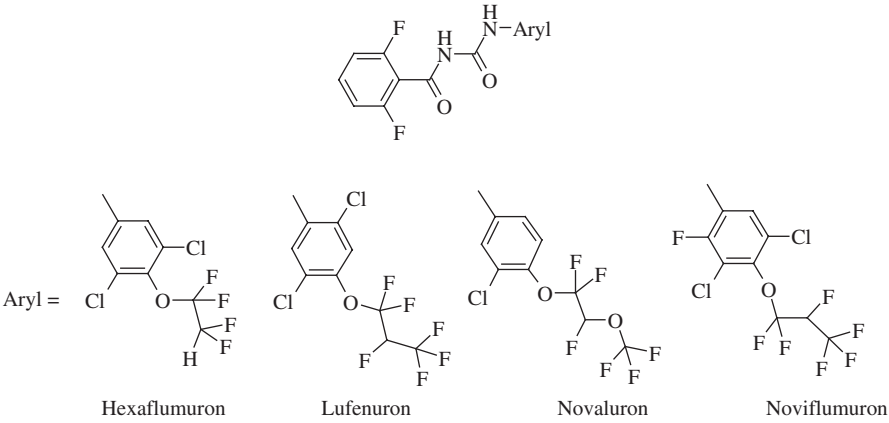

Fungicides. The triazole fungicides represent one of the most significant chemical classes of commonly used agrochemicals [123]. The triazole fungicide tetraconazole (Eminent®, Lospel®, Domark®) [124] is an example of tetrafluoroethoxy-containing agrochemical. The 1,1,2,2-tetrafluoroethyl ether group is introduced by the addition of tetrafluoroethylene to the hydroxy group of an alcohol or phenol in the presence of a base [125].

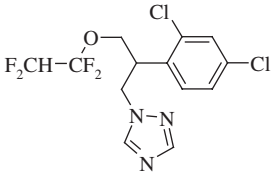

Fludioxonil (Saphire®, Maxim®, Celest®, Wispect®) [126] belongs to the phenyl pyrrole family of fungicides, originally developed from the natural product lead pyrrolnitrin, which is an antifungal secondary metabolite produced by *Pseudomonas pyrrocinia* [127]. Fludioxonil is used for the control of a broad spectrum of foliar pathogens in vegetables, grapes, stone fruits, and other crops.

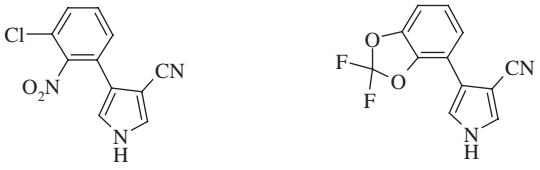

The phenyl pyrroles can be prepared in a variety of ways [128,129]. Lithio-2,2-difluoro-1,3-benzodioxole, obtained from the reaction of 2,2-difluoro-1,3-benzodioxole with *n*-butyl lithium at −10°C, was reacted with ethyl ethoxymethylene

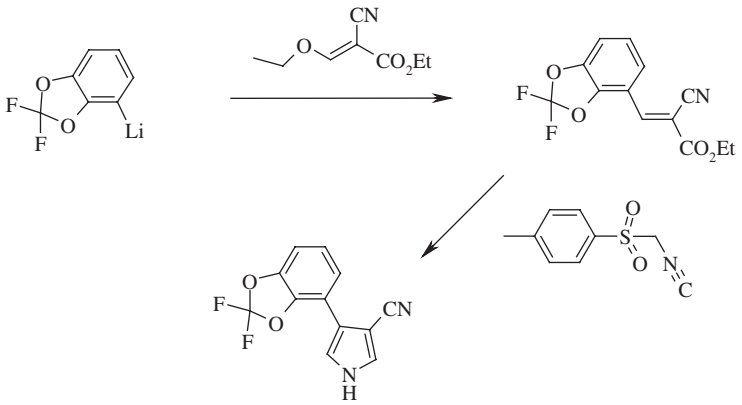

Fludioxonil

Fig. 30. Synthesis of the fungicide fludioxonil.

cyanoacetic ester to give ethyl 2-cyano-2-(2,3-difluoro-1,3-benzodioxol-4-yl)-2-propenoic ester, which was immediately reacted with *p*-toluenesulfonylmethyl isocyanide to produce fludioxonil (Fig. 30).

2.2.4.2. Miscellaneous fluoroalkyl groups attached to nitrogen

N-Difluoromethyl. The difluoromethyl group directly attached to nitrogen is not commonly encountered in agrochemical research. Two examples of *N*-difluoromethylated agrochemicals are sulfentrazone (Authority®, Boral®, Capaz®) [130,131] and carfentrazone-ethyl (Aim®, Affinity®, Aurora®) [132], both herbicides belonging to the same class, Protox. Nitrogen difluoromethylation is obtained from the reaction of the triazolinone with chlorodifluoromethane and a base. A structure–activity study of aryl triazolinones revealed the need for the *N*-difluoromethyl group for optimum activity in this class of herbicides (Fig. 31) [133].

N-Trifluoromethyl. The fungicide, insecticide, acaricide thiadiflur (Cropotex®) [134] is one of the few compounds that have been commercialized that has the unusual *N*-trifluoromethyl group. Thiadiflur was prepared from the di-aza-2,4-diene intermediate $CF_3N = CFCF = NCF_3$ [135].

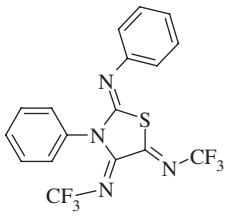

Thiadiflur

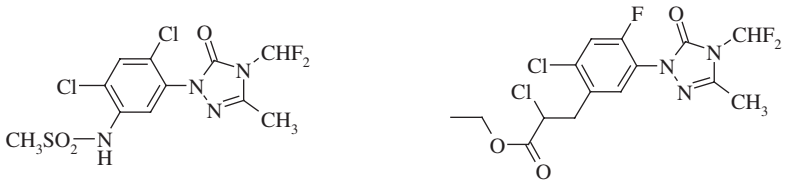

Sulfentrazone Carfentrazone-ethyl

Order of biological potency of triazolinone ring N-substituents

CHF_2 >> Et, i-Pr > CH_2F > Me

Fig. 31. Structure–activity of *N*-substituted triazolinone Protox herbicides.

2.3. Aromatic fluorine compounds

The industrial routes to the synthesis of aromatic fluorine compounds, in which fluorine is directly bonded to an aromatic ring carbon, have been previously reviewed [136]. In contrast to the synthesis of aromatic chlorine and bromine compounds, aromatic fluorine-containing molecules require the use of specialized chemical equipment and additional safety precautions. The reason for these measures is the toxicity and corrosive nature of fluorine reagents.

There are two basic industrial approaches to the introduction of fluorine into an aromatic ring: (1) diazotization procedures and (2) halogen exchange (Halex). A third – and the most promising – approach is aromatic electrophilic fluorination.

Diazotization procedures. Widely used for the production of aromatic fluorine is the Balz–Schiemann reaction. The approach involves diazotization of the aniline and isolation of the insoluble tetrafluoroborate salt, followed by decomposition under heating conditions (Fig. 32). Initially introduced in 1927 [137,138], it did not achieve commercial utility until the mid-1980s. A modification of the Balz–Schiemann reaction involves replacing the tetrafluoroborate with other counterions such as a fluorine anion [139].

Halogen exchange (halex). This procedure involves the displacement of an activated aromatic halogen with a fluorine anion [140,141]. It has been extensively used for the synthesis of fluorinated aromatic intermediates, such as 2,6-difluorobenzonitrile (Fig. 33) [142].

Aromatic electrophilic fluorination. Much research recently has been focused on aromatic electrophilic fluorinations [143], though the approaches studied were limited to small-scale work. A search for alternative routes to the synthesis of the carfentrazone-ethyl herbicide intermediate, 4-chloro-2-fluorophenyl triazolinone, resulted in the investigation of a number of aromatic electrophilic reagents. These investigations have made significant progress toward developing practical and cost-effective large-scale industrial use of these reagents. Among the various

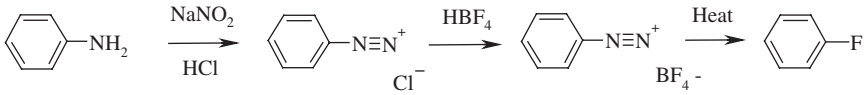

Fig. 32. Balz–Schiemann synthesis of fluorinated aromatic rings.

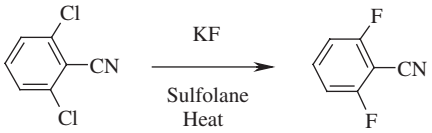

Fig. 33. Synthesis of 2,6-difluorobenzonitrile.

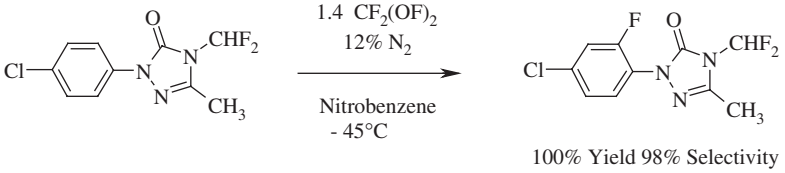

Fig. 34. Electrophilic fluorination of aromatic rings.

reagents that have been studied are F_2/N_2, X_2F_2, $(CF_3SO_2)_2NF$, Selectfluor®, $CF_2(OF)_2$, CF_3OF, $CH_3C(O)OF$, and $CF_3C(O)OF$ (Fig. 34) [144,145].

2.3.1. Herbicides

Several aromatic fluorine-containing herbicides were discussed earlier – diflufenican in Section 2.1.1.1 and flufenacet in Section 2.1.2.1– or will be discussed in more detail below – picolinafen and beflubutamid in Section 3.1. Another is fluroxypyr, a postemergence herbicide introduced by Dow AgroSciences in the UK in 1985 [146].

Auxin herbicides. Auxins are plant hormones, the most important naturally occurring auxin is indole-3-acetic acid. Fluroxypyr, and its ester derivatives, act as a synthetic auxin, in a manner similar to the herbicide 2,4-dichlorophenyl acetic acid (2,4-D), providing control of broadleaf weeds in small grain crops. Fluroxypyr is prepared in several steps starting with the chlorination of pyridine to give pentachloropyridine, which is readily converted to 3,5-dichloro-2,4,6-trifluoropyridine. Treatment with ammonia gives 4-amino-3,5-dichloro-2,6-difluoropyridine, which is readily hydrolyzed at the 2 position to give 4-amino-3,5-dichloro-6-fluoro-2-hydroxypyridine, which is then carboxymethylated to give fluroxypyr [147].

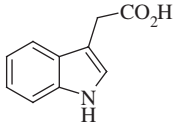

Indole-3-acetic acid

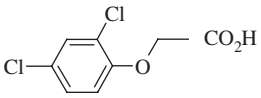

2,4-D Herbicide

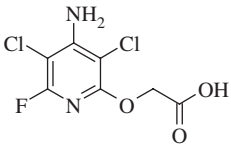

Fluroxypyr

A new class of plant auxin herbicides are the phytotropins, exemplified by the semicarbazone diflufenzopyr [148]. Diflufenzopyr is a systemic herbicide for the selective control of broadleaf and perennial weeds in corn. Unlike the early auxin herbicides, such as 2,4-D and dicamba, which acted as mimics of indole-3-acetic acid, phytotropins prevent polar auxin transport in sensitive plants, causing stunting and loss of tropic response [149].

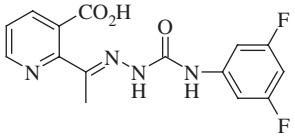

Diflufenzopyr

Protox herbicides. A number of Protox herbicides share a 2-fluorophenyl group. Initial investigations into an alternative synthesis of 2-fluoro-4-chlorophenyl triazolinones resulted in the very promising use of newer fluorinating reagents. The actual synthesis of carfentrazone-ethyl involved the use of 2-fluoroaniline as the starting material (Fig. 35) [150].

ALS herbicides. Two classes of ALS-inhibiting herbicides are the sulfonylurea herbicides, discussed in Sections 2.1.2.1 and 2.2.3.1, and the imidazolinone herbicides. A third class of ALS-inhibiting herbicides is the 1,2,4-triazolo [1,5-a]pyrimidine-2-sulfonanilides. The triazolopyrimidine sulfonanilides act by disrupting the biosynthesis of branched chain amino acids in plants. Representatives of this class of herbicides include florasulam (Boxer®, Nikos®) [151], initially introduced in Belgium in 1999 and used for the postemergence control of broadleaf weeds in cereals and corn, and flumetsulam (Broadstrike®) [152], used alone or in combination with other herbicides for the control of broadleaf weeds in soybean and corn.

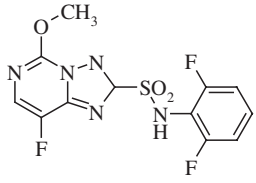

Florasulam

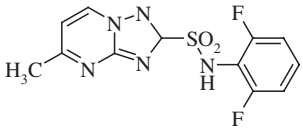

Flumetsulam

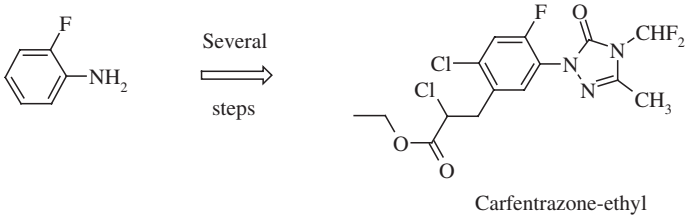

Carfentrazone-ethyl

Fig. 35. Synthesis of the herbicide carfentrazone-ethyl.

2.3.2. Insecticides

Benzoylphenyl urea. Substitution at the anilide portion of the molecule, particularly at the 4 position, has resulted in a variety of different commercial benzoylphenyl urea insecticides; diflubenzuron (Dimilin®), with chlorine at the 4 position of the anilide, provides one of the earliest examples [153]. The trifluoromethyl-containing benzoylphenyl ureas flufenoxuron and bistrifluron were discussed in Section 2.1.1.2, and chlorfluazuron was discussed in Section 2.1.2.2. Teflubenzuron (Nemolt®) is used for the control of lepidoptera, coleoptera, diptera, and hemiptera larvae on vines, pome fruit, cabbages, vegetables, and cotton.

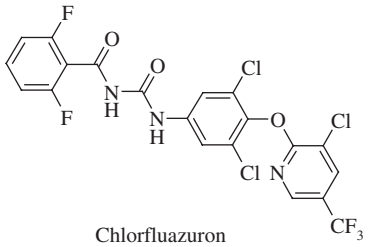

Chlorfluazuron

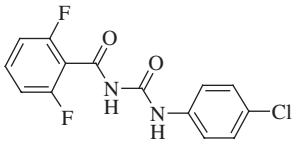

Diflubenzuron

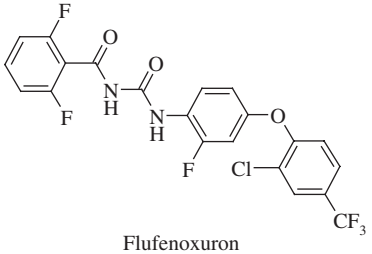

Flufenoxuron

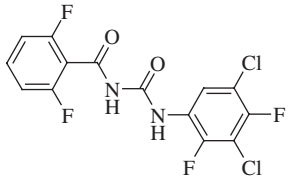

Teflubenzuron

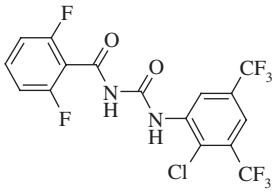

Bistrifluron

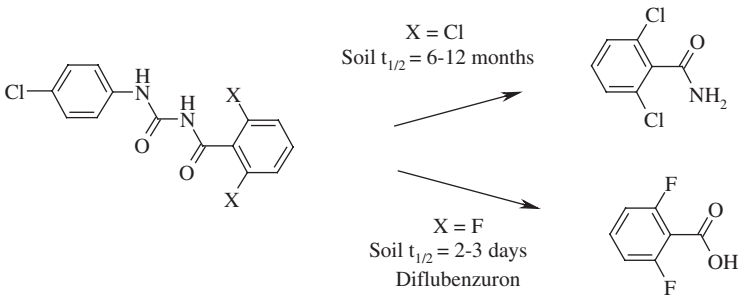

Fig. 36. Influence of fluorine on soil stability of benzoylphenyl urea insecticides.

Aromatic fluorine plays a decisive role in the biological activity of benzoylphenyl urea insecticides. Extensive quantitative structure–activity relationships, or QSAR, was performed by Verloop and Ferrell on the larvicidal activity of *Pieris brassicae* using a number of substituted benzoylphenyl ureas containing aromatic fluorines [154]. The results of the study showed that an electron-withdrawing and hydrophobic group, as well as a small-size substituent such as fluorine, are necessary for optimal biological activity at the 2 and 6 aromatic positions. Interestingly, the 2,6-difluorophenyl modification was originally undertaken to reduce persistence in soil by impacting environmental stability such as soil degradation (Fig. 36) [4].

The 2,4-diaryloxazoline etoxazole [155] is a highly active insecticide and acaricide that was commercialized in 1998. Its mode of action appears to be similar to that of other benzoylphenylurea IGRs [156]. Etoxazole is highly active against eggs, larvae, and nymphs of a number of mites. It also controls green rice leafhoppers, aphids, and diamondback moth. In addition to its broad spectrum of biological activity, etoxazole has a favorable environmental profile, with low mammalian toxicity and short environmental persistence [157].

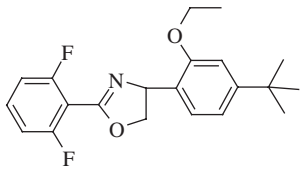

Etoxazole

Pyrethroids. Following the successful introduction of the first commercial pyrethroid insecticides in the 1970s, new pyrethroid molecules, such as cyfluthrin (Baythroid®), the first fluorine-containing pyrethroid [158], were introduced in the1980s. Cyfluthrin was several times more active than cypermethrin for the control of cotton pests [159]. Later, in 1988, tefluthrin (Force®, Forza®) [160] was introduced as an insecticide with soil applications.

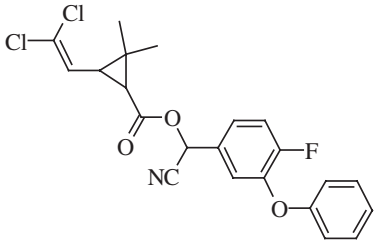

Cyfluthrin

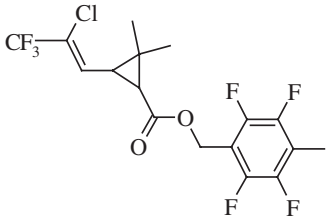

Tefluthrin

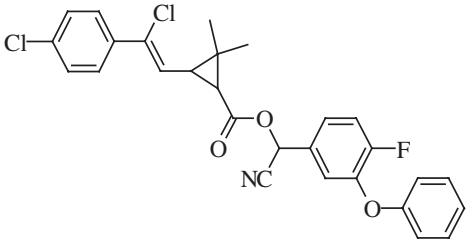

Flumethrin

In addition to the classical ester pyrethroids previously discussed in Sections 2.1.1.2, 2.2.3.2, and 2.2.4.1, two non-ester pyrethroid molecules were reported by the FMC Corporation in the late 1980s and early 1990s: protrifenbute [161] and eflusilanate [162]. Structure–activity investigations of eflusilanate found that removal of the fluorine atom resulted in a 10-fold loss of biological activity [163].

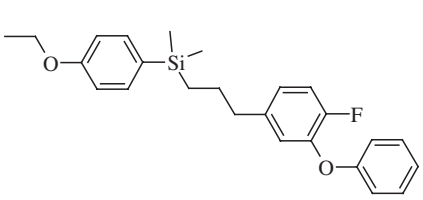

Eflusilanate

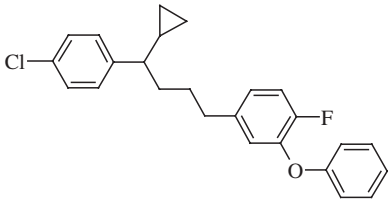

Protrifenbute

2.3.3. Fungicides

In addition to the trifluoromethylphenyl sterol biosynthesis inhibitors discussed in Section 2.1.1.3, a number of fluorine phenyl-containing azoles were introduced in the years 1984 through 1993. Though these molecules share some common structural features, such as the triazole heterocycle and a 4-fluorophenyl ring in at least three of the four fungicides shown below, each also has unique chemical features. For instance, in the case of flusilazole (Punch®, Nustar®, Triumph®, Olymp®) [164], a silicon atom is present. This represented that first time silicon

was present in a commercial agrochemical. Later, another silicon-containing fungicide, simeconazole, was introduced. Structure–activity studies of simeconazole, RS-2-(4-fluorophenyl)-1-(1H-1,2,4-triazol-1-yl)-3-trimethylsilylpropan-2-ol, revealed the importance of the 4-fluoro group in the phenyl ring for effective fungicidal activity against *Rhizoctonia solani* and *Blumeria graminis* [165]. In the other three fungicides, respectively, oxygen is present as an alcohol in flutriafol [166], an epoxide is present in epoxiconazole [167], and a carbonyl is present in fluquinconazole [168]. The fungicide flutriafol, introduced in 1983 for the control of powdery mildew, rusts, and *Septoria* spp., in cereals, was originally prepared in several steps from fluorobenzene and chloroacetyl chloride in the presence of aluminum chloride to give 4-fluorophenacyl chloride. Addition of 2-fluoroaryl Grignard to 4-fluorophenacyl chloride gives the corresponding chlorohydrin, which is reacted with 1,2,4-triazole to give flutriafol [54].

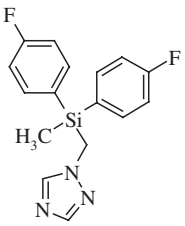

Flusilazole

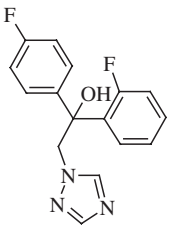

Flutriafol

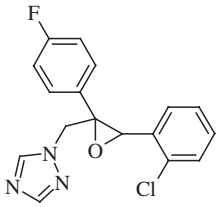

Epoxiconazole

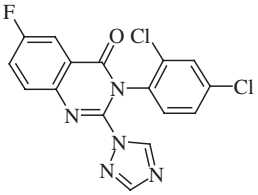

Fluquinconazole

Nuarimol (Gauntlet®) [169] is a systemic foliar fungicide introduced in 1980 by Dow Elanco for the control of *Cercosporella* spp., *Septoria* spp., *Ustilago* spp., powdery mildew, and other fungi in cereals.

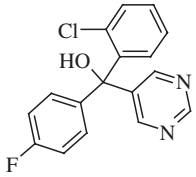

Nuarimol

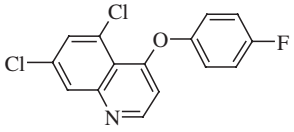

Quinoxyfen

Quinoxyfen is a fungicide that is used for the control of powdery mildew diseases by interfering with germination, and, in some cases, such as barley powdery mildew, appressorium formation [170].

2.4. Aliphatic and olefinic fluoroalkyl groups

Pyrethroid insecticides. Continued interest in and research into this important class of insecticides has resulted in a number of important discoveries, one of which involved replacement of the vinylic chlorine of traditional pyrethroids with trifluoromethyl to give λ-cyhalothrin (Cyhalon®, Grenade®) (ICI/Zeneca) [171], in

1980, and bifenthrin (Talstar®) (FMC) [172] and tefluthrin (Force®, Forza®) [160], in 1988. Tefluthrin was discussed in Section 2.3.2, on aromatic fluorine compounds. Replacement of vinylic chlorine with trifluoromethyl resulted in a significant increase in biological activity. These compounds are prepared from the esterification of the acid with the appropriate alcohol. The acid portion is obtained from the reaction of the olefin with trichloro-2,2,2-trifluoroethane under free radical conditions, followed by ring formation with sodium butoxide in 1,2-dimethoxyethane (Fig. 37) [173]. Several approaches are available for the synthesis of the trifluoromethyl vinyl ester portion of pyrethroids [174].

The non-ester pyrethroid flufenprox is a broad spectrum insecticide with residual activity against hemiptera, lepidoptera, and coleopteran insects in rice. It is reported that flufenprox is safe to beneficial insects such as spiders and predaceous mites [175].

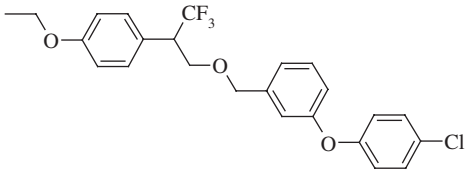

Flufenprox

3. FLUORINE-CONTAINING AGROCHEMICALS: RECENT DEVELOPMENTS

This section will primarily focus on fluorinated agrochemicals in advanced stages of development that have been assigned an ISO name since 2001. Some important sources of information are the latest edition of Global Insecticide Directory, Agranova, and *The Pesticide Manual*. However, in many cases, only limited information is available about the synthesis, biology, mode of action, and structure–activity characteristics of the molecules.

New agrochemicals introduced in the past five years include new chemistries with known modes of action, such as the protoporphyrinogen inhibitor bencarbazone, the phytoene desaturase picolinafen and beflutamid, and sodium channel pyrethroids; new chemistries with possibly new modes of action, such as flonicamid and pyridalyl; and new chemistries with established new modes of actions, such as flubendiamide, which activates ryanodine-sensitive intracellular calcium release channels, ryanodine receptors RyR, in insects.

We have also noticed renewed interest in the use and synthesis in agrochemicals containing the pentafluorosulfanyl group, first in the early 1990s, mostly from work done at Zeneca in the UK. In those early patents, the $-CF_3$ group was replaced with $-SF_5$ in known diphenyl ether herbicides and in insecticides such

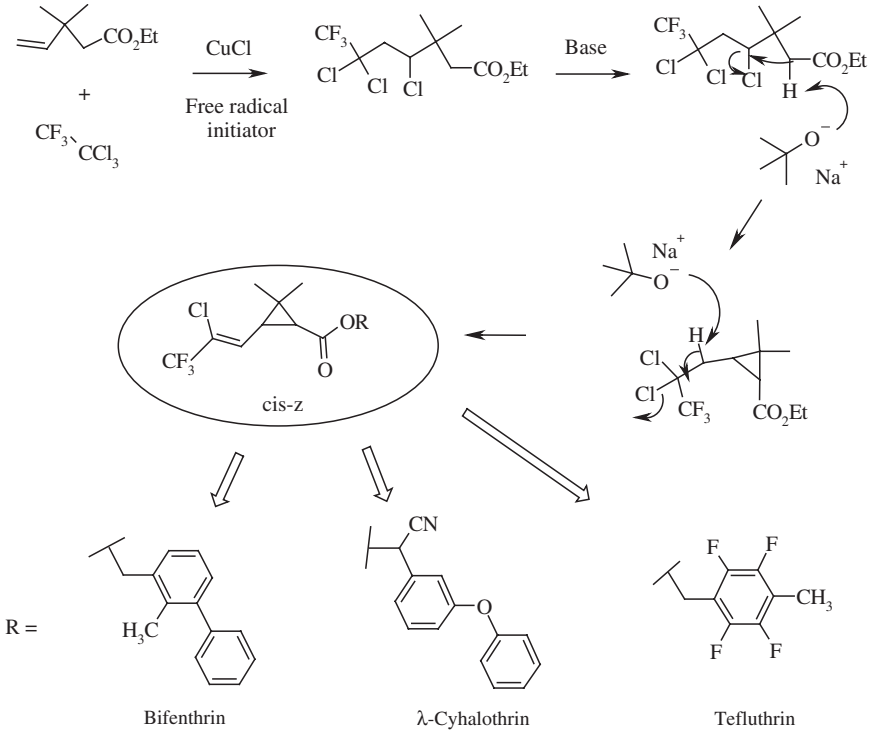

Fig. 37. Preparation of the ester portion of trifluoromethyl vinyl-containing pyrethroids.

as fipronil (Fig. 38) [176]. The $-SF_5$ is a strong electron-withdrawing group, with an electronic para sigma value of 0.68, in between that of $-CF_3$ (0.54) and $-NO_2$ (0.78). The $-SF_5$ is also a highly lipophilic group with a hydrophobic π value of 1.23, slightly more lipophilic than either $-CF_3$ (0.88) or $-OCF_3$ (1.04). As expected, replacement of chemical groups CF_3 and OCF_3 with SF_5 yields various outcomes from one chemical class to another. In one case, comparative screening for herbicidal activity between CF_3 and SF_5 analogs of a series of diphenyl ether herbicides showed that the SF_5 group did not offer any advantages over CF_3. However, the SF_5 analog of diflufenican was comparable in biological activity to its CF_3 analog. In a third example, the SF_5 analog of fipronil was superior in biological activity to its CF_3 analog [177].

Though great advances have been made in the preparation of SF_5 raw materials, more process research needs to be done before SF_5-containing agrochemicals are commercially viable. The initial synthesis of pentafluorosulfur phenyl derivatives from silver difluoride and aryl disulfides resulted in low yields (Fig. 39) [178,179]. Later, this procedure was improved by adjusting the temperature of the reaction, but it still relied on the use of expensive AgF_2 [177,180].

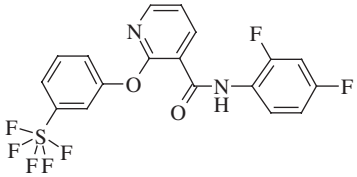

SF_5 analog of herbicide diflufenican

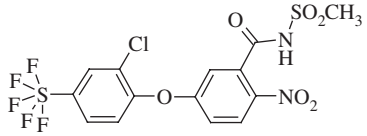

SF_5 analog of diphenyl ether herbicides

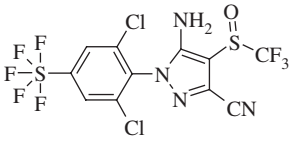

SF_5 analog of fipronil

Fig. 38. SF_5 analogs of known CF_3-containing herbicidal and insecticidal agrochemicals.

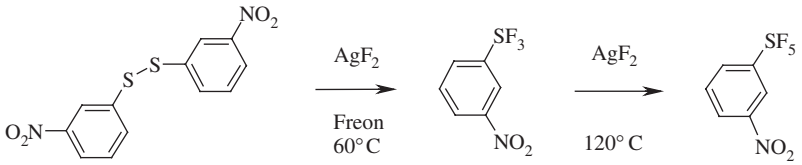

Fig. 39. Synthesis of pentafluorosulfur phenyl derivatives with AgF_2.

An alternative method of preparing the SF_5 group was developed in the 1990s using elemental fluorine and an arylthiol. In this process, elemental fluorine is used both as an oxidant and a fluorinating agent. Despite the fact that in the final fluorination, the conversion of SF_3 to SF_5 is difficult and results in a number of by-products from ring fluorination side reactions, it provides a more realistic route to the preparation of many pentafluorosulfur phenyl derivatives (Fig. 40) [181].

3.1. Herbicides

Two phytoene desaturase herbicides have been introduced since 2000: picolinafen (Pico®) [182], introduced in 2001 by BASF, and beflubutamid [183], introduced in 2003 by Ube Industries. The primary mode of action of picolinafen and beflutamid is interference of carotenoid biosynthesis at the phytoene desaturation level, causing bleaching of the plant affected. As in previously developed phytoene desaturase herbicides, a meta-substituted trifluoromethylphenyl group is key for activity in this class of herbicides, pointing to the need for a lipophilic and electron-withdrawing group at this position of the molecule.

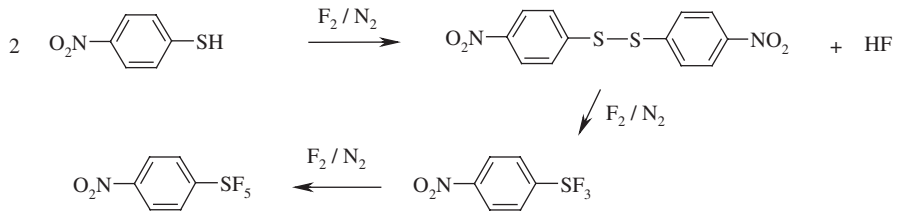

Fig. 40. Preparation of SF_5 phenyl derivatives with elemental fluorine.

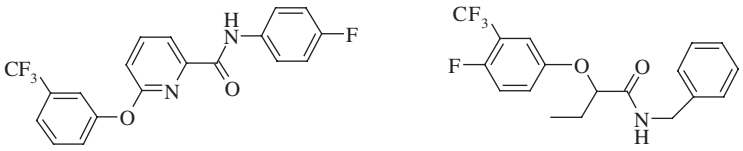

Metamifop (Pizero®) [184] is a new arylphenoxypropionic acid experimental postemergence herbicide for the selective control of grasses such as barnyard grass in rice.

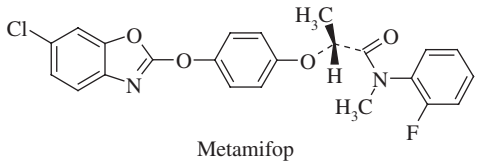

A number of recent herbicide entries include bencarbazone [185], pyrasulfotole [186], and pyrimisulfan [187]. Bencarbazone, whose ISO common name was approved in 2005, has all the features associated with Protox herbicides, particularly that of the Protox herbicide sulfentrazone. Pyrasulfotole is a newly developed herbicide from Bayer CropScience for use on cereals. Pyrimisulfan, a difluoromethylsulfonamide-containing, herbicide, is a new ALS herbicide for the control of perennial weeds.

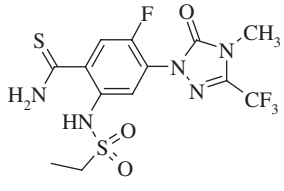

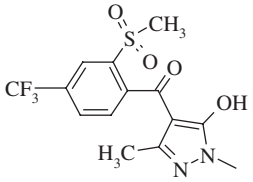

Pyrasulfotole

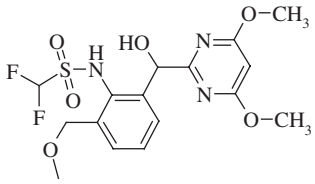

Pyrimisulfan

Flucetosulfuron [188,189] is a sulfonylurea experimental postemergence herbicide for controlling grasses such as barnyard grass in rice and broadleaf weeds such as Galium aparine in cereals. It shares with previously introduced sulfonylurea herbicides a common mode of action, inhibition of the ALS enzyme, a key enzyme in the biosynthesis of branched amino acids, such as leucine, isoleucine, and valine [76].

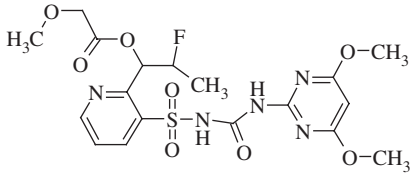

Flucetosulfuron

3.2. Insecticides

Three decades after the first IGRs were introduced in the mid-1970s, new chitin biosynthesis inhibitors, such as noviflumuron (Recruit III®) [190], were developed. Noviflumuron is particularly effective for the control of ants, termites, cockroaches, and fleas.

Amidoflumet is a highly effective experimental miticide for the control of *Tyrophagus putrescientae*, *Dermatophagoides farinae*, and chelatid mites.

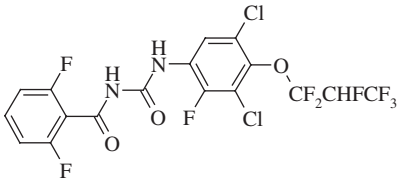

Noviflumuron

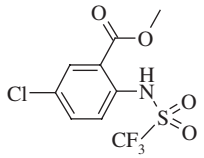

Amidoflumet

Flufenerim [191], an insecticide that acts by inhibition of the mitochondrial electron transport of complex I, is under development by Ube Industries. Flufenerim, which is chemically related to pyrimidifen, is reported to control aphids and whiteflies.

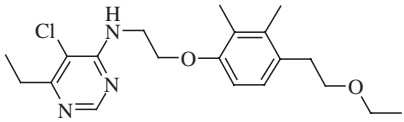

Pyrimidifen

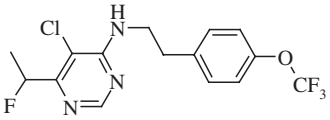

Flufenerim

Dimefluthrin [192] and metofluthrin [193] are two pyrethroid insecticides recently introduced by Sumitomo. In both dimefluthrin and metofluthrin, the vinylic chlorides of early pyrethroids have been replaced, in dimefluthrin by two methyl groups, and in metofluthrin by one methyl and one hydrogen group. They both share a 2,3,5,6-tetrafluorophenyl group, as in the pyrethroid tefluthrin.

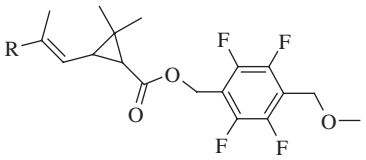

$R = CH_3$ Dimefluthrin
$R = H$ Metofluthrin

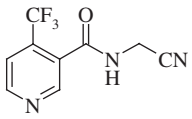

Flonicamid

Flonicamid is a new systemic insecticide discovered by Ishihara [194] for the control of aphids, whiteflies, thrips, and leafhoppers. FMC was granted exclusive licensing for the development of flonicamid in the American and European markets. Also recently introduced by Sumitomo is pyridalyl (Cleo®) [195], belonging to a new class of insecticides with a new mode of action. Investigation into the biological activity of a number of 5-substituted pyridalyl derivatives revealed that the trifluoromethyl group was essential to providing the best activity [196]. Pyridalyl controls lepidopterous pests in cotton and vegetables, but its mode of action is still under investigation [197].

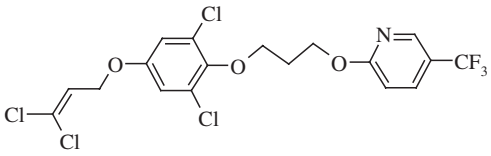

Pyridalyl

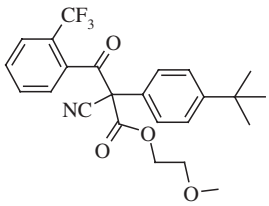

Cyflumetofen

Cyflumetofen [198] is an experimental acaricide/miticide for use in vegetables and fruits. Pyriprole and pyrafluprole are two experimental insecticides introduced by Nihon Nohyaku and related, both in chemistry and mode of action to the highly successful insecticide fipronil. Fipronil acts at the GABA receptor to block the chloride channel.

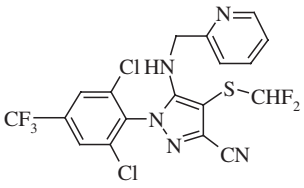

Pyriprole

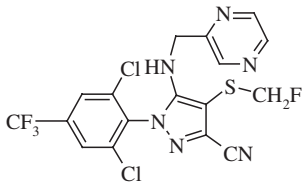

Pyrafluprole

A new development in the field of agrochemicals is the use of the heptafluoroisopropyl group in the aromatic ring of the active molecule flubendiamide [199,200]. Flubendiamide is an insecticide discovered by Nihon Nohyaku, and co-developed with Bayer CropScience [201,202], that belongs to a new chemistry class – the benzenedicarboxamides, or phthalic acid diamides, as they are also known – with a novel mode of action. Flubendiamide activates ryanodine-sensitive intracellular calcium release channels, ryanodine receptors, RyR, in insects [203]. Flubendiamide is prepared in several steps involving 3-iodophthalic anhydride and the key intermediate 4-heptafluoroisopropyl-2-methylaniline, which is prepared from 2-toluidine and heptafluoroisopropyl iodide, in the presence of sodium dithionite and sodium hydrogen carbonate (Fig. 41) [204]. With flubendiamide moving into development, it is clear that whatever the costs added by the incorporation of this exotic group, they are more than compensated by the insecticide's increased biological activity, and the resulting lower application rate.

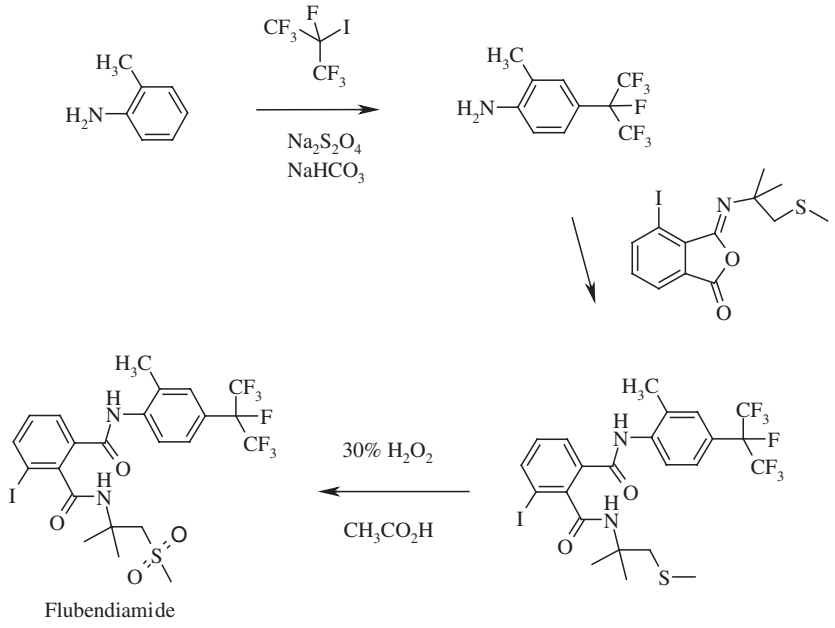

Flubendiamide

Fig. 41. Synthesis of the insecticide flubendiamide.

DuPont has also introduced a new class of insecticides, the anthranilic diamides, such as DP-23 [205], which, like flubendiamide, also act by activating the ryanodine receptor [206].

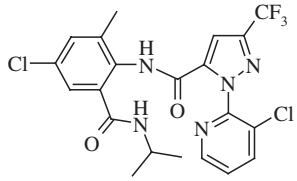
DP-23

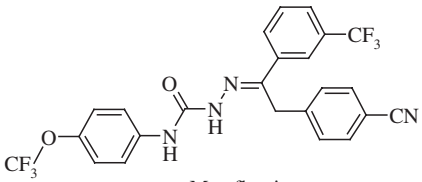
Metaflumizone

Metaflumizone [207], initially discovered in the 1990s by Nihon Nohyaku, is currently under development by BASF. Metaflumizone belongs to a class of sodium channel insecticides, the semicarbazones, which eventually led to the discovery of the successful insecticide indoxacarb.

3.3. Fungicides

The need to control a wide spectrum of plant diseases in a variety of crops demands the discovery and development of new fungicides that are both specific to plant pathogens and safe to human health. In addition, resistance – decreased sensitivity of a given pathogen species to a particular chemical, resulting in poor disease control – requires the constant discovery of new chemistries and modes of action [208]. Over 16 new fungicidal compounds have been announced since 2000, including six strobilurins, such as picoxystrobin, pyraclostrobin, and fluoxastrobin, and several oomycete-specific compounds. Only one new fungicide – Nippon Soda's cyflufenamid – was submitted during 2003 for EU approval [209]. Cyflufenamid (Pancho®) [210] controls powdery mildew in the cereal market. Cyflufenamid has both curative and preventive properties and can be applied to all winter and spring wheats and barleys.

Fluoxastrobin (Fandango®, Bariton®) [211–213], a new strobilurin fungicide with curative and leaf-systemic activity, was developed by Bayer CropScience, for use as both a seed treatment and a foliar spray to treat a variety of diseases in cereals. Fluoxastrobin initially was submitted for registration as an (*E*)/(*Z*) isomer mixture and later changed to the (*E*)-isomer.

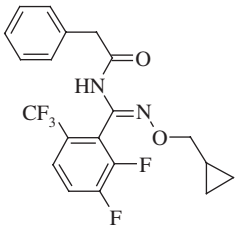
Cyflufenamid

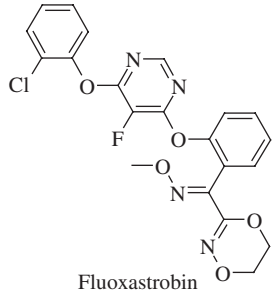
Fluoxastrobin

Flumorph [214] is a new systemic fungicide discovered in 1994 at Shenyang Research Institute of Chemical Industry. Flumorph provides good control at 100–200 mg /L of oomycetes such as cucumber downy mildew, cabbage downy mildew, grape downy mildew, and tomato late blight. Oomycetes are a large group of important species that include both saprophytes and significant parasites of animals, insects, and plants (*Pythium*, *Phytophthora*, white rusts, and downy mildews). Flumorph also has proven to be highly active against both metalaxyl-sensitive and resistant isolates of *Pseudoperonospora cubensis*.

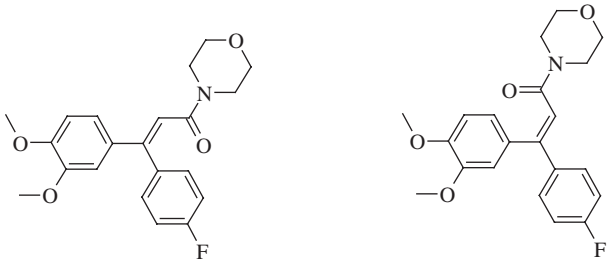

(*E*)-Isomer (*Z*)-Isomer

Flumorph

Amisulbrom [215] is a new fungicide from Nissan Chemical Industries that has been reported to control clubroot disease, *Plasmodiophora brassicae*, in Chinese cabbage [216].

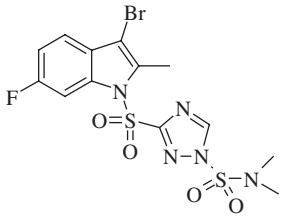

Amisulbrom

Fluopicolide [217] is a Bayer CropScience fungicide for the control of oomycete diseases such as downy mildew, damping-off, and late blight in vegetables, cucumber, tomatoes, cereals, and coffee.

Penthiopyrad [218,219] is a new carboxamide fungicide under development by Mitsui Chemicals that shows good activity against *Botrytis*, powdery mildew, and apple scab.

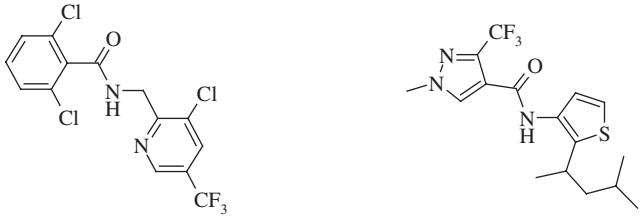

Fluopicolide Penthiopyrad

Benthiavalicarb-isopropyl (Mamorotto®) [220] is a new fungicide from Kumiai Chemical Industries that is active against the oomycete fungal plant pathogen *Plasmopara viticola*, which causes downy mildew in grapevines. Benthiavalicarb-isopropyl has demonstrated good prophylactic and local activity in intact plants and detached leaves and low translaminar activity [221]. With two asymmetric centers, of the four possible optical enantiomers of benthiavalicarb-isopropyl, only one is biologically active, that of isopropyl [(*S*)-1-{(*R*)-1-(6-fluorobenzothiazol-2-yl)ethylcarbamoyl}-2-methylpropyl}carbamate. The bulk agricultural form of benthiavalicarb-isopropyl contains the active (*S*,*R*)-benthiavalicarb-isopropyl and traces of [(*S*)-1-[(*S*)-1-(6-fluorobenzothiazol-2-yl)ethylcarbamoyl]-2-methylpropyl] carbamate, and neither of the two remaining isomers [222].

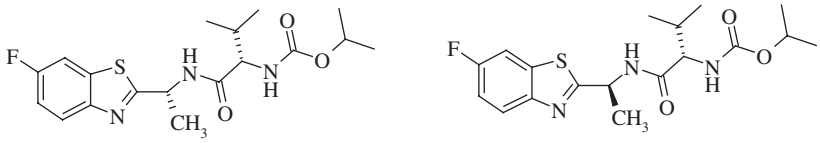

(*S*,*R*)-Isomer (*S*,*S*)-Isomer

Benthiavalicarb-isopropyl

4. SUMMARY

It was recently stated that the field of fluorine chemistry is experiencing a renaissance [223]. The pivotal role of fluorine in the development of new agrochemicals in the past two decades is likely to intensify in the future as improvements continue to be made in the industrial preparation of key fluorinated materials. The higher cost of fluorinated building blocks remains a factor that limits their wider use. Certain fluorinating approaches, such as Halex, the halogen-exchange reaction, are inherently wasteful, both from a cost and an environmental point of view, due to the need to introduce and then remove chlorine as a means of introducing fluorine [224]. Electrophilic fluorinating agents [143,225], such as those described in Section 2.3 on aromatic fluorination, offer clear advantages in that fluorine can be introduced later in the synthesis of a molecule, resulting in potentially lower costs and environmentally cleaner processes [145].

With the increased number of new commercial fluorine-containing agrochemicals introduced over the past decade, there is a growing need to continue to understand the environmental fate of these materials, particularly perfluoroalkyl substituents, such as the trifluoromethyl group [226]. Given the strong carbon–fluorine bond of fluorine-containing molecules, the likelihood of fluorine being released into the environment in the form of hydrogen fluoride is negligible. This is an important point given the ongoing investigations into the risks to

animals and plants of hydrogen fluoride that is released into the environment from fluorinated water effluents and from certain fluoride-generating industries such as coal and ceramics [227,228].[2]

Although the introduction of fluorine often has a dramatic impact on the biological activity of many agrochemicals, it is not always predictable. Improvements in activity with any of the various available fluorinated groups depends on the specific molecule, its mode of action, its physical chemical properties, and application method, among other factors. Part of the difficulty of predicting the outcome of the use of fluorinated groups is the fact that molecular substitution can impact biological activity at different stages: the molecular level, where a molecule interacts with a binding site; transport of a molecule through plant or insect barriers; metabolism by the target organism; and photostability. A better understanding of quantitative structure–activity relationships for different classes of agrochemicals as they are affected by these different factors would go a long way toward promoting the rational design of biologically active molecules.

REFERENCES

[1] H.Martin, C.R.Worthing (Eds.), The Pesticide Manual5th edition, BCPC, Croydon, England, 1977.
[2] C.D.S.Tomlin (Ed.), The Pesticide Manual13th edition, BCPC, Alton, Hampshire, 2003.
[3] G.T. Newbold, Organofluorine chemicals and their industrial applications, in: R.E. Banks, (Ed.), Society of Chemical Industry, Ellis Horwood LTD, Chichester, England, 1979, pp. 169–187.
[4] P. Jeschke, The unique role of fluorine in the design of active ingredients for modern crop protection, ChemBioChem. 5 (2004) 570–589.
[5] A. Haas, Fluorine modified compounds: synthesis and biological activities, L'actualite′ Chimique 5 (1987) 183–188.
[6] F. Leroux, P. Jeschke, M. Schlosser, α-Fluorinated ethers, thioethers, and amines: anomerically biased species, Chem. Rev. 105 (2005) 827–856.
[7] P. Maienfisch, R.G. Hall, The importance of fluorine in the life science industry, Chimia 58 (3) (2004) 93–99.
[8] C. Hansch, T. Fujita (Eds.), Classical and Three-Dimensional QSAR in Agrochemistry, ACS Symp. Ser. 606, Washington, DC, 1995.
[9] R.E.Banks, B.E.Smart, J.C.Tatlow (Eds.), Organofluorine Chemistry: Principles and Commercial Applications, Plenum Press, New York, 1994.
[10] M. Hudlicky, A.E. Pavlath (Eds.), Chemistry of Organic Fluorine Compounds II, A Critical Review, ACS Monogr. 187, 1995, Washington, DC
[11] P.H. Olesen, The use of bioisosteric groups in lead optimization, Curr. Opin. Drug Disc. Dev. 4 (2001) 471–478.
[12] B. Langlois, Organofluorine Chemistry: Principles and Commercial Applications, in: R.E. Banks, B.E. Smart, J.C. Tatlow (Eds.), Plenum Press, New York, 1994, pp. 221–235.

[2] [*Note of the Editor: The effects of fluoro-organics on plants and organisms are presented in details in this series by A. W. Davison and L. H. Weinstein*.]

[13] R.J. Alberts, E.C. Kooymann, Halogenation of aromatics. IX. Vapor-phase chlorination and bromination of benzotrifluoride, Recl. Trav. Chim. Pays-Bas. 83 (8) (1964) 930–936.
[14] N. Ishikawa, Aromatic fluorine compounds as intermediates for pharmaceuticals, agrochemicals and dyes, Senryo to Yakuhin 26 (6) (1981) 106–113.
[15] C.L. Coon, M.E. Hill, US Patent 3,714,272, 1973.
[16] M.B. Green, G.S. Hartley, T.F. West, Chemicals for Crop Protection and Pest Control, 3rd edition, Pergamon Press, Oxford, 1987.
[17] G.W. Probst, W.H. Wright, Herbicides, Chemistry, Degradation, and Mode of Action, P.C. Kearney, D.D. Kaufman, (Eds.), Marcel Dekker, New York, 1975, p. 453.
[18] G.T. Newbold, Organofluorine chemicals and their industrial applications, in: R.E. Banks, (Ed.), Society of Chemical Industry, Ellis Horwood LTD, Chichester, England, 1979, p. 173.
[19] E. Kühle, E. Klauke, Fluorinated isocyanates and their derivatives as intermediates for biologically active compounds, Angew. Chem., Int. Ed. Engl. 16 (1977) 735.
[20] M. Matringe, J.M. Camadro, R. Labbe, R. Scalla, Protoporphyrinogen oxidase as a molecular target for diphenyl ether herbicides, Biochem. J. 260 (1989) 231–235.
[21] F.E. Dayan, S.O. Duke, Herbicide Activity: Toxicology, Biochemistry and Molecular Biology, R.M. Roe, J.D. Burton, R.J. Kuhr (Eds.), IOS Press, Amsterdam, 1997, pp. 11–35.
[22] H.F. Wilson, D.H. McRae, US Patent 3,080,225, 1963.
[23] R.J. Theissen, US Patent 3,652,645, 1972.
[24] R.Y. Yih, C. Swithenbank, New potent diphenyl ether herbicides, J. Agric. Food Chem. 23 (3) (1975) 592–593.
[25] W.O. Johnson, G.E. Kollman, C. Swithenbank, R.Y. Yih, RH-6201 (Blazer): a new broad spectrum herbicide for postemergence use in soybeans, J. Agric. Food Chem. 26 (1) (1978) 285–286.
[26] H.O. Bayer, R.Y. Yih, US Patent 3,928, 416, 1975.
[27] H.O. Bayer, R.Y. Yih, US Patent 3,798, 276, 1974.
[28] R.D. Clark, Porphyric Pesticides: Chemistry, Toxicology, and Pharmaceutical Applications, S.O. Duke, C.A. Rebeiz (Eds.), ACS Symp. Ser. 559, Washington, DC, 1994, pp. 34–47.
[29] W.O. Johnson, US Patent 4,031,131, 1997.
[30] G. Sandman, P. Boger, in: R.M. Roe, J.D. Burton, R.J. Kuhr (Eds.), Herbicide Activity: Toxicology, Biochemistry and Molecular Biology, IOS Press, Amsterdam, 1997, pp. 1–10.
[31] G.Sandman, P.Boger (Eds.), Target Sites of Herbicide Action, CRC Press, Boca Raton, FL, 1989.
[32] E.G. Teach, US Patent 4,069,038, 1978.
[33] F.X. Woolard, Synthesis and Chemistry of Agrochemicals III, D.R. Baker, J.G. Fenyes, J.J. Steffens (Eds.), ACS Symp. Ser 504, Washington, DC, 1992, pp. 81–90.
[34] C.F.A. Kyndt, M.T.F. Turner, J. Rognon, Proc. Br. Prot. Conf. Weeds 1 (1985) 29–34.
[35] F. Reicheneder, R. Kropp, A. Fischer, US Patent 3,697,522, 1972.
[36] C.E. Ward, US Patent 4,568,376, 1986.
[37] D.D. Rogers, B.W. Kirby, J.C. Hulbert, M.E. Bledsoe, L.V. Hill, A. Omid, C.E. Ward, Proc. Br. Prot. Conf. Weeds 1 (1987) 69–75.
[38] C.E. Ward, W.C. Lo, P.B. Pomidor, F.E. Tisdell, A.W.W. Ho, C.-L. Chiu, D.M. Tuck, C.B. Bernardo, P.J. Fong, A. Omid, K.A. Buteau, Synthesis and Chemistry of Agrochemicals, D.R. Baker, J.G. Fenyes, W.K. Moberg, B. Cross (Eds.), ACS Symp. Ser. 355, Washington, DC, 1987, pp. 65–73.
[39] B.M. Luscombe, K.E. Pallet, P. Loubiere, J.C. Millet, J. Melgarejo, T.E. Vrabel, Proc. Br. Prot. Conf. Weeds 1 (1995) 35.

[40] K.E. Pallet, S.M. Cramp, J.P. Little, P. Veerasekaran, A.J. Crudace, A.E. Slater, Isoxaflutole: the background of its discovery and the basis of its herbicidal properties, Pest Manage. Sci. 57 (2) (2001) 133.
[41] F. Colliot, K.A. Kukorowski, D.W. Hawkins, D.A. Roberts, BCPC Conf. Pests Dis. 1 (1992) 29.
[42] J.R. Bloomquist, Ion channels as targets for insecticides, Annu. Rev. Entomol. 41 (1996) 163–190.
[43] M. Casado, L-R. Pierre, V. Pevere, EP 668,269, 1995.
[44] K.K. Ngim, S.A. Mabury, D.G. Crosby, Elucidation of fipronil photodegradation pathways, J. Agric. Food Chem. 48 (2000) 4661–4665.
[45] K.A. Hassall, The Chemistry of Pesticides, Macmillan, London, 1982, p. 164.
[46] W. Mass, R. van Hes, A.C. Grosscurt, D.H. Deul, in: R. Wedler, (Ed.), Chemie der Pfalnzenschutz- und Schädlingsbekämpfungsmittel, Band 6, Springer, Berlin, 1981, p. 424.
[47] J.J. van Daalen, J. Meltzer, R. Mulder, K. Wellinga, Selective insecticide with a novel mode of action, Naturwissenschaften 59 (7) (1972) 312–313.
[48] M. Anderson, EP 161,019, 1985.
[49] J.H. Kim, Y.W. Shin, J.N. Heo, E.D. Kim, J.S. Park, H.S. Song, WO 98/00394, 1998.
[50] D. Cartwright, D.J. Collins, EP 3,416, 1979.
[51] E. Sugden, K. Williams, D. Sammataro, Fluvalinate – use it right or lose it, Bee Culture 123 (2) (1995) 80–81.
[52] J.A. Frank, P.L. Sanders, BCPC Conf. Pests Dis. 2 (1994) 871–876.
[53] P. Margot, F. Huggenberger, J. Amrein, B. Weiss, BCPC Conf. Pests Dis. 2 (1998) 375–382.
[54] P.A. Worthington, Synthesis and Chemistry of Agrochemicals, D.R. Baker, J.G. Fenyes, W.K. Moberg, B. Cross (Eds.), ACS Symp. ser. 355, Washington, DC, 1987, pp. 302–317.
[55] A. Nakata, Proc. 5th Cong. Pest. Chem. Abs. No. 116-9, Kyoto, 1982.
[56] K. Ikura, K. Katsuura, A. Nakada, M. Mizuno, US Patent 4,208,411, 1980.
[57] K.H. Buchel, F. Grewe, H. Kaspers, British Patent 1,237,509, 1971.
[58] M. Wilcox, I.Y. Chen, P.C. Kennedy, Y.Y. Li, L.R. Kincaid, N.T. Helseth, Proc. Plant Growth Regul. Working Group 4 (1997) 194.
[59] M. Wilcox, US Patent 4,169,721, 1979.
[60] D.J. Bowler, I.D. Entwistle, A.J. Porter, BCPC Conf. Pests Dis. 2 (1984) 397.
[61] B.A. Dreikorn, G.O.P. O'Doherty, A.J. Clinton, K.E. Kramer, BCPC Conf. Pests Dis. 2 (1979) 491.
[62] B.A. Dreikorn, G.O.P. O'Doherty, in: P.S. Magee, G.K. Kohn, J.J. Menn (Eds.), Pesticide Synthesis Through Rational Approaches, American Chemical Society, Washington, DC, 1983, pp. 45–63.
[63] D.E. Burton, A.J. Lambie, J.C.L. Ludgate, G.T. Newbold, A. Percival, D.T. Saggers, 2-Trifluoromethylbenzimidazoles: a new class of herbicidal compounds, Nature 208 (5016) (1965) 1166–1169.
[64] R.K. Pfeiffer, 2nd Symp. New Herbicides, European Weed Research Council, 1965, pp. 19–28.
[65] G.O.P. Doherty, German Patent DE 2,165,021, 1972.
[66] H.F.W. Rochling, K-H. Buchel, F.W.A. Korte, US Patent 3,459,759, 1969.
[67] K.-H. Buchel, F.W.A. Korte, R.B. Beechey, Uncoupling of the oxidative phosphorylation in mitochondria by NH-acidic benzimidazoles, Angew. Chem., Int. Ed. Engl. 4 (1965) 788–789.
[68] R.B. Beechey, The uncoupling of respiratory-chain phosphorylation by 4,5,6,7-tetrachloro-2-trifluoromethylbenzimidazole, Biochem. J. 98 (1) (1966) 284–289.
[69] S.O. Duke, C.A. Rebeiz (Eds.), Porphyric Pesticides: Chemistry, Toxicology, and Pharmaceutical Applications, in ACS Symp. Ser. 559, Washington, DC, 1994.

[70] G. Theodoridis, J.T. Bahr, F.W. Hotzman, S. Sehgel, D.P. Suarez, New generation of protox-inhibiting herbicides, Crop Prot. 19 (2000) 533–535.
[71] G. Theodoridis, J.T. Bahr, S. Crawford, B. Dugan, F.W. Hotzman, L.L. Maravetz, S. Sehgel, D.P. Suarez, Synthesis and Chemistry of Agrochemicals VI, D.R. Baker, J.G. Fenyes, G.P. Lahm, T.P. Selby, T.M. Stevenson (Eds.), ACS Symp. Ser 800, Washington, DC, 2002, pp. 96–107.
[72] L.F. Lee, EP 135,491, 1985.
[73] W.F. Goure, K.L. Leschinsky, S.J. Wratten, J.P. Chupp, Synthesis and Chemistry of Agrochemicals III, D.R. Baker, J.G. Fenyes, J.J. Steffens (Eds.), ACS Symp. Ser. 504, Washington, DC, 1992, pp. 161–176.
[74] H. Foerster, R.R. Schmidt, H.J. Santel, R. Andree, FOE 5043. A new selective herbicide from the oxyacetamide group, Pflazenschutz Nachr. 50 (2) (1997) 105–116.
[75] B.M. Berger, M. Muller, A. Eing, Quantitative structure–transformation relationships of sulfonylurea herbicides, Pest Manage. Sci. 58 (7) (2002) 724–735.
[76] T. Akagi, A new binding model for structurally diverse acetolactate synthase (ALS) inhibitors, Pest. Sci. 47 (4) (1996) 309–318.
[77] B. Hashizume, Jpn. Pestic. Inf. 57 (1990) 27–30.
[78] S.R. Teany, L. Armstrong, K. Bentley, D. Cotterman, D. Leep, P.H. Liang, C. Powley, J. Summers, S. Cranwell, F. Lichtner, R. Stichbury, Proc. Br. Prot. Conf. Weeds 1 (1995) 49.
[79] R. Neumann, W. Guyer, 10th Int. Cong. Plant Prot. Conf. 1 (1983) 445–451.
[80] D.A. Hunt, M.F. Treacy, Insecticides with Novel Modes of Action, I. Ishaaya, D. Degheele (Eds.), Springer, Berlin, 1998, pp. 138–151.
[81] R.W. Addor, T.J. Babcock, B.C. Black, D.G. Brown, R.E. Diehl, J.A. Furch, V. Kameswaran, V.M. Kamhi, K.A. Kremer, D.G. Kuhn, J.B. Lovell, G.T. Lowen, T.P. Miller, R.M. Peevey, J.K. Siddens, M.F. Treacy, S.H. Trotto, D.P. Wright Jr., Synthesis and Chemistry of Agrochemicals III, D.R. Baker, J.G. Fenyes, J.J. Steffens (Eds.), ACS Symp. Ser. 504, Washington, DC, 1992, pp. 283–297.
[82] D.G. Kuhn, V.M. Kamhi, J.A. Furch, R.E. Diehl, S.H. Trotto, G.T. Lowen, T.J. Babcock, Synthesis and Chemistry of Agrochemicals III, D.R. Baker, J.G. Fenyes, J.J. Steffens (Eds.), ACS Symp. Ser. 504, Washington, DC, 1992, pp. 298–305.
[83] J.A. Frank, P.L. Sanders, BCPC Conf. Pests Dis. 2 (1994) 871–876.
[84] J.R. Godwin, D.W. Bartlett, J.M. Clough, C.R.A. Godfrey, E.G. Harrison, S. Maund, BCPC Conf. Pests Dis. 1 (2000) 533–540.
[85] R. Kirstgen, K. Oberdorf, F. Schuetz, H. Theobald, V. Harries, WO 96/16047, 1996.
[86] P. O'Reilly, S. Kobayashi, S. Yamane, W. Phillips, P. Raymond, B. Castanho, BCPC Conf. Pests Dis. 1 (1992) 427.
[87] H.J. Santel, B.A. Bowden, V.M. Sorensen, K.H. Muller, BCPC Conf. Pests Dis. 1 (1999) 23–28.
[88] G.P. Lahm, S.F. McCann, C.R. Harrison, T.M. Stevenson, R. Shapiro, Agrochemical Discovery: Insect, Weed, and Fungal Control, D.R. Baker, N.K. Umetsu (Eds.), ACS Symp. Ser. 774, Washington, DC, 2001, pp. 20–34.
[89] H.H. Harder, S.L. Riley, S.F. McCann, S.N. Irving, BCPC Conf. Pests Dis. 2 (1996) 449.
[90] S.F. McCann, G.D. Annis, R. Shapiro, D.W. Piotrowski, G.P. Lahm, J.K. Long, K.C. Lee, M.M. Hughes, B.J. Myers, S.M. Griswold, B.M. Reeves, R.W. March, P.L. Sharpe, P. Lowder, P. Tseng, W.E. Barnette, K.D. Wing, Synthesis and Chemistry of Agrochemicals, D.R. Baker, J.G. Fenyes, G. P. Lahm, T.P. Selby, T.M. Stevenson (Eds.), ACS Symp. Ser. 800, Washington, DC, 2002, pp. 166–177.
[91] I. Hammann, W. Sirrenberg, Laboratory evaluation of SIR 8514, a new chitin synthesis inhibitor of the benzoylated urea class, Pflanzenschutz-Nachr. 33 (1) (1980) 1–34.

[92] W. Blass, Method for the determination of triflumuron residues in foodstuffs of plant origin after alkaline hydrolysis to 4-trifluoromethoxyphenylurea, Pflanzenschutz-Nachr. 51 (1) (1998) 79–96.
[93] G.H. Alt, W.G.P. Phillips, J.K. Pratt, G.H. Srouji, US Patent 5,045,554, 1991.
[94] R.L. Benefiel, E.V. Krumkalns, US Patent 4,002,628, 1977.
[95] W. Rademacher, Growth retardants: effect on gibberellin biosynthesis and other metabolic pathways, Annu. Rev. Plant Physiol. Plant Mol. Bio. 51 (2000) 501–531.
[96] R.L. Robey, J.C. Smirz, EP 39,157, 1981.
[97] J. D. Davenport, R.E. Hackler, H.M. Taylor, British Patent 1,218,623, 1971.
[98] R.D. Trepka, J.K. Harrington, J.E. Robertson, J.T. Waddington, Fluoroalkanesulfonanilides, a new class of herbicides, J. Agric. Food Chem. 18 (6) (1970) 1176.
[99] R.D. Trepka, J.K. Harrington, J.W. McConville, K.T. McGurran, A. Mendel, D.R. Pauly, J.E. Robertson, J.T. Waddington, Synthesis and herbicidal activity of fluorinated *N*-phenylalkanesulfonamides, J. Agric. Food Chem. 22 (6) (1974) 1111.
[100] W.A. Gentner, Agric. Res. 20 (2) (1971) 5.
[101] T.L. Fridinger, D.R. Pauly, R.D. Trepka, G.G.I. Moore, Proc. 166th ACS Natl. Meet., Washington, DC, 1974.
[102] R.K. Vander Meer, C.S. Lofgren, D.F. Williams, Synthesis and Chemistry of Agrochemicals, D.R. Baker, J.G. Fenyes, W.K. Moberg, B. Cross (Eds.), ACS Symp. Ser. 355, Washington, DC, 1987, 226–240.
[103] R.G. Schenellmann, R.O. Manning, Perfluorooctane sulfonamide: a structurally novel uncoupler of oxidative phosphorylation, Biochim. Biophys. Acta 1016 (3) (1990) 344–348.
[104] T.R. Roberts, D.H. Hutson (Eds.), Metabolic Pathways of Agrochemicals, The Royal Society of Chemistry, Cambridge, England, 1999, pp. 786–788
[105] J. Phillips, M.T. Pilato, T. Wu, WO 98/28277, 1998.
[106] C.L. Haas, M.T. Pilato, T.-t Wu, DE 19,653,417, 1997.
[107] J.K. Siddens, S. Raghu, US Patent 4,405,529, 1983.
[108] J.K. Siddens, US Patent 4,407,760, 1983.
[109] B.R. Langlois, Improvement of the synthesis of aryl difluoromethyl ethers and thioethers by using a solid–liquid phase-transfer technique, J. Fluorine Chem. 41 (2) (1988) 247–261.
[110] W. Maurer, H.R. Gerber, J. Rufener, Proc. Br. Prot. Conf. Weeds 1 (1987) 41–48.
[111] S.J. Sanni, Weeds and Weed Control 1 (1986) 37–41.
[112] R.W. Pfluger, US Patent 4,542, 216, 1985.
[113] R. Hassig, US Patent 4,692,524, 1987.
[114] Y. Miura, M. Ohnishi, T. Mabuchi, I. Yanai, Proc. Br. Prot. Conf. Weeds 1 (1993) 35.
[115] D.R. Penman, R.B. Chapman, Exp. Appl. Acarol. 4 (1988) 265.
[116] W.K. Whitney, K. Wettstein, BCPC Conf. Pests Dis. 2 (1979) 387.
[117] W.-G. Jin, G.-H. Sun, Z.-M. Xu, BCPC Conf. Pests Dis. 2 (1996) 455.
[118] C. Hansch, A. Leo, Exploring QSAR, Fundamentals and Applications in Chemistry and Biology, American Chemical Society, Washington, DC, 1995, p. 517
[119] K. Fujii, Y. Fukuda, Y. Yamanaka, JP Patent 04235976, 1992.
[120] G. Pinochet, Acrinathrin: an acaricide for vineyards and orchards, Phytoma 428 (1991) 54–57.
[121] K.R.S. Ascher, N.E. Nemny, The ovicidal effect of PH-60-40 [1-(4-chlorophenyl)-3-(2,6-dichlorobenzyl)-urea] in *Spodoptera littoralis* Boisd. Phytoparasitica, 2 (1974), 131–133.
[122] I. Ishaaya, A.R. Horowitz, in: I. Ishaaya, D. Degheele (Eds.), Insecticides with Novel Modes of Action, Springer, Berlin, 1998, pp. 1–24.
[123] M. Henningsen, Modern fungicides, Chem. Unserer Zeit. 37 (2) (2003) 98–111.
[124] C. Garavaglia, L. Mirenna, O. Puppin, E. Spagni, BCPC Conf. Pests Dis. 1 (1988) 49–56.

[125] D.C. England, L.R. Melby, M.A. Dietrich, R.V. Lindsey, Nucleophilic reactions of fluoroolefins, J. Am. Chem. Soc. 82 (19) (1960) 5116–5122.
[126] K. Gehmann, R. Nyfeler, A.J. Leadbeater, D. Nevill, D. Sossi, BCPC Conf. Pests Dis. 2 (1990) 399.
[127] K. Arima, H. Imanaka, M. Kousaka, A. Fukuda, G. Tamura, Pyrrolnitrin, a new antibiotic. I. Isolation and properties of pyrrolnitrin, J. Antibiot., Ser. A 18 (5) (1965) 201–204.
[128] P. Ackermann, H.-R. Kanel, B. Schaub, US Patent 5,514,816, 1996.
[129] R. Nyfeler, P. Ackermann, Synthesis and Chemistry of Agrochemicals III, D.R. Baker, J.G. Fenyes, J.J. Steffens (Eds.), ACS Symp. Ser. 504, Washington, DC, 1992, pp. 395–404.
[130] G. Theodoridis, US Patent 4,818,275, 1989.
[131] W.A. Van Saun, J.T. Bahr, G.A. Crosby, Z.A. Fore, H.L. Guscar, W.N. Harnish, R.S. Hooten, M.S. Marquez, D.S. Parrish, G. Theodoridis, J.M. Tymonko, K.R. Wilson, M.J. Wyle, Proc. Br. Prot. Conf. Weeds 1 (1991) 77.
[132] W.A. Van Saun, J.T. Bahr, L.J. Bourdouxhe, F.J. Gargantiel, F.W. Hotzman, S.W. Shires, N.A. Sladen, S.F. Tutt, K.R. Wilson, Proc. Br. Prot. Conf. Weeds 1 (1993) 19.
[133] G. Theodoridis, J.S. Baum, F.W. Hotzman, M.C. Manfredi, L.L. Maravetz, J.W. Lyga, J.M. Tymonko, K.R. Wilson, K.M. Poss, M.J. Wyle, Synthesis and Chemistry of Agrochemicals III, D.R. Baker, J.G. Fenyes, J.J. Steffens (Eds.), ACS Symp. Ser. 504, Washington, DC, 1992, pp. 134–146.
[134] H.J. Scholl, E. Klauke, F. Grewe, I. Hamman, British Patent 1,326,853, 1970.
[135] P.H. Ogden, R.A. Mitsch, Isomerization of perfluoro-alpha, omega-bisazomethines, J. Am. Chem. Soc. 89 (19) (1967) 5007–5011.
[136] J.S. Moilliet, in: R.E. Banks, B.E. Smart, J.C. Tatlow (Eds.), Organofluorine Chemistry: Principles and Commercial Applications, Plenum Press, New York, 1994, pp. 195–219.
[137] G. Balz, G. Schiemann, Aromatic fluorine compounds. I. A new method for their preparation, Chem. Ber. 60 (1927) 1186.
[138] H. Suschitzky, The Balz–Schiemann reaction, Advances in Fluorine Chemistry 4 (1965) 1–27.
[139] P. Osswald, O. Scherer, DE 600,706, 1934.
[140] A.K. Barbour, L.J. Belf, M.W. Buxton, in: M. Stacey, J.C. Tatlow, A.G. Sharpe (Eds.), Advances in Fluorine Chemistry, Butterworths, London, 1963, pp. 181–270.
[141] L. Dolby-Glover, Halogen exchange – 'new ions for old', Chem. Ind. 15 (1986) 518–523.
[142] G. Fuller, DE 2,902,877, 1979.
[143] G.S. Lal, G.P. Pez, R.G. Syvret, Electrophilic NF fluorinating agents, Chem. Rev. 96 (5) (1996) 1737–1756.
[144] J.S. Goudar, US Patent 6,218,545, 2001.
[145] R.G. Syvret, W.J. Casteel Jr., G.S. Lal, J.S. Goudar, Selective fluorination of an aryl triazolinone herbicide intermediate, J. Fluorine Chem. 125 (2004) 33–35.
[146] H. Trozelli, Fluroxypyr – a new herbicide in cereals, Weeds and Weed Control 27 (1) (1986) 65–75.
[147] L.H. McKendry, US Patent 4,108,629, 1979.
[148] S. Bowe, M. Landes, J. Best, G. Schmitz, M. Graben, Proc. Br. Prot. Conf. Weeds 1 (1999) 35–40.
[149] K. Grossmann, Chemistry of Crop Protection, G. Voss, G. Ramos (Eds.), Wiley-VCH, Weinheim, 2003, pp. 131–142.
[150] G. Theodoridis, J.T. Bahr, B.L. Davidson, S.E. Hart, F.W. Hotzman, K.M. Poss, S.F. Tutt, Synthesis and Chemistry of Agrochemicals IV, D.R. Baker, J.G. Fenyes, G.S. Basarab (Eds.), ACS Symp. Ser. 584, Washington, DC, 1995, pp. 90–99.
[151] A.R. Thomson, Proc. Br. Prot. Conf. Weeds 1 (1999) 73.

[152] W.A. Kleschick, C.M. Carson, M.J. Costales, J.J. Doney, B.C. Gerwick, J.B. Holtwick, R.W. Meikle, W.T. Monte, J.C. Little, N.R. Pearson, S.W. Snider, M.V. Subramanian, J.C. VanHeertum, A.P. Vinogradoff, Synthesis and Chemistry of Agrochemicals III, D.R. Baker, J.G. Fenyes, J.J. Steffens (Eds.), ACS Symp. Ser. 504, Washington, DC, 1992, pp.17–25.
[153] A.C. Grosscurt, BCPC Conf. Pests Dis. 1 (1977) 141–147.
[154] A. Verloop, C.D. Ferrell, Pesticide Chemistry in the 20th Century, J.R. Plimmer (Ed.), ACS Symp. Ser. 37, Washington, DC, 1977, pp. 237–275.
[155] S. Miyamoto, J. Suzuki, Y. Kikuchi, K. Toda, Y. Itoh, T. Ikeda, T. Ishida, Y. Hariya, Y. Tsukidate, US Patent 5,141,948, 1992.
[156] J. Suzuki, T. Ishida, Y. Kikuchi, Y. Ito, C. Morikawa, Y. Tsukidate, I. Tanji, Y. Ota, K. Toda, Nihon Noyaku Gakkaishi, Synthesis and activity of novel acaricidal/insecticidal 2,4-diphenyl-1,3-oxazolines, J. Pest. Sci. 27 (1992) 1–8.
[157] M.A. Dekeyser, Acaricide mode of action, Pest Manage. Sci. 61 (2) (2005) 103–110.
[158] W. Behrenz, A. Elbert, R. Fuchs, Cyfluthrin (FCR 1272) a new pyrethroid with long-lasting activity for the control of public health and stored-product pests, Pflanzenschutz-Nachr. 36 (2) (1983) 127–176.
[159] K. Naumann, in: W.S. Bowers, W. Ebing, D. Martin, R. Wegeler (Eds.), *Chemistry of Plant Protection 4*, Synthetic Pyrethroid Insecticides, Springer, Berlin, 1990, p. 43.
[160] R.J. Gouger, A.J. Neville, A.R. Jutsum, BCPC Conf. Pests Dis. 3 (1986) 1143–1150.
[161] G.A. Meier, T.G. Cullen, S. McN. Sieburth, K.A. Boyler, S. Sehgel, D.P. Suarez, A. Fritz, Synthesis and Chemistry of Agrochemicals IV, D.R. Baker, J.G. Fenyes, G.S. Basarab (Eds.), ACS Symp. Ser. 584, Washington, DC, 1995, pp. 236–244.
[162] S. McN. Sieburth, US Patent 4,709,068, 1989.
[163] S. McN. Sieburth, C.N. Langevine, D.M. Dardaris, Organosilane insecticides. Part II: chemistry and structure–activity relationships, Pest. Sci. 28 (1990) 309–319.
[164] T.M. Fort, W.K. Moberg, BCPC Conf. Pests Dis. 2 (1984) 413.
[165] M. Tsuda, H. Itoh, S. Kato, Systemic activity of simeconazole and its derivatives in plants, Pest. Manage. Sci. 60 (2004) 881–886.
[166] P.A. Worthington, Synthesis of 1,2,4-triazole compounds related to the fungicides flutriafol and hexaconazole, Pest. Sci. 31 (4) (1991) 457–498.
[167] E. Ammermann, F. Loecher, G. Lorenz, B. Janssen, S. Karbach, N. Meyer, BCPC Conf. Pests Dis. 2 (1990) 407–414.
[168] P.E. Russell, A. Percival, P.M. Coltman, D.E. Green, BCPC Conf. Pests Dis. 1 (1992) 411–418.
[169] J.D. Davenport, R.E. Hackler, H.M. Taylor, British Patent 1,218,623, 1971.
[170] D.W. Hollomon, I.E. Wheeler, K. Dixon, C. Longhurst, G. Skylalakis, Defining the resistance risk of the new powdery mildew fungicide quinoxyfen, Pest. Sci. 51 (3) (1997) 347–351.
[171] M.J. Robson, R. Cheetham, D.J. Fettes, J. Crosby, BCPC Conf. Pests Dis. 3 (1984) 853–857.
[172] H.J.H. Doel, A.R. Crossman, L.A. Bourdouxhe, Meded. Fac. Landbouwwet. Univ. Gent. 49 (1984) 929–937.
[173] R.K. Huff, British Patent, 2,000,764, 1980.
[174] P.D. Bentley, R. Cheetham, R.K. Huff, R. Pascoe, J.D. Sayle, Fluorinated analogs of chrysanthemic acid, Pest. Sci. 11 (2) (1980) 156–164.
[175] R.F.S. Gordon, R. Pascoe, T. Enoyoshi, BCPC Conf. Pests Dis. 1 (1992) 81.
[176] R. Salmon, WO 93/06089, 1993.
[177] P.J. Crowley, G. Mitchell, R. Salmon, P.A. Worthington, Synthesis of some arylsulfur pentafluoride pesticides and their relative activities compared to the trifluoromethyl analogues, Chimia 58 (3) (2004) 138–142.
[178] W.A. Sheppard, Arylsulfur trifluorides and pentafluorides, J. Am. Chem. Soc. 82 (1960) 4751–4752.
[179] W.A. Sheppard, Arylsulfur pentafluorides, J. Am. Chem. Soc. 84 (1962) 3064.

[180] A.G. Williams and N.R. Foster, WO 94/22817, 1994.
[181] F.M. Carlini, S. Miteni, Aryl-sulfur pentafluorides: a new building-block generation for life sciences applications, Chim. Oggi 21 (3/4) (2003) 14–16.
[182] R.H. White, W.S. Clayton, Proc. Br. Prot. Conf. Weeds 1 (1999) 47–52.
[183] S. Takamura, T. Okada, S. Fukuda, Y. Akiyoshi, F. Hoshide, E. Funaki, S. Sakai, Proc. Br. Prot. Conf. Weeds 1 (1999) 41–46.
[184] D.W. Kim, H.S. Chang, Y.K. Ko, J.W. Ryu, J.C. Woo, D.W. Koo, J.S. Kim, WO 2000/05956, 2000.
[185] H.-J. Wroblowsky, R. Thomas, WO 97/33876, 1997.
[186] M. Schmitt, A. Van Almsick, R. Preuss, L. Willms, T. Auler, H. Bieringer, F. Thuerwaechter, WO 2001/074785, 2001.
[187] I. Yoshimura, M. Miyazaki, S. Suzuki, M. Nakaya, M. Tamaru, Y. Ono, T. Ida, K. Yanagisawa, H. Sadohara, JP 11060562, 1999.
[188] S.-J. Koo, J.-H. Cho, J.-S. Kim, S.-H. Kang, K.-G. Kang, D.-W. Kim, H.-S. Chang, Y.-K. Ko, J.-W. Ryu, WO 02/30921, 2002.
[189] D.S. Kim, S.J. Koo, J.N. Lee, K.H. Hwang, T.Y. Kim, K.G. Kang, K.S. Hwang, G.H. Joe, J.H. Cho, D.W. Kim, Flucetosulfuron: a new sulfonylurea herbicide, BCPC Int. Cong.: Crop Sci. Technol., Glasgow 1 (2003) 87–92.
[190] R.J. Sbragis, G.W. Johnson, L.L. Karr, J.M. Edwards, B.M. Schneider, WO 98/19542, 1988.
[191] F. Obata, K. Fujii, A. Oaka, Y. Yamanaka, EP 665,225, 1995.
[192] T. Mori, EP 1,004,569, 2000.
[193] K. Ujihara, T. Iwasaki, EP 939,073, 1999.
[194] T. Tadaaki, T. Koyanagi, M. Morita, T. Yoneda, C. Kagimoto, H. Okada, US Patent 5,360,806, 1994.
[195] S. Saito, S. Isayama, N. Sakamoto, K. Umeda, K. Kasamatsu, BCPC Conf. Pests Dis. 1 (2002) 33–38.
[196] N. Sakamoto, S. Saito, T. Hirose, M. Suzuki, S. Matsuo, K. Izumi, T. Nagatomi, H. Ikegami, K. Umeda, K. Tsushima, N. Matsuo, The discovery of pyridalyl: a novel insecticidal agent for controlling lepidopterous pests, Pest Manage. Sci. 60 (1) (2004) 25.
[197] S. Isayama, S. Saito, K. Kuruda, K. Umeda, K. Kasamatsu, Pyridalyl, a novel insecticide: potency and insecticidal selectivity, Arch. Insect Biochem. Physiol. 58 (4) (2005) 226–233.
[198] N. Takahashi, S. Gotoda, N. Ishil, Y. Sasama, US Patent 6,899,886, 2005.
[199] M. Tohnishi, H. Nakao, E. Kohno, T. Nishida, T. Furuya, T. Shimizu, A. Seo, K. Sakata, S. Fujioka, H. Kanno, EP 1,006,107, 1999.
[200] M. Tohnishi, H. Nakao, T. Furuya, A. Seo, H. Kodama, K. Tsubata, S. Fujioka, T. Hirooka, T. Nishimatsu, DC AGRO-9, Abstr. Pap., 230th ACS Natl. Meet., Washington, DC, 2005.
[201] W. Andersch, D. Stubler, R. Fischer, U. Heinemann, W. Kramer, J. Konze, U. Wachendorff-Neumann, M. Jautelat, DE 10310906, 2004.
[202] J. Konze, W. Andersch, D. Stubler, R. Fischer, DE 10248257, 2004.
[203] P. Lummen, U. Ebbinghaus-Kintscher, N. Lobitz, T. Schulte, C. Funke, R. Fische, AGRO-25, Abstr. Pap., 230th ACS Natl Meet., Washington, DC, 2005.
[204] M. Onishi, A. Yoshiura, E. Kohno, K. Tsubata, EP 1,006,102, 1999.
[205] G.P. Lahm, T.P. Selby, J.H. Freudenberger, T.M. Stevenson, B.J. Myers, G. Seburyamo, B.K. Smith, L. Flexner, C.E. Clark, D. Cordova, Insecticidal anthranilic diamides: a new class of potent ryanodine receptor activators, Bioorg. Med. Chem. Lett. 15 (22) (2005) 4898–4906.
[206] D. Cordoba, E.A. Benner, M.D. Sacher, J.J. Rauh, J.S. Sopa, G.P. Lahm, T.P. Selby, T.M. Stevenson, L. Flexner, S. Gutteridge, D.F. Rhades, L. Wu, R.M. Sith, Y. Tao, AGRO (late addition, paper not included in Abstracts), 230th ACS Natl. Meet., Washington, DC, 2005.

[207] K. Takagi, T. Ohtani, T. Nishida, H. Hamaguchi, T. Nishimatsu, A. Kanaoka, EP 462,456, 1991.
[208] M.J. Henry, G.D. Gustafson, in: G. Voss, G. Ramos (Eds.), Chemistry of Crop Protection, Wiley-VCH, Weinheim, 2003, pp. 89–98.
[209] Agro Reports 2004, New Developments in Fungicides.
[210] I. Kasahara, H. Ooka, S. Sano, H. Hosokawa, H. Yamanaka, US Patent 5,847,005, 1998.
[211] U. Heinemann, H. Gayer, P. Gerdes, B.-W. Kruger, B. Gallenkamp, U. Stelzer, A. Marhold, R. Tiemann, S. Dutzmann, G. Hanssler, K. Stenzel, WO 97/27189, 1997.
[212] U. Heinemann, H. Gayer, P. Gerdes, B.-W. Kruger, B. Gallenkamp, U. Stelzer, A. Marhold, R. Tiemann, S. Dutzmann, G. Hanssler, K. Stenzel, US Patent 6,103,717, 2000.
[213] S. Dutzmann, A. Maulet-Machnik, F. Kerz-Mohlendick, J. Applegate, U. Heinemann, BCPC Conf. Pests Dis. 1 (2002) 365.
[214] C.H.L. Liu, W.C.H. Liu, Z.C.H. Li, BCPC Conf. Pests Dis. 2 (2000) 549–556.
[215] T. Hamada, T. Takeyama, JP 187786, 2001.
[216] H. Suzuki, M. Hasunuma, JP 2005082479, 2005.
[217] B.A. Moloney, D. Hardy, E.A. Saville-Stones, WO 99/42447, 1999.
[218] H. Katsuta, S. Ishii, K. Tomiya, K. Kodaka, US Patent 6,239,282, 2001.
[219] K. Tomiya, Y. Yanase, BCPC Int. Cong.: Crop Sci. Technol., Glasgow, 1 (2003) 99–104.
[220] Y. Miyake, J. Sakai, I. Miura and K. Nagayama, BCPC Int. Cong.: Crop Sci. Technol., Glasgow, 1 (2003) 105–112.
[221] M. Reuveni, Activity of the new fungicide benthiavalicarb against *Plasmopara viticola* and its efficacy in controlling downy mildew in grapevines, Eur. J. Plant Pathol. 109 (3) (2003) 243–251.
[222] H. Mizutani, J. Suzuki, Y. Saito, M. Ikeda, A. Yagi, Residue analysis of the fungicide benthiavalicarb-isopropyl and its degradation products in upland field soil, J. Pest. Sci. 29 (2004) 87–95.
[223] W.R. Dolbier, Fluorine chemistry at the millennium, J. Fluorine Chem. 126 (2005) 157–163.
[224] S.J. Tavener, J.H. Clark, Can fluorine chemistry be green chemistry? J. Fluorine Chem. 123 (2003) 31–36.
[225] P.T. Nyffeler, S.G. Duron, M.D. Burkart, S.P. Vincent, C.-H. Wong, Selectfluor: mechanistic insight and applications, Angew. Chem., Int. Ed. Engl. 44 (2005) 192–212.
[226] B.D. Key, R.D. Howell, C.S. Criddle, Fluorinated organics in the biosphere, Environ. Sci. Technol. 31 (9) (1997) 2445–2454.
[227] L.H. Weinstein, A.W. Davison (Eds.), Fluorides in the Environment: Effects on Plants and Animals, CABI Publishing, Wallingford, UK, 2004.
[228] T.F.X. Collins, R.L. Sprando, Fluoride-toxic and pathologic aspects: review of current literature on some aspects of fluoride toxicity, Rev. Food Nutr. Toxicity 4 (2005) 105–141.

This page intentionally left blank

CHAPTER 5

Fluorine: Friend or Foe? A Green Chemist's Perspective

Stewart J. Tavener,* and James H. Clark

Clean Technology Centre, Department of Chemistry, University of York, Heslington, York YO10 5DD, UK

Contents

Abstract

The contribution of fluorine chemistry to the field of clean chemical technology is reviewed. The roles of fluorochemicals in the environment and the ways in which they may be involved in inherently 'greener' processes are discussed.

1. INTRODUCTION

A great deal has been written in recent years about *clean chemical technology* or *green chemistry*, and the role of the 'green' chemist is to find workable and economically attainable solutions for the chemical industry with the minimum impact on our environment. An important axiom of green chemistry is that an inherently efficient process is greatly preferable to treatment or recycling of waste [1]. A 'green' process should have the smallest possible burden on the environment and, in general, this means using renewable resources where possible, ensuring that the atom economy of the process is high – i.e. as much of the substrate and reagents as possible find their way into the final product – and that

*Corresponding author. Email: sjt4@york.ac.uk;

FLUORINE AND THE ENVIRONMENT, VOLUME 2
ISSN 1872-0358 DOI: 10.1016/S1872-0358(06)02005-7

the use of auxiliary compounds such as solvents and promoters is minimised or eliminated. Frequently, the conclusions are the same as those that would be reached from an economic point of view: less substrate, fewer reagents, less solvent and a consequent reduction in energy requirement will all contribute to financial savings. Fluorine chemistry has an important role to play in clean technology, in catalyst, solvent and manufacturing technologies, as well as several other areas [2]. Fluorine is a very light element with extreme electronic properties, and provides excellent value in terms of activity-per-gram. It is also recognised that fluorochemicals are frequently more effective and are required in smaller quantities than non-fluorinated compounds – in the case of fluorine, 'small is beautiful'. High effect, low dosage fluorinated formulations allow reductions in the use of materials and energy all along the production and supply chain: fewer non-renewable feedstocks are consumed, transport and packaging are reduced, and the quantity of post-consumer waste is minimised. However, fluorochemicals have also been involved in some of the more negative aspects of the chemical industry. In this review, we consider the effects of fluorine and fluorochemicals in the environment, their position in industry, and describe some of the ways in which they are involved in clean chemical technology.

2. THE FLUOROSPHERE

Readers of this volume may already be more aware than many of the extent to which we are surrounded by the element fluorine. It is present in the air we breathe, the water we drink and the rocks beneath us, as well as in numerous synthetic polymers, pharmaceuticals, agrochemicals and other formulations. Fluorine in the atmosphere, oceans, biosphere and crust might be grouped together as the *fluorosphere* (Fig. 1), and, in order to understand the effects of human activities on the environment, it is worthwhile briefly considering the reservoirs and flux of fluorine compounds, both natural and anthropogenic, which occur around us [3,4].[1]

Fluorine is the 13th most abundant element on the planet, and is found in significant quantities in the oceans, atmosphere and in the Earth's crust (Table 1). Human beings are fluorine-enriched organisms, with a concentration of 37 ppm, significantly higher than that of seawater. This equates to 2.6 g for an average 70 kg person, which implies that the human race, with a population of 6000 million, is currently carrying a mass of 15,600 tonne of fluorine.[2] The distribution of fluorine is significantly affected by human activity, and organofluorine

[1] The role of fluorine in the environment has been reviewed in detail elsewhere – see Ref. [3].

[2] One observer has commented that the average fluorine chemist may contain considerably more than this value! Population data from U.S. Census, for the year 1999.

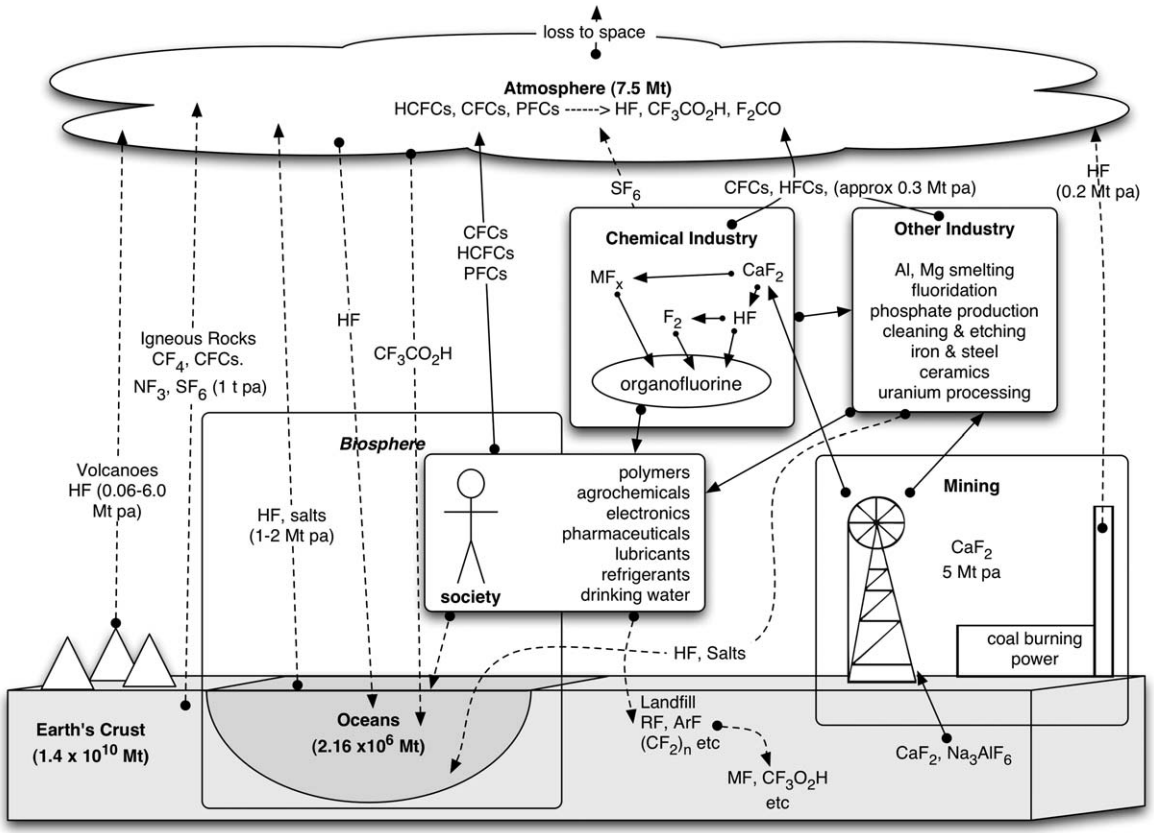

Fig. 1. The Fluorosphere: A schematic representation of fluorine reservoirs and flux on Earth, with approximate volumes. Solid arrows indicate deliberate manipulation of fluorine-containing products and minerals. Dotted arrows indicate unintentional by-products, emissions to the environment and natural processes. Sources of data are indicated in the text.

Table 1. Estimated quantities of fluorine in the atmosphere, hydrosphere and lithosphere

Reservoir	Fluorine concentration	Total mass of fluorine (million tonnes)
Atmosphere	2.2 ppbv[a]	7.5[b]
Hydrosphere	1.3 ppm	2.16×10^6
Lithosphere (Earth's crust)	585 ppm	1.4×10^{10}

Note: Values taken from Ref. [5] except:
[a] Value taken from Luo et al. [20].
[b] Calculated using value for mass of atmosphere based on a mixing ratio of 2.2 ppbv of fluorine, a total atmospheric mass of 5.2×10^{18} kg, and the assumption that the tropospheric concentration (the troposphere contains 90% of the atmospheric mass) is representative of the whole atmosphere. See figures from Jacob [22].

compounds in particular have come under scrutiny because of their role in ozone depletion, global warming effects and bioaccumulation in mammals.

The primary mineral source of fluorine for chemical and other industrial use is fluorspar (mostly CaF_2, also known as fluorite). World production of fluorspar is estimated at 4–5 million tonnes per annum [6], with over half of this coming from China. Other major producers include France, Spain, Mongolia, Mexico and the UK. Japan and the USA have little or no domestic fluorspar production and rely entirely on imports and use of government stockpiles to satisfy its demand for fluorspar. About 90% of the 600,000 tonne consumed in the USA each year is used for the manufacture of HF, aluminium fluoride and cryolite (Na_3AlF_6). Another important fluorine source is fluorosilicic acid, of which approximately 65,000 tonne per annum are generated as a by-product of phosphate manufactured for fertiliser use [6,7]. Some of this is sold for fluoridation of drinking water or conversion to AlF_3, but it is not usually an economically viable source of fluorine for hydrogen fluoride manufacture [7]. Hydrogen fluoride is manufactured by reaction of acid grade ($>97\%$ CaF_2) fluorspar with concentrated sulphuric acid, and it has a wide range of applications including uranium processing, glass etching and metal treatment as well as preparation of various fluoride salts, fine chemical use, and as a catalyst for aromatic alkylation reactions. Elemental fluorine is produced *via* electrolysis of potassium bifluoride, and both HF and F_2 are used to produce fluorocarbons for a range of applications that including refrigerants, aerosol propellants and anaesthetics [51]. The major use of cryolite (in conjunction with CaF_2 and AlF_3) is as an electrolytic medium for the production of aluminium. However, the volume of cryolite produced by mining is insufficient to supply global demand for aluminium smelters, and so synthetic cryolite is produced by reaction of HF with alumina and sodium hydroxide. Although, in theory, the electrolysis process should not consume the fluoride salts, the reality is that

the fluoride reacts with the carbon electrodes to form perfluorocarbons (CF_4 and C_2F_6), and this is a significant source of PFC emissions [8,9]. On average, about 21 kg of fluoride salts are consumed for every tonne of aluminium metal produced. Recent advances in the efficiency of smelters should improve this situation; older equipment requires 40 kg/tonne, while newer smelters may require as little as 10 kg/tonne of aluminium metal, although the time lag in replacing plants means that the effect of the change on environmental burden will be slow [6,7].

Fluorinated compounds are utilised in other metallurgical processes. CaF_2 is used directly as a flux to lower the melting point of slag in iron production [6]. Sulphur hexafluoride is used as a blanket gas during magnesium smelting to ensure that reoxidation does not occur. However, it is one of the most potent greenhouse gases known, with a *global warming potential* (GWP) of 23,900 times that of CO_2 [8], and is therefore now being replaced with HFCs and PFCs in this application. Draft EU regulations will ban the use of SF_6 in magnesium casting industry where the annual consumption is greater than 850 kg. SF_6 is also used as an electrical insulator in switch gear, with an estimated 500 tonne currently in use in the UK [10]. SF_5CF_3 is also used for this purpose. Emissions from this source are expected to rise as existing equipment is decommissioned. Recent data on industrial applications of inorganic fluorides can be found in Ref. [85].

An important area of the chemical industry that has been subject to major change in recent years is the manufacture of halogenated organic molecules. Chlorofluorocarbons (CFCs), which were identified as having a significant contribution to the destruction of stratospheric ozone, through liberation of chlorine radicals *via* photolysis, were phased out as a result of the 1987 Montreal Protocol [11]. HCFCs were introduced as interim replacements for CFCs in refrigeration and blowing agent applications, and these have in turn been replaced by hydrofluorocarbons (HFCs). Importantly, HFCs are chlorine-free and are believed to have no significant contribution to ozone destruction [12], although they may still act as greenhouse gases. Table 2 gives GWPs for some fluorine-containing compounds currently in use [8,13]. Of course, production of these chlorine-free replacements require larger quantities of fluorine than their predecessors, and manufacture of HFCs, HCFCs, fluoropolymers and other fluorocarbon compounds is one of the largest uses of HF [6,7].

HFCs and perfluorocarbons have themselves come under scrutiny because of their large GWPs (it has even been suggested that the correct mixture of fluorinated gases could be used to warm Mars sufficiently to make it inhabitable by humans! [14]). HFCs in general, and HFC134a in particular, have been used since the early 1990s as drop-in replacements for CFCs in vehicle air conditioning units, and emissions from these systems are projected to contribute the equivalent of 50 million tonnes of CO_2 per annum by 2010. The EU Environment

Table 2. Global warming potentials (GWP) for some representative organofluorine compounds [8,13]. A range of values is given where sources differ

Compound	GWP (CO_2 equivalents)	Residence time (years)
CO_2	1 (defined)	
CH_4	23	10
HCF_3 (HFC-23)	12,000–13,000	243
CH_2CF_2 (HFC-32)	550–710	5.6
CHF_2CF_3 (HFC-125)	3400–3600	32.6
CH_2FCF_3 (HFC-134a)	1300	13.6
$CF_3CH_2CF_3$ (HFC-236fa)	6300–8400	226
CF_4	5700	50,000
C_2F_6	9200	10,000
C_6F_{14}	9000	3200
CFC-11	4500	45
CFC-12	10,600	100
NF_3	10,800	740
SF_6	23,900	3200

Commission is considering legislation to tackle this in the near future, although it is not yet clear what alternatives are available at acceptable cost [15]. A complete phase-out of volatile HFCs and PFCs is anticipated and already being discussed in legislative circles [16], which could be counter-productive, impeding the growth of fluorous-phase chemistry and supercritical solvent systems which have great potential as clean methods for chemical synthesis – some of these methods are discussed further below. There is political pressure to phase out fluorinated gases with GWP greater than 150 CO_2 equivalents in motor vehicle manufacture, which will restrict use of HFC 134a (GWP = 1300) but will still allow HFC152a (GWP = 140) [17]. CO_2 air conditioning units seem to be the most promising replacements for this, and carry the advantage that the compressible gas does not need to be recovered and recycled at the end of the unit's life. These units are already in use in some vehicles in Japan, although there are still some doubts about the energy efficiency of the CO_2-based systems, which must, of course, be considered when assessing their effectiveness in reducing environmental impact. HFC emissions from refrigeration and air conditioning units in vehicles in the UK were found to increase by 40% in 2004, indicating that leakage from these units is significant. Although recycling and recovery of CFCs from older refrigerators is now mandatory in the developed world, there is concern over the efficiency of this process, with a national survey suggesting that only 64% of the gases are actually recovered [18]. Overall levels of CFCs in the atmosphere appear to be falling, but HCFC and HFC levels are estimated to be rising by 3–7% and 12–17%, respectively, and HFC emissions may triple by 2015 [19].

It should be remembered that despite their high GWPs, fluorinated gases make a relatively minor contribution (*ca*. 1%) to the total GWP of mankind's emissions (*see in this series, the chapters of R. Tuckett and A. Sekiya et al. devoted to the green house effect of SF_5CF_3 and to CFCs and HCFCs substitutes, respectively*).

Stratospheric HF is believed to be the dominant stable reservoir of free fluorine atoms released from photolysis of CFCs and HCFCs [20]. The only route for removal of HF from the stratosphere is diffusion down to the troposphere where it may be rained out: HF therefore has a long stratospheric lifetime. Concentrations of tropospheric fluorine have increased in recent decades, showing a rise from below 0.5 ppbv in 1970 to over 2.0 ppbv in 1995, although there is evidence from satellite studies of the mesosphere of a slowdown in the rate of increase of atmospheric fluorine [21]. The total atmospheric reservoir thus contains approximately 7.5 million tonnes of fluorine [22].

Many HCFCs and HFCs (including HCFC-123 and HFC-134a) contain trifluoromethyl groups, which are resistant to degradation in the environment; HFCs may have lifetimes in the atmosphere from 15 to 400 years [12]. The final degradation product of CF_3-containing compounds is trifluoroacetate (TFA), which is eventually rained out of the atmosphere as trifluoroacetic acid and accumulates in surface water. TFA has no known loss mechanisms in the environment, but is not believed to be highly toxic to plants or animals [12,23]; it is not metabolised by humans, and has a half-life in the human body of 16 h [24]. Rain and snow in Switzerland have recently been found to contain an average of 151 ng L^{-1} trifluoroacetic acid, which translates to 230 g km^{-2} $year^{-1}$, of which 150 g finds its way into soil and groundwater, and the rest is removed in river water [25]. Similar measurements in Canada found a lower level of 21 ng L^{-1} trifluoroacetic acid in rainwater [12]. With a global surface area of 5.10×10^8 km^2, these figures suggest that somewhere between 10,000 and 117,000 tonne of trifluoroacetic acid may be rained out of the atmosphere each year.[3] Another published estimate based on global average rainfall puts this value at 42,000 tonne per annum [24].

As well as atmospheric sources, pyrolysis of fluorine-containing polymers, which may occur in engine oil additives, non-stick cookware or incinerated medical equipment (i.e. syringes) and household waste, may also produce TFA. This process may also produce perfluorinated alkanes and cycloalkanes, which have significant GWP, and have estimated tropospheric half-lives of more than 2000 years. Trifluoroacetate may also be produced by metabolism of trifluoromethyl-containing drugs such as Prozac, and anaesthetics including halothane and isofluorane [4].

[3] Calculation based on global surface area, not an average rainfall. Surface area figure from CRC handbook of Chemistry and Physics.

Burning of coal also contributes to atmospheric fluorine, with an estimated 100 mg of fluorine per kg of coal [26]. How much of this is released to the atmosphere depends upon both the efficiency of burning and the treatment of exhaust gases: for China alone this has been conservatively estimated at 65,000 tonne of fluorine per annum. If this figure is representative of global trends, then burning of coal may contribute more than 270,000 tonne of fluorine to the atmosphere per annum,[4] although a lower estimate of 180,000 tonne has been reported elsewhere [27].

In addition to anthropogenic sources, there are natural sources of atmospheric fluorine-containing compounds. Perhaps, the largest of these are volcanoes, which are estimated to produce somewhere between 60,000 and 6 million tonnes of fluorine per annum, mostly in the form of hydrogen fluoride and fluorosilicates [27]. Emissions will vary greatly from year to year, depending upon volcanic activity. For example, eruption of the Baitoushan volcano in China in 969AD produced a calculated 42 ± 11 megatonnes of volatile fluorine [28], in prehistoric times Mt Roza in Washington, USA liberated 1780 megatonnes of HF over a ten-year period [29], and much more recently Mt Erebus in Antarctica was found to be a significant source of halogens, emitting from 3000 to 6000 tonne per annum of HF [30](*see also in this series the chapter of C. Oppenheimer and G. Sawyer devoted to fluorine emissions from volcanoes*). Some eruptions produce severe fluoride contamination of surrounding grazing land: the 1970 eruption of Hekla in Iceland led to the death of about 7500 sheep, both through fluoride poisoning and through brittle teeth syndrome (also known as 'tephra teeth'), in which high concentrations of fluoride damage the teeth of livestock and prevent them from grazing. Volcanic gases have also been found to contain up to 160 ppb of halocarbon gases, including $CFCl_3$, CF_2Cl_2 and $HCFCl_2$ [31]. Igneous and metamorphic rocks are now recognised as significant sources of CF_4, CF_2Cl_2, $CFCl_3$, NF_3 and SF_6, with CF_4 being the most important. These compounds have been found in samples of fluorite, granite and other rocks from around the world, with an annual flux into the atmosphere of approximately 0.1–1.0 tonne [32]. With a lifetime in the environment of $>200{,}000$ years, this is sufficient to account for the background level of 6×10^5 tonne of CF_4 in the atmosphere. This could also be a source of trifluoroacetic acid, and, by slowly building up over geological time, could account for the high levels found in seawater, which exceed those expected from purely anthropogenic sources [33].

Several fluorochemicals have recently come under scrutiny for their persistence in the environment, the most notable being perfluorooctylsuflonate (PFOS), which was withdrawn from sale by manufacturers 3M in 2000 because of concerns over its bioaccumulation in organisms [34]. This compound has been found

[4] Based on global coal consumption reported in BP Statistical Review of World Energy, June 2002, BP p.l.c., London.

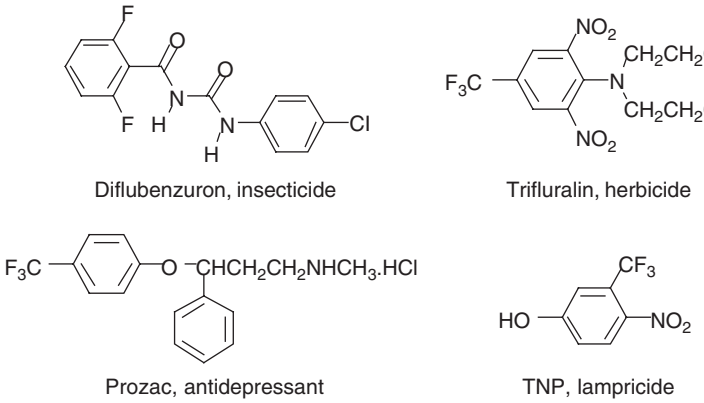

Fig. 2. Representative bioactive fluorinated aromatics.

to be a widespread global contaminant and has been detected at significant levels in the fat, tissue and blood of humans and other mammals, birds, fish, reptiles and amphibians [35], and there is some evidence that this alters the properties of cell membranes [36]. PFOS and related compounds were used extensively as waterproofing agents and stain-repellent coatings. The UK government has since announced restrictions on the use of PFOS with the aim of phasing out its use completely, and a European ban is anticipated. Substitution of this compound in the short term is likely to be by shorter chain length perfluoroalkylsulphonates (e.g. perfluorobutane sulphonate) which are reported to show lower toxicity and do not bioaccumulate. Use of perfluoralkyl alcohols (fluorotelomer alcohols) has also been suggested, although these are suspected sources of perfluorooctanoic acid in the environment and, while less bioaccumulative than PFOS, are also known carcinogens and widespread environmental pollutants [37]. PFOS also has applications in fire fighting, chrome plating, hydraulic fluids for aircraft and in the semiconductor industry for photoresists and control of optical effects [38]. Current use in the EU is estimated at 12,250 tonne per annum, with the majority being consumed by electroplating.

Aromatic molecules with fluorine or fluorine-containing substituents frequently have high bioactivity [39] and are therefore used for medical and agrochemical applications, in which they are deliberately introduced to organisms and/or the environment (Fig. 2). They are typically less bioaccumulative and less environmentally persistent than saturated fluorocarbons, and may be degraded oxidatively under aerobic conditions, where defluorination may or may not occur.[5] The world market for fluoroaromatics was estimated at 10,000 tonne per annum in

[5] Biotransformation of fluorinated molecules in the environment is beyond the scope of this review but is covered in depth. See Ref. [40].

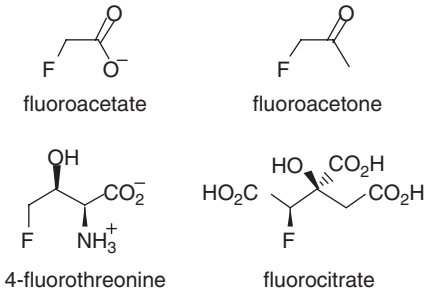

Fig. 3. Fluorine-containing natural products.

1994 [4], and global capacity for production of these compounds was 35,000 tonne per annum in 2000 [41]. Compounds-containing aromatic F–C bonds may also be degraded by nucleophilic attack, but trifluoromethyl functions are generally resistant to defluorination and it is likely that the final sink for fluorine atoms will, in these cases, be trifluoroacetate. This has been shown to be in the case of 3-trifluoromethyl-4-nitrophenol (TNP), which is used to control the sea lamprey: TNP breaks down under photolysis in water to produce trifluoroacetic acid [42].

Organofluorine compounds are often perceived as being entirely man-made. This is not, in fact, the case, and there are several biogenic sources of fluorinated natural products. When grown in fluoride-rich soil, several species of plants produce and accumulate fluoroacetate, which acts as a defence mechanism as it is extremely toxic to animals. However, animals that graze in regions where these plants are common have evolved with an increased tolerance to fluoroacetate, and this resistance has been found to extend further up the food chain. For example, falcons and owls which prey on rodents in areas rich in fluoroacetate-accumulating plants also have resistance to its toxic effects [43]. Sodium fluoroacetate poisoning in humans causes coma-like symptoms and respiratory failure, but if the subject survives, complete recovery may occur within a few days [44]. To date, only about 12-fluorinated natural products have been identified, which include fluoroacetate, fluorocitrate, fluoroacetone and 4-fluorothreonone, as well as fluorinated fatty acids (Fig. 3).[6] Considering the abundance of fluorine in the oceans and crust, it is perhaps surprising that there are not more naturally occurring organofluorine compounds, and there may be several that are, as yet, undiscovered. It is not clear what contribution biogenic organofluorine compounds make to atmospheric fluorine burden, although, as most of these compounds are reactive and are expected to have relatively short atmospheric lifetimes, it is likely that their effect is insignificant.

[6] For reviews of fluorine-containing natural products, see Ref. [45].

3. THE ROLE OF FLUORINE COMPOUNDS IN CLEAN SYNTHESIS

3.1. Fluorous separation technologies

Although the spectre of legislation is looming over many halogenated compounds, it would be unfortunate if organofluorine compounds were to become the subject of the wide-reaching restrictions that now affect chlorine- and bromine-containing compounds, as the unique properties of fluorine could have an important role to play in the advancement of clean chemical synthesis. In particular, the immiscibility of compounds containing perfluoroalkyl groups with some hydrocarbons and most polar organic solvents has led to the development of fluorous biphasic chemistry and other fluorous solvent technologies, in which the ease of separation of product or catalyst is greatly improved. The reason for this low miscibility has been debated and a 'special' attraction within the fluorous phase is occasionally proposed, but consideration of the cohesive pressures (perfluoroheptane = 136 MPa, hexane = 225 MPa and water = 2300 MPa) make it probable that the very weak interactions between highly fluorinated alkanes and the non-fluorous molecules are insufficient to pay back, thermodynamically, the free energy required to disrupt the non-fluorous phase [46]. Fig. 4 shows how fluorous liquids may be utilised in a biphasic system to facilitate recycling of a catalyst and solvent: at low temperatures the phases are immiscible, but on heating become a single phase allowing reaction to proceed at useful rates. Cooling leads to separation of the two phases and allows ready recovery of solvent, catalyst and product from the mixture. This gives improved efficiency and reduces waste.

The use of small-molecule sources of oxygen, including O_2, H_2O_2 and NaOCl (with an additional catalyst if required), is preferable on both economic and environmental grounds to stoichiometric, metal-based oxidants such as $KMnO_4$ and $K_2Cr_2O_7$ [1,47]. As oxidations will typically give products of greater polarity than

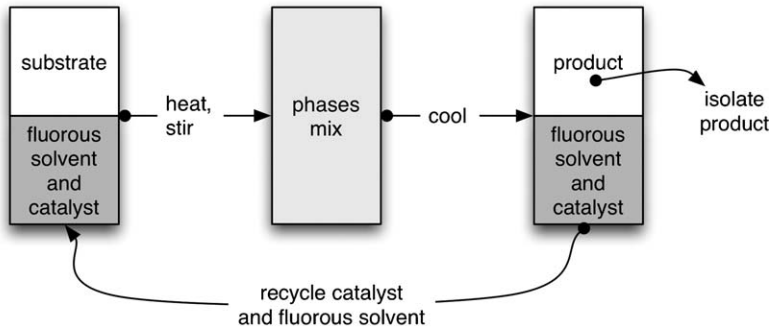

Fig. 4. Schematic diagram of a fluorous biphase process in which a fluorous solvent and fluorous catalyst are recycled together.

Table 3. Solubility of oxygen in selected perfluorinated solvents [46]

Solvent	Solubility of O_2 in ml per 100 ml solvent
n-Perfluorooctane C_8F_{18}	52.1
Perfluorotributylamine $(C_4F_9)_3N$	38.4
Perfluorooctyl bromide $C_8F_{17}Br$	52.7

the substrates, these reactions are very suitable candidates for fluorous biphasic processes. For example, if an alkene is oxidised to a more polar product (e.g. an epoxide or diol) in a fluorous biphase, the product should be less soluble in the fluorous phase than the substrate, and this will lead to the product being 'ejected' from the fluorous phase giving improved separation. Their low cohesive pressures allow perfluorinated solvents to dissolve extremely high quantities of oxygen (and other gases) (Table 3) and so the fluorous biphase is an ideal system in which to conduct oxidation reactions using elemental oxygen.

Although ideally suited to reactions involving gases, the fluorous approach to oxidations is not limited to use of elemental oxygen. A fluorous analogue of DMSO has been used to perform Swern reactions [48], a widely used method of oxidising an alcohol to an aldehyde which is unsatisfactory from the environmental point of view due to its production of stoichiometric quantities of dimethyl sulphide. Using fluorous biphase methodology, this stoichiometric reaction may be made pseudo-catalytic (Fig. 5). After reaction, the sulphide is extracted into perfluorohexane and recycled.

Heterogeneous reactions lend themselves to continuous flow reactors, which are desirable as they minimise the reacting volume. This reduces operation risks, and allows smaller, more efficient plants to be built. Flow reactors designed for fluorous reactions with both liquid and gaseous substrates have been demonstrated to be effective, at least on a bench scale [49]. Fluorous solvents have also recently found applications as liquid membranes to control the rate of addition of reagents and so control exothermic reactions such as alkene bromination (Fig. 6), and demethylation of anisoles by reaction with boron tribromide [50]. This has potential as a clean route as the kinetic control gives improved selectivity.

Fluorous biphase reactions have been reviewed extensively in the past few years, and most important types of reaction may now be conducted under fluorous conditions [46,51]. However, partitioning of catalysts and reagents into the fluorous phase is seldom perfect – even a loss of 1–2% of an expensive catalyst may be unacceptable. Solubility and partitioning between phases relies on a complex balance of properties and interactions, and rather than simply adding more fluorocarbon chains to a catalyst (which is a common approach to the problem of leaching of catalyst from the fluorous phase), studies have indicated that the partition coefficients of fluorous compounds may better be optimised by

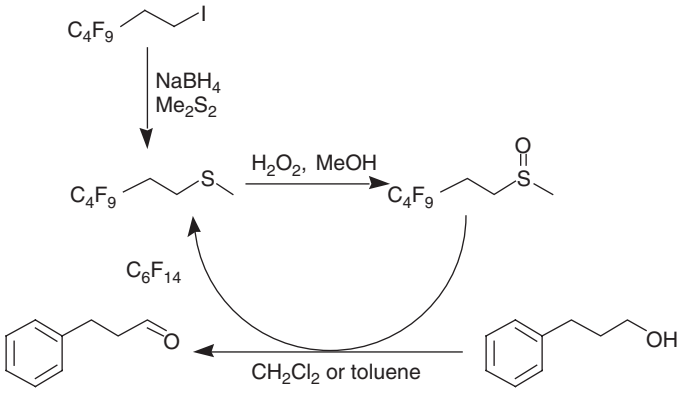

Fig. 5. A Swern oxidation under fluorous conditions allows reuse of the suphoxide reagent.

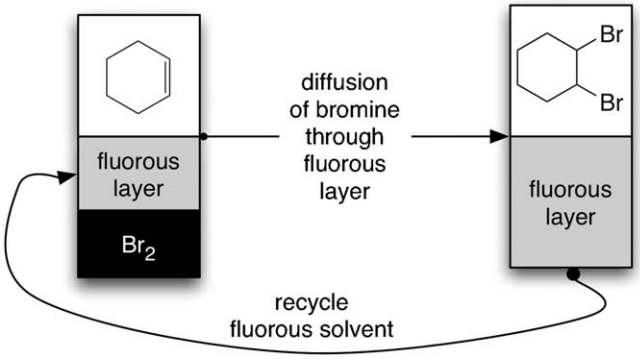

Fig. 6. Alkene bromination using a fluorous liquid membrane to control diffusion rates.

careful adjustment of the composition of the solvent phases [52]. The polarity of a liquid perfluorocarbon may be increased by addition of perfluoroalkyl ethers, while the polar organic phase becomes more fluorophobic on addition of small amounts of water. While the principle is an interesting and potentially useful one, the solvent systems reported unfortunately involved the use of DMF, which is toxic and a known carcinogen. Fluorine-containing groups benefit other alternative reaction solvents: fluorine is increasingly found in the cations of ionic liquids where it is used to fine-tune the viscosity, density, conductivity, miscibility and other important properties of the liquid [53], and is present in the near-ubiquitous BF_4^- and PF_6^- anions. Silica gel, which is normally a very polar surface [54], may be made compatible with fluorous reagents and solvents by grafting a perfluoroalkyl group to the surface using a silane reagent [55] – a fluorous technology which requires no perfluorinated solvent. The resultant solids, know as

fluorous reverse phase silica gel (FRPSG), have very low surface energies and so should only be wetted by liquids with correspondingly low surface tensions, i.e. highly fluorinated compounds. The FRPSGs may thus be used as a chromatography support for separation and purification of fluorous reagents, or as a tool for preferentially adsorbing them from a reaction mixture. In a chromatographic system, compounds without fluorous groups are first eluted using a polar solvent (in which the fluorous compounds have little solubility), and then a less polar solvent is used to elute the fluorous compound. Whereas effective partitioning into a fluorous liquid phase generally requires two or three perfluoroalkyl groups to be attached, FRPSG techniques require much lower fluorine content for separation to be effective. This approach has been applied to separation of chiral mappicines [56], and to isolate and reuse Lewis acid and metal catalysts with fluorous ligands [57]. It may also be used to recover fluorous amides from reaction mixtures *via* solid-phase extraction without recourse to additional purification steps, giving a cleaner overall synthesis [58]. A recent, and ingenious, example of the use of heterogeneous fluorinated systems to recover homogeneous catalysts has involved the use of Teflon tape as the immobilisation phase [59]: a thermomorphic rhodium catalyst containing perfluorinated-phosphine ligands was found to be efficiently recovered by cooling the mixture in the presence of the tape. Here, the authors recognise an additional potential advantage: the required quantity of catalyst may be delivered by cutting lengths of the tape, rather than by accurate weighing of small amounts. It is worth noting here that other workers have studied the diffusion properties of fluorinated and non-fluorinated aromatics at Teflon surfaces and suggest that these systems do not act in a truly 'fluorous' manner, but are closer to supported-liquid membranes in their behaviour [60].

As discussed in Section 2, a major problem restricting the implementation of these fluorous technologies is the high GWP of volatile fluorinated compounds, although a switch to perfluoroalkyl ethers, which break down faster in the environment, may overcome this hurdle. Despite the environmental problems and anticipated legislative controls of perfluorinated solvents and reagents, research into fluorous technologies has continued undeterred, with reports of increasingly sophisticated multi-phasic systems involving, for example, fluorous, organic and aqueous-liquid phases [61]. A survey of use of the word 'fluorous' in titles of publications in the *Web of Knowledge* database [62] reveals 451 articles, increasing rapidly in frequency between 1995 and 2002 (Fig. 7). The number of publications has since levelled, which may indicate that the technology is at the peak of its popularity, at least in academic circles. Despite the market presence of a company dedicated to fluorous products, the uptake of this technology by industry has not yet reached the potential that seemed possible five years ago, and the relatively high prices and environmental concerns over highly fluorinated reagents may ultimately limit their use to specialist applications.

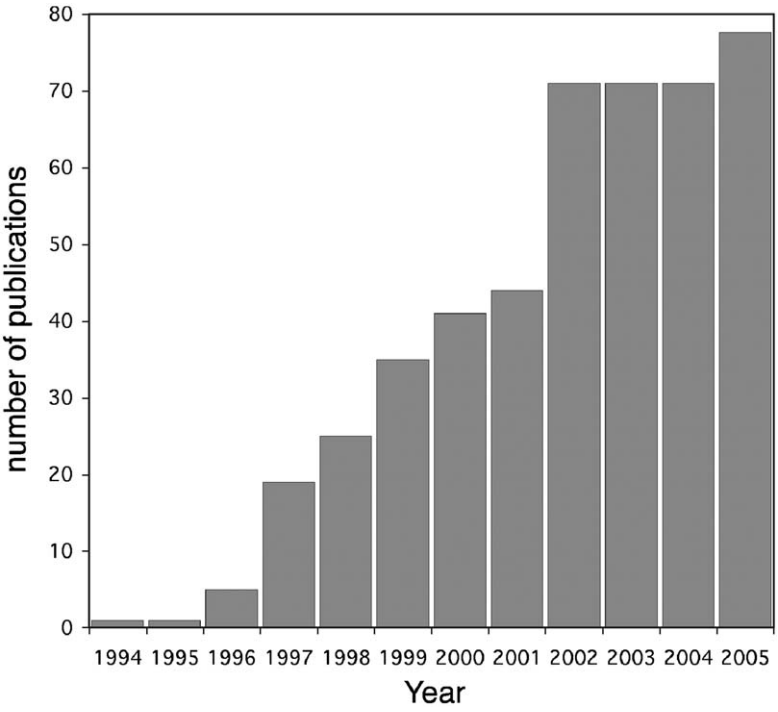

Fig. 7. Yearly publications of journal articles containing the word 'fluorous' in the title.

3.2. The use of fluorinated groups in supercritical CO_2

Supercritical CO_2 is considered to be close to zero in its environmental impact as it is normally condensed from, and returned to, the atmosphere (although the energy involved in its use must be accounted for). For this reason supercritical CO_2 is finding many applications as a solvent in clean synthesis and extraction, and it has the addition advantages of being non-toxic and may be completely removed from the reaction product simply by releasing the reactor pressure [46]. However, it is not a particularly powerful solvent and does not, by itself, dissolve many compounds. Fluorous compounds find applications in these systems because of their solubility, and ability to act as ligands and surfactants to bring other compounds into the supercritical phase [63]. Once again it is the weakness of the intermolecular forces between fluorous molecules that makes this possible. Despite studies using a range of spectroscopic techniques, the exact cause of this compatibility with supercritical CO_2 is not well understood, and there is some disagreement in the literature over whether or not specific interactions between

the fluid and the fluorous group occur [64]. What is certain is that the combination of supercritical CO_2 and fluorous modifier is a very powerful, tuneable and potentially clean reaction medium.

Hydrogen peroxide, which produces only water and O_2 as by-products and is generally considered to be a clean oxidant, may be generated in $scCO_2$. The anthraquinone (or *AQ*) process, in which an alkyl anthraquinone is first hydrogenated and then oxidised, is used to supply almost all of the global demand for H_2O_2 [65]. The AQ process may be successfully performed in $scCO_2$ if the anthraquinone catalyst is made compatible with the fluid phase by functionalisation with perfluorinated chains [66]. Moreover, the H_2O_2 produced in this way may be utilised in the same reactor (i.e. a one-pot process), for the epoxidation of alkenes (Fig. 8). The compatibility of fluorinated compounds with supercritical CO_2 has facilitated the replacement of CFCs as a medium for polymerisation of Teflon and other fluoropolymers on an industrial scale. DuPont recently built a $275 million plant capable of making 1000 tonne of polymer per year. The plant uses carbon dioxide technology in a process that generates less waste during manufacture, and produces a grade of polymer that the manufacturer claims has enhanced performance and processing capabilities [67]. It is expected to begin commercial production in 2006.

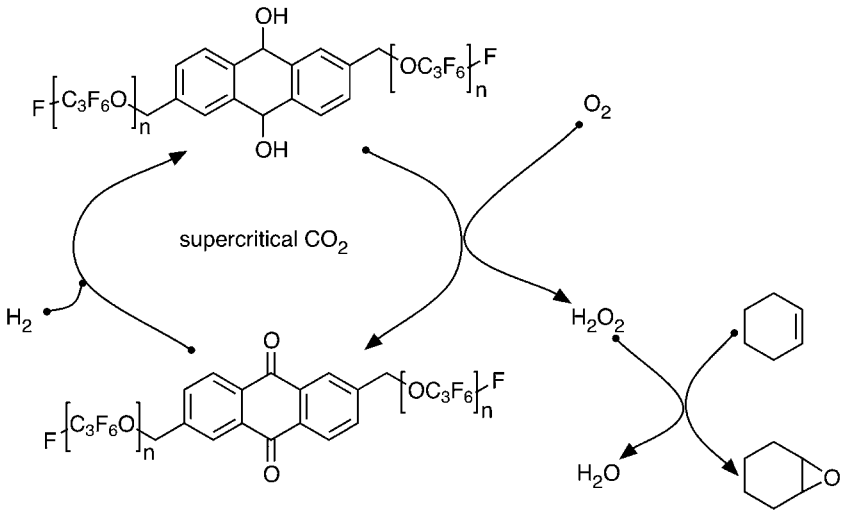

Fig. 8. Generation of H_2O_2 in supercritical CO_2 using a fluorous anthraquinone catalyst, and *in situ* use as an oxidant.

3.3. Safe fluorination with F_2 using microreactor technology

Where electrophilic fluorination is required, it has been commonplace to utilise the so-called 'F^+' reagents in which the electrophilic fluorine is bound to an organic nitrogen centre [68]. While these reagents are effective, they have the drawbacks of being expensive, requiring use of elemental fluorine in their manufacture, and of course the atoms in the organic amine carrier have no role in the final product – essentially those atoms are wasted and the process has a poor atom economy. There is no fundamental reason why elemental fluorine itself should not be viewed as a suitable reagent for clean synthesis. Generally, F_2 is used to replace a C–H bond with a C–F function, producing HF as a by-product, and if the HF is recycled the atom economy may be very high indeed. Because of its reactivity, fluorination with F_2 proceeds without the need for catalysts, and may be performed in the gas phase without solvent. However, this supreme reactivity is itself a problem because of the large quantity of heat liberated during the reaction, which can lead to increased reaction rates, reduced selectivity and, in the worst case scenario, a runaway reaction. While this must be avoided on safety grounds, the loss of selectivity is also of concern from a green chemistry of view. Fluorinations may be made significantly more selective simply by dilution of F_2 in an inert carrier gas (usually nitrogen) [69]. One potential method for scale up of reactions simply by running many tiny *microreactors*, often as small as a few microlitres volume, in parallel, which could, in the future, intensify processes and reduce the size of chemical plants [70]. Microreactor systems are already showing great potential for selective reactions using elemental fluorine and the extremely small volume contributes greatly to the safe running of these systems by ensuring that only small quantities of F_2 are present in the reactor. Also, heat may be removed from the reaction much more efficiently, moderating the exotherm and thus giving much greater control – which is ideal for selective introduction of fluorine. For example, the fluorination of ethyl acetoacetate, using 10% F_2 in N_2, in a microreactor gave 73% selectivity at 99% conversion for the monofluorinated product, as shown in Fig. 9 [71], which compares very favourably with 85% selectivity at only 15% conversion observed in a similar bulk reactor [72]. Selective fluorination of toluene and other aromatics in microreactors have also been reported [73]. Reactors with as many as 30 parallel channels are already in

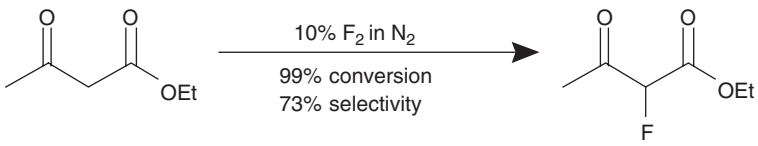

Fig. 9. Fluorination of ethyl acetoacetate with elemental fluorine using a microreactor.

use which, despite very low flow rates and capacities, may produce 100 g of product overnight [74].

3.4. Comparison of synthetic routes to fluoroaromatics

Fluoroaromatics are an important class of chemicals with applications that include pharmaceuticals (see Section 2), agricultural chemicals, polymers and liquid crystals [75]. As well as direct fluorination by HF, there are several other methods for preparation of fluoroaromatics, and four of the most important – Halex, Balz–Schiemann, direct fluorination and a recently reported route involving CuF_2 (Fig. 10) – are compared here in terms of their inherent hazards and efficiency. An ideal synthesis for fluoroaromatics should involve a good fluorinating agent in terms of reactivity, cost, ease of handling and safety, and would give high yields with low levels of by-products.

The oxidative fluorination route has high atom efficiency, incorporating all of the fluorine into the aromatic, and producing only water as a by-product [76]. Be-

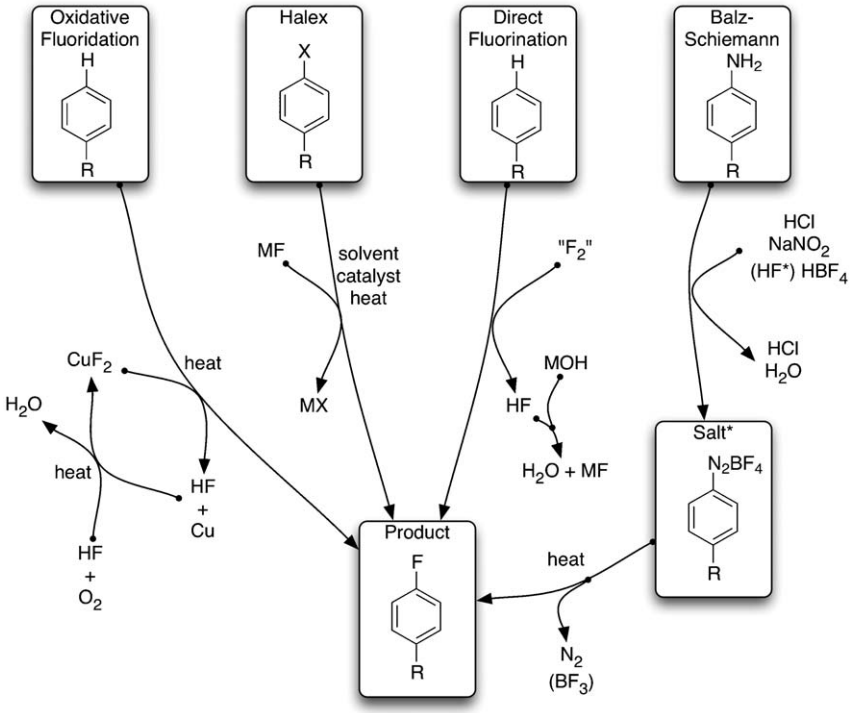

Fig. 10. Summary of four routes for preparing fluoroaromatics (see also Table 4). *Indicates the modified Schiemann reaction which may be performed in anhydrous HF or HF-pyridine. The salt intermediate in this case is a diazonium fluoride.

cause it replaces an aromatic hydrogen directly with fluorine, no precursor group is required. Copper(II) fluoride, used as the fluorinating agent, was selected on the basis of examination of metal redox potentials. The metal must be sufficiently oxidising that it reacts with the C–H bond, yet not so oxidising that it is impossible to regenerate. This system gives moderate yields (5–35% conversion in a single pass through the reactor), very good selectivity ($>95\%$) towards the monofluorinated-aromatic product, requires no solvent, and, appears to be very promising as a clean, atom efficient route to fluoroaromatics. However, very high temperatures are required for both the reaction (400–550°C) and regeneration (400°C) steps. The high temperatures mean that while this may well be a suitable method for the fluorination of benzene and simple alkylbenzenes, many functional groups would not survive these conditions. In addition, the energy required to heat the reactor makes a substantial contribution to the process cost and any advantages gained in terms of atom efficiency must be offset against this.

Direct fluorination is potentially very efficient in terms of utilisation of reagents, requiring no existing functional group: the C–H is replaced directly with C–F. The drawbacks are that the reaction is frequently unselective, giving polysubstituted products (although see the discussion on direct fluorination, above), energy is required to cool the system, and acid HF waste is produced which must be neutralised and disposed of. Unlike chlorination and bromination reactions, it is not possible to oxidise the HF back to F_2 by *in situ* use of H_2O_2 – the oxidation potential for F_2 is too high. The Halex, or halogen exchange, route to fluoroaromatics starts with a chloroaromatic substrate (or nitro group in analogous fluorodenitration reactions), which is inherently wasteful from an atom efficiency perspective, as the chlorine will not appear in the final product. A fluoride salt, usually KF, and quaternary ammonium or phosphonium salt catalyst are also required. Halex reactions work best in polar aprotic solvents, which are frequently toxic and tend to break down under reaction conditions. The quaternary salt is generally not reusable, and high temperatures are required. The Balz–Schiemann route involves two steps, and requires treatment with HCl, $NaNO_2$ and HBF_4, although the nitrogen, chlorine and boron that appear in these reagents are not found in the final fluorinated product. An improvement on this route is the *modified Schiemann reaction* which eliminates the need for BF_3 but must be performed in anhydrous HF or HF-pyridine. The aniline substrate may already have produced substantial waste during its manufacture *via* nitration and subsequent reduction. These methods are, however, applicable to a wider range of substrates than some of the other methods, and remain popular methods for fluoroaromatic manufacture.

There are many factors that contribute to the 'greenness' of a chemical reaction, and there is no clear preferred route, although the two systems that replace C–H directly are, on paper at least, cleaner than those that require functional group exchange. These reactions are summarised in Table 4.

Table 4. Overall evaluation of manufacturing methods for fluoroaromatics

Route	Waste	Risk	Energy and materials	Cost	Simplicity	Maximum atom efficiency[a]
Oxidative fluorination	Water only	HF	Very high temperatures	Energy HF handling	One step with recycling of fluoride	80%
			Special reactors			
Halex	Salt	Corrosion	High temperature	Activated aromatics; expensive solvents, catalyst	One step (omitting Ar-X manufacture)	$<$86% (omitting Ar-X manufacture)
	Lost or decomposed solvent	Decomposition of (toxic) solvent				
Direct fluorination	Salt (neutralised HF)	F_2, HF	Cooling	F_2 generation and handling	One step	70%
			Special reactors			
Balz–Schiemann	Salt	Unstable intermediate HF, BF_3	Cooling	Anilines	Two steps (omitting aniline manufacture)	44% (omitting aniline manufacture)
	Lost solvent BF_3		Special reactors			
Modified schiemann	Salt	Unstable intermediate HF handling	Cooling Special reactors	Anilines	Two steps (omitting aniline manufacture)	48% (omitting aniline manufacture)
	Lost solvent					

[a] At 100% yield, assumes aromatic group is C_6H_5.

4. FLUOROCHEMICALS FACILITATE MINIATURISATION OF END-PRODUCTS

Employment of fluorine technology may contribute to clean chemistry by virtue of its unique atomic properties. Fluorine's small size and superior electronegativity allow manipulation of dielectric properties of molecules (specifically, the dielectric anisotropy), making it an essential building block for liquid crystal engineering [77]. This has led to rapid advances in visual display unit and *thin film transistor* (TFT) flat screens are replacing conventional cathode ray tube devices. The computer display market is estimated at US$ 100,000 million per year, and flat screen technology has rapidly penetrated the market, rising from just 5% of the market share in 1999 to 70% in 2005; it is predicted to reach 94% by 2008 [78]. TFT visual display screens, which use significantly less energy than conventional cathode ray tube (CRT) screens, rely on fluorine-containing compounds that behave as *twisted nematic* liquid crystals (Fig. 11).

These flat screens have allowed miniaturisation of the whole computer screen assembly, and substantially less plastic, glass and electrical components are required. In addition, transport and packaging are reduced, and the enormous volume of these products means that even small improvements may have major environmental benefits. Ongoing work at York University has discovered that these liquid crystal molecules may be effectively recovered from TFT screens *via* a supercritical extraction process, giving the potential for reuse of these useful high value fluorinated compounds [79].

Fluorine plays another important role in display screen technology, albeit replacing another type of fluorine technology. F_2 is often considered to be a dangerous harmful chemical (indeed it has been referred to as the *Tyrannosaurus Rex* of the elements [80]). However, its very reactivity ensures that it cannot persist in the environment, although its by-products may. The major hazards

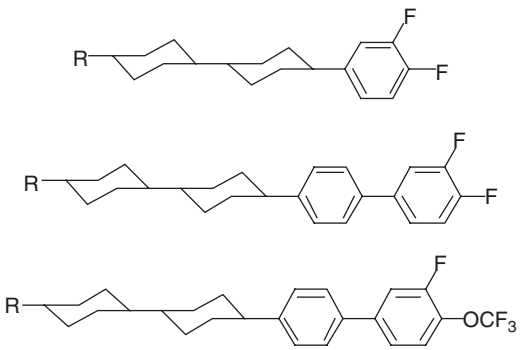

Fig. 11. Examples of fluorinated-liquid crystals used in TFT display screens (R = alkyl group).

associated with use of F_2 are transport and storage of quantities of the reactive gas. Advances in electrochemical fluorine gas production have led to the development of on-demand F_2 generators that may be installed on location at the manufacturing site [81]. Cleaning of TFT screen and silicon chip manufacturing equipment requires removal of deposits formed during electrochemical vapour deposition, and this is normally performed using fluorine radicals generated from CF_4, NF_3, C_2F_6 and other related compounds by microwave-plasma methods. Use of locally generated F_2 gas as a source of the F radicals avoids the use of these environmentally persistent greenhouse gases.

The unique properties of fluorine – its small size, high electronegativity, and the hydrophobicity/lipophilicity imparted by introduction of small fluorinated groups (CF_3, OCF_3, SCF_3, etc.) – allow careful tuning of the biological properties of the molecule, and the use of fluorine in medicines and agrochemicals has become widespread [82]. Incorporation of fluorine or a small fluorocarbon group can impart several benefits, all of which may improve the bioavailibility of the drug and allow lower doses to be used. This may reduce waste and energy requirements along the entire supply chain. Three major effects of using fluorine in medicines are [81,83]

(i) Blocking of metabolically labile C–H sites by replacement with fluorine atoms often leads to molecules with increased metabolic stability.
(ii) Control of the basicity and lipohilicity of the molecule can improve the ability of the drug to permeate through cell membranes.
(iii) Binding constants are normally increased by the introduction of fluorinated groups.

Fluoroquinolines (Fig. 12), for example, are highly active antibacterial agents with binding affinities up to 17-fold higher, and cell penetration increased by up to 70-fold, compared to non-fluorinated counterparts. Mankind has a long tradition of utilising natural products as medicines, and the discovery and recent understanding of the biosynthesis of natural organofluorine compounds may allow development of new families of fluorinated medicines to be developed using biosynthetic pathways [84].

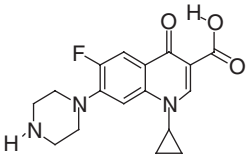

Fig. 12. Example of a fluoroquinoline antibacterial agent.

5. CONCLUSIONS

From a green chemist's point of view, an ideal product, be it a recyclable solvent, a car or a laptop computer, is one that is designed to be robust during use, have a long-working lifetime, yet may easily be recycled at the end of its life and will, if released into the environment, break down rapidly into benign components. This is clearly not an easily achievable goal as durability and biodegradation do not necessarily go hand-in-hand. Because of the tendency of fluorine to form very strong bonds with other elements, fluorochemicals generally perform well in terms of durability (e.g. Teflon), and the unique properties of fluorous solvents and reagents facilitate recycling. However, some of the environmental problems associated with organofluorine compounds are direct results of their inherent durability, and many highly fluorinated species have few decomposition mechanisms, long environmental lifetimes and may accumulate to dangerous levels in organisms. Recognition of these problems allows for design of better chemical products with lower environmental impact.

Fluorine-containing compounds are found widely in the environment, and although some of these may be attributed to the activities of human beings in general, and the chemical industry in particular, there are also many natural processes that contribute to fluorine reservoirs. Although certain fluorine-containing compounds have been identified as being involved in ozone depletion, global warming effects and health concerns, legislative measures have been, or are being, put in place where necessary to reduce this impact. Fluorine-containing compounds have a great potential for clean synthesis, and utilisation of the high activity that fluorinated groups can impart may help to produce smaller, more effective, and therefore greener chemical products.

ACKNOWLEDGEMENTS

We thank Prof. John Goodby and Dr Avtar Matharu of the University of York for discussions about the use of fluorine in liquid crystal devices, and Prof. Alan Davison of the University of Newcastle and Dr Archie McCulloch of Marbury Technical Consulting for helpful suggestions regarding fluorochemicals in the environment.

REFERENCES

[1] J.H. Clark, Chem. Brit. October 34 (10) (1998) 43; J.H. Clark, Green Chem. 1 (1999) 1; M. Lancaster, Green Chemistry: An Introductory Text, RSC, Cambridge, 2002.
[2] T. Kitazume, J. Fluorine Chem. 105 (2000) 265; S.J. Tavener, J.H. Clark, J. Fluorine Chem. 123 (2003) 31–36.

[3] A. McCulloch, J. Fluorine Chem. 123 (2003) 21; J. Lucas, J. Fluorine Chem. 41 (1988) 1; The Handbook of Environmental Chemistry, Vol. 3, Part N: Organofluorines, A.H. Neilson (Ed.), Springer, Berlin, 2002; J.P. Friend, Natural Chlorine and Fluorine in the Atmosphere, Water and Precipitation, Scientific Assessment of Stratospheric Ozone, in World Meterological Organisation Global Ozone Project Report, 1989 No. 20,Vol. 2, p. 429.
[4] B.D. Key, R.D. Howell, C.S. Criddle, Environ. Sci. Technol. 31 (1997) 2445.
[5] CRC Handbook of Chemistry and Physics, 76th Edition, CRC Press, Boca Raton, 1995.
[6] M.M. Miller, U.S. Geological Survey Minerals Yearbook 2003: Flourspar Report, 2003; *ibid.*, 2001, *ibid.*, 1998; Mineral Profile: Flurorspar, British Geological Society, Nottingham, July 2003.
[7] M.M. Miller, U.S. Geological Survey Minerals Commodities Summaries, U.S. Geological Survey, Reston, VA, USA, January 2002 and February 1997.
[8] Inventory of U.S. Greenhouse Gas Emission and Sink 1990–2000, U.S. Enviornmental Protection Agency, Washington, 2002; Inventory of U.S. Greenhouse Gas Emission and Sinks 1990–2003; U.S. Enviornmental Protection Agency, Washington, 2005; Internation Panel on Climate Change, Third Assessment Report – Climate Change 2001, Cambridge University Press, Cambridge, 2001, Chapter 4.
[9] T.E. Norgate, W.J. Rankin, Proc.Int. Symp. Greenhouse Gases in the Metalurgical Industries, Toronto, 2000.
[10] Environmental Data Service, ENDS Rep. 329 (2002) 8.
[11] A. McCulloch, J. Fluorine Chem. 100 (1999) 163.
[12] A.R. Ravishankara, A.A. Turnipseed, N.R. Jensen, S. Barone, M. Mills, C.J. Howard, S. Soloman, Science 263 (1999) 71.
[13] T.J. Wallington, O.J. Nielson, Handbook of Environmental Chemistry, Vol. 3, Springer, Berlin, 2002, Chapter 3, Part N.
[14] M.F. Gerstell, J.S. Francisco, Y.L. Yungm, C. Boxe, E.T. Aaltonee, Proc. Natl. Acad. Sci. USA 98 (2001) 2154.
[15] Environmental Data Service, ENDS Rep. 337 (2003) 46.
[16] Environmental Data Service, ENDS Rep. 328 (2002) 50.
[17] Environmental Data Service, ENDS Rep. 355 (2004) 30.
[18] Environmental Data Service, ENDS Rep. 360 (2005) 16.
[19] Environmental Data Service, ENDS Rep. 358 (2004) 11; *ibid.*, 363 (2005) 9.
[20] M. Luo, R.J. Cicerone, J.M. Russell III, T.Y.W. Huang, J. Geophys. Res. 99 (1994) 16691.
[21] G. Considine, L. Deaver, E. Fremsberg, J.M. Russell III, Geophys. Res. Lett. 24 (1997) 3217.
[22] D.L. Jacob, Introduction to Atmospheric Chemistry, Princeton University Press, Princeton, 1999.
[23] D.A. Ellis, S.A. Mabury, J.W. Martin, D.C.G. Muir, Nature 412 (2001) 321.
[24] K.R. Solomon, X. Tang, S.R. Wilson, P. Zanis, A.D. Bais, Photochem. Photobiol. Sci. 2 (2003) 62; X. Tang, S. Madronich, T. Wallington, D. Calamari, J. Photochem. Photobiol. B: Biol. 46 (1998) 83.
[25] M. Berg, S.R. Müuller, J. Müthlemann, A. Wiedmer, R.P. Schwartzenbach, Environ. Sci. Technol. 34 (2000) 2675.
[26] K.L. Luo, L.R. Xu, R.B. Li., L.H. Xiang, Chin. Sci. Bull. 47 (2002) 1347.
[27] R.B. Symonds, W.I. Rose, M.H. Reed, Nature 334 (1988) 415; R.D. Cadle, Rev. Geophys. Space Phys. 18 (1980) 746.
[28] S. Horn, H.U. Schmincke, Bull. Vulcanol. 61 (2000) 537.
[29] Th. Thordarson, S. Self, J. Vulcanol. Geotherm. Res. 74 (1996) 49.
[30] G. Zreda-Gostynska, P.R. Kyle, D.L. Finnegan, Geophys. Res. Lett. 20 (1993) 1959–1962.
[31] V.A. Isidorov, I.G. Zenkevich, B.V. Ioffe, J. Atmos. Chem. 10 (1990) 329.

[32] J. Harnisch, M. Frische, R. Bochers, A. Eisenhauer, A. Jordan, Geophys. Res. Lett. 27 (2000) 1883.
[33] A. McCulloch, J. Fluorine Chem. 123 (2003) 21.
[34] Environmental Data Service, ENDS Rep. 354 (2004) 28.
[35] K. Kannan, S. Corsolini, J. Falandysz, G. Fillman, K. Senthil Kumar, B.G. Loganathan, M. Ali Mohd, J. Olivero, N. Van Wouwe, J. Ho Yang, K.M. Aldous, Environ. Sci. Technol. 38 (2004) 4489; J.P. Giesy, K. Kannan, Environ. Sci. Technol. 35 (2001) 1339.
[36] W.Y. Hu, P.D. Jones, W. DeCoen, L. King, P. Fraker, J. Newsted, J.P. Giesey, Comp. Biochem. Physiol. Part C 135 (2003) 77.
[37] N.L. Stock, F.K. Lau, D.A. Ellis, J.W. Martin, D.C.G. Muir, S.A. Mabury, Environ. Sci. Technol. 38 (2004) 991; D.A. Ellis, J.W. Martin, A.O. De Silva, S.A. Mabury, M.D. Hurley, M.P. Sulbaek Anderson, T.J. Wallington, Environ. Sci. Technol. 38 (2004) 3316.
[38] Environmental Data Service, ENDS Rep. 355 (2004) 42; *ibid.*, 358 (2004) 55.
[39] D. O'Hagan, H.S. Rzepa, Chem. Commun. (1997) 645. J.C. Biffinger, H.W. Kim, S.G. DiMagno, Chem. Bio. Chem. 5 (2004) 622.
[40] B.D. Key, R.D. Howell, C.S. Criddle, Environ. Sci. Technol. 31 (1997) 2445; A.H. Neilson, A.-S. Allard, The Handbook of Environmental Chemistry, Vol. 3, Part N: Organofluorines, A.H. Neilson, (Ed.), Springer, Berlin, 2002, Chapter 6.
[41] R. Bryant, Pharmaceutical Fine Chemicals Global Perspectives, Informa Chemicals Industry Report, Kent, UK, 2000.
[42] D.A. Ellis, S.A. Mabury, Environ. Sci. Technol. 34 (2000) 632.
[43] G.R. Martin, L.E. Twigg, Wildlife Res. 29 (2002) 75.
[44] R.F. Robinson, J.R. Griffith, W.R. Woolwich, M.C. Nahata, Vet. Human Toxicol. 44 (2002) 93.
[45] D. O'Hagan, D.B. Harper, J. Fluorine Chem. 100 (1999) 127; D.B. Harper, D. O'Hagan, Nat. Prod. Rep. 11 (1994) 123; G.W. Gribble, Handbook of Environmental Chemistry, Vol. 3, Springer, Berlin, 2002, Part N, Chapter 5.
[46] D.J. Adams, P.J. Dyson, S.J. Tavener, Chemistry in Alternative Reaction Media, Wiley, Chichester, 2003.
[47] R.A. Sheldon, J. Chem. Tech. Biotechnol. 68 (1997) 381.
[48] D. Crich, S. Neelamkavil, J. Am. Chem. Soc. 123 (2001) 7449; D. Crich, S. Neelamkavil, Tetrahedron 58 (2002) 3865.
[49] E. Perperi, Y. Huang, P. Angeli, G. Manos, C.R. Mathison, D.J. Cole-Hamilton, D.J. Adams, E.G. Hope, Chem. Eng. Sci. 59 (2004) 4983; A. Yoshida, X.H. Hao, J. Nishikido, Green Chem. 5 (2003) 554; E. Perperi, Y. Huang, P. Angeli, G. Manos, C.R. Mathison, D.J. Cole-Hamilton, D.J. Adams, E.G. Hope, Dalton Trans. (14) (2004) 2026.
[50] I. Ryu, H. Matsubara, S. Yasuda, H. Nakamura, D.P. Curran, J. Am. Chem. Soc. 124 (2002) 12946.
[51] A.P. Dobbs, M.R. Kimberley, J. Fluorine Chem. 118 (2003) 3; E.G. Hope, A.M. Stuart, J. Fluorine Chem. 100 (1999) 75; E. de Wolf, G. van Koten, B.J. Deelman, Chem. Soc. Rev. 28 (1999) 37.
[52] M.S. Yu, D.P. Curran, T. Nagashima, Org. Lett. 7 (2005) 3677.
[53] H. Xue, Jean'ne Shreeve, Eur. J. Inorg. Chem. (13) (2005) 2573.
[54] S.J. Tavener, J.H. Clark, G.W. Gray, P.A. Heath, D.J. Macquarrie, Chem. Commun. (1997) 1147.
[55] D.P. Curran, Synlett 9 (2001) 1488.
[56] D.P. Curran, Z. Lee, Green Chem. 3 (2001) G3.
[57] B. Croxtall, E.G. Hope, A.M. Stuart, FBC7 in Abstracts of the RSC Annual Conference 2001. O. Yamazaki, X. Hao, A. Yoshida, J. Nishikido, Tetrahedron. Lett. 44 (2003) 8791.
[58] T. Nagashimi, Y. Lu, M.J. Petro, W. Zhang, Tetrahedron Lett. 46 (2005) 6585.

[59] L.V. Dinh, J.A. Gladysz, Angew. Chem. Int. Ed. 44 (2005) 4095.
[60] H. Zhao, K. Ismail, S.G. Weber, J. Am. Chem. Soc. 126 (2004) 13184.
[61] S. Shirakawa, Y. Tanaka, K. Maruoka, Org. Lett. 6 (2004) 1429.
[62] ISI web of knowledge, http://wok.mimas.ac.uk, Survey conducted on 3rd January 2006.
[63] J. Eastoe, S. Gold, Phys. Chem. Chem. Phys. 7 (2005) 1352.
[64] A. Dardin, J.B. Cain, J.M. DeSimone, C.S. Johnson, E.T. Sanulski, Macromolecules 30 (1997) 3592; E.J. Beckman, Chem. Commun. (2004) 18. C.R. Yonker, B.J. Palmer, J. Phys. Chem. A 105 (2001) 8; J.T. Gerig, J. Am. Chem. Soc. 127 (2005) 277.
[65] W.R. Sanderson in Handbook of Green Chemistry and Technology, J.H. Clark, D.J. Macquarrie (Eds.), Blackwell, Oxford, England, 2002, p. 256.
[66] D. Hâncu, J. Green, E.J. Beckman, Acc. Chem. Res. 35 (2002) 757.
[67] M. McCoy, Business 77 (1999) 11; M. McCoy, Chem. Eng. News June (1999) 11; Unattributed article, Chem. Week, 27 March (2002)
[68] G.S. Lal, G.P. Pez, R.G. Syvret, Chem. Rev. 96 (1996) 1737.
[69] G. Sandford, Tetrahedron 59 (2003) 437.
[70] P.D.I. Fletcher, S.J. Haswell, E. Pompo-Villar, B.H. Warrington, P. Watts, S.Y.F. Yong, X. Zhang, Tetrahedron 58 (2002) 4735; S.J. Haswell, R.J. Middleton, B. O'.Sullivan, V. Skelton, P. Watts, P. Styring, Chem. Commun. (2001) 391.
[71] R.D. Chambers, R.C.H. Spink, Chem. Commun. (1999) 833. R.D. Chambers, D. Holling, R.C.H. Spink, G. Sandford, Lab on a Chip 1 (2001) 132.
[72] R.D. Chambers, M.P. Greenhall, J. Hutchinson, Tetrahedron 52 (1996) 1.
[73] N. de Mas, A. Günther, M.A. Schmidt, K.F. Jensen, Ind. Eng. Chem. Res. 42 (2003) 698.
[74] S.K. Ritter, C&EN, 14th February (2005) 35. R.D. Chambers, M.A. Fox, D. Holling, T. Nakano, T. Okazoe, G. Sandford, Lab on a Chip 5 (2005) 191.
[75] J.H. Clark, D. Wails, T.W. Bastock, Aromatic Fluorination, CRC Press, Boca Raton, 1996.
[76] M.A. Subramanian, L.E. Manzer, Science 297 (2002) 1665; M.A. Subramanian, T.G. Calvarese, Fluorine and the Environment: Agrochemicals, Archaeology, Green Chemistry and Water, Advances in Fluorine Science, Chapter 6.
[77] G.W. Gray, M. Hird, D. Lacey, K.J. Toyne, Perkin Trans. 2 (1989) 2041; G.W. Gray, M. Hird, K.J. Toyne, Mol. Cryst. Liquid Cryst. 195 (1991) 221; A.S. Matharu, D.J. Byron, R.C. Wilson, Liquid Cryst. 19 (1995) 39.
[78] N. Bardsley, Display search, Survival of the fittest, talk given at USDC investor's conference, New York, March 15th 2005.
[79] J.W. Goodby, A.S. Matharu, University of York, personal communication.
[80] J. Holloway, Lecture given at University College, London, January 2005.
[81] G. Hodson, B.O.C Edwards, On site fluorine generation in the electronics industry, talk given at 'Fluorum' Fluorine technology Bureau Meeting, Manchester, 9th December 2005.
[82] H.-J. Böhm, D. Banner, S. Bendels, M. Kansy, B. Kuhn, U. Obst-Sander, M. Stahl, Chem. Bio. Chem. 5 (2004) 637.
[83] P. Jeschke, Chem. Bio. Chem. 5 (2004) 570.
[84] G.W. Gribble, J. Chem. Ed. 81 (2004) 1441.
[85] D. Meshri, Industrial applications of inorganic fluorides, Advances Inorganic Fluorides, T. Nakajima, B. Zemva, A. Tressaud (Eds.), Elsevier, 2000, Chapter 20, pp. 661–682.

Note from the Editor

See also in this series the chapters by R. Tuckett and A. Sekiya *et al*. devoted to the green house effect of SF_5CF_3 and to CFCs and HCFCs substitutes, respectively.

See also in this series the chapter of C. Oppenheimer and G. Sawyer devoted to fluorine emissions from volcanoes.

CHAPTER 6

Emerging ''Greener'' Synthetic Routes to Hydrofluorocarbons: Metal Fluoride-Mediated Oxyfluorination

M.A. Subramanian,* and T.G. Calvarese

DuPont Central Research and Development, Experimental Station, Wilmington, DE 19880-0328, USA

Contents

Abstract

Current technologies used in the manufacture of aliphatic and aromatic hydrofluorocarbons (HCFs) generate large quantities of waste, particularly hydrochloric acid, which is under severe environmental scrutiny and needs to be eliminated. Although highly desirable, direct and selective conversion of a C–H bond to a C–F bond using HF is not feasible due to the thermodynamic considerations. An environmentally ''greener'' process for the synthesis of fluorocarbons can be envisioned through an intermediate inorganic metal fluoride that is capable of fluorinating a C–H bond of a desirable hydrocarbon and could be regenerated to the appropriate oxidized metal fluoride with oxygen and HF. This process, when successfully implemented, will eliminate H_2O as the only by-product. In this chapter, we review on our research efforts to achieve oxyfluorination of a C–H bond to C–F bond using HF recyclable inorganic metal fluorides (e.g. CuF_2, AgF) to form many industrially important aliphatic and aromatic hydrofluorocarbons used in the manufacture of refrigerants, etching agents, industrial polymers, pharmaceuticals and agrochemicals.

*Corresponding author.;
E-mail: subramanian@usa.dupont.com

FLUORINE AND THE ENVIRONMENT, VOLUME 2
ISSN 1872-0358 DOI: 10.1016/S1872-0358(06)02006-9

1. INTRODUCTION

Green chemistry is defined as ''The utilization of a set of principles that reduces or eliminates the use or generation of hazardous substances in the design, manufacture and application of chemical products'' [1]. The tools of green chemistry are alternative feedstocks, solvents and reagents and zero-waste stoichiometric processes. Future environmentally benign chemical technologies should focus on the redesign, at the atomic and molecular level, of manufacturing processes with the aim of reducing or eliminating the generation of hazardous wastes. In this regard, one area receiving much attention in recent years is the industrial scale production of fluorinated aliphatic and aromatic hydrocarbons as they broadly fulfill many important societal needs such as health care, agricultural production, climate control and food storage, to name a few. In this chapter, we will review some of the current fluoroorganics manufacturing technologies, the environmental issues associated with their process chemistries, and emerging greener routes for achieving the ultimate goal of zero-waste processes.

1.1. Fluoroaliphatics

The first commercial catalytic system, $SbCl_5$, for the production of aliphatic chlorofluorocarbons (CFCs) was based on the pioneering work of Swartz [2] during the 1890s. DuPont developed and commercialized CFCs during the 1930s. Since then, these marvelously stable, nontoxic and nonflammable compounds have found their way into many aspects of modern lifestyle [3]. Refrigeration, air conditioning, energy-conserving foams, cleaning of electronic circuit boards and firefighting are just a few of the applications of CFCs. A landmark paper [4] published by Molina and Rowland in 1974 showed that CFCs are probably responsible for the destruction of ozone layer through chlorine atom catalyzed reaction cycle in the stratosphere [4]. During the 1980s, the incredible stability of CFCs was scientifically linked to the depletion of the earth's ozone layer by the NASA Ozone Trends Panel. The Montreal Protocol, an international United Nations agreement, signed by many nations of the world in 1987, called for the phase out of CFCs [3]. This created a major challenge for industrial catalytic scientists and engineers to identify, develop and commercialize an entirely new family of products that were environmentally safer yet still satisfied the needs of society.

The CFC replacements need to be nontoxic, nonflammable and have significantly lower, or zero ozone depletion potentials. Many organic- and aqueous-based systems, that do not contain chlorine or fluorine, have been developed for some applications while others use hydrochlorofluorocarbons (HCFCs) and hydrofluorocarbons (HFCs). Unlike hydrocarbon catalysis, the presence of hydrogen, chlorine and fluorine in the same molecule creates a very large number of

Table 1. Some important HFC substitutes for CFCs

Market	Phased out CFC	CFC alternative
Refrigerants	CFC-12 (CF_2Cl_2)	HFC-134a (CF_3CFH_2) HCFC-22 (CHF_2Cl) HFC-32 (CH_2F_2) HFC-125 (CF_3CF_2H) HCFC-124 (CF_3CHFCl) HFC-152a (CH_3CHF_2) (Blends)
Blowing agents	CFC-11 ($CFCl_3$)	HCFC-141b (CH_3CFCl_2) HCFC-123 (CF_3CHCl_2) HCFC-22 (CHF_2Cl) (Blends)
Cleaning agents	CFC-113 ($CF_2ClCFCl_2$)	Blends/azeotropes Hydrocarbons

isomeric possibilities. As a result of many years of careful study, the early list of >800 potential candidates has been narrowed down to less than a dozen viable molecules and their blends and azeotropes [5]. Many of these are now being commercially manufactured by DuPont and other chemical companies (Table 1).

1.2. Fluoroaromatics

Fluorinated aromatics are widely used in the synthesis of pharmaceuticals and agrochemicals with a volume exceeding 5000 tons per year. The efficacy of pharmaceuticals and agrochemicals can be improved by the incorporation of fluorine in the structure. Figure 1 shows the chemical structure of Sustiva®, an AIDS drug and Nustar®, a fungicide based on fluoroaromatics, developed by DuPont. The reagents used as starting material for the industrial scale manufacture of many fungicides and drugs are fluorinated derivatives of benzenes. The manufacturing steps of many complex fluoroaromatics still involve classical fluorination chemistries [6,7] that generate wastes and need to be addressed.

2. ALIPHATIC FLUORINATION

2.1. Current catalytic routes to HCFCs and HFCs

In this section, we briefly summarize current synthetic methods to CFC alternatives. More comprehensive reviews with many examples have been published

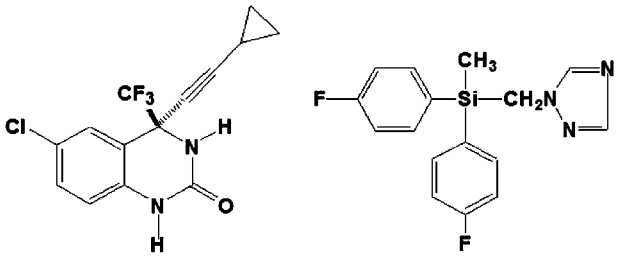

Fig. 1. Structures showing fluoroaromatic molecules used in pharmaceutical and agriculture applications.

elsewhere [8–10]. Current technology for the manufacture of HCFCs and HFCs involves stepwise formation of a C–Cl bond from a C–H bond followed by halogen exchange with HF to give a C–F bond. This can be done in one step using vapor phase chlorofluorination catalysis or in multiple steps involving separate chlorination followed by fluorine exchange. Once the desired starting material is selected, the carbon–fluorine bonds can be increased or rearranged by a variety of transformations through heterogeneous catalysis. Some of the reaction mechanisms used are addition of HF across the double bond, halogen exchange, isomerization, disproportionation, conproportionation, hydrodehalogenations, dehydrohalogenation and coupling reactions [8–10]. When an olefin or chloro-olefin is the starting material, the initial step is HF addition to the double bond. In many cases this is followed by halogen exchange to make highly fluorinated analogues.

2.2. HCl waste issue

Although highly desirable, direct and selective conversion of a C–H bond to a C–F bond using HF (with elimination of H_2) is not feasible due to the thermodynamic considerations based on relative bonds strengths [11] of H–F (565 kJ mol^{-1}) and C–H (411 kJ mol^{-1}) in the reactant side, C–F (485 kJ mol^{-1}) and H–H (432 kJ mol^{-1}) in the hypothetical product side. Hence, fluorocarbon catalysis is still largely dominated by halogen exchange reactions involving initial formation of a C–Cl bond and halogen exchange with HF [8–10]. These reactions generate very large quantities of HCl as a by-product, which is under severe environmental scrutiny and needs to be disposed of after neutralizing with alkali or else recycled. For every mole of C–F bond produced from C–H bond, two moles of HCl are generated (equations (1) and (2)).

$$C-H + Cl_2 \rightarrow C-Cl + HCl \quad (1)$$

$$C-Cl + HF \rightarrow C-F + HCl \quad (2)$$

For example, the production of CF_3–CFH_2 (134a) from ethylene eliminates 10 moles of HCl for every mole of CF_3–CFH_2 (134a) as shown below.

$$CH_2 = CH_2 + 4Cl_2 \rightarrow CCl_2 = CCl_2 + 4HCl \quad (3a)$$

$$CCl_2 = CCl_2 + 4HF + Cl_2 \rightarrow CF_3-CFCl_2 + 4HCl \quad (3b)$$

$$CF_3-CFCl_2 + 2H_2 \rightarrow CF_3-CFH_2 + 2HCl \quad (3c)$$

$$CH_2 = CH_2 + 5Cl_2 + 4HF + 2H_2 \rightarrow CF_3-CFH_2 + 10HCl\ (\text{Net}) \quad (3d)$$

Because the supply exceeds demand, the HCl generated often cannot be sold or reused even after purification. Although electrochemical fluorinations have been practiced commercially for many years, the main products of the reactions are typically perfluorocarbons since C–H bonds rarely survive. New methods, which avoid the need to feed chlorine and disposal of HCl are needed to prepare HCFCs and HFCs are obviously desirable.

2.3. Oxy(chloro)fluorination and oxyfluorination

Although the direct synthesis of C–F bonds from C–H bonds using HF is thermodynamically unfavorable, C–F bond formation can take place in the absence of chlorine under oxidative conditions. This can be achieved by the presence of oxygen in the reactants and subsequent formation of water providing a thermodynamic driving force for the oxy(chloro)fluorination (equation (4)) or oxyfluorination (equation (5)) reactions to proceed. In equation (4), HCl is believed to be oxidized *in situ* to Cl_2, which is then followed by chlorination and HF exchange. Handling of Cl_2 is eliminated and the HCl disposal is significantly reduced. It has been shown that methane can be converted into CCl_2F_2 using oxy(chloro)fluorination with conversion and selectivity greater than 90% [12].

$$2C-H + 2HCl + 2HF + O_2 \rightarrow 2C-F + 2H_2O + 2HCl \quad (4)$$

$$2C-H + O_2 + 2HF \rightarrow 2C-F + 2H_2O \quad (5)$$

The successful implementation of oxyfluorination technology (equation (5)) could have significant environmental and economic impacts as this reaction scheme eliminates handling of Cl_2 and HCl disposal and produces H_2O as the only by-product. Earlier work at DuPont [13] on the reaction of HF/toluene/PbO_2 to $F_2CHC_6H_5$ and $FCH_2C_6H_5$ is further evidence that metal oxides and HF (or metal fluorides) are capable of fluorinating hydrocarbons. An intriguing reaction was reported many years ago [14] involving the oxidative fluorination of ethylene to vinyl fluoride using Pd–Cu catalysts. Yet, there are only very few reported examples which make C–F bonds directly from hydrocarbons without going through a chlorinated intermediate.

2.4. Oxyfluorination of aliphatics through inorganic fluorides

An environmentally ''greener'' process for the synthesis of HFCs can be envisioned through an intermediate inorganic metal fluoride that is capable of fluorinating a C–H bond of a desirable hydrocarbon and could be regenerated to the appropriate oxidized metal fluoride with oxygen and HF. The general synthetic approach is shown in equations (6a) and (6b) and the net reaction is shown in equation (6c).

$$C-H + M-F_x \rightarrow M-F_{x-2} + C-F + HF \text{ (Fluorine carrier reaction)} \quad (6a)$$

$$M-F_{x-2} + 2HF + 1/2O_2 \rightarrow M-F_x + H_2O \text{ (Metal fluoride regeneration)} \quad (6b)$$

$$2C-H + 2HF + O_2 \rightarrow 2C-F + 2H_2O \text{ (Net)} \quad (6c)$$

Key to the economic success of the above process is finding a metal fluoride that is capable of oxidizing a C–H bond to C–F bond and could be regenerated to the appropriate oxidized metal fluoride with oxygen and HF. A survey of oxidation–reduction potentials of some of the selected metals is shown in Table 2. The metal fluorides with $E > 1$ are strong oxidizing agents and can only be regenerated with elemental fluorine (e.g. CoF_3, AgF_2). This process is not economically viable because of high cost of elemental fluorine. Those metal fluorides with $E < 0$ are easy to prepare from HF and O_2, but are not strong enough to oxidize a C–H bond (e.g. ZnF_2, CoF_2). The most attractive candidates are the ones with reduction potential in the range $1 < E > 0$. Copper(II) fluoride and silver(I) fluorides provide an excellent platform for this chemistry [15].

Reactions of methane and ethane with HF recyclable metal fluorides to give fluorocarbons have been reported briefly in the patent and journal literature [16–18]. Reaction of methane with hydrogen fluoride in the presence of oxygen and the salt or oxide of a variable valency metal as catalyst yielded small amounts of fluoromethane and difluoromethane at temperatures above 500°C. Olsen *et al.* [17] reacted copper(II) fluoride with methane at high temperatures (>600°C) and found products that always included copper metal, hydrogen fluoride, fluoromethane and carbon. Although activity was first detected around

Table 2. Oxidation–reduction potential for metals in various oxidation states

$E^0 > 1$	$1 > E^0 > 0$	$E^0 < 1$
$Co^{3+} + e^- \Leftrightarrow Co^{2+}$	$Cu^{2+} + 2e^- \Leftrightarrow Cu^0$	$Zn^{2+} + 2e^- \Leftrightarrow Zn^0$
$Ag^{2+} + e^- \Leftrightarrow Ag^{1+}$	$Ag^{1+} + e^- \Leftrightarrow Ag^0$	$Mg^{2+} + 2e^- \Leftrightarrow Mg^0$
$Pb^{4+} + 2e^- \Leftrightarrow Pb^{2+}$	$Te^4 + 4e^- \Leftrightarrow Te^0$	$Al^{3+} + 3e^- \Leftrightarrow Al^0$
$Ce^{4+} + e^- \Leftrightarrow Ce^{2+}$	$Hg^{2+} + 2e^- \Leftrightarrow Hg^0$	$Co^{2+} + 2e^- \Leftrightarrow Co^0$

Note: E^0, reduction potential = 0.0 for $2H^+ + 2e^- \Leftrightarrow H_2$.

600°C, appreciable yields of products were not produced until 750°C. Reaction of ethylene with pure CuF_2 or CuF_2 dissolved in a eutectic melt of alkali and alkaline earth fluorides between 450°C and 700°C yielded vinyl fluoride and HF and Cu metal. A similar reaction with propylene at 400°C yielded 2-fluoropropene [19]. The reaction cycle is shown in equations (7a) and (7b) and the net reaction scheme is shown in equation (7c).

$$C{-}H + CuF_2 \rightarrow C{-}F + HF + Cu \tag{7a}$$

$$Cu + O_2 + 2HF \rightarrow CuF_2 + 2H_2O \tag{7b}$$

$$2C{-}H + O_2 + 2HF \rightarrow 2C{-}F + 2H_2O \text{ (Net)} \tag{7c}$$

Copper metal powder formed is oxidized at 400°C by air and reacted with hydrogen fluoride at 350°C to regenerate CuF_2. This can be achieved either sequentially or in one step. It has been shown that regenerated CuF_2 reacted with hydrocarbons with identical yields of the HFCs demonstrating that the reaction cycle may be carried out without loss of activity [18]. The above observation is a proof of concept for oxyfluorination reaction using HF recyclable inorganic fluorides. Although the CuF_2-based reactions yielded HFCs with good selectivity, the yields are very low (2–5%) at moderate temperatures ($\leqslant$600°C) making it difficult to implement in commercial production.

Recent work at DuPont [19] has shown that when ethylene gas is reacted with AgF at 260 °C, selective formation of vinyl fluoride ($CH_2 = CHF$) is formed. During the course of the reaction AgF is simultaneously converted into an interesting solid silver cluster compound with a molecular formula, $Ag_{10}F_8C_2$ and Ag metal. The crystal structure of $Ag_{10}F_8C_2$ (along *ac* plane) is shown in Fig. 2. The compound crystallizes in a tetragonal structure with $a = 7.474(1)$ and $c = 10.348(1)$ Å (space group P4/*n*) [19–21]. In this structure, Ag_9 atoms form corners of a cage with short Ag–Ag distances and the 10th Ag atom is located outside the cage forming a ‘chandelier-like’ arrangement. A single chandelier unit with bridging fluorine atoms is also shown in Fig. 2. The C_2 groups are located inside the Ag_9 cages with a C–C distance close to 1.22 Å [19–21] indicating a carbon–carbon triple bond. Neutron and synchrotron X-ray diffraction crystal structure refinements pointed out that there is a large degree of dynamic and static disorder in carbon and fluorine sites at room temperature. Variable temperature ^{13}C and ^{19}F magic-angle spinning NMR showed evidence for crystallographic phase transition in the range 240–260 K and above, the transition C_2 units undergo rapid re-orientational motion and F^- ions migrate from site to site in an ion-diffusion process. The above results indicate that $Ag_{10}F_8C_2$ is a metastable phase.

$Ag_{10}F_8C_2$ compound is stable in air at room temperature. Remarkably, this phase is decomposed at 350°C in N_2 yielding stoichiometric amounts of CF_3–CF_3 (FC-116), AgF and Ag. Alternatively, further reaction of $Ag_{10}F_8C_2$ with ethylene at

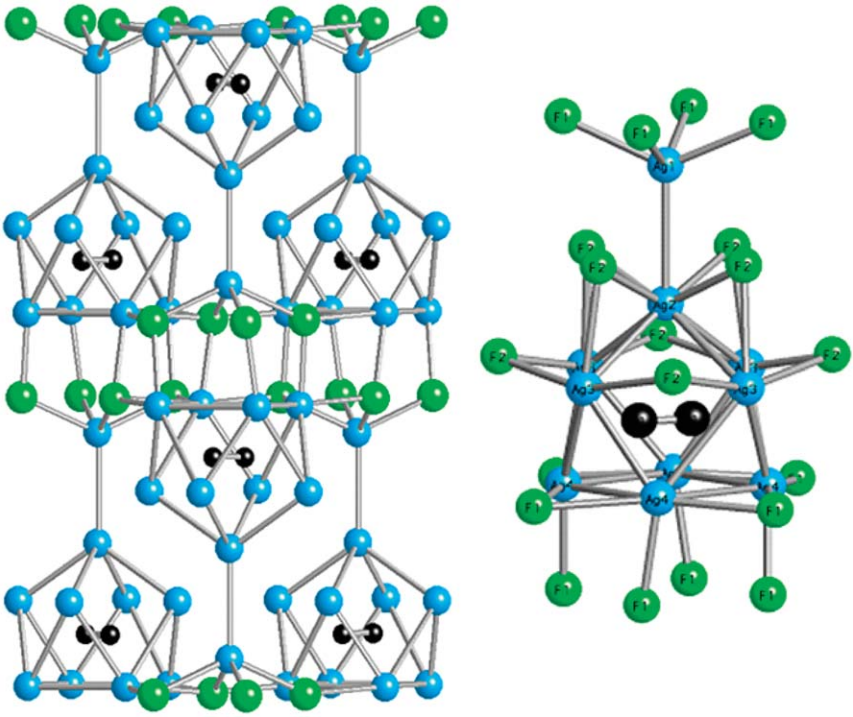

Fig. 2. Crystal structure of $Ag_{10}F_8C_2$. The Ag atoms are shown in blue, fluorine atoms are in green and carbon atoms are in black.

330°C produced commercially important HFCs: $CH_2F–CF_3$ (HFC-134a), $CHF_2–CF_3$ (HFC-125), $CF_3–CF_3$ (FC-116), and $CH_2 = CF_2$ (HFC-1132a) [19]. This shows that the $Ag_{10}F_8C_2$ is a better fluorinating agent than the starting AgF. The AgF–ethylene reaction cycle is shown in Fig. 3. The solid leftover in the reactor after the completion of the reaction cycle is Ag metal and the conversion is stoichiometric. The reaction cycle could be repeated without loss of activity during the regeneration step.

3. AROMATIC FLUORINATION

Aromatic fluorination chemistry has a remarkably long history, and the first successful synthesis of aryl C–F bonds was reported in 1870 [22]. Significant developments in the area in the early part of the 20th century included the discovery of Balz–Schiemann reaction [23,24] involving diazotization of an aromatic amine in the presence of tetrafluoroboric acid and the reaction scheme is shown in Fig. 4. The above reaction produces large quantities of waste (such as $NaBF_4$,

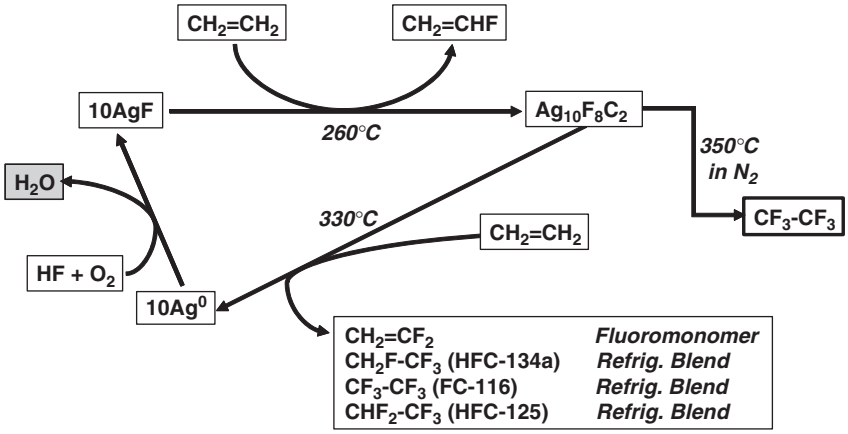

Fig. 3. AgF–ethylene reaction scheme showing the conditions of reactions and the HFCs isolated. The by-product of the reaction cycle is H_2O.

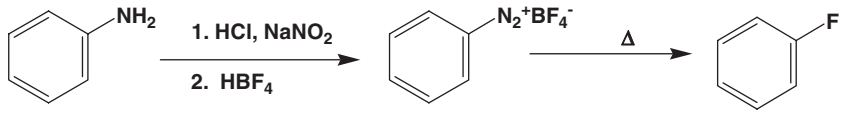

Fig. 4. Balz–Schiemann aromatic fluorination reaction.

NaCl) and is typical of the poor atom economy associated with fine chemical manufacturing. Recent industrial advances [25] use HF in place of the fluoroboric acid, however, stoichiometric amounts of NaF and NH_4F salts are produced as waste with the fluorobenzene. Other approaches using HF exchange of chlorobenzene also generate HCl as a waste [7].

3.1. Aromatic oxyfluorination using HF recyclable inorganic fluorides

Recently, Subramanian [15,26] has shown that vapor-phase reaction of benzene over CuF_2 formed fluorobenzene selectively with conversion efficiencies as high as 35% for a single pass. This can be achieved at relatively low temperatures when compared with fluorination of aliphatics with CuF_2 as discussed earlier. The reaction scheme is shown in Fig. 5. In a typical experiment, an Inconel reactor is charged with 25 g of copper oxide, heated to 400°C in a flow of HF to generate the CuF_2. After 3 h, a stream of vaporized benzene with N_2 as carrier gas is passed over the catalyst. On-line GC mass spectrometer is used to follow the course of the reaction. We find the reaction to be very specific (selectivity to fluorobenzene is $>95\%$) and the conversion is temperature dependent. At 400°C, the conversion rate is 10% and rising to 35% at 550°C. X-ray diffraction analysis (Fig. 6) of CuF_2

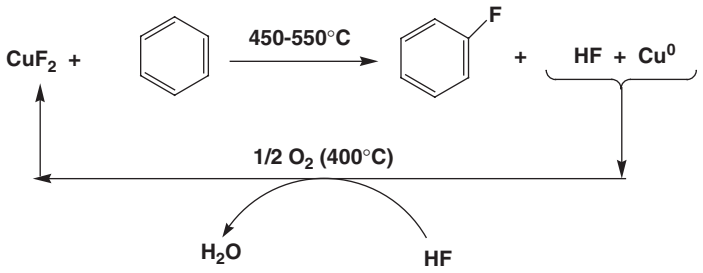

Fig. 5. CuF_2–benzene reaction cycle to form fluorobenzene. The by-product of the reaction is H_2O.

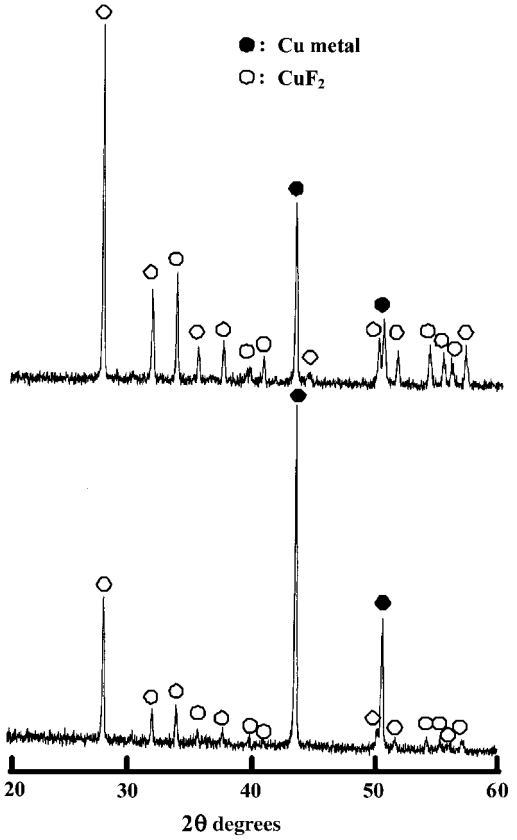

Fig. 6. Powder X-ray diffraction plots for CuF_2 after reaction with benzene: 5 min (top) and 15 min (bottom) at 500°C.

after exposing to benzene vapor for 5 and 15 min at 550°C showed the progressive formation of copper metal during the reaction, and the reaction is stoichiometric. When the conversion begins to fall, the benzene feed is switched off and an HF/O_2

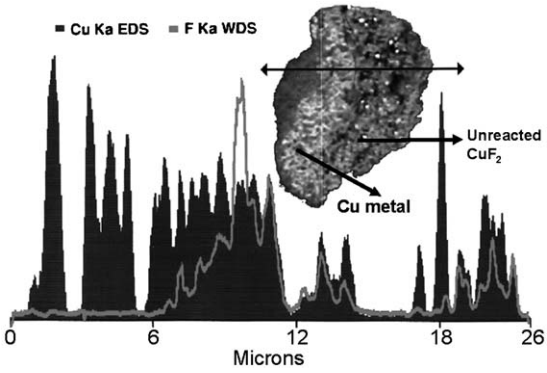

Fig. 7. X-ray chemical analysis scan for CuF_2 particle exposed to benzene at 550°C showing fluorine depletion on the surface (grey line).

stream is passed over the catalyst for 3 h at 400°C to regenerate CuF_2. The reaction cycle can be repeated without a loss of activity during the fluorination step.

X-ray profile chemical analysis scan across a particle of CuF_2 (~25 μm) exposed to benzene vapor for 15 min at 550°C is shown in Fig. 7. The inset shows the cross-section SEM image of the same particle. As the reaction progressed, the particle gets covered with copper metal and the eventual drop in the reaction rate is due to the inaccessibility of inner core CuF_2 for the reaction. This showed that the fluorobenzene conversion not only depends on the temperature, but also on the surface area of the CuF_2. We have found that AlF_3 is an excellent support for CuF_2, since it is stable to HF and not oxidized with air to the oxide. Depending on the surface area of the AlF_3, it is possible to disperse the CuF_2 and gain higher conversions. Reaction of AgF with benzene yielded stoichiometric amounts of fluorobenzene at 300°C and mixture of mono- and di-fluorobenzene at 350–400°C.

4. CONCLUSIONS

Heterogeneous catalysis has played a key role in the synthesis of CFC alternatives. However, for the process to be environmentally safer, the HCl must be recycled or disposed of safely. The ''greener'' processes discussed in this chapter, although intriguing, are still in the conceptual state and need to be optimized for large-scale production. Although HFCs do not destroy stratospheric ozone, there are growing concerns about their widespread usage as they are powerful greenhouse gases. For instance, HFC-134a is 1300 times more harmful than CO_2, according to the International Panel on Climate Change. In addition to safer processes for HFC production, much work is in progress in industrial and government laboratories to develop environmentally safer, ''third generation'' CFC alternatives.

Note of the Editor: see also in this series the chapter by A. Sekiya *et al*. devoted to CFCs and HCFCs substitutes [27].

ACKNOWLEDGMENTS

We thank L.E. Manzer, V.N.M. Rao, A.E. Feiring and B.E. Smart for many helpful discussions during the course of this work. We also thank A.J. Vega and R.L. Harlow for NMR and X-ray diffraction studies of $Ag_{10}F_8C_2$, respectively.

REFERENCES

[1] P.T. Anastas, J. Warner, Green Chemistry Theory and Practice, Oxford University Press, Oxford, 1998.
[2] F. Swartz, Bul. Acad. R. Belg. 24 (1892) 309; 35 (1898) 301.
[3] M. Molina, R.S. Rowland, Nature 249 (1974) 810.
[4] L.E. Manzer, Science 249 (1990) 31.
[5] M.O. McLinden, D.A. Didion, Quest for alternatives–a molecular approach; inevitable in seeking refrigerants, ASHRAE J. (1987) December 3.
[6] R.E.Banks, B.E.Smart, J.C.Tatlow (Eds.), Organofluorine Chemistry: Principles and Commercial Applications, Plenum, New York, 1994.
[7] J.H. Clark, D. Wails, T.W. Bastock, Aromatic Fluorination, CRC Press, Boca Raton, FL, 1996.
[8] V.N.M. Rao, L.E. Manzer, Adv. Catal. 39 (1993) 329.
[9] Z. Ainbinder, L.E. Manzer, M.J. Nappa, Catalytic routes to hydro (chloro) fluorocarbons, Environ. Catal. (1999) 197–212.
[10] L.E. Manzer, M.J. Nappa, Appl. Catal. 221 (2001) 267.
[11] J.E. Huheey, Inorganic Chemistry: Principles of Structure and Reactivity, 3rd edition, Harper & Row, New York, 1983.
[12] W.J.M. Pieters, E.J. Carlson, Patent US 4,039,596, 1977.
[13] A.E. Feiring, Patent US 4,051,168, 1977.
[14] T. Kuroda, Y. Takamitsu, Patent JP 52-122,310, 1977.
[15] M.A. Subramanian, L.E. Manzer, Science 297 (2002) 1665.
[16] G.M. Whitman, Patent US 2,578,913, 1951.
[17] D.H. Olsen, Patent US 3,398,203, 1968.
[18] J.H. Moss, R. Ottie, J.B. Wilford, J. Fluorine Chem. 6 (1975) 393.
[19] M.A. Subramanian, Patent 6,096,932, 2000.
[20] M.A. Subramanian, R.L. Harlow, A. Vega, unpublished results.
[21] G.C. Guo, G. Zhou, Q. Wang, T.C.W. Mak, Angew. Chem. 37 (1998) 630.
[22] R. Schmitt, H. Von Gehren, J. Prakt. Chem. 1 (1870) 394.
[23] G. Balz, G. Schiemann, Chem. Ber. 60 (1927) 1186.
[24] C.D. Hewitt, M.J. Silvester, Aldrichim. Acta 21 (1988) 3.
[25] M. Krackov, Patent EP 330420, 1988.
[26] M.A. Subramanian, Patent US 6,166,273, 2000.
[27] A. Sekiya, M. Yamabe, K. Tokuhashi, Y. Hibino, R. Imasu, H. Okamoto, Evaluation and Selection of CFC Alternatives, in: A. Tressaud, (Ed.), Advances in Fluorine Science, Vol. 1, Elsevier, 2006, pp. 33–88.

CHAPTER 7

Fluorine Analysis by Ion Beam Techniques for Dating Applications

M. Döbeli,[1,*] A.A.-M. Gaschen,[2] and U. Krähenbühl[2]

[1]*Paul Scherrer Institute, c/o ETH Zurich, HPK H32, CH-8093 Zurich, Switzerland*
[2]*Laboratory for Radio- and Environmental Chemistry, University of Berne, Freiestrasse 3, 3012 Berne, Switzerland*

Contents

*Corresponding author. Tel.: +41-44-633-2045; Fax: +41-44-633-1067;

FLUORINE AND THE ENVIRONMENT, VOLUME 2
ISSN 1872-0358 DOI: 10.1016/S1872-0358(06)02007-0

Abstract

Megaelectron volt (MeV) ion beam techniques offer a number of non-destructive analysis methods that allow to measure depth profiles of elemental concentrations in material surfaces. Elements are identified by elastic scattering, by specific nuclear reaction products or by emission of characteristic X-rays. With nuclear microprobes raster images of the material composition at the surface can be obtained. Particle-induced gamma-ray emission (PIGE) is especially suited for fluorine detection down to the ppm concentration level.

The technical aspects of fluorine detection by nuclear reactions as well as its applications to fluorine analysis in geological and archaeological objects are reviewed. Special attention is given to the determination of exposure ages of meteorites on the Antarctic ice shield and burial durations of archaeological bones and teeth. This information can be acquired by evaluation of the shape and penetration depth of the diffusion profile of fluorine that was incorporated by the sample from the environment. For a quantitative assessment of the data, several factors like ambient conditions and diagenetic state of the material have to be taken into account.

1. INTRODUCTION

Many investigations about fluorine uptake are reported in literature. The goal of these examinations is to unravel the exposure duration of different materials to various environmental conditions. Here, the application of ion beam analysis in studies on terrestrial contamination of meteorites from Antarctica and diffusion profiles in bones from archaeological burial sites is presented.

Fluorine detection by nuclear methods is a well-established experimental technique. More than 200 publications on the subject can be found in the literature. In the 1960s, it was recognized that the thorough and precise knowledge on nuclear scattering and reactions offered a very valuable means for accurate elemental analysis of materials. The main reason for the high accuracy of ion beam techniques is the fact that the interaction of projectile and target particle takes place at an energy range far above electronic binding energies and can be treated as the encounter of two ‘‘naked’’ nuclei. Thus, no corrections for the atomic or molecular electronic structure have to be taken into account and virtually no ‘‘matrix effect’’ exists. In addition, the techniques are virtually non-destructive and straightforward to perform. By these reasons, the field of Megaelectron volt (MeV) ion beam physics evolved fast and found many applications for the compositional and structural characterization of surfaces. It also made its way into research areas such as geology, mineralogy, biology, medicine, environmental science and archaeology. A comprehensive handbook on all techniques used in ion beam analysis was published in 1977 [1] and 1995 [2].

Owing to a number of very suitable resonant nuclear reactions with high cross-sections and relatively unambiguous reaction products that can be used as ‘‘fingerprints’’, fluorine has become one of the popular chemical elements

investigated by ion beam analysis. For information on the development of the experimental fluorine detection techniques we may refer the reader to a comprehensive review on its principles and applications by Coote in 1992 [3]. Additional technical information not compiled therein can be found in Refs [4–20]. A significant fraction of applications of fluorine analysis by ion beams lies in the fields of biology and biomedicine. Among these, by far the largest number deals with investigations of fluorine in human teeth. The remaining work was done in archaeology, geology and environmental sciences.

The idea to use fluorine trace concentrations in archaeometry is more than 150 years old [21]. Since the 1980s, the potential of fluorine depth profiling by nuclear techniques for dating purposes in archaeology and geology was subject of several investigations. The pioneering work of Coote [3,22–30] concentrated on the dating of ancient bones and teeth. The same method was then expanded to study the exposure history of flints and meteorites [16,31–40]. A review on this subject will be given in the second part of this article.

In the following, those ion beam analysis techniques that allow for fluorine detection will be presented. By far, the most important technique in this respect is nuclear reaction analysis (NRA). Although it can be rather complex to perform, it is the most often applied technique for fluorine trace element studies, due to a number of convenient and prolific resonant nuclear reactions which make it very sensitive to fluorine in most host matrices. NRA is often combined with particle-induced X-ray emission (PIXE) which allows for simultaneous determination of the sample bulk composition and concentrations of heavier trace elements. By focusing and deflecting the ion beam in a microprobe, the mentioned techniques can be used for two- or even three-dimensional multielemental imaging.

2. ANALYSIS TECHNIQUES

2.1. Nuclear reaction analysis

Long before nuclear reactions were used for materials analysis, nuclear physicists used to identify contaminants in targets and background from stray beam by the characteristic γ-emission produced in reactions with the unwanted nuclear species. During the 1960s, this process was developed into a useful analytical technique. The basic principle of identifying atomic species by their nuclear reaction products was called NRA. If reactions with resonant cross-sections are used the method is called NRRA (nuclear resonant reaction analysis). In the special case where no massive particles but emitted γ-rays are detected the method is named particle- (or proton) induced gamma-ray emission (PIGE). The acronym PIGME is sometimes used as a synonym.

2.1.1. Basics

In principle, light particles from protons to ^{4}He can be used to excite nuclear reactions in fluorine. There has been some work on NRA by ^{19}F(d,p)^{20}F, ^{19}F(d,α)^{17}O and ^{19}F(α,p)^{22}Ne (for details see Ref. [2]), but by far the most popular are the proton-induced reactions leading to γ-emission. They have the benefit that γ-detectors can be placed outside the vacuum chamber and there is no background from scattered beam particles. Reactions with charged products are only of advantage for depth profiling in energy regions exhibiting a plateau in the cross-section.

If protons of an energy up to a few MeV are used, two basically different nuclear processes lead to γ-ray emission from ^{19}F. The first is inelastic scattering of the type ^{19}F(p,p$'\gamma$)^{19}F, which produces two intense low-energy γ-lines at 110 and 197 keV.This radiation is detected best by a small Ge (Li) detector with a low Compton background (see Fig. 1). Yield curves for the two lines have been published by Stroobants *et al.* [41], Demortier *et al.* [42] and Grambole *et al.* [43]. The second reaction is ^{19}F(p,$\alpha\gamma$)^{16}O which has a *Q*-value of 8.114 MeV and emits a γ-ray triplet with energies of 6.129, 6.917 and 7.117 MeV. These high-energy γ-rays are easily detected by Ge, NaI or bismuth germanium oxide (BGO) detectors (see Fig. 1) and absorption in material surrounding the sample is not important (1 cm of steel absorbs only 20% of γ-rays in this energy range). The γ-yield is not strongly dependent on the angle to the incident beam [18] and detector positions between 45 and 135° have been used. Excitation curves for this reaction have been measured among others by Dababneh *et al.* (1993) [13]. Their result is displayed in Fig. 2. The excitation function exhibits a number of isolated, sharp resonances, the most important being at 340, 668, 872, 935 and 1371 keV. The 872 keV resonance has the highest cross-section of 661 mb. It is followed by the 1371 keV (300 mb), 935 keV (180 mb) and 340 keV (102 mb) peaks. The strongest resonance at 872 keV has a width of 4.5 keV [2].

Owing to the high reaction cross-section, the intensive and sharp resonances, and the relatively background-free high-energy γ-lines the ^{19}F(p,$\alpha\gamma$)^{16}O reaction has become the standard process used for fluorine NRA.

2.1.2. Thick target yields

When a bulk material is probed by a proton beam with an initial energy E_0, the protons are slowed down by the stopping force and thus pass along the excitation

Fig. 1. (Top): γ-Ray energy spectrum of the reaction ^{19}F(p,$\alpha\gamma$)^{16}O measured by a 3-inch NaI detector. Proton energy is 2.7 MeV, sample material is fluorapatite. (Middle): γ-Ray energy spectrum for the same reaction acquired by a high purity germanium detector. The sample is meteoritic material. Low energy lines from several other nuclear reactions can be identified. (Bottom): Low-energy γ-ray spectrum from ^{19}F(p,p$'\gamma$)^{19}F inelastic scattering recorded with a thin Ge(Li) detector. Reproduced with permission from Grambole and Noll [59].

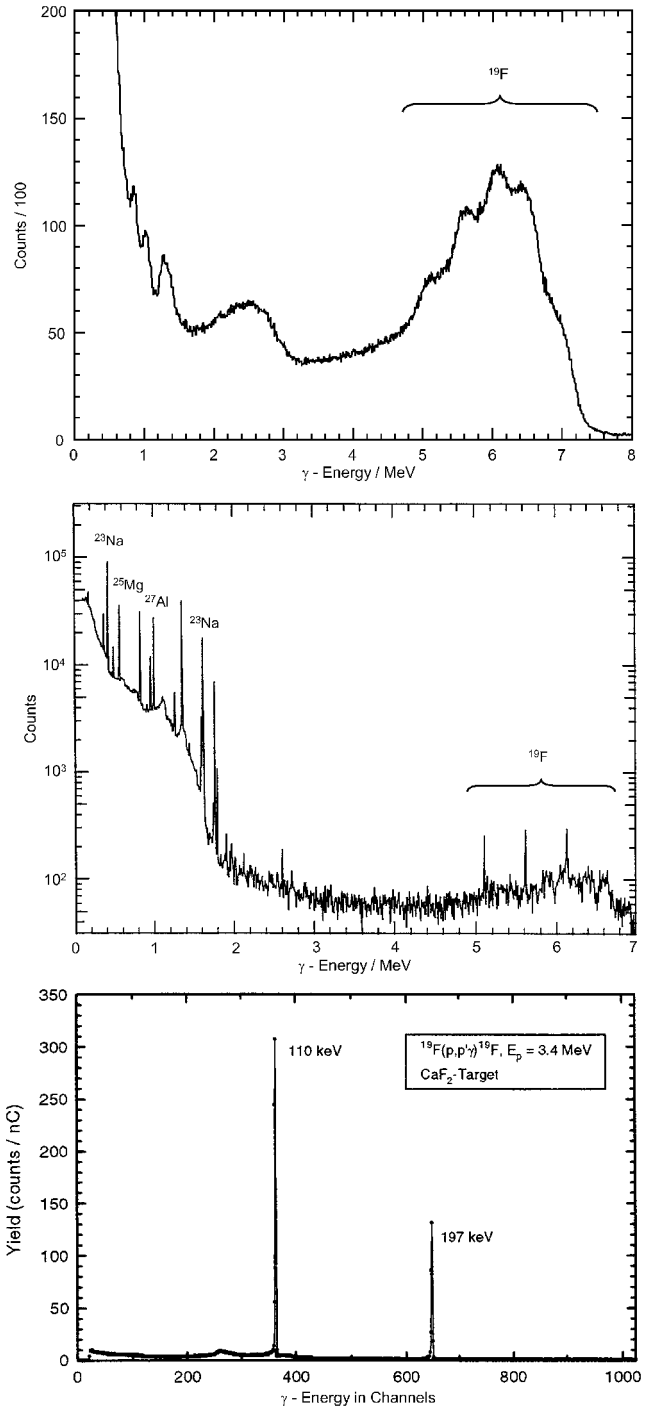
19F
Counts / 100
γ - Energy / MeV
23Na
25Mg
27Al
23Na
19F
Counts
γ - Energy / MeV
110 keV
197 keV
19F(p,p'γ)19F, Ep = 3.4 MeV
CaF2-Target
Yield (counts / nC)
γ - Energy in Channels

function from E_0 to zero energy. For a homogeneous atomic fluorine concentration C, the number N_γ of detected γ-rays per incident proton is

$$N_\gamma = AC \int_0^{E_0} \frac{\sigma(E)}{S(E)} \mathrm{d}E \tag{1}$$

where the constant A takes care of the solid angle and efficiency of the detector, $\sigma(E)$ is the reaction cross-section and $S(E)$ is the stopping power of the material in units of energy per atom per unit area. In principle, N_γ can be calculated if A, $\sigma(E)$ and $S(E)$ are given. In practice, this is not advisable since A and σ are often not known to the necessary precision. Therefore, standards are used for calibration of the yield. For a standard sample with a fluorine concentration C_{St} the number of detected γ-rays per incident proton is

$$N_{\gamma,\mathrm{St}} = AC_{\mathrm{St}} \int_0^{E_0} \frac{\sigma(E)}{S_{\mathrm{St}}(E)} \mathrm{d}E \tag{2}$$

where $S_{\mathrm{St}}(E)$ is the stopping power of the standard material. The $S(E)$ curves are very similar in shape for all materials [44] and can be scaled by a proper energy normalization. Therefore, the integral in Equations (1) and (2) can be replaced by the ratio of an average cross-section $\bar{\sigma}$ and a representative stopping power value $\bar{S}$ in most cases without loosing significant accuracy.

$$N_\gamma = AC\frac{\bar{\sigma}}{\bar{S}} \quad \text{and} \quad N_{\gamma,\mathrm{St}} = AC_{\mathrm{St}}\frac{\bar{\sigma}}{\bar{S}_{\mathrm{St}}} \tag{3}$$

From this, the fluorine concentration C of a measured sample can be obtained as

$$C = C_{\mathrm{St}} \frac{N_\gamma}{N_{\gamma,\mathrm{St}}} \frac{\bar{S}}{\bar{S}_{\mathrm{St}}} \frac{Q_{\mathrm{St}}}{Q} \tag{4}$$

Here, Q and Q_{St} are the integrated beam currents to which the sample and the standard material have been exposed. The best choice for $\bar{S}$ has been investigated in detail by Kenny *et al.* [8]. However, good results will be obtained by taking the stopping power at the centroid of the excitation function since most of the systematic errors will cancel out to a large extent with the division of $\bar{S}$ by $\bar{S}_{St}$. If a single resonance is used, S has of course to be evaluated at the resonance energy. The stopping power curves provided by the semiempirical model of Ziegler *et al.* [44] are presently widely accepted. Their estimated accuracy for protons in the low MeV energy range is below 5%.

2.1.3. Depth profiling

In case of a non-constant fluorine concentration with depth, two different profiling methods can be applied depending on the investigated depth range. For deep profiles of tens of microns to millimetres, the sample can be cross-sectioned and

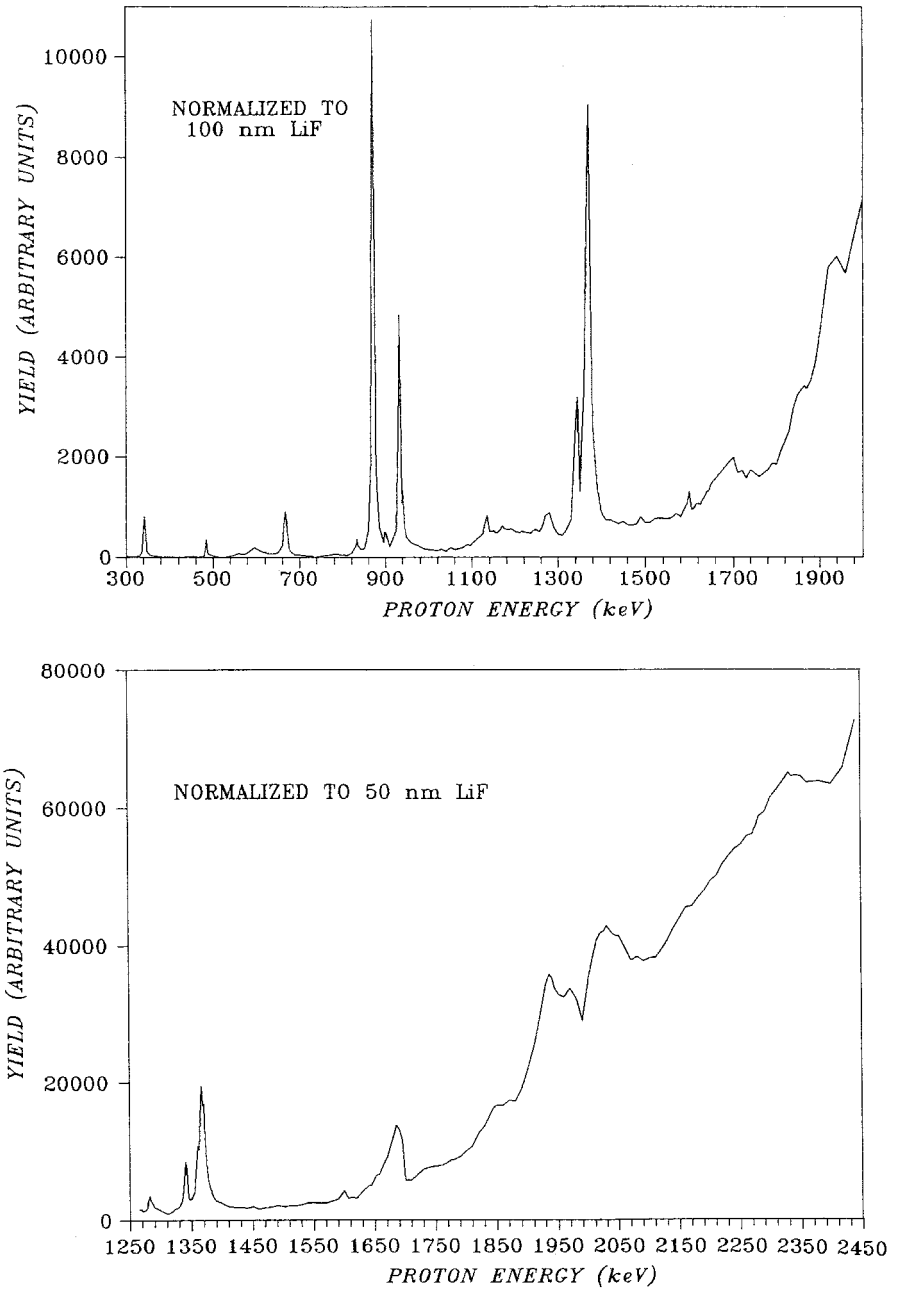

Fig. 2. Overview of the $^{19}F(p,\alpha\gamma)^{16}O$ excitation curve from $E = 0.3$–2.45 MeV, including the narrow resonances (left) and the beginning of the continuum (right). Reproduced with permission from Dababneh *et al.* [13].

scanned by a focused beam. The depth resolution in this case is given by the width of the beam spot. For shallow profiles, one of the sharp resonances can be used to probe the sample at a well-defined depth. This technique had first been published by Möller and Starfelt in 1967 [45]. The situation is depicted in Fig. 3. The particle beam is entering the sample with an initial energy E_0 which is usually above a resonant energy E_R. As the projectiles continuously lose energy on their way through the material the probability for a reaction with fluorine follows the excitation function from E_0 to zero energy. At a depth d_R below the surface, the particles reach the resonant energy E_R and the reaction will take place in a certain depth interval until their energy falls below the resonant energy again. If there are further resonances at lower energies E_R, the process will repeat itself. In an idealized situation with a single isolated resonance, the beam would probe the fluorine concentration only at a well-defined depth d_R given by

$$d_R = -\int_{E_0}^{E_R} S^{-1}(E)\mathrm{d}E \tag{5}$$

In this idealized case, the profile can be obtained by varying the incident particle energy E_0 stepwise within a certain interval. Yield calibration is done by a standard in an analogous way as described in equation (4). Close to the surface equation (5) can be simplified by the so-called surface approximation which consists in replacing $S(E)$ by $S(E_0)$, i.e. by the value of the energy loss at the surface. The expression for the depth scale is then simply $d_R(E_0) = (E_0 - E_R)/S(E_0)$.

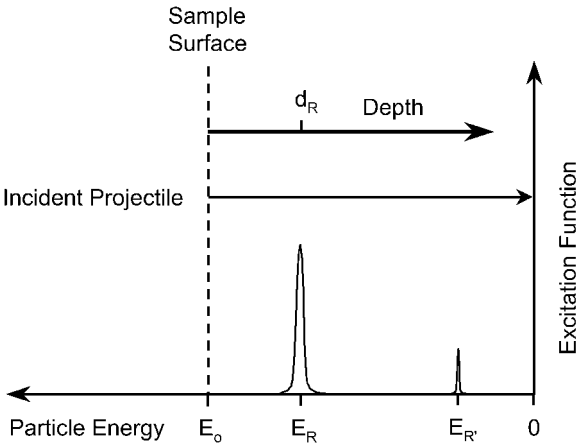

Fig. 3. Schematic illustration of nuclear resonance profiling. The sample surface is to the left. The particle energy continuously decreases from left to right as the projectiles pass through the material. The resonance energy E_R is reached at a certain depth d_R where the reaction takes place.

The variation of E_0 can be obtained either by changing the acceleration energy or, within a smaller range, by applying a high voltage to the target.

While the simplified data analysis technique described above might lead to a first estimate of the concentration profile in some cases, the situation is much more complex in reality. First of all, there are virtually no usable single resonances with the excitation function going to zero outside of the resonance peak. This means that other resonances at lower energies and off-resonance contributions have to be taken into account. Thus, the measured γ-yield at a certain beam energy is normally a complicated convolution between the fluorine concentration profile, the excitation function of the reaction and the stopping power in the material. The composition of the sample might as well be depth-dependent leading to a stopping power which is not only a function of energy but also of depth. The problem has been extensively discussed in literature and several algorithms and computer codes for profile deconvolution have been developed [16,46–51]. One important consequence of off-resonance and low energy resonance contributions is the limitation of the dynamic range of detectable fluorine concentrations within a profile, as there is always a background from reactions taking place at larger depths. In fortunate cases of flat fluorine profiles, simple subtraction of the resulting flat background leads to acceptable results.

Secondly, the situation is complicated by factors affecting the shape of the depth window probed by a particular resonance. The width and shape of the layer in which the particles are under resonance condition is not only given by the energy width of the resonance peak but is also influenced by energy loss straggling which is due to the stochastic nature of the slowing down process of ions in matter [2,44]. This effect becomes of growing importance with increasing depth. For measurements close to the surface using narrow resonances, the initial energy spread of the particle beam and Doppler broadening due to the thermal movement of atoms have to be considered as well [52]. The depth resolution function is in general non-Gaussian as the resonance peaks are better described by Lorenzians.

The depth resolution for resonance profiling at the sample surface where energy straggling can be neglected can be calculated in first order by dividing the width of the resonance by the stopping power of the material. For the $^{19}F(p,\alpha\gamma)^{16}O$ reaction this is generally a few tens of nanometres. For example, the stopping power of protons in typical bone material is around 44 keV/μm at the 872 keV resonance energy (SRIM [44]). The width of the resonance is 4.5 keV [2] which is normally larger than the Doppler broadening and the energy spread of the proton beam. This leads to a depth resolution of approximately 100 nm. If the low-energy resonance at 340 keV with a width of 2.4 keV is used, the corresponding stopping power is 78 keV/μm resulting in a depth resolution of about 30 nm close to the surface. Even with the narrowest resonances and taking advantage of glancing incidence the achievable depth resolution has a lower limit of a few nanometres.

For resonance profiling, the accessible depth is given by the distance to the next resonance peak at higher energy. For the 872 keV resonance the next strong peak appears at 935 keV (disregarding the small resonance at 902 keV). In our example of bone material this results in a maximum interference-free probing depth of approximately 1.4 μm. If the 10 times weaker resonance at 668 keV is used, the next interfering peak only appears at 832 keV, leaving an accessible depth of more than 3 μm. However, as mentioned above, energy straggling and off-resonance contributions lead to fast deterioration of the profile quality with depth. A representative example of nuclear resonance profiling is provided by Mandler *et al.* (1973) [53] who determined the fluorine concentration in tooth enamel to a depth of more than 2 microns. More details on fluorine profiling by this technique can be found in a number of publications [43,45,47,48,53–56]. Compilations of the energy, strength and width of $^{19}F(p,\alpha\gamma)^{16}O$ nuclear resonances by which the experimental parameters for profiling can be optimized have been provided, for example, by Dieumegard [57] and Dababneh [13]. A similar list is reproduced in the ion beam analysis handbook of Tesmer *et al.* [2].

2.1.4. Sensitivity

The sensitivity of PIGE to fluorine is determined in a fairly complex way by the sample composition, the specific reaction and the experimental set-up. The $^{19}F(p,\alpha\gamma)^{16}O$ low-energy resonances have total cross-sections of the order of 100 mb. Therefore, absolute count rates have to be taken into consideration for an estimate of detection limits in the case of resonance profiling. Representative examples are given for a typical set-up by Dieumegard *et al.* [57]. Following their data, count rates of about 400 counts/μC can be expected from a CaF_2 calibration target for the 340 keV resonance. Thus, for samples with a fluorine concentration lower than about 100 ppm the count rate will fall below 1/μC. Apart from off-resonance contributions and background from reactions with other elements this can become a severe restriction for trace-level detection. If thick target measurements with proton energies above 2 MeV are performed, the γ-ray yield is usually so high that counting statistics is not a sensitivity limiting factor. In Ref. [2], thick target yields are given as a function of proton energy between 1 and 4 MeV. Following these values, count rates can rise well above 10 counts/μC under typical experimental conditions for a 1 ppm concentration. Therefore, measurements in the ppm range should be possible within minutes with a reasonable statistical error. In this case, background from other reactions become dominant. In the γ-energy window between 4 and 7 MeV contributions from the abundant elements Al and Na have to be expected for low-resolution and high-efficiency detectors such as BGO or NaI [58]. This flat background can be subtracted to a certain extent by estimating the Al and Na contents in the sample by the low energy γ-lines which are also present in the spectra (see Fig. 1). This subtraction technique

was established by Bird and Clayton [58] for background contributions of Al, Na, Li, B, Cu, Fe, Zn, Mg, Si and Ta. It was applied by Noll *et al.* [38,59] for the determination of low-level fluorine traces in meteorites.

If the low-energy γ-lines at 110 and 197 keV from inelastic scattering $^{19}F(p,p'\gamma)^{19}F$ are used there exists a true interference with the same γ-energies from the $^{18}O(p,\gamma)^{19}F$ reaction with ubiquitous oxygen. This has first been investigated by Stroobants *et al.* [41] and later by Grambole *et al.* [19].

If proper care is taken a fluorine detection limit of roughly 1 ppm in thick targets can be obtained with both the $^{19}F(p,\alpha\gamma)^{16}O$ and the $^{19}F(p,p'\gamma)^{19}F$ reaction. As a general rule of thumb it can be said that 0.1% of fluorine can usually be detected without difficulties, while 1 ppm can only be reached under optimized conditions. Additional information on sensitivity can be found in literature (e.g. [1,2,41,60]). Although published data can be of help in evaluating the appropriate analytical technique, it should not be the substitute for a practical experimental test in the case of an unknown matrix.

2.1.5. Accuracy

As discussed in the previous paragraph, count rates are usually high enough to determine the number of γ-rays from a sample with a statistical error below a few percent with ease. Thus, statistical precision is normally not a severe limitation. The absolute accuracy of measured fluorine concentrations is more determined by systematic errors. The precise solid angle and efficiency of a detector and the absolute integrated beam current are difficult to measure to a satisfactory degree. In addition, the differential reaction cross-section for a particular detection angle or projectile energy might not be known well enough. Even if cross-section values are published, the precise integration over a γ-ray energy spectrum poses a severe problem as handling of escape peaks, tails and Compton part has to be decided. Therefore, continuous normalization to a standard is recommended rather than absolute yield measurements. Following Equation (4), systematic errors can be introduced by the accuracy of the standard material and by the calculation of the stopping powers. As stated above, the accuracy of stopping powers is approximately 3–5%. Depending on the integration or averaging procedure by which the correction is performed, an additional contribution to the error has to be taken into account. Often, the fluorine concentration and with it the count rate of the standard material is significantly different from that of unknown samples. In this case, either dead time and pile-up corrections have to be applied or the beam current has to be adjusted to obtain similar count rates which necessitates a careful observation of beam current integration and background events. For many applications, samples are non-conductive which requires special precautions concerning the beam current measurement. All in all, the total non-statistical error will usually amount to 5–10%. For measurements at the fluorine detection limit, accuracy is determined by the background subtraction procedure.

2.1.6. Imaging

Nuclear microprobes allow to focus and raster scan the analysing ion beam across the sample surface to obtain a line scan or a two-dimensional image of the fluorine concentration. State-of-the-art microprobes have a lateral resolution of the order of 1 μm [61,62]. At this focal size the beam current is usually below 1 nA but increases fast with increasing spot size. Thus, depending on the image resolution, one has to accept a reduced sensitivity and statistical precision. If resonance profiling is performed with a rastered beam, a true three-dimensional image of the fluorine content can be produced. However, this is often of limited use because the accessible depth for profiling is normally by far smaller than the lateral size of the raster field. Likewise, the depth resolution is much better than the lateral resolution, especially close to the surface. An increasing number of nuclear microprobes is equipped with an exit window to extract the ion beam into air [62,63]. This allows to analyse objects that are not suited for transfer into a vacuum vessel.

2.1.7. Charged particle activation

In PIGE the γ-emission is usually prompt. If very low amounts of trace elements have to be detected it can be advantageous to use a delayed decay. In this case, the technique is called charged particle activation (CPA) and is an analogue to neutron activation analysis (NAA). It has the advantage that the prompt background from interfering reactions is completely removed as irradiation and analysis are completely separated in time. This also allows to remove external contaminants in the short time between irradiation and measurement which further improves detection limits. A comprehensive description of the technique can be found in the ion beam analysis handbook [2]. For ^{19}F CPA is conceivable in special cases *via* the ^{19}F(d,dn)^{18}F reaction. However, we have found only one application in the literature [64].

2.2. Elastic scattering

For the sake of completeness, fluorine detection by elastic scattering has to be mentioned as well. Elastic scattering is experimentally the most simple and therefore the most widespread ion beam analytical technique. It relies on the fact that the energy of an MeV ion elastically scattered from a target material is a function of the target atomic mass and the depth at which the scattering took place. Both, the scattered projectile ion and the recoiling target atom, carry the information on the elemental depth distribution of the sample. The corresponding techniques are Rutherford backscattering spectrometry (RBS) and elastic recoil detection analysis (ERDA), which are well described in the literature (e.g. [2,65,66]). For fluorine analysis, ERDA is better suited than RBS and a sensitivity

of approximately 0.01–0.1% can be obtained by this method. No standards are required since scattering cross-sections are well known. A complete concentration depth profile is obtained with a single measurement of a few minutes. Maximum depth of analysis is of the order of 1 μm. Although ERDA is a very fast and quantitative analysis technique, only few applications to fluorine detection have been published [67,68]. No work for dating purposes has been done so far.

2.3. PIXE

PIXE is the analogue to EDX/WDX (energy/wave dispersive analysis of X-rays) done with electron microprobes. Elements in the sample are identified by the characteristic X-rays emitted during MeV particle bombardment. PIXE is not well suited for fluorine detection because of the low energy of the corresponding X-rays. However, it is often performed simultaneously with other ion beam techniques and gives very valuable information on the bulk composition and other trace element concentrations in the sample.

3. APPLICATIONS

The time-dependant mutual effects of several elements with silicates and bones found great attention in archaeological studies in the past. The enrichment of fluorine by adsorption on the surface of silicates and their diffusion into the interior of minerals were studied by several authors already in the first-half of the last century. Among others, flintstones, meteorites and bones or teeth were the materials investigated most often [33,69,70]. In some cases only the integral uptake of fluorine was reported. From diffusion theory and studies it is quite evident that concentration profiles are developed through time, when a material is in contact with a reservoir of different concentration of the element under investigation. Therefore, the course of the formed concentration profile contains much more information than an integral report only.

The development of the profile of interest is a function of the chemical potential (a function itself of the chemical binding forces involved and the concentrations in the investigated reservoirs). For bones it is important to understand alterations induced by environmental factors of the burial site such as pH, humidity, prolonged draught periods or temperature. Furthermore, it is possible that distinct changes of the exposure conditions occur throughout burial duration, e.g. changes of the present concentration of fluoride ions through time (e.g. changes in groundwater table). It is quite obvious that diagenetic processes may blur some basic information stored in the investigated bone specimen.

To learn more about the influence of the discussed factors modern and archaeological bones were doped with artificial fluoride solutions for different

durations and at different temperatures to evaluate realistic diffusion parameters. With this parameter at hand it seems to be easier to unravel the archaeological age of an unearthed bone specimen.

3.1. Fluorine diffusion in Antarctic meteorites

Concentration profiles of all halogens were investigated in meteorites by Langenauer and Krähenbühl [70,71]. Meteorite samples were tested for their release of halogens by leaching with water. After 5 days of contact with water less than 4% of the F enrichment on the surface could be leached whereas for Cl the respective value reached 15%. So, the diffusion profiles are best conserved for F among all the halogens. Therefore, the interest was focused to the investigation of contamination of meteorites by fluorine. The first analyses of fluorine on Antarctic meteorites were performed on powders resulting from mechanical removal of thin layers and measurement of their F concentrations. This was obtained by ion-sensitive electrodes after expelling the halogens in presence of water vapour and V_2O_5 at 1000°C forming the respective hydrogen halides which were absorbed in NaOH. By this technique, a depth resolution of 0.5 mm could be obtained at best [71]. It was therefore replaced by the NRA technique using protons, due to its superior space resolution and ease of use. The proton irradiation profile presented in Fig. 4 indicates the improved resolution compared to the earlier technique [38].

Since the contamination of fluorine on Antarctic meteorites only occurs when they are lying on the ice, the contamination level is a measure for the duration of the exposure to the Antarctic environment. Parallel to this higher contamination on the surface the diffusion into the interior is proceeding for a longer period. Therefore, the degree of contamination on the surface of the meteorite and the depth to which the diffusion can be recognized is proportional and is given by the diffusion laws. Such results are presented in Fig. 5. For a detailed discussion it is necessary to make some assumptions regarding the reservoirs from which F might have contaminated the meteorites in Antarctica. What are the sources for the concentration of F resulting in the atmosphere and are these values constant? Sea spray delivers an important fraction of the F in the atmosphere. But for a given place in Antarctica the distance to the open sea (extension of the ice shelf) may change with time. In addition, exhalations of volcanoes contribute an essential fraction of the F budget over time.[1]

The terrestrial age of meteorites is based on the measurement of long-lived radio nuclides such as ^{14}C, ^{26}Al, ^{36}Cl, ^{53}Mn and more recently of ^{41}Ca, the half-lives of which rank from 5730 years up to 3.7 million years. It is not possible with such measurements to distinguish which fraction of the terrestrial age the

[1] Note of the Editor: See also in this series the chapter of C. Oppenheimer and G. Sawyer devoted to Fluorine Emissions from Volcanoes.

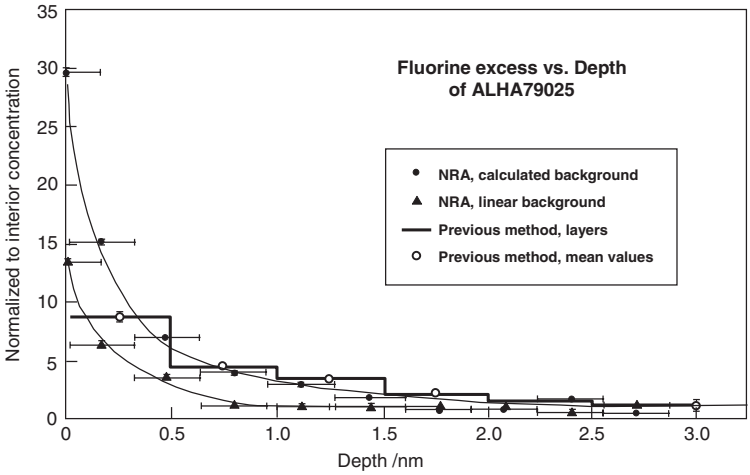

Fig. 4. Profile of the normalized F concentration for the Antarctic Meteorite ALHA79025 by NRA compared to the earlier classical analysis of thin layers (see text). Reproduced with permission from Noll *et al.* [38].

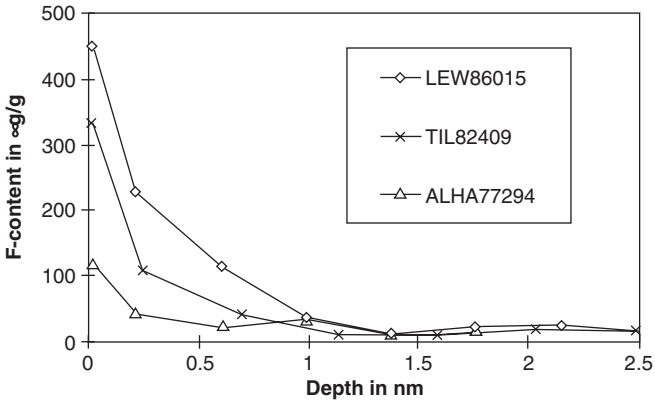

Fig. 5. Concentration profiles for three Antarctic meteorites of different exposition duration on the ice sheet (see Table 1 for details). Reproduced with permission from Noll [59].

meteorite was lying enclosed in the ice or free to the atmosphere on top of the ice. In contrast to the usual terrestrial ages Noll *et al.* [40] came up with exposure ages (duration on the ice) based on F contamination levels compared to terrestrial ages. These relations are presented in Table 1.

Obsidian and flints are natural glasses. Such samples show a uniform diffusion in any direction. In contrast, the diffusion of F into meteorites must be a function of the grain size of the material. The apparent diffusion is a mixture of volume diffusion and grain-boundary diffusion. Grain-boundary diffusion is much faster

Table 1. Comparison of terrestrial age and surface exposure for three Antarctic chondrites [110]

Sample location	Signature	Exposure duration on the ice in years	Terrestrial age in years	Class
Lewis Cliff	Lew86015	13,700	80,000 ± 50,000	H6
Thiel Mountains	Til82409	9200		H5
Allan Hills	ALHA77294	3100	10,000	H5

than volume diffusion. Therefore, meteorites, for which almost no grains can be discerned, demonstrate a diffusion rate that is more than 10 times lower (comparison of H5 and H6 chondrites by Langenauer and Krähenbühl [71]) (the petrographic classification H3 means coarse grained, H6 very fine grained almost no grain boundaries visible).

Weathering of meteorites influences the oxidation state of the material besides an alteration of the composition of many elements. Since meteorite studies allow to gain information on the early solar system not accessible by any other means it is important to know which fraction of the solid meteorite under investigation has not undergone any secondary alteration and therefore has preserved its pristine composition. This may be of essential interest for additional detailed investigations of extraterrestrial material. For meteorites, weathering is proportional to the exposure duration on the Antarctic ice shield which is given by the F contamination as explained above and not by the terrestrial age of the observed meteorite.

3.2. Diffusion profiling in archaeological bones and teeth

3.2.1. Introduction

Archaeological fragments of bones and teeth take up fluorine from the surrounding soil and accumulate it in their mineral phase when they are exposed to a humid environment. Geological time spans are needed for this process to reach equilibrium and for the fluorine distribution to become uniform. In cortical parts of long bone diaphysis, an initially U-shaped fluorine concentration profile can be observed, which decreases from the outer surface and the marrow cavity towards the inner parts of the bone and carries information on the exposure duration of the buried object in its shape. The time dependence of the profile slope is usually described in a simplified way by a diffusion model. The quantitative mathematical evaluation of these profiles may provide information on the exposure duration and the physical condition of the samples. Therefore, several attempts to use fluorine profiling as a dating method have been undertaken [3,39]. The distribution of

fluorine in an archaeological sample however is strongly influenced by the environmentally induced processes of bone diagenesis, i.e. the alteration in the structure and composition of the mineral phase and degradation of organic components of bone that may make the time information indistinct [72,73]. The primary chemical composition of bones can thus be superimposed by diagenesis within tens, hundreds or thousands of years. This depends more on the taphonomic and diagenetic ambience than on the geological age.

The initial step of fluorine uptake is the percolation of ground water into the pores and fissures. Hereupon, the fluorine ions are adsorbed onto the surface of the matrix, where an ion exchange takes place *via* the recrystallization of hydroxyapatite (HAP), the main component of bone and tooth material, affording chemically more stable fluorapatite (FAP), by which the hydroxyl groups are replaced by fluorine ions. After recrystallization, the substitution in the bone material proceeds both by grain-boundary diffusion and solid-state diffusion. Especially in specimens which have undergone diagenesis and where the number of pores and fissures is high, percolation becomes more and more dominant as a transport mechanism.

In a physiological context, the term ‘‘bone’’ describes a large variety of materials with a complex physical and chemical structure, whose basic building block consists of mineralized collagen fibres. Plate-shaped crystals of carbonated apatite (‘‘dahllite’’, $(Ca,Na,Mg)_5(HPO_4,PO_4,CO_3)_3(OH,CO_3)$ are formed within a collagen framework during bone growth (‘‘biomineralization’’). Studies on the microcomposition of modern bone have been done by Weiner *et al*. [74,75]. After the death of the individual, the proportions of the major components of bone, protein (20–30 wt%, mainly collagen), poorly crystalline mineral (60–70 wt%) and water (10 wt%), vary with the time elapsed since the bone material was deposited as it goes through diagenesis. During burial time, the material is in contact with sediments, soils and interstitial water. These structural features and the preservation state of the mineral and organic phase must be taken into consideration when fluorine uptake and movement within the body of the fossil bone is described.

3.2.2. History and related investigations

First attempts to date archaeological remains by their fluorine content were undertaken in Great Britain by J. Middleton in London and K.P. Oakley at the University of Oxford [21,76], where especially Oakley became well known for his work on the ‘‘Piltdown Man’’. By comparing the total fluorine content of a skull and a mandible, which had deliberately been faked to simulate fossil specimens and secretly placed in a ditch in Sussex, with original remains from the Lower Pleistocene period found in the same ditch, he concluded that the questionable specimens must have been significantly younger, as they contained less fluorine [69]. The Piltdown Skull had widely been held as a crucial discovery of modern

palaeontologic research, being the missing link between man and ape. In this particular case, it was possible to use total fluorine analysis as a relative dating method, as the fluorine contents of the original specimens were very high and the fraudulent samples deposited thousands of years later could be clearly identified. But Oakley himself pointed out the aggravating circumstances of environmental impact, which would influence the rate of fluorine uptake into the samples by changing the ''material'', this is, the bone structure and its diffusion characteristics. In later studies, the amount of fluorine acquired by a bone during fossilization was found to be also a function of the ''sample surroundings'' like sediment permeability and hydrology [77,78].

G. E. Coote was the first to doubt the homogeneous enrichment of fluorine in bones and disbelieved the simple bulk analysis. He found out that a decrease in concentration could be observed from the surface towards the inner parts of the sample. Based on these facts he proposed the idea of examining the fluorine diffusion profile of a sample cross-section to develop a dating method instead of considering the total fluorine content only [23], although he was well conscious of the difficulties of deriving valuable information out of so inhomogeneous and variable material as bone. However, the profiling method was hardly seized in the scientific community, and more than 15 years later studies were performed dealing with dating by determination of the total fluorine content of a bone sample [79].

Several studies have been made on fluorine uptake in archaeological bone specimens for relative or absolute dating [39,80,81]. As bone represents an open system with respect to many elements in soil, the uptake particularly of uranyl ions from soil water is a fundamental problem while developing a dating method for bone samples based on the decay series of uranium [82–84]. Even though purely inorganic systems like meteorites, flintstone or obsidian, might show more homogeneous physical structure, the process of diffusion ''*in vivo*'' is nowhere as simple as previously thought. The presumption that their composition shows less variation over time has proved to be a fallacy. So attempts at exposure dating by fluorine depth profiling also exist for chipped flints [34], where the fluorination depth is extremely shallow. The results of these investigations will be described by Reiche in this compendium. As described above, the varying uptake of F, Cl, Br and I into meteorites has been compared in Refs [40,70,71] and successfully related to their sites of recovery. Attempts for quartz hydration dating have been undertaken by Ericson *et al.* [85], where NRA methods were used to determine the hydration front in the sample. This is a further development of the obsidian hydration dating [86], where the diffusion fronts of water/hydrogen were determined by optical microscopy. Dating obsidian artefacts by determination of the hydration diffusion fronts of H_2O, which may interfere with regions of increased fluorine content, similarly involves difficulties caused by the unknown environmental context and the subsequently varying diffusion rate [87].

The spectrum of scientific literature dealing with bone diagenesis is in general manifold and only an incomplete outline can be presented here including Refs [72,88–90]. Special work on the decay and degradation of the organic matrix has been done by several authors [91–93]. Changes in the mineral components are described by Reiche *et al*. [94] and Trueman *et al*. [95]. Recent studies on bone dissolution and recrystallization have shed light on the behaviour of bone in a humid environment [74,96]. There has been interest in the uptake of Sr, Ba, Fe, Mn, Zn or Cr by bone. These elements are either absorbed from the soil after burial, thus carrying information on the palaeoenvironment or are part of metabolism during bone growth [97–99].

3.2.3. Diffusion theory and methods of analysis

In humid environments, hydroxyapatite ($Ca_5(PO_4)_3OH$), the main component of the inorganic bone and tooth matrix, is transformed into the more stable fluorapatite ($Ca_5(PO_4)_3F$). In an idealized sample, fluorine uptake from the environment leads to a U-shaped concentration profile, which slowly develops into the bulk from the outer surface and from the marrow cavity inwards according to Fick's second law

$$D\Delta c(\vec{r}, t) = \frac{\delta c}{\delta t}(\vec{r}, t)$$

where D is the diffusion constant of the material; c the concentration of the element, r the distance from the surface position; and t the time.

The shape of the profile alters with time, until it becomes completely flat and the inner concentration of fluorine corresponds to the one measured on the periosteal surface. This equation is used to describe diffusion processes if there is a concentration gradient only along one axis, i.e. if diffusion is one-dimensional. If diffusion and environmental conditions are constant (e.g. a constant supply of fluorine due to invariant soil humidity), the profile shape and its penetration depth carry the information on exposure time t. The profile will be more developed if the sample has been exposed to this environmental system for a longer time (Fig. 6). This fact leads to the idea of a mathematical evaluation of the ''diffusion length'' Dt (the parameter that describes how far the diffusion front has penetrated into the material), which allows the calculation of the burial time t, i.e. the age of the archaeological sample, if the diffusion constant is known [80].

Of the many structural types of bone, only the ''lamellar'', plexiform bone in the diaphysis compacta of long bones is of importance for fluorine dating, because only this material is homogeneous enough for the development of a dominant profile that starts from the periosteal surface. Especially in haversian bone (e.g. human bone), profiles may be forming at a number of points in the bone and in a number of different directions, stemming from surfaces within the bone (e.g. Haversian canals) or from the medullary cavity. These profiles often hide the true

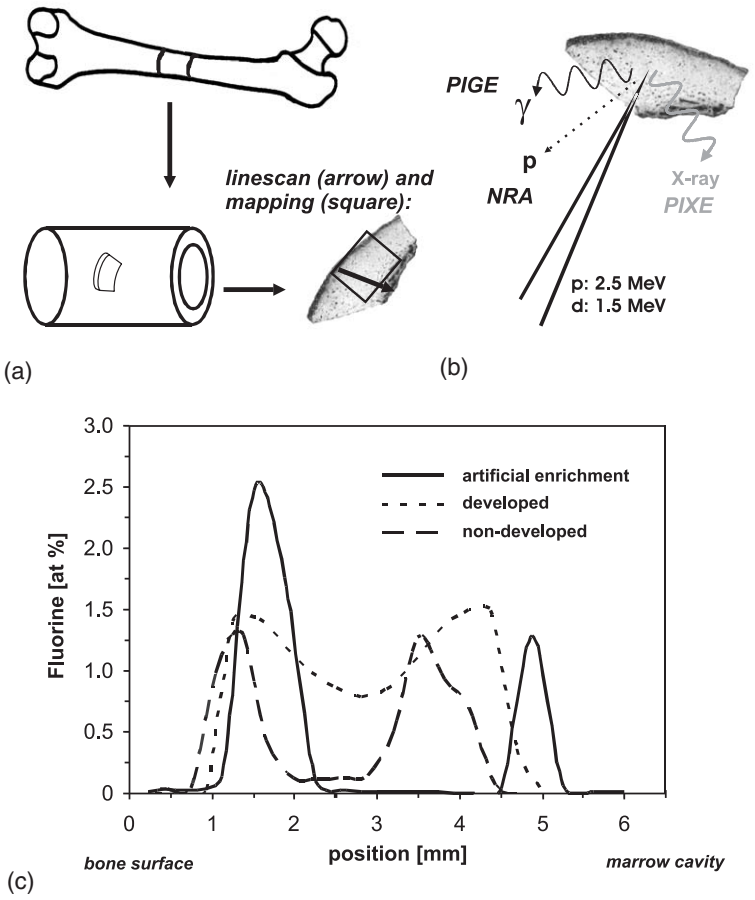

Fig. 6. (a) Samples of the mid-sections of long bones are best suited for fluorine profiling, as this skeletal position provides the most uniform conditions. All scans were performed in the direction from the periosteal surface towards the marrow cavity. Two-dimensional maps were collected in some samples. (b) Fluorine was analysed by PIGE (proton-induced γ-emission), while the distributions of Ca, Fe, Mn and Zn were detected by PIXE (proton-induced X-ray emission). C and N were analysed by NRA and emitted protons were detected in both cases. (c) Examples of ''developed'' and ''non-developed'' fluorine profiles in archaeological bone samples. The profile of an artificially fluorine enriched fresh bone sample is shown for comparison.

shape of the dominant profile, which is discussed in Ref. [81]. Even an intact long bone becomes an open system to the environment; soon after burial due to the degradation of soft tissues and due to the existence of foramina and various minor nerve canals and blood vessels, water (containing fluorine) will always find

its way into the marrow cavity. So a diffusion front arising from the marrow cavity can be observed in many cases.

In the diffusion model presented here, the value of the diffusion constant D remains constant, which is not the case for natural bone systems. The problems arising from bone diagenesis will be discussed in Section 3.2.7 and by Reiche in this compendium.

3.2.4. Micromapping with PIGE, PIXE and NRA

In a large majority of cases [3,23,24,34,39,40,73,80,81,100–103,105], PIGE is used for the determination of the fluorine concentration profiles. As the simultaneous processes of bone alteration and fluorine uptake and its diffusive transport are complex, complementary analytical tools are needed to reveal the interaction of diagenesis and diffusion and to gain information on the history of fluorine profile development. During PIGE measurements in a nuclear microprobe, it is obvious to make a simultaneous assessment of the material composition by PIXE, i.e. by a simple analysis of the excited characteristic X-rays [26]. Recently, Gaschen *et al.* have combined the analytical methods of PIGE/PIXE/NRA and infrared spectroscopy with optical and electron microscopy to gain additional information on the concentration and distribution of fluorine as a function of bone constitution and degradation [100–103]. An outline of the measurement set-up is presented in Fig. 7.

PIGE is a fast and precise analytical technique for a non-destructive determination of the quantitative fluorine content and its distribution in cross-sections of bone and tooth specimens. The γ-rays from the nuclear reaction $^{19}F(p,\alpha\gamma)^{16}O$ were used to quantify the fluorine concentration in the samples, and the simultaneous detection of the Ca-signal by PIXE provided additional information on the sample topography, as cracks, alteration halos and the typical porosity occurring in human bone samples are parameters which have direct influence on the fluorine uptake and transport during burial. The elements C and N were analysed by NRA ($^{12}C(d,p0)^{13}C$ and $^{14}N(d,p_5)^{15}N$ reactions) to gain information on the distribution of organic material in the samples. Mapping was performed where required (Figs 8 and 9), otherwise the samples were scanned from the periosteal surface towards the marrow cavity.

The major peculiarities for a diagenetically altered bone are an increase in crystal size and a decrease in protein content [104], thus complementary information on the state of degradation can be obtained by FT-IR (Fourier transform infrared spectroscopy). The characteristic splitting of the double peak at 563–604 cm^{-1} corresponds to the phosphate vibrations ν_4 $(PO_4)^{3-}$ indicating mineral-phase modifications, e.g. changes in crystallinity. A low value for the splitting factor ''SF'' indicates a high amount of amorphous material in the mineral phase and was obtained as described in Ref. [105].

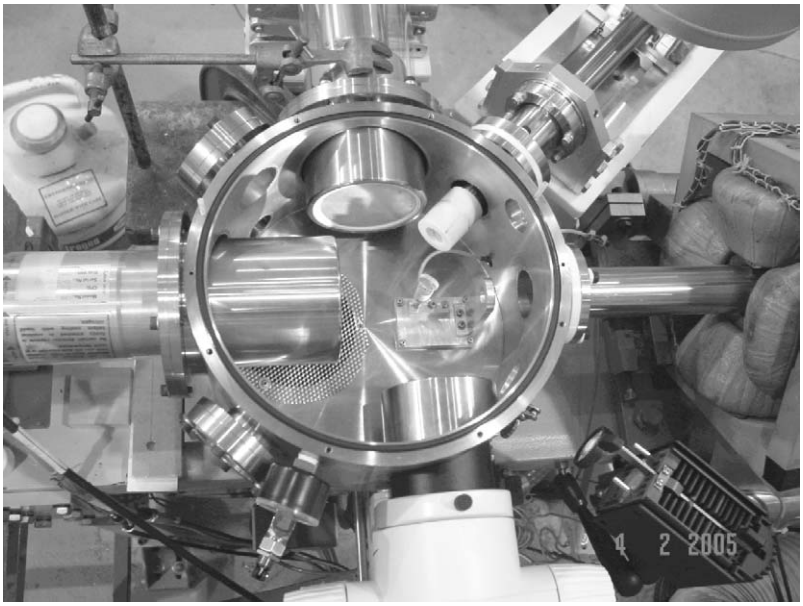

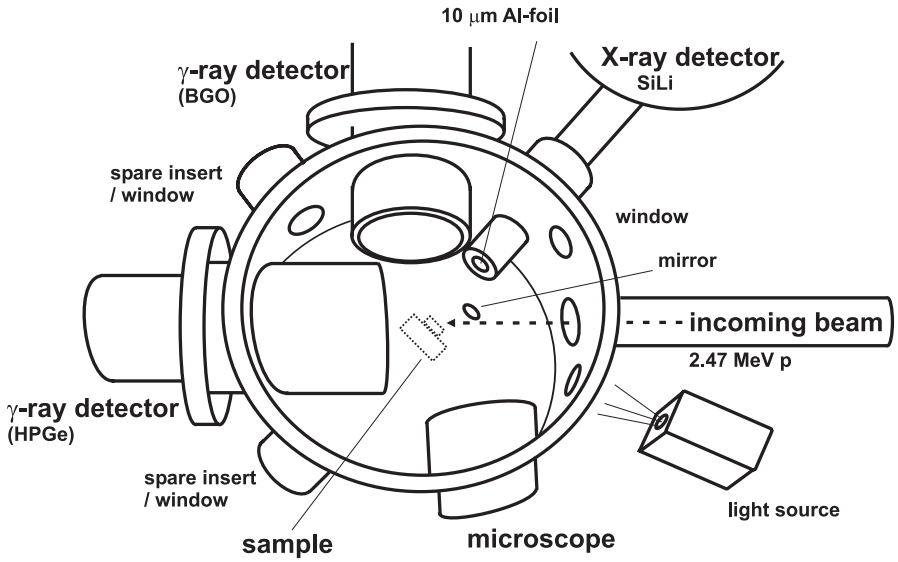

Fig. 7. Close-up of the Oxford vacuum chamber and the detectors at GNS (for abbreviations see body text): The incoming beam hits the samples at an angle of 45°. A small mirror and an optical microscope allowed the exact location of the beam position on the sample. For NRA measurements a SBD detector was additionally mounted on the lid of the chamber close to the SiLi detector at a position of 30° to the beam.

Fig. 8. Fluorine scans obtained by PIGE: Fluorine-containing soil water enters the tooth mainly through the nerve canal into the pulpa. The cementum also readily takes up fluorine which slowly diffuses into the dentine, while the enamel crown forms a barrier. Fluorine enters a long bone as well from the periosteal surface as from the marrow cavity. The thickness of the bone wall does not influence the shape of the diffusion front itself, but limits the time window where age determination is possible, as the profile becomes flat much faster. (Human molar, Seeberg BE, Switzerland, ~3750 BC, and human tibia, grave 132, Büren a. A. BE, Switzerland, medieval).

3.2.5. Profile evaluation by error function-fitting

To gain quantitative information on the profile characteristics, the profile shape must be evaluated mathematically. The parameter *Dt* (*D*, diffusion constant; *t*, exposure time) that describes the depth of the diffusion front that penetrated into the sample was determined by fitting the data with an error function (erf). The resulting curve describes the result of an undisturbed diffusion process. If the exposure time *t* is known, e.g. by radiocarbon dating, the diffusion constant *D*, a material constant, can be derived from this data.

The process of mathematical fitting is error-prone, and especially two different issues have to be considered, the first one dealing with the boundary conditions of the fitting procedure itself: A pure diffusion process is considered here as the only transport mechanism for fluorine in the sample. A constant value for the diffusion constant *D*, invariant soil temperatures and a constant supply of fluorine (e.g. a constant soil humidity) are assumed, the latter effect theoretically resulting in a constant surface fluorine concentration for samples collected at the same burial site. In mathematical terms, *Dt* is influenced by the spatial resolution of the scanning beam, the definition of the exact position of the bone surface, which usually coincides with the maximum fluorine concentration, and by the original fluorine concentration in the bulk of the object, which in most cases is still detectable. A detailed description on

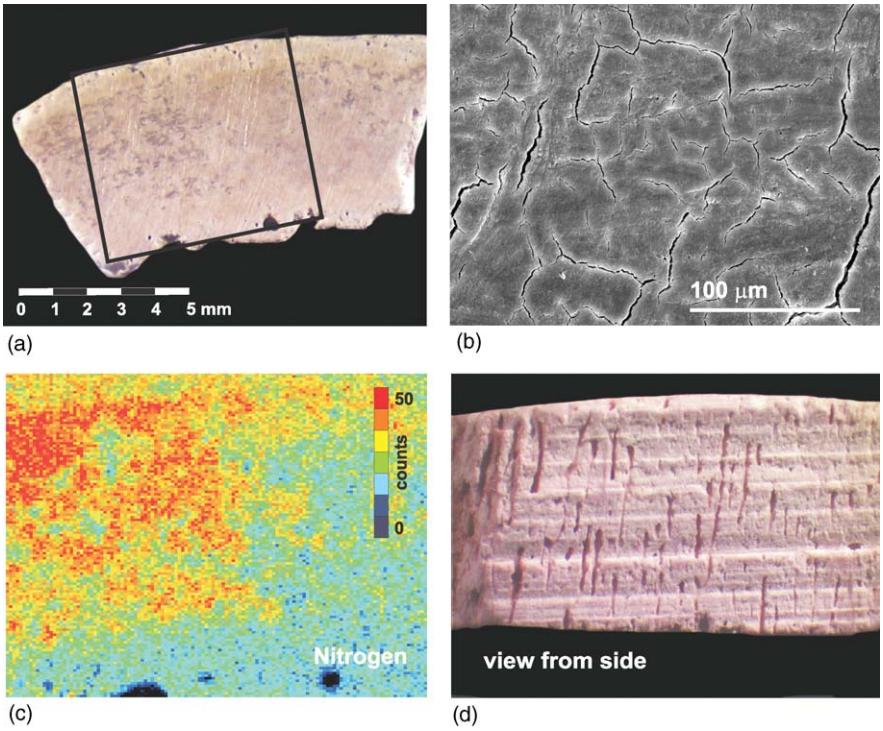

Fig. 9. (a) In some archaeological samples a ''patchy'' preservation of material could be observed even by eyesight. (b) NRA- and FT-IR analyses revealed that these regions differ in their content of organic material (human femur, grave 438, Büren a. A., medieval). (c) SEM-pictures of the macro- and micro-fissures pattern in a well-preserved archaeological bone (bos taurus, metatarsus, Seeberg, ~3750 BC). (d) The porosity pattern and the interconnection of the pores influence the resulting fluorine distribution in a buried bone sample, as fluorine ions migrating through the pores may reach certain regions of the bone far easier by percolation than by solid-state diffusion. The samples were submerged in fuchsine solution to visualize water percolation (human femur, grave 438, Büren a. A., medieval, a similar sample than depicted in (a)).

boundary conditions of fitting procedures has been written by Kottler *et al.* [39], whereas situations in which the fitting procedure failed are described in Ref. [103].

The evaluation of D by fitting an error function, which is based upon an undisturbed diffusion model in a single component system, will not lead to a proper description of the fluorine uptake in a natural multi-component system.

3.2.6. Artificial fluorine enrichment

Modern and archaeological bone samples were artificially enriched with fluorine to comprehend the uptake behaviour in a simplified environment [103]. Profiles were generated by immersing samples of about 0.5 g into aqueous solutions of NaF. These studies under controlled laboratory conditions (defined temperature, water fluorine content and exposure time) revealed that in fresh bone material which has not undergone alteration yet, solid-state and grain-boundary diffusion is indeed one of the most relevant mechanisms of fluorine transport in the sample. This artificial enrichment of archaeological samples revealed that ''pure'' diffusion is superimposed to the effects of bone alteration. Thus, fluorine incorporation in archaeological specimens mainly occurs in regions where bone diagenesis has provided the space for water percolation.

Compared to fossil samples where fluorine penetrates inwards quite readily, the transport seems to be impeded in fresh samples, which may be due to the intimate cohesion of the organic and the inorganic matrix of fresh lamellar bone [74,75]. A typical profile developed in a fresh bovine femur which was kept in a NaF-solution is shown in Fig. 10 (bottom, artificial fluorine enrichment, $[F]_{solution} = 1000\,\mu g/g$, $T = 35^{\circ}C$, $t = 14\,d$). Compared to human bones, bovine bones have much smaller pores if any, and the fluorine distribution is smoother as the formation of additional profiles becomes less important. The central parts of the sample show the initial low fluorine concentration even after enrichment, and so far it has not been possible to achieve thorough fluorine saturation in fresh samples. The surface concentration is very high, reflecting the strongly increased fluorine concentration in laboratory compared to natural soil waters and soils (≈ 0.1 mg/g or up to several mg/g, respectively, depending on geology).

Fluorine profiles generated under laboratory conditions show the expected evolution with time [101,103]. The parameter Dt increases with time and with increased temperature in the environment and the fluorine front penetrates further in samples that have undergone diagenesis. While the diffusion constant D was found to be time-independent in all cases, it was significantly increased in archaeological material (medium values for artificial enrichment: $D = 2 \times 10^{-8}$ mm^2/s for modern bone, $D = 20 \times 10^{-8}\,mm^2/s$ for well-preserved old material, and $D = 90 \times 10^{-8}\,mm^2/s$ for highly degraded material).

Thus, the generation of profiles under laboratory conditions, i.e. the simulation of the fluorine uptake, is possible. Furthermore, the fluorine profile reacts to different parameters of a very simple artificial system provided in the laboratory. Although it could be shown that in an undisturbed system under laboratory conditions, diffusion indeed is the most important of many relevant mechanisms for fluorine uptake into bone [103], in experimental work the above conditions are unlikely to be fulfilled, limiting the practical realization of fluorine exposure dating

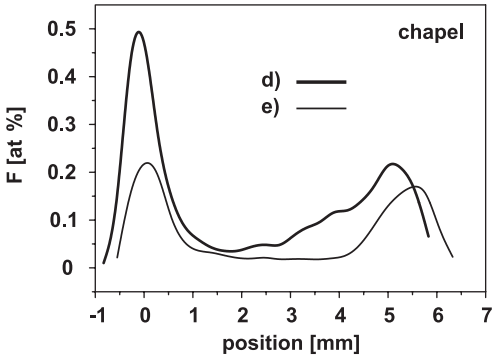

d) grave 50, 963 ± 50 AD
D = (2.5 ± 0.8) x 10^{-11} mm^2/s
robust skeleton,
but heavily degraded.

e) grave 78, 1407 ± 41 AD
D = (1.7 ± 0.5) x 10^{-11} mm^2/s
graceful skeleton,
better preserved,
resulting in similar D.

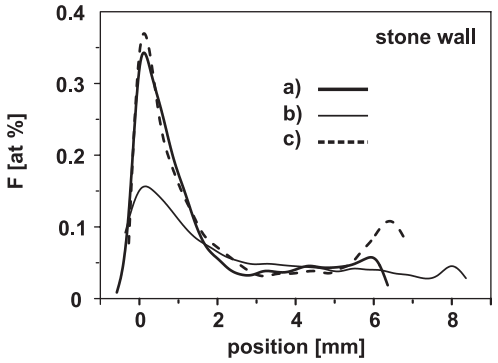

a) grave 438, 1138 ± 62 AD
D = (1.7 ± 0.3) x 10^{-11} mm^2/s

b) grave 162, 1188 ± 61 AD
D = (4.6 ± 0.8) x 10^{-11} mm^2/s
lowest collagen content,
remodeling of mineral
phase, intensive incorporation
of foreign material,
but no differences in density
compared to sample 132 and 438.

c) grave 132, 1209 ± 55 AD
D = (2.5 ± 0.8) x 10^{-11} mm^2/s

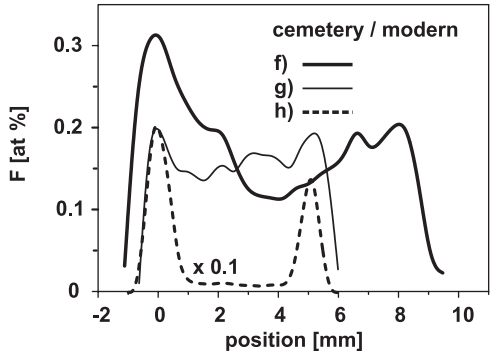

f) grave 168, 934 ± 50 AD
D = (9.5 ± 7.7) x 10^{-11} mm^2/s
collagen well preserved
in middle parts of specimen.

g) grave 174, 1011 ± 59 AD
D = (12.9 ± 10.9) x 10^{-11} mm^2/s
rather degraded, low density,
increased pore diameter.

h) modern bovine femur

Fig. 10. Fluorine profiles in samples from three different locations within the same burial place (Büren a. A., Switzerland). The exposure age was determined by radiocarbon dating. The diffusion constants D were determined by evaluation of the left front of the fluorine profile. The values are calibrated. Samples from the same burial place show qualitatively similar profile shapes. Differences can be explained by material characteristics.

for archaeologists to a level of comparison of the total fluorine content and profile shape for relative age classification.

3.2.7. The effect of the material itself

Even samples from the same burial site which were buried in close vicinity to each other, show different values for their diffusion constant *D*, which by definition is an invariant material parameter. However, the profile shape stays qualitatively similar for sections of long bones originating from neighbouring skeletons (Fig. 10). Nevertheless, a simple relation of this profile shape or the sample preservation state to the geological age is not possible. In most cases, variation of profile shapes may be explained by specific soil and material characteristics. This leads to the conclusion that future fluorine profile analyses should not be performed without simultaneous thorough sample characterization by microscopical and spectroscopic methods. At least the simultaneous detection of the Ca signal is inevitable, as it is of great importance when determining the exact position of the sample surfaces during the mathematical fitting procedure. An analysis of the adherent soil is desirable, unfortunately soil samples are rarely collected during excavations. It is surely reasonable to limit the choice of sample materials to long bone compacta only with a minimal wall thickness of 4 mm, as the values for *D* may differ up to 30% within a few centimetres [39], depending on the skeletal position.

The undisturbed organic and the inorganic matrix in a bone form a very stable network which is the reason for the extreme stability of bone. So a mineralized collagen can survive into the archaeological record under certain circumstances and an intact collagen phase can prevent fluorine from penetrating into the sample (Fig. 9). A well-preserved bone may thus show a less-developed profile than a far degraded sample of the same age.

The observation that moving water can increase pore diameters by inducing material loss has been made [72,105]. An increased porosity will facilitate microbial attack and collagen degradation, which in turn will expose mineral compounds to acidic decomposition. During diagenesis a bone's internal surface area decreases and its porosity increases [104]. These processes, which reinforce each other will result in high values of the diffusion constant *D*, which would influence dating. Studies on porosity changes in bones during diagenesis have been published by Nielsen-Marsh and Hedges [106]. It is important to include samples of both human and animal origin in studies on bone degradation. Bones of human and animal origin can be clearly distinguished by their different porosity. Pores in human bone compacta have a typical diameter of 60 μm [107], in contrast to animal bones, where the diameter of Haversian canals is much smaller [108,109]. However, compact bone itself has a large porosity (0.35 cm^3/g) and a high internal surface area (85–170 m^2/g, [106]), so that water movement is possible and profile formation can be observed all the same in a very well-preserved

animal bone of high density. Besides the diameter and the number of the pores, also their interconnection must be considered.

The skeletal age, which is not necessarily identical with the calendar age of the individual, has an important impact on the fluorine uptake, because osteoporosis is a process that fundamentally influences the bone structure. The disease pattern becomes visible in material loss within both the trabecular and the compact bone structure. Furthermore, the mineral density even in a healthy individual is not uniform in compact bone, but is a function of bone stress at this skeletal position and is increased at the point where muscles and tendons are fixed.

The collagen molecule (Type I) which occurs in vertebrates is a very ''conservative'' molecule, i.e. there is hardly any variation in its structure and composition. Differences between animal species mainly exist when the meso-structural arrangement of the bone components is discussed. The fluorine ion penetrating into a piece of bone encounters a different area, depending on the bone being haversian (as in human individuals) or plexiform (as in animals that grow fast, e.g. cattle). The remodelling during lifetime, which results in a transmutation of primary into secondary bone, also provides altering conditions for the penetrating fluorine ions.

Once bone diagenesis introduces fissures and causes collagen degradation and mineral recrystallization, these effects become indeed dominant over the small impacts that variations in the bone meso-structure may have on the fluorine uptake. But the initial bone structure steers and controls the specifications of the early diagenesis. Therefore, small variations in the initial bone structure may become very relevant within geological ages.

It has to be assumed that grain-boundary diffusion is not the only possible transport mechanism of ions in a bone, but that a significant amount of aqueous fluorine is transported through microfissures into a sample by capillary effects (Fig. 9). Diagenetic parameters influencing the uptake of fluorine into archaeological bone are discussed in detail by Reiche in this compendium.

3.2.8. Tooth as an alternative matrix

Generally, dissolved fluorine enters a human tooth *via* the nerve canal during alteration processes and adsorbs on the walls of the pulpa, from where it penetrates into the dentine. The enamel cap protects the dentine from contact with fluorine and does not incorporate any fluorine itself. Whereas this area of the dentine is well protected from the environmental milieu, the roots are exposed to microbial attack and all other factors of diagenesis. Sample damage also often starts from the pulpa, especially when the teeth are separated from the protective connection with the jawbone. During burial, a crack is formed between the dentine and the enamel crown. This is well known by anthropologists, and they report that in old specimens the enamel easily falls off during handling.

The reason to extend the experiments to tooth material was the idea that the matrix would have a less porous structure compared to human haversian bone and be less exposed to diagenetic alteration. While the porosity in human bone is mainly determined by a complicated network between the Haversian system and the Volkmann canals that are perpendicular to it, especially enamel is a far denser material than human bone and its organic content is significantly less (2% of organic material only). But in contrast to the enamel, dentine has a similar composition of the organic and the inorganic matrix compared to bone, and it has a high microporosity due to nerve canals that start from the pulpa and stop close to the enamel–dentine junction (edj). However, these nerve canals have a smaller diameter than a haversian pore (70 μm) and the canals are orientated parallel and are not connected with each other. So a fluorine ion cannot percolate from one pore to another, as it is the case in a human bone, but it has to overcome the distance from one canal to the next one by diffusion. So the permeability is low and this results in a smaller diffusion rate *D*.

Oakley [76] was already conscious about possible advantages of teeth relative to bones, and intensive work on teeth was done by Coote and Nelson [80]. Unfortunately, the construction of animal teeth (especially those from horses, sheep, goats, pigs or cattle, which are abundant in the archaeological record), is far more complicated than that of a human molar, because the enamel is folded during tooth growth and appears in several layers in the mature tooth.

The migration of water in teeth was tried to be visualized using fuchsine dye as a colorant ([103], rosaniline hydrochloride $C_{19}H_{17}N_3$ HCl). Fresh human molars were immersed into a slightly acidic aqueous fuchsine solution. As was expected, the water penetrated fast *via* the nerve canal into the pulpa and especially the roots were dyed red from fuchsine migrating inwards as well from the sample surface as from the nerve canal. After several days, it could be observed that water had migrated into the gap between the enamel and the dentine (edj). Generally the intensity of the colour increased with time, and the dentine took up the colour more readily than the enamel.

Generally, the diffusion rates that were measured at similar points within the same sample showed good consistency and also agreed well with known data. The positions where fluorine profiling is possible have to be carefully selected in tooth samples. The most clear diffusion fronts arise from the enamel–dentine junction (edj), as this is a region of a minimal environmental impact and of maximum homogeneity of the sample matrix. Water penetrates into this fissure by capillary effects, and a neat profile can develop. This process would be most favoured in a milieu where water is in constant motion (e.g. annual dry and wet cycles) and not in a waterlogged site. The major impediment restricting so far our ability to apply fluorine profiling in teeth is the fact that our knowledge on the formation of the gap between the enamel crown and the dentine is insufficient. Especially, we cannot estimate the time duration needed for these cracks to develop and how fast this occurs in different milieus.

Values for the diffusion rates of naturally grown fluorine profiles in teeth can be seen in Fig. 11. As can be expected from the material properties, they are significantly lower than those for human bone compacta. Artificial fluorine enrichment of a modern human molar resulted in increased diffusion rates compared to the naturally grown profiles as it was the case for artificial enriched bone samples, too ($[F]_{solution} = 360\,\mu g/g$, $T = 45^{\circ}C$, $t = 36\,h$, $D = 8 \times 10^{-9}\,mm^2/s$ for profiles arising from the nerve canal in the root of a human molar).

3.2.9. The reconstruction of the change of D during time

In natural soils, environmental impacts are variously combined and assessed in each individual case resulting in a great variety of material properties. However, hydrological conditions may vary during the exposure time of the artefact in an archaeological site.

The estimation of the exposure time of a bone sample by fluorine diffusion profiling is based upon the knowledge of the diffusion constant *D* of the material. Though the degree of bone conservation is highly variable and dependent on the environment, as ''bone'' is not a static medium. Diffusion has been found to be just one of the many relevant mechanisms for fluorine uptake in bone. Whatever the mechanism of fluorine uptake in a specific sample is, the process is closely related to others. The observed distribution of fluorine in an archaeological bone sample is always the result of site-specific and sample-specific parameters which strongly influence the evolution of the fluorine profile with time during the diffusion process. The time frame where dating is possible is dependent on the diffusion velocity in the medium. Unlike the concentration decrease of the ^{14}C isotope used for radiocarbon dating, the alteration of the bone matrix is not a constant process during geological eras. Archaeological bone whose structure and composition is modified during diagenesis, has turned out to be a complex system for diffusion processes for many reasons, which may reinforce and entail each other in turn, and a model based on the knowledge of the material constant *D* is a difficult approach for the development of a dating technique. The factors influencing the uptake of fluorine into bone can be summarized as follows:

(1) Structure of living bone: plexiform, haversian, osteoporotic;
(2) Funeral practices and conditions of burial: starting conditions of early diagenesis;
(3) Bone diagenesis: change of matrix during time;
(4) Soil pH and hydrology: fluorine availability;
(5) Transport mechanisms of fluorine and water: different rates of diffusion and percolation.

Even if the present value of *D* can be determined, its value cannot be related to a corresponding age, as the mechanism how the profile has developed, cannot

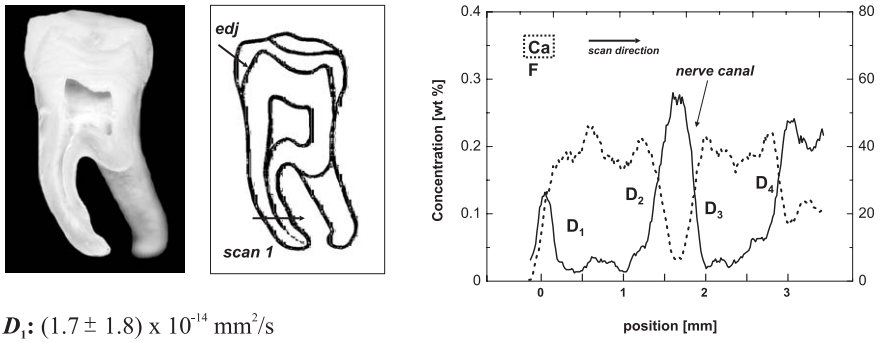

D_1: $(1.7 \pm 1.8) \times 10^{-14}$ mm^2/s
D_2: $(3.2 \pm 1.2) \times 10^{-13}$ mm^2/s
D_3: $(2.4 \pm 0.8) \times 10^{-14}$ mm^2/s
D_4: $(1.5 \pm 0.4) \times 10^{-13}$ mm^2/s

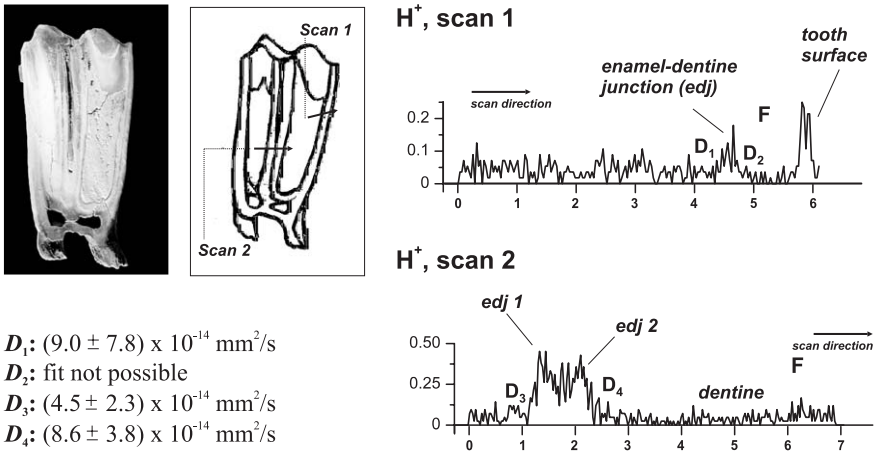

D_1: $(9.0 \pm 7.8) \times 10^{-14}$ mm^2/s
D_2: fit not possible
D_3: $(4.5 \pm 2.3) \times 10^{-14}$ mm^2/s
D_4: $(8.6 \pm 3.8) \times 10^{-14}$ mm^2/s

Fig. 11. Fluorine profiles in two tooth samples (Seeberg, Switzerland, ~3750 BC, top, and Radfeld, Austria, 1200–750 BC). The clearest fluorine profiles arise from the enamel–dentine junctions (edj) and from the nerve canals (in human tooth only). The diffusion constants of these naturally grown profiles are similar in both tooth samples, although their provenance and age is very different. But, the values differ significantly from those measured in human bone compacta (Fig. 9).

be retraced and is different for each bone specimen. We only know the ''end-state'' of the sample. A constant increase of D is not plausible under natural conditions. We assume that D may either stay constant for a certain time duration or even decrease, e.g. during times of water shortage. Once the intimate cohesion between organic and inorganic matrix is broken, the bone matrix undergoes a rapid change during early diagenesis, until a stable crystal structure is formed

which does not undergo further alteration. Diagenesis therefore is referred to as a self-limiting process.

It is not possible to reconstruct the remodelling of the bone matrix and the subsequent changes of the diffusion constant D during bone history, so far. So the preliminary conditions for grain-boundary diffusion vary and similarly the diffusion constant D may alter for a given sample in function of time. In this case, a simple diffusion model fails to describe the fluorine uptake. Therefore, this model was proved to represent a good approximation for fluorine uptake in intact or slightly altered bone matrices, but not for far degraded or very porous samples: here, other processes than pure diffusion interfere once a critical degree of degradation has been achieved, by which the fitting error becomes increasingly important. An age determination based on the analysis of D becomes more and more uncertain.

It has to be considered that fluorine uptake is not a phenomenon occurring in a bone that may simultaneously go through diagenesis, but that the formation of FAP itself is one of many manifestations of bone diagenesis. But all efforts within the scientific community to relate the state of preservation of an archaeological sample to the exposure time rather than to the burial milieu have failed so far.

We would like to point out the distinct dependence of the diffusion constant D on the physical bone appearance and the interaction of various parameters entailing the resulting fluorine distribution in an archaeological bone sample. This study brings up the paradox of the ''altering constant'' D and highlights the large spectrum of uncertainties in a multi-variate system of bone, soil and time. One of the main problems that remain to be solved is the possibility to deduce the time duration during which a single influencing factor has been of relevance. Further studies on fluorine dating should integrate the change of the diffusion constant D over time into their model.

4. SUMMARY

Diffusion tends to equilibrate concentration differences between two reservoirs upon contact; fluorine concentration profiles develop at the boundary of the two compartments as a function of time. Studies of the distribution of this trace element in archaeological samples such as bones, teeth or flints allow to gain some age information on the excavated objects of a burial site. The presented technique using beams of accelerated protons allows to measure fluorine diffusion profiles with an excellent space resolution. The surface exposure duration was deduced by the same method for Antarctic meteorites.

A severe limitation of the methods to unravel age information or dating of objects is given by the time-dependent changes of the value of the diffusion constant D as well as by all the transformations any material undergoes through time.

ACKNOWLEDGEMENTS

The authors would like to thank Dr. S. Ulrich-Bochsler, Historical Anthropology, University of Berne, and Dr. M. Nussbaumer, Natural History Museum, Berne, for providing of archaeological samples. We thank Dr. K. Noll for the data he has provided for this article.

APPENDIX:. ACRONYMS AND GLOSSARY

PIGE (or PIGME)	particle-induced gamma-ray emission
NRA	nuclear reaction analysis
PIXE	particle-induced X-ray emission
NRRA	nuclear resonant reaction analysis
BGO	bismuth germanium oxide
CPA	charged particle activation
RBS	Rutherford backscattering spectrometry
ERDA	elastic recoil detection analysis
EDX/WDX	energy/wave dispersive analysis of X-rays
Chondrites	rock of meteoric origin containing peculiar rounded granulae of some mineral, which give the name of chondrites
Diagenesis	the physical, chemical or biological alteration of sediments into sedimentary rocks, this term may also be used for alteration phenomena occurring in bones and teeth and any other archaeological material after deposition
HAP	hydroxyapatite
FAP	fluorapatite
erf	error function

REFERENCES

[1] J.W.Mayer, E.Rimini (Eds.), Ion Beam Handbook for Material Analysis, Academic Press, New York, 1977.
[2] J.R.Tesmer, M.Nastasi (Eds.), Handbook of Modern Ion Beam Materials Analysis, MRS, Pittsburgh, 1995.
[3] G.E. Coote, Ion-beam analysis of fluorine – its principles and applications, Nucl. Instr. Meth. B66 (1992) 191–204.
[4] F. Bodart, G. Demortier, Interferences of neutron-induced γ-ray emission in Ge(Li) detectors in elemental analysis by proton-induced γ-ray emission, Radiochem. Radioanal. Lett. 31 (1977) 215–224.

[5] R.B. Bouiton, G.T. Ewan, Simultaneous analysis of light elements using prompt nuclear reaction gamma rays, Anal. Chem. 49 (1977) 1297–1303.
[6] M. Kregar, J. Muller, P. Rupnik, F. Spiler, Concentration profile measurements using multiply resonant nuclear reactions, Fizika 9 (1977) 81.
[7] J.R. Bird, M.D. Scott, L.H. Russell, M.J. Kenny, Analysis using ion induced gamma rays, Nucl. Instr. Meth. 149 (1978) 336.
[8] M.J. Kenny, J.R. Bird, E. Clayton, Proton induced gamma-ray yields, Nucl. Instr. Meth. 168 (1980) 115–120.
[9] M.J. Kenny, Thick target gamma yields from fluorine, Aust. J. Phys. 34 (1981) 35–41.
[10] I. Khubeis, J.F. Ziegler, Microanalysis of fluorine using the $^{19}F(p,\alpha_o)^{16}O$ reaction, Nucl. Instr. Meth. B24-B25 (1987) 691–694.
[11] Zheng-Zhihao, Wang-Yongqiang, A simple simulation method for profiling elements, Nucl. Tech. 13 (1990) 409–413.
[12] H.E. Zschau, F. Plier, J. Vogt, G. Otto, H. Duschner, J. Arends, D. Grambole, F. Herrmann, R. Klabes, R. Salomonovic, Z. Hulek, M. Setvak, Test of a new standard for fluorine determination with PIGE, Nucl. Instr. Meth. B68 (1992) 158–160.
[13] S.O.F. Dababneh, K. Toukan, I. Khubeis, Excitation function of the nuclear reaction $^{19}F(p,\alpha\gamma)^{16}O$ in the proton energy range 0.3–3.0 MeV, Nucl. Instr. Meth. B83 (1993) 319–324.
[14] C. Olivier, H.L. Van-Niekerk, On the use of LiF as non- and analyte spike for the determination of fluorine by PIGE, Nucl. Instr. Meth. B B85 (1994) 128–132.
[15] G. Demortier, Analysis of light elements with a nuclear microprobe – a review, Nucl. Instr. Meth. B104 (1995) 244–254.
[16] J. Jin, D.L. Weathers, J.P. Biscar, B.F. Hughes, J.L. Duggan, F.D. McDaniel, S. Matteson, Convolution fitting and deconvolution methods for fluorine depth profiling by resonant NRA, AIP Conf. Proc. 392 (1997) 681–684.
[17] J.D. Borgardt, M.D. Ashbaugh, L.C. McIntyre, J.O. Stoner, R.B. Gregory, M. Azrak, J. Wetzel, Detection and depth profiling of ^{19}F using a resonance at 2313 keV in the $^{19}F(\alpha,p)^{22}Ne$ nuclear reaction, Nucl. Instr. Meth. B136–B138 (1998) 528–532.
[18] A. Fessler, T.N. Massey, B.J. Micklich, D.L. Smith, Thick target photon yields and angular distributions for the $^{19}F(p,\alpha\gamma)^{16}O$ source reaction at incident proton energies between 1.5 and 4.0 MeV, Nucl. Instr. Meth. A450 (2000) 353–359.
[19] D. Grambole, C. Neelmeijer, K. Noll, F. Herrmann, $^{19}F(p,p'\gamma)^{19}F$ and $^{18}O(p,\gamma)^{19}F$ gamma-ray interferences studied on liquids, Nucl. Instr. Meth. B161–B163 (2000) 269–274.
[20] A.P. Jesus, B. Braizinha, J.P. Ribeiro, Excitation function and cross-sections of the reaction $^{19}F(p,p'g)^{19}F$, Nucl. Instr. Meth. B161–B163 (2000) 186–190.
[21] J. Middleton, On the fluorine in bones, its source and its application to the determination of the geological age of fossil bones, Geol. Soc. Lond. Proc. 4 (1944) 431–433.
[22] G.E. Coote, N.E. Whitehead, G.J. McCallum, Rapid method of obsidian characterization by inelastic-scattering of protons, J. Radioanal. Chem. 12 (1972) 491–496.
[23] G.E. Coote, R.J. Sparks, New Zealand J. Archaeol. 3 (21) (1981) 806–810.
[24] G.E. Coote, R.J. Sparks, P. Blattner, Nuclear microprobe measurement of fluorine concentration profiles, with application in archaeology and geology, Nucl. Instr. Meth. 197 (1982) 213–221.
[25] G.E. Coote, S. Holdaway, in: W. Ambrose, P. Duerden (Eds.), Archaeometry: An Australasian Perspective, Australian National University, Canberra, 1982, pp. 251–261.
[26] G.E. Coote, I.C. Vickridge, Application of a nuclear microprobe to the study of calcified tissues, Nucl. Instr. Meth. B30 (1988) 393–397.
[27] G.E. Coote, T. Molleson, Archaeometry: Australasian Studies, J. R. Prescott (Ed.), Physics Department, University of Adelaide, 1988, pp. 99–104.

[28] G.E. Coote, Fluorine as an indicator of changes in bones and teeth, Trace elements in New Zealand: environmental, human and animal, Proc. New Zealand Trace Elements Group Conf., 1989, pp. 183–188.
[29] G.E. Coote, W.J. Trompetter, Strontium and fluorine markings in shells of a mollusk (Paphies-Subtriangulata) with potential importance in biology and archaeology, Nucl. Instr. Meth. B77 (1993) 501–504.
[30] G.E. Coote, R.W. Gauldie, W.J. Trompetter, I.C. Vickridge, A. Markwitz, Twenty years of proton microprobe research in biominerals: a tribute to Graeme Ernest Coote, 1935–1997, Nucl. Instr. Meth. B158 (1999) 1–5.
[31] R.E. Taylor, Fluorine diffusion: a new dating method for chipped lithic materials, World Archaeol. 7 (1975) 125–135.
[32] R.O. Allen, P.J. Clark, Fluorine in meteorites, Geochim. Cosmochim. Acta 41 (1977) 581–585.
[33] P. Walter, M. Menu, I.C. Vickridge, Fluorine depth profiles as a relative dating method of chipped flints, Nucl. Instr. Meth. B45 (1990) 119–122.
[34] P. Walter, M. Menu, J.C. Dran, Dating of archaeological flints by fluorine depth profiling – new insights into the mechanism of fluorine uptake, Nucl. Instr. Meth. B64 (1992) 494–498.
[35] U. Krähenbühl, K. Noll, M. Döbeli, D. Grambole, F. Herrmann, L. Tobler, Exposure of ALH84001 and other achondrites on the Antarctic ice, Meteor. Planet. Sci. 33 (1998) 665–670.
[36] K. Noll, M. Döbeli, L. Tobler, D. Grambole, U. Krähenbühl, Fluorine profiles in achondrites and chondrites from Antarctica by nuclear reaction analysis (NRA), Meteor. Planet. Sci. 32 (1997) ; A101.
[37] K. Noll, M. Döbeli, D. Grambole, F. Herrmann, U. Krähenbühl, Fluorine enrichment on the surface of Antarctic C30 and H chondrites by nuclear reaction analysis (NRA) and the sources of this terrestrial fluorine, Meteor. Planet. Sci. 33 (1998) A118–A119.
[38] K. Noll, M. Döbeli, U. Krähenbühl, Fluorine profiles in Antarctic meteorites by nuclear reaction analysis, Fresenius J. Anal. Chem. 361 (1998) 713–715.
[39] C. Kottler, M. Döbeli, U. Krähenbühl, M. Nussbaumer, Exposure age dating by fluorine diffusion, Nucl. Instr. Meth. B188 (2002) 61–66.
[40] K. Noll, M. Döbeli, U. Krahenbühl, D. Grambole, F. Herrmann, C. Koeberl, Detection of terrestrial fluorine by proton induced gamma emission (PIGE): a rapid quantification for Antarctic meteorites, Meteor. Planet. Sci. 38 (2003) 759–765.
[41] J. Stroobants, F. Bodart, G. Deconninck, G. Demortier, G. Nicolas, in: O. Meyer, C. Linker, F. Kappeler (Eds.), Ion Beam Surface Layer Analysis, Plenum, New York, 1976, pp. 933–943.
[42] G. Demortier, J. Stroobants, G. Deconninck, F. Bodart, LARN Report, 724 (1983).
[43] D. Grambole, C. Bauer, P. Gippner, C. Heiser, W. Rudolph, H.J. Thomas, Fluorine determination in the near surface region of solids using the $^{19}F(p,p'\gamma)^{19}F$ resonance reaction, J. Radioanal. Nucl. Chem. Articles 83 (1984) 107–115.
[44] J.F. Ziegler, J.P. Biersack, U. Littmark, The Stopping and Range of Ions in Solids, Pergamon Press, New York, 1985. Computer code available at http://www.srim.org.
[45] E. Möller, N. Starfelt, Microanalysis of fluorine in zircaloy by use of $^{19}F(p,\alpha\gamma)^{16}O$ reaction, Nucl. Instr. Meth. 50 (1967) 225.
[46] D.J. Land, D.G. Simons, J.G. Brennan, M.D. Brown, in: O. Meyer, C. Linker, F. Kappeler (Eds.), Ion Beam Surface Layer Analysis, Plenum, New York, 1976, p. 851.
[47] B. Maurel, G. Amsel, J.P. Nadai, Depth profiling with narrow resonances of nuclear reactions: theory and experimental use, Nucl. Instr. Meth. 197 (1982) 1–13.
[48] G. Deconninck, B. Van-Oystaeyen, High resolution depth profiling of F, Ne and Na in materials, Nucl. Instr. Meth. 218 (1983) 165–170.

[49] P.J.M. Smulders, A deconvolution technique with smooth non-negative results, Nucl. Instr. Meth. B14 (1986) 234–239.
[50] I. Vickridge, G. Amsel, Spaces – a PC implementation of the stochastic-theory of energy-loss for narrow-resonance depth profiling, Nucl. Instr. Meth. B45 (1990) 6–11.
[51] J. Rickards, Fluorine studies with a small accelerator, Nucl. Instr. Meth. B56–B57 (1991) 812–815.
[52] G. Amsel, B. Maurel, High resolution techniques for nuclear reaction narrow resonance width measurements and for shallow depth profiling, Nucl. Instr. Meth. 218 (1983) 183–196.
[53] J.W. Mandler, R.B. Moler, E. Raisen, K.S. Rajan, Determination of fluoride concentration profile in tooth enamel using a nuclear-resonance technique, Thin Solid Films 19 (1973) 165–172.
[54] F. Bodart, G. Deconninck, Concentration depth profiling in fluorine implanted iron, Nucl. Instr. Meth. 197 (1982) 59–63.
[55] A.W. Crawford, W.J. Sampson, H.J. Debruin, Shallow fluorine depth profiles of cementum in periodontal disease – a pilot-study, J. Dent. Res. 62 (1983) .
[56] J.D. Borgardt, M.D. Ashbaugh, L.C. McIntyre Jr., J.O. Stoner Jr., R.B. Gregory, M. Azrak, J. Wetzel, Detection and depth profiling of ^{19}F using a resonance at 2313 keV in the $^{19}F(\alpha,p)^{22}Ne$ nuclear reaction, Nucl. Instr. Meth. B 136–138 (1998) 528–532.
[57] D. Dieumegard, B. Maurel, G. Amsel, Microanalysis of fluorine by nuclear reactions. I. $^{19}F(p,\alpha_o)^{16}O$ and $^{19}F(p,\alpha\gamma)^{16}O$ reactions, Nucl. Instr. Meth. 168 (1980) 93–103.
[58] J.R. Bird, E. Clayton, The PIGME method for fluorine determination, Nucl. Instr. Meth. 218 (1983) 525–528.
[59] K. Noll, PhD Thesis, University of Berne, Switzerland, 1998.
[60] R.A. Jarjis, On the determination of fluorine concentration profiles in magnesium alloy scales using the $^{19}F(p,\alpha\gamma)^{16}O$ reaction, Nucl. Instr. Meth. B154 (1978) 383–387.
[61] D.N. Jamieson, B. Rout, R. Szymanski, P. Spizzirri, A. Sakellariou, W. Belcher, C.G. Ryan, The new Melbourne nuclear microprobe system, Nucl. Instr. Meth. B190 (2002) 54–59.
[62] G.W. Grime, M.H. Abraham, M.A. Marsh, The new external beam facility of the Oxford scanning proton microprobe, Nucl. Instr. Meth. B181 (2001) 66–70.
[63] T. Calligaro, J.C. Dran, J. Salomon, P. Walter, Review of accelerator gadgets for art and archaeology, Nucl. Instr. Meth. B226 (2004) 29–37.
[64] Y.I. Bondarenko, V.S. Rudenko, Determination of fluorine by deuteron activation, J. Radioanal. Chem. 52 (1979) 127.
[65] W.K. Chu, J.W. Mayer, M.A. Nicolet, Backscattering Spectrometry, Academic Press, New York, 1978.
[66] J. Tirira, Forward Recoil Spectrometry, Plenum, New York, 1996.
[67] E. Arai, A. Zounek, M. Sekino, K. Takemoto, O. Nittono, Depth profiling of porous silicon surface by means of heavy-ion TOF ERDA, Nucl. Instr. Meth. B85 (1994) 226–229.
[68] J. Paivasaari, M. Putkonen, L. Niinisto, A comparative study on lanthanide oxide thin films grown by atomic layer deposition, Thin Solid Films 472 (2005) 275–281.
[69] K.P. Oakley, C.R. Hoskins, New evidence on the antiquity of piltdown man, Nature 4193 (1950) 379–382.
[70] M. Langenauer, U. Krähenbühl, Halogen contamination in Antarctic H5 and H6 chondrites and relation to sites of recovery, Earth Planet. Sci. Lett. 120 (1993) 431–442.
[71] M. Langenauer, U. Krähenbühl, Depth-profiles and surface enrichment of the halogens in four Antarctic H5 chondrites and in two non-Antarctic chondrites, Meteoritics 28 (1993) 98–104.

[72] C.M. Nielsen-Marsh, R.E.M. Hedges, Patterns of diagenesis in bone I: the effects of site environments, J. Archaeol. Sci. 27 (2000) 1139–1150.
[73] I. Reiche, C. Vignaud, L. Favre-Quattropani, L. Charlet, M. Menu, Diffusion in archaeological bones, Defect and Diffusion Forum Vols. 194–199 (2001) 953–960.
[74] F. Berna, A. Matthews, S. Weiner, Solubilities of bone mineral from archaeological sites: the recrystallization window, J. Archaeol. Sci. 31 (2004) 867–882.
[75] S. Weiner, P.A. Price, Disaggregation of bone into crystals, Calcified Tissue Int. 39 (1986) 365–375.
[76] K.P. Oakley, The fluorine-dating method, Yearbook of Physical Anthropology, Volume 5, Wiley-Liss, New York, 1949, pp. 44–52.
[77] H. Toots, R.B. Parker, Factors affecting fluorine content of fossil bones and teeth, Contrib. Geol. University of Wyoming 18 (1979) 69–70.
[78] A.R. Millard, R.E.M. Hedges, The role of the environment in uranium uptake by buried bone, J. Archaeol. Sci. 22 (1995) 239–250.
[79] D. Chlubek, I. Nocen, E. Dabkowska, B. Zyluk, Z. Machoy, B. Kwiatkowska, Fluoride accumulation in human skulls in relation to chronological age, Fluoride 29 (3) (1996) 131–134.
[80] G.E. Coote, P. Nelson, Diffusion profiles of fluorine in archaeological bones and teeth: their measurement and application, in: G. Ward (Ed.), Archaeology at ANZAAS, Canberra Archaeological Society, Canberra, 1984, pp. 22–27.
[81] S. Holdaway, Fluorine Profiling: A New Method for the Relative Dating of Bone, Dissertation for BA, Anthropology Department, University of Otago, 1981.
[82] A.R. Millard, R.E.M. Hedges, A diffusion–adsorption model of uranium uptake by archaeological bone, Geochim. Cosmochim. Acta 60 (12) (1996) 2139–2152.
[83] A.W.G. Pike, R.E.M. Hedges, P. Van Calsteren, U-series dating of bone using the diffusion–adsorption model, Geochem. Cosmochem. Acta 66 (2002) 4273–4286.
[84] A.M. Rae, R.E.M. Hedges, M. Ivanovich, Further studies for uranium-series dating of fossil bone, Appl. Geochem. 4 (1989) 331–337.
[85] J.E. Ericson, O. Dersch, F. Rauch, Quartz hydration dating, J. Archaeol. Sci. 31 (2004) 883.
[86] W.R. Ambrose, Obsidian hydration dating, in: D.R. Brothwell, A.M. Pollard (Eds.), Handbook of Archaeological Sciences, Wiley, New York, 2004, pp. 81–92.
[87] F. Leach, H. Naylor, Dating New Zealand obsidians by resonant nuclear reactions, New Zealand J. Archaeol. 3 (1981) 33–49.
[88] R.E.M. Hedges, Bone diagenesis: an overview of processes, Archaeometry 44 (3) (2002) 319–328.
[89] H. Piepenbrink, Examples of chemical changes during fossilisation, Appl. Geochem. 4 (1989) 273–280.
[90] S. Weiner, O. Bar-Yosef, States of preservation of bones from prehistoric sites in the near east: a survey, J. Archaeol. Sci. 17 (1990) 187–196.
[91] A.M. Child, Towards an understanding of the microbial decomposition of archaeological bone in the burial environment, J. Archaeol. Sci. 22 (1995) 165–174.
[92] C.N. Trueman, D.M. Martill, The long-term survival of bone: the role of bioerosion, Archaeometry 44 (2002) 371–382.
[93] N. Tuross, Alterations in fossil collagen, Archaeometry 44 (2002) 427–434.
[94] I. Reiche, C. Vignaud, M. Menu, The crystallinity of ancient bone and dentine: new insights by transmission electron microscopy, Archaeometry 44 (2002) 447–459.
[95] C.N.G. Trueman, A.K. Behrensmeyer, N. Tuross, S. Weiner, Mineralogical and compositional changes in bones exposed on soil surfaces in Amboseli National Park, Kenya: diagenetic mechanisms and the role of sediment pore fluids, J. Archaeol. Sci. 31 (2004) 721–739.
[96] C.M. Nielsen-Marsh, R.E.M. Hedges, Dissolution experiments on modern and diagenetically altered bone and the effect on the infrared splitting factor, Bull. de la Sociéte de Géologie de France 168 (1997) 485–490.

[97] St Jankuhn, T. Butz, R.-H. Flagmeyer, T. Reinert, J. Vogt, B. Barckhausen, J. Hammerl, R. Protsch von Zieten, D. Grambole, F. Herrmann, K. Bethge, Ion microprobe analyses of ancient human bone, Nucl. Instr. Meth. B136–B138 (1998) 329–333.
[98] I. Reiche, L. Favre-Quattropani, T. Calligaro, J. Salomon, H. Bocherens, L. Charlet, M. Menu, Trace element composition of archaeological bones and post-mortem alteration in the burial environment, Nucl. Instr. Meth. B150 (1999) 656–662.
[99] C.N. Trueman, N. Tuross, Trace elements in recent and fossil bone apatite, Rev. Mineral. Geochem. 48 (2002) 489–521.
[100] A.A.-M. Gaschen, U. Krähenbühl, M. Döbeli, A. Markwitz, B. Barry, Studies on fluorine diffusion in archaeological bones, Bull. de la Société Suisse d'Anthropologie 10 (1) (2004) 23–33.
[101] A.A.-M. Gaschen, U. Krähenbühl, M. Döbeli, A. Markwitz, B. Barry, Artificial fluorine enrichment in bones: diagenesis as restricting factor for exposure age dating by fluorine diffusion, Proc. 34th Int. Symp. Archaeometry, Zaragoza, 2004.
[102] A.A.-M. Gaschen, U. Krähenbühl, M. Döbeli, A. Markwitz, B. Barry, Fluorine and calcium profiling by PIGE/PIXE for exposure age dating in archaeology, accepted, scheduled for a special issue of the International Journal of PIXE, 15, 1–2, 2005
[103] A.A.-M. Gaschen, Relevance of fluorine diffusion for exposure age dating in archaeological bones and teeth, Unpublished PhD Thesis, University of Bern, 2005.
[104] R.E.M. Hedges, A.R. Millard, A.W.G. Pike, Measurements and relationships of diagenetic alteration of bone from three archaeological sites, J. Archaeol. Sci. 22 (1995) 201–209.
[105] I. Reiche, L. Favre-Quattropani, C. Vignaud, H. Bocherens, L. Charlet, M. Menu, A multi-analytical study of bone diagenesis: the Neolithic site of Bercy (Paris, France), Meas. Sci. Technol. 14 (2003) 1608–1619.
[106] C.M. Nielsen-Marsh, R.E.M. Hedges, Bone porosity and the use of mercury intrusion porosimetry in bone diagenesis studies, Archaeometry 41 (1999) 165–174.
[107] L. Harsányi, Differential diagnosis of human and animal bone, in: G. Grupe, A.N. Garland (Eds.), Histology of Ancient Bone: Methods and Diagnosis, Springer, Berlin, 1993, pp. 79–94.
[108] D.H. Enlow, S.O. Brown, A comparative histological study of fossil and recent bone tissues – part I, Tex. J. Sci. 8 (1956) 405–443.
[109] B. Herrmann, S. Hummel, H. Schutkowski, G. Grupe, H. Piepenbrink, Prähistorische Anthropologie: Leitfaden der Feld- und Labormethoden, Springer, Berlin, 1990.
[110] K.C. Welten, L. Lindner, C. Alderliesten, K. van der Borg, Terrestrial ages of ordinary chondrites from the Lewis Cliff stranding area, East Antarctica, Meteor. Planet. Sci. 34 (1999) 558–570.

CHAPTER 8

Fluorine and Its Relevance for Archaeological Studies

Ina Reiche*

Laboratoire du Centre de Recherche et de Restauration des Musées de France, UMR 171 CNRS, Palais du Louvre – Porte des Lions, 14, Quai François Mitterrand, 75 001 Paris, France

Contents

*Corresponding author.;
E-mail: ina.reiche@culture.gouv.fr

FLUORINE AND THE ENVIRONMENT, VOLUME 2
ISSN 1872-0358 DOI: 10.1016/S1872-0358(06)02008-2

Abstract

This paper represents a review of the importance of studying fluorine (F) in archaeological artefacts. Fluorine is an element which is omnipresent in water and soil environments. Thus, it is incorporated into archaeological artefacts as bones or flints in different ways during their burial depending on the geochemical conditions and on the artefact conservation state. The incorporation pathways of F lead to different F distribution patterns in the artefacts. Therefore, these artefacts can be considered as geochemical archives for the reconstruction of their burial history. Moreover, studies of F in ancient bone material or flints can give precious information that are relevant for archaeological purposes as e.g. post-mortem diagenesis. In some cases, relative dating or evidence for heat processes of artefacts is possible.

In the introduction, the paper gives a review of general questions in archaeology and relevant examples where analytical studies can give answers to.

Then, ancient materials where F is found are presented. The study of F in archaeology is particularly important for materials as bones and flints. Therefore, the majority of the paper is dedicated to the study of these materials and the information deduced on the past.

The knowledge of the composition and structure of both types of material is necessary for the understanding of the F incorporation, and is briefly reviewed. Furthermore, postulated incorporation mechanisms of the F uptake over time are reported.

In the next paragraph, the most commonly applied analytical methods for F detection in archaeological artefacts are presented. Specific problems related with the analysis of precious and unique artefacts are discussed.

Significant archaeological case studies are shown and discussed to highlight the importance of F studies in archaeological artefacts. However, these examples enable us to evidence the limits of F relevance in archaeology and the precautions to take when using these data for archaeological interpretations. Finally, conclusions and an outlook are presented.

1. INTRODUCTION

This paper reviews studies of fluorine in artefacts of cultural heritage and archaeology. F is an element which is omnipresent in water and soil environments. It can be incorporated into archaeological artefacts such as bones or flints in different ways during their burial, depending on geochemical conditions and artefact conservation states.

Generally, archaeological artefacts are studied in human sciences by a stylistic approach, their burial context and by comparison of the material with written sources. However, some relevant questions in archaeology also concern the material origin, fabrication technologies and dating of the objects. Indeed, a part of this information is recorded in the chemical composition or structure of the artefacts at different levels. It can be assessed by analysing major, minor or trace constituents or by investigating the specific signatures impregnated on the macro-, micro- or even nanoscopic scale of the material. Therefore, the analysis of objects of cultural heritage can be very helpful to gain complementary information on past populations and their level of technological knowledge. The fields of physico-chemical studies of archaeomaterials – often called archaeometry – have developed several objectives as e.g. the determination of the exact nature of materials, their provenance, chronology and the study of fabrication techniques. It also includes the study of alteration phenomena in order to better evaluate the informative potential of the archaeological artefacts and to develop well suited conservation strategies. Biological, geological and remote sensing studies also belong to the fields of archaeometry.

In this viewpoint, analytical studies of the F concentrations and distributions in archaeological artefacts can also give information about their state of preservation or inversely their post-mortem alteration processes (diagenesis) that have affected the material composition and structure. In some special cases, relative dating of the objects or evidence of technological knowledge of past populations is possible. Indeed, the idea to use F uptake in bone material for dating purposes is not new and was already proposed in the 19th century by Middleton and Carnot [1,2].

2. FLUORINE-CONTAINING ANCIENT MATERIALS OF ARCHAEOLOGICAL INTEREST

The study of F in archaeological materials is mostly focussed on bone materials or flints. Therefore, this paper is mainly dedicated to the study of these materials and their potential for revealing information on the past; some applications of F studies in obsidian and teeth are also mentioned. The following examples illustrate the importance of the chemical and isotopic analysis for archaeological studies, in general. Prior to the presentation of F studies in archaeological bone material and flint, it is important to review their main characteristics in order to be able to adequately evaluate the output and limits of investigations.

2.1. Bone material (bone, teeth, antler)

Bones or objects made of bone material are an important part of the archaeological remains and can largely contribute to the understanding of ancient societies

as they give evidence of human or fauna occupation, climatic and environmental conditions. They are used to identify the species, their age and sex, their relativity degree, their sanitary state, to enumerate the individuals that lived at one archaeological site, to get information on their exploitation of animal herds and to deduce the use of these materials as a function of their morphology or of traces observed on the artefacts (mode of use, treating with primary materials, fabrication techniques). Concerning prehistorical times, these objects are of particular importance since there are no written sources and all information obtained on the past have to be deduced from the material discovered and their spatial distribution on an archaeological site. Basically, prehistoric remains are bone, stones, objects made of these materials, pigments and later ceramics and wood. Therefore, it is necessary to extract as much information as possible from these materials.

As a biomaterial, bone provides various information on diets and environmental conditions during the life of the individual. It also records the age in its chemical and isotopic composition. Generally, these researches on bone materials are based on specific trace elements, isotopes or isotopic ratios and more recently also on DNA studies. Namely for dating, the $^{14}C/^{12}C$ ratio and the U-Th disequilibrium are used [3,4]. Some authors also proposed the use of F penetration for dating purposes of bone [2,5–9], even if this dating method cannot be used without precautions as can be seen later in this chapter. The study on palaeodiets is based on the isotopic compositions $\delta^{13}C$ and $\delta^{15}N$ of bone. For instance, using $\delta^{15}N$ and $\delta^{13}C$ data of remaining collagen from ancient bones, Bocherens (1997) found that Neanderthal men from a Pleistocene site in Marillac (Charente, France) were essentially carnivore species and effective predators [10].

Thanks to the analysis of trace element ratios Ba/Sr/Ca, the diets at the Chalcolithic site of Pico Ramos, Basque Country, and Spain could be reconstructed [11]. At this site, archaeologists observed a late introduction of Neolithic habits suspecting a diet based on hunting or seafood because of the absence of some indicators of Neolithic lifestyle like agriculture.

An interesting application of isotopic studies in bone and teeth is the comparative analysis of Sr isotopes ($^{87}Sr/^{86}Sr$) for evidencing migration processes between childhood and adulthood. Indeed, the Sr isotopic ratio is characteristic of the geological environment of the site. Therefore, this ratio is different in soil water on the sites depending on the geological formation conditions of the rocks. Because Sr can substitute for Ca, Sr is integrated into bone minerals of the individuals. Comparing the Sr isotopic ratio in teeth and in bone allows the determination of migration processes as – contrary to teeth reflecting childhood living conditions – bone is continuously renewed and its composition thus reflects the environment of the adulthood [12].

The morphology and structure of artefacts at different levels can also give precious insights into ancient diseases [13]. In addition, bone material was transformed in tools or sometimes even works of art [14,15]. Bone also served as combustible;

thus, the evidence of a heat treatment is very important to understand the use of primary material in the past and during the evolution of past populations [16–20].

It is important to understand the alteration phenomena of old artefacts, especially for the conservation of objects of our cultural heritage. This understanding enables a better evaluation of the reliability of the information that can be extracted from the investigation and observation of the objects. Furthermore, it allows the establishment of adequate conservation and restoration treatments. Therefore, many studies are devoted to the estimation of the state of preservation of archaeological objects [21–34]. Among them, several studies treat the uptake of trace elements including F in bone as an indicator of specific alteration processes [27–29,31–34].

2.2. Flint

Flints are materials largely used during prehistoric times, thanks to their hardness and relative homogeneity on a macroscopic scale. Their structure – fine silica grains at the microscopic scale – enables cutting which makes them perfect primary materials for the fabrication of different kinds of tools. After the cut, a new surface is created with a composition and structure corresponding principally to the heart of the stone. The various uses of the flint object leave traces on this surface depending on the kind of utilisation (use wear) and the burial environment. Often this surface alteration is accompanied by the transport or diffusion of chemical elements. The advancement of this process depends on many parameters and mainly on the surface state of the chipped flint and on the burial time. Therefore, some authors proposed to use – analogously to relative dating of bone using F depth profiles – these F profiles for dating chipped flints [35].

2.3. Obsidian

Obsidian, a volcanic glass, is generally formed when volcanic lava comes in contact with water. Often the lava pours into a lake or an ocean and is cooled quickly. This process produces a glassy texture. Many studies are devoted to the determination of source sites as it is a very widespread material in prehistory used for tools [36]. Coote *et al*. [37] examined 120 specimens by means of proton-induced γ-ray emission (PIGE) and found that the F/Na ratio is well suited to distinguish between different source sites. Melanesian obsidian was studied using the same method [38,67].

3. DESCRIPTION OF THE CHEMICAL COMPOSITION AND THE STRUCTURE OF BONE MATERIAL AND FLINT

The knowledge of the composition and structure of both types of material is necessary to understand a possible F incorporation process. These features and their use for archaeological purposes will be briefly reviewed below.

3.1. Characteristics of bone material

3.1.1. Chemical composition

Bone, dentine, ivory and antler are composite materials made of an organic and inorganic fraction, which are intimately mixed on a nanometric scale. The organic phase (20–30 wt.%) is mainly composed of a collagen matrix. Collagen is a protein macromolecule whose formula can be resumed as $(Gly\text{-}X\text{-}Y)_{338\pm2}$, where Gly is the amino acid glycine, and X and Y are other amino acids such as proline and hydoxyproline. The inorganic phase (60–70 wt.%) corresponds to a poorly crystalline carbonate-hydroxyapatite ($Ca_{10}(PO_4)_{6-x}(CO_3)_x(OH)_{2+x}$, carb.HAP) with a hexagonal crystal lattice ($P6_3/m$). In addition, bones contain about 10 wt.% of water. The dentine apatite phase is amorphous, whereas irregular nanometric apatite crystals can be found in bone [17]. Antler shows more acicular crystals [33]. Bone, dentine, ivory and antler can be considered having similar composite chemical compositions, even if the structure of dentine or ivory is slightly more complex than that of bone and antler due to a different arrangement of collagen fibres [39,40].

The F content in recent bone or dentine apatite is normally less than 0.1 wt.%. For ancient specimen, F is known to diffuse during burial into bone material. Its enrichment is generally a part of many complex diagenetic changes of bone and tooth, which remains after their deposit. Fluorine can react with the bone and dentine mineral phase to form calcium fluoride compounds. It usually substitutes for hydroxyl ions in hydroxyapatite, leading to the less soluble fluorapatite compound ($Ca_{10}(PO_4)_6(F)_2$, FAP).

3.1.2. Macrostructure and mesostructure of bone

Compact bone like long bones, most abundant among archaeological bone remains, shows basically two different parts: a central one called diaphysis, mainly composed of compact bone, and two extremities called epiphysis which are more porous. It contains a fundamental substance – a mixture of the organic and mineral phase – and cells that remodel continuously the bone material as well as the so-called Haversian systems containing channels that provide the nutrition to the bone cells as they accommodate blood vessels and nerves. The Haversian channels exhibit diameters between 10 and 70 μm [26]. The periosteum closes the bone at its outside and the medullar cavity at the inside accommodating the bone marrow [40].

3.1.3. Micro- and nanostructure of bone

The key of the mechanical and physico-chemical properties of bone lies in its micro- and nanostructure. The apatite crystals of the mineral phase are nanocrystalline and irregular platelet shaped with dimensions in the range of

$(25 \times 50 \times 2)$ nm. These crystals are embedded in the organic fraction, which builds the bone's fundamental structure. About 1000 amino acids form each of the three protein chains (two $\alpha 1$ and one $\alpha 2$) that are arranged forming a triple helix of 3000 Å length and of a diameter of 15 Å. These fibrils are staggered and are more or less aligned with the fibril axis to form a three-dimensional framework of the collagen fibres in which the crystals can, at least partly, be embedded as proposed by the model of Hodge and Petruska (1963) [39]. The holes between fibrils are continuous and form a channel or groove of a width of 680 Å. Apatite crystals can thus be located in the channels or gaps inside or outside the fibrils [39]. These structural features are very important for the study of diffusion of chemical species in archaeological bone and seem to have been neglected by many authors when having determined the diffusion coefficients [5,41–47].

3.2. Characteristics of teeth

Teeth are composed of different parts: enamel at the outer surface, then mainly dentine, cementum and pulp. Dentine has basically the same composition as bone, in contrast to enamel, which is composed of 96 wt.% of well crystalline carb. HAP. The enamel crystals can reach up to 1 μm length.

3.3. Characteristics of antler

Antler is the outgrowth of bones of animal scalps. It is made of bone tissue covered with velour during growth. This tissue is formed by porous bone in the centre and compact bone outside [48]. Antler has the particularity that it is lost and renewed every year. So, it is a very rapidly growing material. Antler has a chemical composition very similar to bone and dentine. It also bears two different components: an organic matrix made of collagen and an inorganic fraction basically composed of HAP. The weight fraction of the organic matrix is slightly higher than in bone or dentine. This feature gives antler very elastic properties. In addition, it contains an amorphous substance formed by glycoprotein and mucopolysaccharide [49]. This later substance permits the growth of antler. The tissue has a lamellar structure that is crossed by longitudinal and circular vessels.

3.4. Characteristics of flint

Compared to bone material, the composition and structure of flint is much simpler. Flint takes part in the big family of silicon-containing sedimentary rocks. It is basically composed of homogeneous microcrystalline silica grains, which give it a homogeneous macroscopic aspect. The name flint especially defines rocks where the cortex is thin and the heart of the stone is characterised by the absence of calcite. The majority of flint is found dispersed in sediments or as subcontinuous

chains. Very often flints also contain microfossils, quartz *lepispheres* and chalcedony, a water-rich form of silica, acting as an interstitial cementum [50].

4. INCORPORATION OF FLUORINE

4.1. Incorporation of F into bone

A diffusion theory and various methods of analysis of F in bone are described in detail by M. Döbeli *et al*. in this volume. Therefore, only a brief summary of F transport phenomena in archaeological bone material is given here. Quite a few data are known and most without description of the supposed transport mechanism. Generally, the reported diffusion coefficients for bone at ambient temperature are much higher than those of enamel. Differences of several orders of magnitude ranging from $10^{-8}\,cm^2/s$ in bone to $10^{-17}\,cm^2/s$ in enamel crystals are observed. Thus, the apatite structure is not an adequate model material to establish a reliable diffusion model for archaeological bones during the burial time. These data show the importance of a pertinent diffusion theory that takes adequately into account the effects of intrinsic material properties of bone-like apatite crystal size, microstructure and porosity as well as the influence of diagenetic modifications, especially the degradation of organic matter, and hydrological parameters of the burial environment.

Consequently, the following incorporation mechanism can be proposed: F is taken up by bone due to the interactions of bone minerals with the pore water transporting F. As the organic fraction is intimately mixed, at the nanometric scale, with the mineral one, it has a protecting effect on the mineral phase. Fluorine can only interact with the apatite phase if the organic fraction is, at least partly, degraded and leave spaces in the bone structure. So the partial degradation of the organic fraction should precede the adsorption and the subsequent substitution of OH by F in the apatite matrix. As another consequence of the degradation of the organic fraction, the bone porosity increases and more pore water can interact with the bone mineral phase. Contrarily to what was formerly presented [5], diffusion of F within the channels of the apatite structure does not influence significantly the F uptake, since the apatite crystal size (smaller than some 10 s of nm) is too small compared to its surface and this process may be thus neglected. Fluorine is taken up by the bone mineral by a transport-reaction mechanism, where F transport takes place at grain boundaries and through interconnected bone pores and then reaction transforms partly or completely carb. HAP into carb. FAP. Simultaneously, the pore water can also contribute to the dissolution of bone hydroxyapatite and partial replacement by precipitation of less-soluble fluorapatite. This mechanism can explain why bone is not enriched in F under dry conditions and also why even old samples with a high content of initial organic matter show a very low F content [51].

4.2. Incorporation of F into tooth

Because of the complex structure of teeth, simple F depth profiles from the outside to the inside of teeth cannot easily be used for dating or other archaeological purposes. Former studies on F enrichment over time in tooth showed that F ions in sediment water enter the tooth through the nerve channel and are deposited on the pulp cavity before they diffuse outward through the dentine and may reach the enamel. An undamaged tooth is well sealed from F, whereas dentine that was exposed to F after the removal of enamel or cementum layer can as easily take up F, as bone. Therefore, interior profiles on dentine were proposed for relative dating of teeth. However, these studies did not give very conclusive results [5]. A review of post-mortem uptake of F by teeth is given in Ref. [52].

4.3. Incorporation of F into flint

The F uptake of flint takes a much longer time than that for bone. Fluorine diffusion into the depth of flint material is controlled by defect clusters. The diffusion coefficient determined by implanting a model compound (amorphous silica bombarded with heavy ions and hydrated at 100°C) is 9.10^{-21} cm^2/s at room temperature. The corresponding penetration depth of F under ambient conditions in a 1000-year-old artefact can be estimated via $x = (Dt)^{1/2} = 0.17\,\mu m$ [50]. Thus, F accumulates only in the first micrometre of the surface. The surface of ancient flint artefacts can be altered by dissolution. The occurrence of this phenomenon is especially important in basic media. However, in some cases, the thickness of the dissolved layer can be neglected compared to the F penetration depth at low temperatures. Therefore, Walter *et al*. [35] proposed relative dating of chipped flint by measuring the full width at half maximum (FWHM) of F diffusion profiles in theses cases.

5. FLUORINE ANALYSIS OF ARCHAEOLOGICAL SAMPLES

5.1. Specific requirements for the analysis of archaeological artefacts

Generally, objects of our cultural heritage are not only characterised by their rareness or precious nature, but they are often heterogeneous and complex materials. Complementary analytical methods and examinations at different scales are necessary to obtain reliable results. These investigations should be as non-invasive as possible. Furthermore, databases established on the analysis of artefacts of known origin and age are needed for comparison. The analytical strategy depends on the archaeological issue, the object type, the quantity and complexity of material, its degree of degradation and whether sampling is possible or not [53].

5.2. Analytical methods for F detection

In the following paragraph, the most commonly applied analytical methods for F detection in archaeological artefacts are presented (Table 1). In art and archaeology, the method of choice for F analysis is without any doubt particle (or proton)-induced γ-ray emission (PIGE, sometimes also called PIGME) [5].

Other analytical methods can also be applied for the detection of F in archaeological artefacts, especially when it is possible to take a sample or to perform microdestructive analysis. These are namely the electron microprobe with a wavelength-dispersive detector (WDX), secondary ion mass spectrometry (SIMS), X-ray fluorescence analysis under vacuum (XRF), transmission electron or scanning electron microscopy coupled with an energy-dispersive detector equipped with an ultrathin window (TEM/SEM-EDX). Fluorine can also be measured by means of classical potentiometry using an ion-selective electrode or ion chromatography.

5.2.1. Particle (or proton)-induced γ-ray emission

PIGE is very sensitive (the limit of detection can be as low as 1 ppm) and non-destructive. It allows analysis of bulk F, F-distribution within one sample on cross-sections or depth profiles using resonant nuclear reaction analysis (RNRA) [35]. The spatial resolution, even using a beam of some micrometres size or RNRA, is however insufficient to detect F on individual bone crystals. The RNRA method is reviewed in detail in the chapter of Döbeli *et al*. [6] in this volume.

Two different nuclear reactions are currently used for PIGE; they are extensively described in Ref. [6].

5.2.1.1. The AGLAE accelerator

PIGE and micro-PIGE have been performed simultaneously with proton-induced X-ray emission (PIXE) at the external beamline of the particle accelerator AGLAE at the Centre of Research and Restoration of the French Museums, Paris, France. AGLAE is an electrostatic tandem 2 MV accelerator (6SDH-2 2 MV tandem Pelletron NEC) [54]. At this beamline, 3 MeV protons are extracted in an He atmosphere through either a 10 μm Al, 2 μm Ti or 0.1 μm Si_3N_4 exit foil. Each spectrum is obtained with a dose of 0.1–0.2 μC and a current of about 0.5 nÅ. The extracted proton beam can be restricted to different beam diameters as a function of the set-up and the exit foil. Using a 10 μm Al or 2 μm Ti exit foil, a focussed beam of ˜150 μm diameter can be obtained (PIGE). The recent development of the exit set-up with an Si_3N_4 exit foil allows the production of a microbeam with a diameter of about 10–100 μm (micro-PIGE) [54]. The beam intensity is monitored by detecting the protons backscattered from the exit foil or, in the case of the

Table 1. Characteristics of analytical techniques used for F detection

Analytical technique	Non-destructive analysis possible (conservation of the sample after analysis)	Sample quantity required	Sample preparation	Analysis type	Spatial resolution	Limit of detection
F electrode	No	100 mg	Dilution in aqueous solution	Surface or bulk analysis as a function of sampling	–	Some tens of ppm
Ion chromato-graphy	No	A few mg	Dilution in aqueous solution	Surface or bulk analysis as a function of sampling	–	200 ppm
SEM/TEM-EDX	Yes	mm or μm sample	Metallisation for SEM/ deposit of powder on Cu or Au grid or thin section for TEM	Surface analysis/ surface or bulk analysis as a function of sampling	Some hundreds of nm/some hundreds of Å	1 wt.%
Electron microprobe WDX	Yes	mm or μm sample	Metallisation	Surface analysis	Some hundreds of nm	0.5 wt.%
X-ray fluores-cence (XRF)	Yes	mm or μm sample	Not necessary	Surface analysis	Some tens of μm in air, sub-μm in vacuum	1 wt.%
SIMS	No	mm or μm sample	Flat surface for analysis under vacuum	Surface analysis, depth profile	Some metre in depth	Some ppm
NRA (PIGE)	Yes	No sampling necessary	Not necessary when analysing in air	Surface analysis (ca. 50 μm analysis depth), depth profile	Some μm in air	50 ppm

microbeam, by detecting the X-rays emitted by Si from the exit foil. Fluorine content has been determined using the nuclear reactions induced by the incident protons $^{19}F(p,p'\gamma)^{19}F$ emitting γ-rays of 110 and 197 keV (Fig. 1). The latter one can also be a product of another nuclear reaction on oxygen-18 ($^{18}O(p,\gamma)^{19}F$). But Coote [5] showed that this interference has only a small influence on F concentration measurement. Its contribution is far below 50 ppm, thus in the range of the statistical error of the measurement. The γ-rays at 6.13 MeV produced by the nuclear reaction $^{19}F(p,\alpha\gamma)^{16}O$ and its escape peaks could also be used for determining the F concentration. Nevertheless, the detector efficiency is not high in this energy region. The γ-rays used for F quantification at 110 and 197 keV are detected by an HPGe detector at about 5 cm from the sample and at an angle of 45° or 90° with the incident beam, depending on the sample size. The detector resolution is 1.7 keV for 1.33 MeV γ-rays from Cobalt-60. A polished geological FAP crystal from Durango is used as an F standard. Its F content (3.27 wt.%) is confirmed from potentiometric measurements using a specific electrode. The limit of detection of this method is about 50 ppm [27,32].

For PIGE measurements, transverse bone sections are cut with a diamond saw and polished with SiC paper, and then placed directly in front of the external proton beam. It is not necessary to coat the sample surface with a conductive layer as the charges are dissipated in air and helium. Step width of the concentration profiles is determined by precisely recorded sample translation in front of the beam. The above experimental conditions were used for F analysis in archaeological bone materials in the applications described in this chapter.

The measurements of F depth profiles in chipped flints have been realised using the 4.7 keV wide 872 keV $^{19}F(p,\alpha_{1\cdot2\cdot3}\gamma)^{16}O$ resonance. This reaction provides a good depth resolution (about 100 nm in SiO_2). The 4–7.5 MeV γ-rays are detected with a BGO (bismuth germanium oxide) detector at 0°C with respect to the incident beam. The flint artefacts can be settled in the vacuum chamber as whole pieces without any sample preparation [35].

5.2.2. Electron microprobe

The electron microprobe provides an adequate tool to measure F. Even if its sensitivity is less compared to that of PIGE and SIMS, it has the advantage to be more easily accessible and to allow F analysis with a spatial resolution in the micrometre range. For F analysis using the electron microprobe, BaF_2 is often used as reference sample, and a W/Si multilayer pseudocrystal is used for the detection of the Kα line of light elements. The sensitivity reached with this method is in the range of 0.5 wt.% [55].

5.2.3. Secondary ion mass spectrometry

SIMS is a very powerful tool to analyse materials with a high depth and lateral resolution in the nm or 10s of nm region, respectively [42]. It has a high

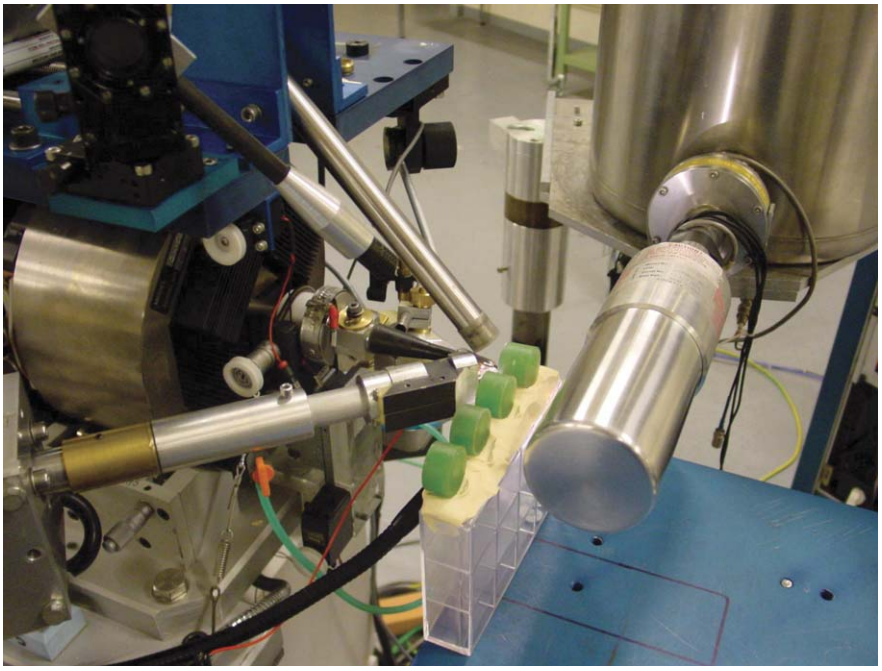

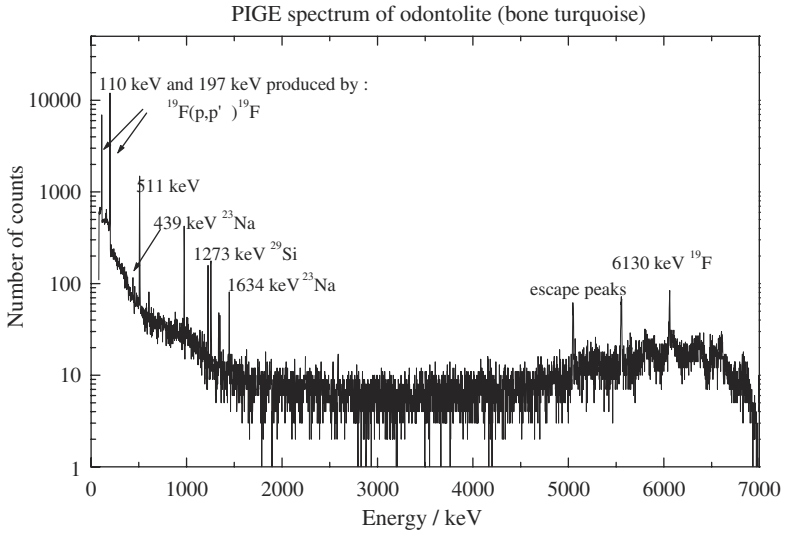

Fig. 1. View of the external microbeamline set-up at the AGLAE accelerator with the sample holder and the detectors (Copyright C2RMF, Paris). 3 MeV PIGE spectrum of odontolite showing the γ-rays used for quantitative F analysis.

elemental and molecular specificity and allows simultaneous analysis of elements down to the ppm or even ppb range depending on the ionisation yield of the material. However, SIMS requires a particular sample preparation for analysis under vacuum conditions and parts of the sample are ablated during analysis [42,56,57]. The sample is bombarded with a mono-energetic-focussed ion beam with energy in the range of 0.2–30 keV. A collision cascade is generated in the material initiating among other phenomena ionisation and emission of atomic or molecular species that are separated by a mass spectrometer. Generally, SIMS can be performed in a static or dynamic mode; the latter one penetrating slowly the sample while analysing. This allows depth profiling and is, therefore, very interesting for many applications in the field of cultural heritage, including the analysis of F depth profiles in bone material or flint. In a study of human and shark teeth, primary negative oxygen ions were used for F depth resolved analysis on prepared cross-sections with sensitivity in the 10 ppm range [58].

5.2.4. Transmission electron or scanning electron microscopy coupled with an energy-dispersive detector

The big advantage in using TEM-EDX for the determination of F in bone is that it allows to measure the F concentration of individual nanocrystals [32–34]. For TEM-EDX measurements, a microsample of bone is grounded manually, because of the problems during the preparation of TEM thin sections. Only 0.1 mm^3 of the sample powder are necessary. A suspension is deposited onto a carbon-coated Au or Cu grid. Energy-dispersive X-ray (EDX) analysis can be performed using an Si(Li) detector equipped with an ultrathin window providing the detection of light elements as F with a detection limit of 1 wt.%.

5.2.5. Potentiometry

An ion-specific electrode can also be used for classical measurement of F in a sample solution. Its principle is the same as that of a pH electrode. A voltage proportional to the F amount in the solution is measured that will be compared to a calibration curve obtained by measuring standard solutions of known F concentration. At least 0.1 g of bone is necessary for each analysis [59]. Fluorine gradients were also measured in the past by stepwise grinding or etching and analysis of successive surface layers. This method is sensitive down to about 50 ppm F [57].

6. EXAMPLES OF ARCHAEOLOGICAL STUDIES

In this paragraph, studies concerning dating of flint by F diffusion profiles, investigation of F in the frame of recording different bone diagenesis pathways depending on the burial environment and effects of heat treatment on F uptake are discussed. Finally, the analysis of a turquoise gemstone imitation mainly

composed of FAP is described. These studies also allow the evidence of the limits of F relevance in archaeology and the precautions to take when using these data for archaeological interpretations. This is especially the case when F depth profiles are used for dating purposes of bones. These later studies being reviewed in the chapter of Döbeli *et al*. [6], have been omitted in the following sections.

6.1. F dating of flints: the case of arrowheads from the Fort Harrouard prehistoric site (Eure et Loir, France)

Fort Harrouard prehistoric site was occupied from the Neolithic (4500 BC) to the roman period (500 AD). A particular archaeological problem occurred during the excavation. A very similar type of bronze and flint arrowheads was found within the same stratigraphical layer suggesting that either Neolithic and Bronze-Age layers have been mixed or that Bronze-Age inhabitants had used Neolithic artefacts. An alternative hypothesis is that bronze and flint technologies existed simultaneously in the Bronze Age. The flint material originates from the Grand Pressigny mine. This kind of flint was widely used in the Western European Upper Neolithic period. Fifteen flint artefacts were studied. The F depth profiles of the artefacts were U-shaped, independently from the measured position on the surface (Fig. 2, see Ref. [35]). Modern flint, e.g. from Grand Pressigny has flat profiles. Artefacts from the same stratum showed similar profile width within the measurement uncertainties. The profile width increases with the estimated age of the artefacts (Fig. 3, see Ref. [35]). These results seem to confirm that relative

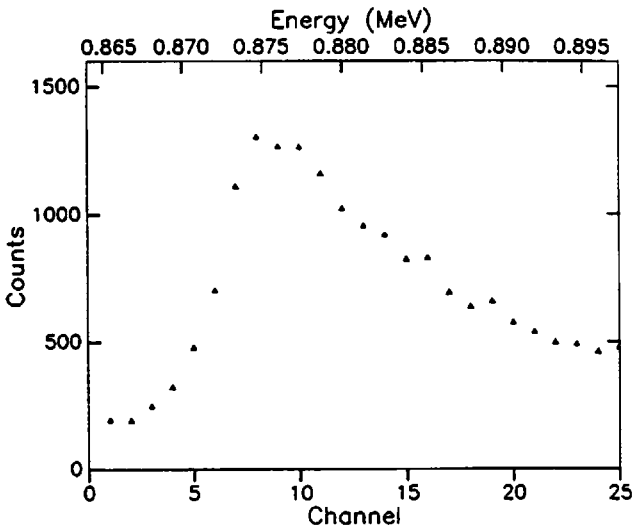

Fig. 2. F concentration profile in Bronze-Age flint from the archaeological site of Fort Harrouard, France (4500 BC–500 AD). (Reproduced by permission of P. Walter *et al*., Nucl. Instrum. Methods Phys. Res. B 45 (1990) 119–122.)

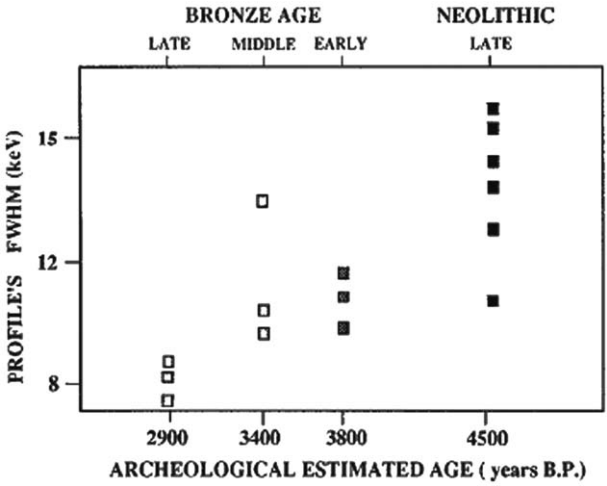

Fig. 3. Correlation between FWMH of the F profile and age of the flint specimens from Fort Harouard site. (Reproduced by permission of P. Walter *et al.*, Nucl. Instrum. Methods Phys. Res. B 45 (1990) 119–122.)

dating of the arrowheads from this site using F depth profiles is possible. The data obtained on flint arrowheads from Bronze-Age stratum evidence that they were still manufactured during Bronze Age. Therefore, the hypothesis that bronze and flint technologies existed simultaneously at this site could be confirmed [35].

6.2. Bone diagenesis studies

If archaeological material is buried, it is constantly in contact with sediments, soils and interstitial water. The chemical composition and structure change consequently by partial or complete dissolution, erosion and transport phenomena from the environment into the artefact and vice versa. The resulting state of preservation can be very variable, from well preserved to complete dissolution. It depends largely on the direct environmental conditions (pH, Eh, chemical composition of the soil and the interstitial water, pressure, biological factors, particle transport depending on grain size and porosity). The modifications can false the archaeological interpretations based on the elemental and isotopic composition of bone and can also be a problem for the conservation of unique artefacts. Thus, it is of utmost importance to understand the alteration processes (diagenesis) in soils, especially the transport processes and the impact of the environmental conditions on bone preservation. As these alteration mechanisms are complex, the study of the state of preservation and of the diffusion processes needs various complementary analytical tools that are also adequate to reveal the particular structure and the modifications of the bone material.

Chemical characterisation of F uptake in archaeological bone has already been developed in the 19th century [1,2] and is now well established [60]. However, relatively few studies use a combined multianalytical approach using trace elemental and microstructure analytical techniques (PIXE/PIGE, TEM-EDX) for evidencing modifications on different microscopic and nanoscopic levels (Fourier transform-infrared spectroscopy (FT-IR), X-ray diffraction (XRD), SEM, TEM) and enabling an objective evaluation of the F uptake mechanisms [32–34,51].

Some examples of the study of F uptake in archaeological bone materials are presented in this paragraph. These investigations are focussed on different tasks:

- F uptake in environments (lakeside/riverside sites) with constant hydrological regime,
- F uptake depending on the conservation of the organic bone fraction,
- F uptake in burned bone,
- F uptake in bone, dentine and antler, and
- F uptake during very long-term fossilisation.

6.2.1. Study sites and material

Examples of bones, dentine and antler fragments from various archaeological (Neolithic and Palaeolithic) and even palaeontological sites are grouped in Table 2. The chemical composition and structure of all samples were investigated. The discussion of the results especially focuses on the F concentration profiles as a function of the geochemistry of the site and of the state of bone material prior to its abandon (e.g. burned bone).

Concerning the study of F uptake in bones in different environments, results from archaeological lakeside sites dating from the Neolithic period at the lake of Chalain (layer O, station 21, 2700–2600 BC, Jura, Eastern France) and at the riverside site of Bercy (Paris, France, 4000 BC) are described in Ref. [17]. The Bercy site has the specificity to provide two different hydrological zones within one archaeological layer: an emerged zone corresponding to the ancient riverbank (N sector) and an immersed zone of the ancient river channel (L sector). The diagenetic pathways can thus be directly studied as a function of the hydrological burial conditions. The sample coming from the immersed zone of the site of Bercy (AB3) is a good example to illustrate the influence of the preservation of the organic matter on F enrichment. Differences of the F uptake phenomena in burned and unburned bones can be observed on samples from the mixed Neolithic layers HK in the lake dwellings (3030–2920 BC, station 19) situated right by the lake of Chalain that have been flooded from time to time (CH19NB3 and CH19B3). To confirm the statements, results obtained on burned bones from another Neolithic site of Gletterens (Gle81 6548 in Ref. [32]) located at the lake of Neuchâtel (3000 BC, Switzerland) are also shown. The F uptake in

Table 2. Types and names of bone, ivory and antler samples

Sample	Provenance	Sample name [32]	Age
Modern sheep bone	Unknown	MB1	–
Modern elephant ivory	Unknown	MD	–
Modern antler	Unknown	MA	–
Undetermined	Emerged Chalain lake site 19 (Jura, Eastern France)	CH19NB3	3030–2920 BC
Undetermined, burned bone	Emerged Chalain lake site 19 (Jura, Eastern France)	CH19B3	3030–2920 BC
Ox bone	Subaquatic Chalain lake site 21 (Jura, Eastern France)	CH21NB1 (AB1 in [17])	3200 BC
Undetermined bone	Subaquatic Chalain lake site 21 (Jura, Eastern France)	CH21NB2	3200 BC
Small vertebrate bone	Gletterens subaquatic lake site (Switzerland)	Gle81 6548	3000 BC
Ox bone (*Bos taurus*)	Bercy, N sector, emerged area (Paris, France)	BE (AB2 in [17])	4000 BC
Aurochs bone (*Bos primigenius*)	Bercy, L sector, immersed area (Paris, France)	BI (AB3 in [17])	4000 BC
Palaeolithic mammoth ivory	Unknown	PD	40,000 a
Palaeolithic antler	Dordogne, France	PA	12,000 a
Mastodon ivory (*Zygolophodon turicensis*)	Rajégats		
	Gers, Southern France	IVFO2 (FD in [17])	Middle miocene, 13–15 Ma
Odontolite (heated mastodon ivory)	Unknown	O3	Unknown

dentine and antler is illustrated, thanks to the analysis of F profiles in Palaeolithic mammoth dentine (PD sample, 40,000 a, unknown provenance) and antler (Magdalenian period, Les Eyzies, France). Finally, long-term fossilisation processes can be illustrated by studying palaeontological remains of mastodon dentine (FD) found in the region of Simorre, Gers, Southern France dating from the middle Miocene (13–16 Ma). For comparison, a modern sheep bone (MB1), a fragment of modern elephant dentine (MD) and of modern antler (MA) were analysed.

6.2.2. *Average F concentrations of archaeological bones, dentine and antler*

The F content of all the specimens was determined using PIGE and micro-PIGE. All ancient specimens are enriched in F in comparison to modern bone material. The detected concentrations vary from some hundreds of ppm in modern bone to 2.6–3.6 wt.% in fossilised dentine (Table 3). The highest F content has been found in fossilised Miocene dentine (FD), which is completely transformed into FAP. Neolithic bones (AB2 and AB3, 4000 BC) can contain a relatively high F amount at the border (about 1 wt.%), whereas the older Palaeolithic samples (PD and PA) only shows F traces. The mean F content is thus not directly related to the age of the sample, but to the hydrological conditions of the corresponding site and to the preservation of the organic fraction of the bone material.

6.2.3. *Fluorine enrichment measured on individual apatite crystals by TEM-EDX*

If the F concentration is high enough (>1 wt.%), it can be measured locally on individual apatite crystals by TEM-EDX. This is the case for FD [32], the degraded surface of one Neolithic bone sample (AB3), and the centre of a burned bone from Chalain 19 (CH19B3) [32]. The other bone and dentine specimens do not contain enough F to quantify or, as in the case of CH19NB3, CH21NB1 or AB1 in Ref. [17], CH21NB2 and PD, to even detect the content. PIGE and micro-PIGE are better suited for quantitative F analysis. In fossilised dentine (FD), 3.6 wt.% of F could be registered homogeneously on individual apatite crystals (Table 3). This value is very close to that of stoichiometric fluorapatite (3.77 wt.% of F).

6.2.4. *Fluorine concentration profiles on cross-sections*

The spatial distribution of F in bone material shows various characteristic patterns. The different profiles can be divided into five groups: (i) type 1: flat profiles with concentrations above or at the physiological level of recent bones, (ii) type 2: U-shaped profiles with a concentration decreasing continuously from the periosteum and from the endosteum, (iii) type 3: inverse U-shaped profiles, (iv) type 4: decreasing profiles where the F concentration is significantly higher at the periosteum (outer border of the bone) than at the endosteum (inner border of long

Table 3. Fluorine concentration of bone, ivory and antler samples determined by TEM-EDX and PIGE. [– = not measured, n.d. = not detected, d. but n.q. = detected but not quantifiable. For PIGE, the relative error lies between 1% and 5%]

Sample	F concentration on individual crystals (TEM-EDX)	Average F concentration (PIGE)/ppm	Central F concentration (PIGE)/ppm	F concentration At the border (PIGE)/ppm	F distribution
MB	n.d.	1200	–	–	Flat
MD	n.d.	145	–	–	Flat
MA	n.d.	300	–	–	Flat
CH19B3	40.7 wt.% (local CaF_2) elsewhere n.d.	1670	2500	600	Inverse U
CH19NB3	n.d.	2000	1100	4000	U
AB1	n.d.	550	n.d.	1800	U
CH21NB2	n.d.	2500	500–2000	6000	Decreasing
Gle81 6548	–	2000	1600–3400	600–1000	Inverse U
AB2	d. but n.q.	9700	9500	13,900	Decreasing
AB3	d. but n.q.	12,500	10,000	15,000	U
PD	n.d.	1200	–	–	–
PA	n.d.	150	60	690	Decreasing
FD	3.6 wt.%	3.6 wt.%	3.7 wt.%	3.5 wt.%	Flat
O3	4.4 wt.%	3.8 wt.%	3.8 wt.%	3.8 wt.%	Flat

bones, next to the medullary cavity) and the content is constantly decreasing from the periosteum to the endosteum, and (v) type 5: irregular profiles.

Flat F profiles (type 1) were either found on extremely old samples as FD with a homogeneous F content of 3.5 wt.% next to the nominal F value of FAP (3.8 wt.%), or at trace levels on recent unaltered bone material (MB1, MA and MD). Long-term fossilisation leads thus to a homogeneous F distribution in bone material.

Generally, the F distribution corresponds to a U-shaped profile (type 2). This distribution was found in specimens that have experienced early diagenetic changes. Examples are bones from the Neolithic lake sites 19 and 21 of Chalain (for instance AB1, Fig. 4) as well as from the immersed zone of the Neolithic river site of Bercy (AB3). In addition, the AB3 sample shows a slight loss of F in the outer parts very close to the periosteum which can be explained by surface erosion. When observing U-shaped profiles, F is only enriched in the bones at the surface and the F saturation level is not reached. Especially in stable, water-logged environments with a constant hydrological regime, transport reactions control the F uptake and diffusive concentration profiles can be formed. A diffusion coefficient in the order of magnitude of 10^{-12} cm^2/s could be estimated from the F concentration profile of AB3.

The measurements on AB3 are a good example of post-burial behaviour that illustrates the influence of the remaining organic fraction on the uptake of F in bone. An inverse correlation of N and F distribution profiles measured by means

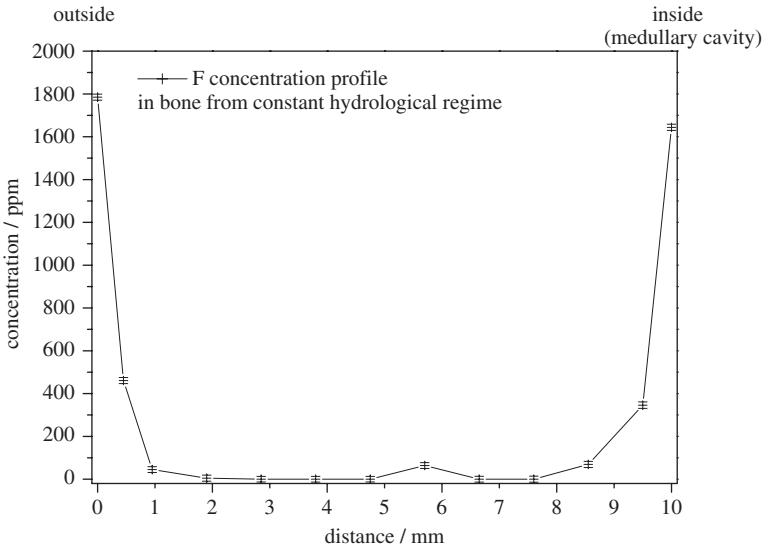

Fig. 4. U-shaped F concentration profile in a Neolithic bone AB1 from constant hydrological regime as in the subaquatic station 21 of the lake of Chalain, France. (Reproduced by permission of I. Reiche *et al.*, J. Trace Microprobe Tech. 20 (2) (2002) 211–231.)

of an electron microprobe and PIGE was observed in this specimen. As the organic fraction has disappeared at the border, it has no protecting effect on the mineral phase anymore and F enrichment is favoured [51]. On the contrary, a high amount of preserved organic matter (3.5 wt.% of N corresponding to 80% of modern bone) and a low F content have been observed in the centre of the bone AB3. Fluorine is only present in high concentrations (about 1 wt.%) at the bone surfaces where nearly no nitrogen, i.e. collagen, is left (see N and F profiles in Ref. [61]). The F transporting seems to be decelerated in this case.

Inverse U-shaped profiles (type 3) are only very rarely observed for exogenous chemical species in ancient bone material. These profiles are characteristic for elements that are present in modern bone, when they were partially leached out. This type of F profile has been also observed in the case of burned bones (Fig. 5). The proposed explanation of this distribution is that the heat process did not transform homogeneously the bone structure. Higher temperatures are reached at the sample surface compared to the bulk resulting first in the partial or complete degradation of the organic matter, and secondly in differentiation of crystallinity at the border and in the centre of the specimen. In addition, differential loss of combustion products can limit the crystal growth in the inner bone parts, but the increase in crystal size can proceed easily in the outer parts. Fluorine in the interstitial water circulates in the porous bone material during burial and can be mainly fixed by a reaction with small crystallites in the bone centre compared to the larger crystals at the bone border. Small apatite crystals provide a larger specific surface for F reaction. This statement was confirmed by TEM. It showed

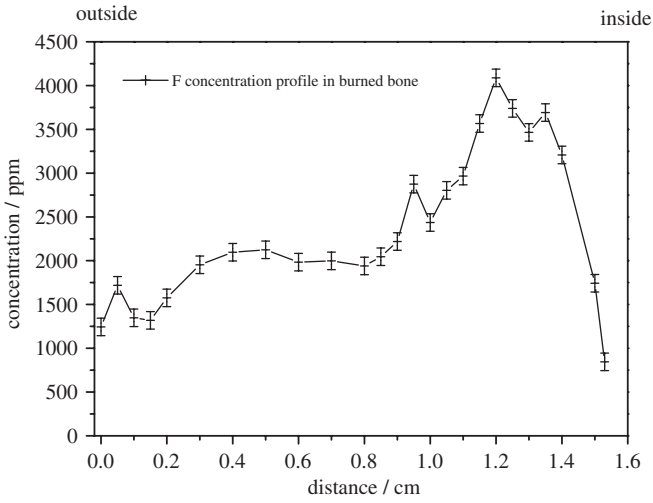

Fig. 5. Inverse enrichment F concentration profile in a Neolithic burned bone from the site of Gletterens, Switzerland. (Reproduced by permission of I. Reiche *et al*., J. Trace Microprobe Tech. 20 (2) (2002) 211–231.)

higher crystal size and a polygonal apatite morphology at the bone surface of burned bone that is different from the smaller crystal size with an irregular or acicular morphology in the centre of the burned samples from Chalain 19 (Fig. 6) [32]. In the bone surface region, the polygonal morphology corresponds to re-crystallisation induced by a heat process [17]. In contrast, needle-shaped crystals in the bone centre are characteristic of dissolution–recrystallisation phenomena. That is why, such inverse U-shaped PIGE profiles correlated to the specific

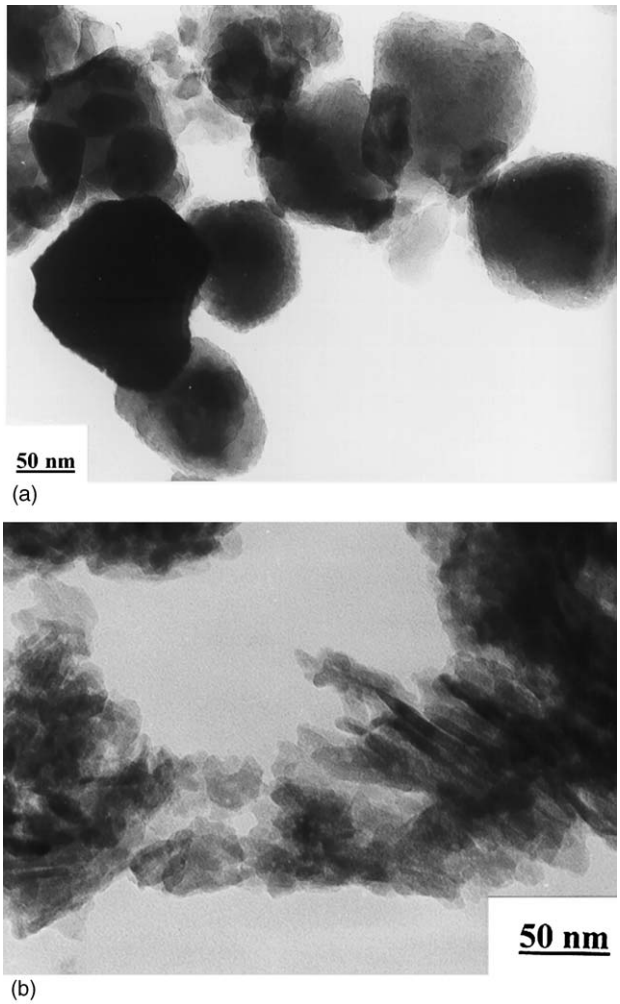

Fig. 6. TEM micrographs of apatite crystals in burned bone (a) at the outside showing higher crystal size and a polygonal apatite morphology, (b) at the inside of the sample with smaller crystal size with an irregular or acicular morphology. Example: burned bone from HK layer, station 19 of Chalain lake. (Reproduced by permission of I. Reiche *et al*., J. Trace Microprobe Tech. 20 (2) (2002) 211–231.)

shapes of apatite crystals observed by TEM could be used as an indicator of heat transformations on ancient bone samples before burial which is crucial information in archaeology, especially for very old sites evidencing first intentional use of fire.

Examples showing a decreasing profile (type 4) are the sample from the emerged zone in the Neolithic riverside site of Bercy (AB2), one bone from Chalain station 21 (CH21NB2) and the Palaeolithic antler [33] (Fig. 7). The F transport-reaction mechanism should be the same as the one leading to the U-shaped profile. However, either the morphology of the artefact is responsible for the formation of this kind of profile or the cycling of the hydrological regime (successive wet and dry periods) favours phenomena as dissolution, precipitation of secondary minerals as well as lixiviation that can accelerate or decelerate the F transporting and thus modify the general F U-shaped distribution.

Last but not least, irregular F concentration profiles (type 5) can be observed indicating an inhomogeneous F distribution. Possible origins of these distribution patterns could be the superimposition of several simultaneous phenomena as F enrichment coupled with the loss of the apatite or the formation of secondary phases as CaF_2.

6.3. Odontolite: a turquoise bone material

A special bone material containing high amounts of F and its use as gemstone is treated in this paragraph. In the Middle Ages, turquoise bone fragments (odontolite) were used among other stones to adorn reliquary objects (Fig. 8). This gem was not immediately recognised as being fossil bone material even if the property of fossilised bone and ivory from Southern France to turn blue upon heating was already known in the Middle Ages [62].

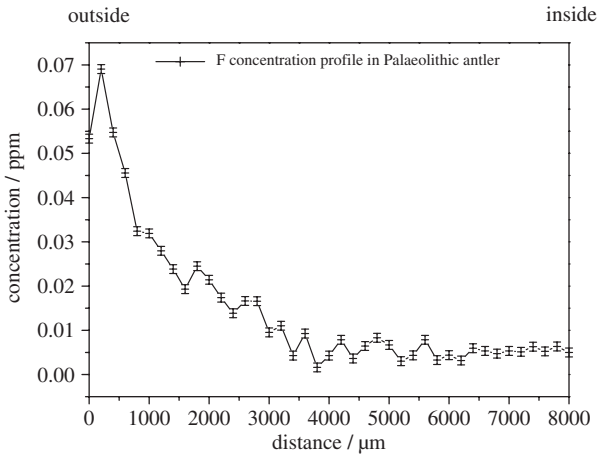

Fig. 7. Decreasing F concentration profile measured on Palaeolithic antler from National Museum of Prehistory, Les Eyzies, Dordogne, France (unpublished data).

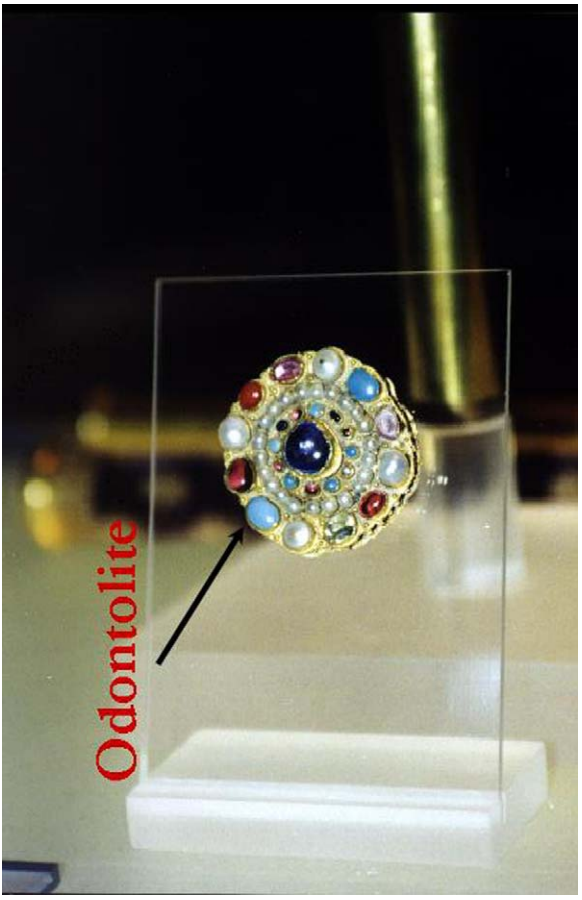

Fig. 8. "Anneau de St. Denis", XIIIth c., France. Object of the Louvre museum containing as adorning stone an odontolite among other turquoises.

In 1715, the famous French naturalist Réaumur reported the existence of a small industry in Southern France which produced turquoise from old bone remains [63]. He observed that these bone artefacts could be transformed into a turquoise-blue material by heating. He thought that the mineral turquoise, a phosphate salt of aluminium and copper ($CuAl_6(OH)_8(PO_4)_4.8H_2O$), was produced this way. However, his hypothesis was solely based on the resemblance with precious turquoise. In 1823, Fischer recognised that odontolite and turquoise mineral were different minerals [64]. Until very recently, the origin of odontolite has remained the object of controversy. In order to shed new light on the nature of this material, spectrochemical analyses were carried out on odontolites from different collections of the National Museum of Natural History, the Louvre museum and the National Museum of the Middle Ages. Furthermore, fossilised ivory fragments

originating from Palaeontological sites (Rajégats and Malartic) in the Gers, Southern France, have been investigated [65]. Indeed, this area is supposed to be the same place where Cistercian monks discovered the fossilised ivory precursor for odontolite production in the Middle Ages. These remains were submitted to successive heating experiments in air at 400/600/800/940°C for 8 h in order to verify that the turquoise-blue colour appears after a simple heat treatment [15,16].

Micro-PIXE and -PIGE were used for the non-destructive and complete analysis of the chemical composition of the artefacts [34]. These methods clearly showed that the collection of odontolites and the fossilised ivory fragments are composed of FAP, containing traces of Fe (230–890 ppm), Mn (220–650 ppm), Ba (160–620 ppm), Pb (40–140 ppm) and U (80–210 ppm). Indeed, the nominal amount of 3.8 wt.% of F in FAP is reached in most of the samples (Fig. 1). As modern bone and ivory bear only trace amounts of F, this homogeneous enrichment as well as those of the other elements mentioned above is indicative of a long-term fossilisation process. The crystal structure of the artefacts was determined by electron diffraction in TEM and corresponds indeed to a well-crystallised FAP (single crystal diameters between 100 and 500 nm) in the odontolites (Fig. 9). In fossilised ivory, the size of FAP crystal varies as a function of the heating temperature. Heated ivory to 600°C shows FAP crystals with sizes of about 10 times larger than that of unheated fossil ivory which presents only grain sizes of 10–30 nm. This observation together with the lack of any remaining

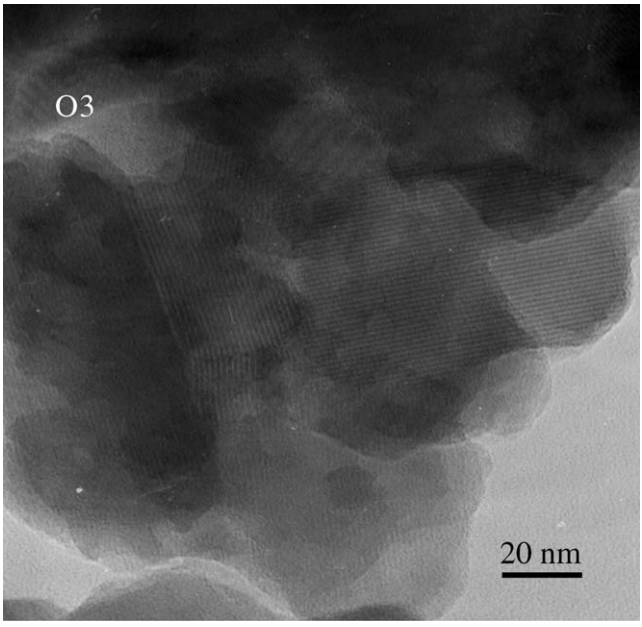

Fig. 9. TEM micrograph of apatite crystals in the odontolite sample (O3) from the mineralogical collections of the National Museum of Natural History, Paris.

organic material is indicative for a heating process [17]. However, the elemental and structural investigation did not provide a proof for the colour origin in the principally FAP-containing bone remains. Therefore, other spectroscopic methods as time-resolved laser-induced luminescence spectroscopy (TR LIF) and X-ray absorption fine structure analysis (XAFS) have to be used [15,66].

Thanks to these analytical methods, the nature of odontolite could be finally clarified. Its formation involves two phenomena: (i) a long-term alteration (fossilisation) including the uptake of different ions as F and Mn followed by their diffusion along grain boundaries, adsorption on apatite crystals and possibly their incorporation in the apatite structure, and (ii) a deliberate heating process in air above 600°C that oxidises Mn^{2+} into Mn^{5+} and induces simultaneously crystal growth of apatite. Thus, odontolite is a material mainly composed of FAP that owes its turquoise colour to an intense O^{2-}-Mn^{5+} charge transfer [15]. It should be noted that such a colouration process was also found in Mn^{5+}-doped synthetic fluorapatites [68].

7. CONCLUSIONS AND FUTURE OF FLUORINE STUDIES IN ARCHAEOLOGY

In this chapter, the contribution of F studies on archaeological bone materials (bone, dentine, antler and teeth) and on chipped flints are reviewed. These studies illustrate the information that can be deduced from F studies in ancient material. The most well-known application of F distribution studies is the F dating method. In a general manner, archaeologists and archaeometrists now agree that F dating of bone and flint can only be considered under very special conditions and when further indications permit to confirm the results obtained by F dating studies. However, other interesting information can be obtained by the study of F contents and profiles in archaeological objects, such as the determination of modifications by different alteration phenomena depending on burial conditions or heat treatments. In addition, a special turquoise bone material, odontolite, composed of fluorapatite and formed by fossilisation including important F uptake and by further deliberate heating is described and its use as a gemstone in medieval reliquary objects is demonstrated.

In the future, detailed studies of fluorine in archaeology will help to better assess modifications of ancient objects in soils and to develop adapted conservation strategies for precious and unique archaeological materials.

ACKNOWLEDGEMENTS

H. Bocherens is thanked for providing samples from the Bercy site, P. Pétrequin for the samples from the Chalain lake sites, D. Ramseyer for the bones from the

Neolithic lakeside site Gletterens, Switzerland, C. Aballéa for the Palaeolithic antler samples from the National Museum of Prehistory in Les-Eyzies-le-Tayac, and A. Casio from the Museum of National Antiquities, St.-Germain-en-Laye for the Palaeolithic mammoth dentine. P.J. Chiappero, H.-J. Schubnel and P. Tassy from the National Museum of Natural History, Paris, are acknowledged for providing odontolite and mastodon ivory samples as well as J. Durand, curator at the Louvre Museum for placing the art and reliquary objects at our disposal. Th. Calligaro and J. Salomon are gratefully acknowledged for their support during experiments at AGLAE, F. Pillier for the preparation of the TEM grids and the help during experimental and so are Y. Adda, L. Charlet, C. Chadefaux, M. Menu, S. Merchel, C. Vignaud and L. Favre-Quattropani for fruitful discussions.

REFERENCES

[1] J. Middleton, On fluorine in bones, its source, and its application to the determination of the geological age of fossil bones, Proc. Geol. Soc. (London) 4 (1844) 431–433.
[2] A. Carnot, Recherche sur la composition générale et la teneur en fluor des os modernes et des os fossiles à différents âges, Ann. Mines 1 (1893) 155–195.
[3] R.E.M. Hedges, I.A. Law, The radiocarbon dating of bone, Appl. Geochem. 4 (1989) 249.
[4] A.R. Millard, A.W.G. Pike, Uranium-series dating of the Tabun Neanderthal: a cautionary note, J. Hum. Evol. 36 (1999) 581–585.
[5] G.E. Coote, Ion beam analysis of fluorine: its principles and applications, Nuclear Instrum. Methods Phys. Res. B 66 (1992) 191–204.
[6] M. Döbeli, A. Gaschen, U. Krähenbühl, Fluorine analysis by ion beam techniques for dating applications, in: A. Tressaud, (Ed.), Advances in Fluorine Science: Fluorine and the Environment, Elsevier, Amsterdam, 2006.
[7] A. Haddy, A. Hanson, Research notes and application reports. Nitrogen and fluorine dating of Moundville skeletal samples, Archaeometry 24 (1) (1982) 37–44.
[8] G. E. Coote, S. Holdaway, Radial profiles of fluorine in archaeological bone and teeth: a review of recent developments, in: W. Ambrose, P. Duerden, (Eds.), Archaeometry : An Australian Perspective, Australian National University, Canberra ACT 2600, 1982, pp. 251–261.
[9] K. Johnsson, Chemical dating of bones based on diagenetic changes in bone apatite, J. Archaeol. Sci. 24 (1997) 431–437.
[10] H. Bocherens, Signatures isotopiques dans le collagène des os anciens, C. R. Soc. Biol. 191 (1997) 493–510.
[11] J.P. Baraybar, C.d.l. Rua, Reconstruction of diet with trace elements of bone at the Chalcolithic site of Pico Ramos, Basque Country, Spain, J. Archaeol. Sci. 24 (1997) 355–364.
[12] T. Douglas Price, R. Alexander Bentley, J. Lüning, D. Gronenborn, J. Wahl, Prehistoric human migration in the Linearbandkeramik of Central Europe, Antiquity 75 (289) (2001) 593–603.
[13] S. Blau, B.J. Kennedy, J.Y. Kim, An investigation of possible fluorosis in human dentition using synchrotron radiation, J. Archaeol. Sci. 29 (2002) 811–817.
[14] E. Schmid, Die altsteinzeitliche Elfenbeinstatuette aus der Höhle Stadel im Hohlenstein bei Asselfingen, Alb-Donau-Kreis, Fundberichte aus Baden-Württemberg, Vol. 14, Stuttgart, 1989, pp. 31–96.

[15] I. Reiche, C. Vignaud, B. Champagnon, G. Panczer, C. Brouder, G. Morin, V.A. Solé, L. Charlet, M. Menu, From mastodon ivory to gemstone: the origin of turquoise color in odontolite, Am. Mineral. 86 (2001) 1519–1524.
[16] I. Reiche, C. Vignaud, M. Menu, Heat induced transformation of fossil mastodon ivory into turquoise ''odontolite''. Structural and elemental characterisation, Solid State Sci. 2 (2000) 625–636.
[17] I. Reiche, C. Vignaud, M. Menu, The crystallinity of ancient bone and dentine: new insights by transmission electron microscopy, Archaeometry 44 (3) (2002) 447–459.
[18] M.C. Stiner, S.L. Kuhn, S. Weiner, Ofer Bar-Yosef differential burning, recrystallisation, and fragmentation of archaeological bone, J. Archaeol. Sci. 22 (1995) 223–237.
[19] N.S. Baer, N. Indictor, J.H. Frantz, B. Appelbaum, The effect of high temperature on ivory, Stud. Conserv. 16 (1971) 1–8.
[20] J.L. Bennett, Thermal alteration of buried bone, J. Archaeol. Sci. 26 (1999) 1–8.
[21] R.E.M. Hedges, Bone diagenesis: an overview of processes, Archaeometry 44 (3) (2002) 319–328.
[22] M.M.E. Jans, H. Kars, C.M. Nielsen-Marsh, C.I. Smith, A.G. Nord, P. Arthur, N. Earl, *In situ* preservation of archaeological bone: a histological study within a multidisciplinary approach, Archaeometry 44 (2002) 343–352.
[23] A.M. Child, Towards the understanding of the microbial decomposition of archaeological bone in the burial environment, J. Archaeol. Sci. 22 (1995) 165–174.
[24] M.J. Kohn, M.J. Schoeninger, W.W. Barker, Altered states: effects of diagenesis on fossil tooth chemistry, Geochim. Cosmochim. Acta 63 (18) (1999) 2737–2747.
[25] V. Michel, P. Ildefonse, G. Morin, Assessment of archaeological bone and dentine preservation from Lazaret cave (Middle Pleistocene) in France, Palaeogeogr. Palaeoclimatol. Palaeoecol. 126 (1996) 109–119.
[26] C.M. Nielsen-March, R.E.M. Hedges, Bone porosity and the use of mercury intrusion porosimetry in bone diagenesis studies, Archaeometry 41 (1) (1999) 165–174.
[27] I. Reiche, L. Favre-Quattropani, T. Calligaro, J. Salomon, H. Bocherens, L. Charlet, M. Menu, Trace element composition of archaeological bones and post-mortem alteration in the burial environment, Nucl. Instrum. Methods Phys. Res. B 150 (1999) 656–662.
[28] C.A. Baud, Fluor et Strontium dans les os anciens, in Actes des 4ème Journées Anthropologiques, Dossier de Documentation archéologique, 1989.
[29] N. Boscher-Barré, P. Trocellier, Nuclear microprobe study of a woman's skeleton from the sixth century, Nucl. Instrum. Methods Phys. Res. B 73 (1993) 413–416.
[30] A.R. Millard, R.E.M. Hedges, Uranium uptake by buried bone, J. Archaeol. Sci. 22 (1995) 239–250.
[31] L. Quattropani, L. Charlet, H. de Lumley, M. Menu, Early Palaeolithic bone diagenesis in the Arago cave at Tautavel, France, Mineral. Mag. 63 (6) (1999) 801–812.
[32] I. Reiche, C. Vignaud, L. Favre-Quattropani, M. Menu, Fluorine analysis in biogenic and geological apatite by analytical transmission electron microscopy and nuclear reaction analysis, J. Trace Microprobe Tech. 20 (2) (2002) 211–231.
[33] C. Chadefaux, C. Aballéa, C. Vignaud, I. Reiche, Multianalytical study of Palaeolithic reindeer antler. Discovery of antler traces in Lascaux pigments, Archaeometry, submitted.
[34] I. Reiche, C. Vignaud, T. Calligaro, J. Salomon, M. Menu, Comparative analysis of odontolite, heated fossil ivory and blue fluorapatite by PIXE/PIGE and TEM, Nucl. Instrum. Methods Phys. Res. B 161-163 (2000) 737–742.
[35] P. Walter, M. Menu, I.C. Vickridge, Fluorine depth profiles as a relative dating method of chipped flints, Nucl. Instrum. Methods Phys. Res. B 45 (1990) 119–122.
[36] L. Bellot-Gurlet, G. Poupeau, O. Dorighel, T.h. Calligaro, J.-C. Dran, J. Salomon, A PIXE/fission-track dating approach to sourcing studies of obsidian artefacts in Colombia and Ecuador, J. Archaeol. Sci. 26 (8) (1999) 855–860.
[37] G.E. Coote, N.E. Whitehead, G.J. McCallum, J. Radioanal. Chem. 12 (1972) 491.

[38] J.R. Bird, L.H. Russell, W.R. Ambrose, M.D. Scott, Obsidian characterized with elemental analysis by proton induced γ-ray emission, Anal. Chem. 50 (14) (1978) 2082–2084.
[39] S. Weiner, W. Traub, Bone structure: from ångstroms to microns, FASEB J. 6 (1992) 879–885.
[40] X.W. Su, F.Z. Cui, Hierarchical structure of ivory: from nanometer to centimeter, Mater. Sci. Eng. C7 (1999) 19–29.
[41] G.J. Flim, Z. Kolar, J. Arends, Diffusion of fluorine ions in dental enamel at pH 7, J. Bioeng. 2 (1978) 95–102.
[42] P.M. Fischer, A.R.E. Lodding, J.G. Noren, Trace elements and dating studies of teeth by secondary ion mass spectrometry (SIMS), in: Y. Maniatis, (Ed.), Archaeometry, Elsevier, Amsterdam, 1989, pp. 109–119.
[43] J. Arends, J. Schuthof, W.L. Jongeblood, Mineral properties of the outer tooth surface. Dental Plaque and Surface Interactons, 1979.
[44] K. Toyoda, M. Tokonami, Diffusion of rare-earth elements in fish teeth from deep-sea sediments, Nature 345 (1990) 607–609.
[45] A.R. Millard, R.E.M. Hedges, A diffusion–adsorption model of uranium uptake by archaeological bone, Geochim. Cosmochim. Acta 60 (12) (1996) 2139–2152.
[46] P. Anderson, S.E.P. Dowker, J.C. Elliott, C.R. Thomas, Synchrotron X-ray fluorescence microprobe analysis in the study of dental mineralized tissues, J. Trace Microprobe Tech. 14 (3) (1996) 541–560.
[47] C. Kottler, M. Döbeli, U. Krähenbühl, M. Nussbaumer, Exposure age dating by fluorine diffusion, Nucl. Instrum. Methods Phys. Res. B 188 (2002) 61–66.
[48] M.-H. Crigel, M. Balligand, E. Heinen, Les bois de cerf: revue de littérature scientifique, Ann. Méd. Vét. 145 (2001) 25–38.
[49] B. Pozzi, Etude comparative entre différents traitements appliqués à la conservation des bois de cerfs gorgés d'eau en vue d'un séchage, Haute école d'arts appliqués du canton de Neuchâtel, 2002, p. 123.
[50] P. Walter, thesis: Etude du comportement du fluor lors des interactions silice-solutions aqueuses-applications archéologiques, in Geochimie, Université Paul Sabatier, Toulouse, 1993, p. 219.
[51] I. Reiche, L. Favre-Quattropani, C. Vignaud, H. Bocherens, L. Charlet, M. Menu, Multi-analytical approach to bone diagenesis: example of the French Neolithic site of Bercy (Paris), Meas. Sci. Tech. 14 (2003) 1608–1609.
[52] T. Molleson, in: G. Grupe, B. Herrmann, (Eds.), Trace Elements in Environmental History, Springer, Berlin, 1989, pp. 67–82.
[53] M. Regert, M.-F. Guerra, I. Reiche, Physico-chimie des matériaux du patrimoine culturel: objectifs, principes, méthodes et exemples d'application, Techniques de l'ingénieur Part 1: P3780 (2006) 1–35; Part 2: P3781 (2006) 1–20.
[54] T. Calligaro, J.-C. Dran, B. Moignard, L. Pichon, J. Salomon, P. Walter, Ion beam analysis with external beams: recent set-up improvements, Nucl. Instrum. Methods Phys. Res. B 188 (2002) 135–140.
[55] J.C. Stormer Jr., M.L. Pierson, R.C. Tacker, Variation of F and Cl X-ray intensity due to anisotropic diffusion in apatite during electron microprobe analysis, Am. Mineral. 78 (1993) 641–648.
[56] M. Dowsett, A. Adriaens, The role of SIMS in cultural heritage studies, Nucl. Instrum. Methods Phys. Res. B 226 (2004) 38–52.
[57] L.G. Petersson, G. Frostell, A. Lodding, Secondary ion microanalysis of fluorine in apatines of biological interest, Zeit. Naturforsch. 29c (1974) 417–420.
[58] P.W.O. Hoskin, SIMS determination of $\mu g\, g^{-1}$-level fluorine in geological samples and its concentration in NIST SRM 610, Geostandards Newslett. 23 (1) (1999) 69–76.
[59] M.R. Schurr, Fluoride dating of prehistoric bones by ion selective electrode, J. Archaeol. Sci. 16 (1989) 265–270.

[60] G.E. Coote, I.C. Vickridge, Application of a nuclear microprobe to the study of calcified tissues, Nucl. Instrum. Methods Phys. Res. B 30 (1988) 393–397.
[61] I. Reiche, C. Vignaud, L. Favre-Quattropani, L. Charlet, M. Menu, Diffusion in archaeological bone, Defect Diffus. Forum 194–199 (2001) 953–960.
[62] G. Astre, Mastodontes à Gimont (Turquoise de Planselve) et à Bédéchan, Bull. Soc. Histoire naturelle de Toulouse 84 (1949) 147–150.
[63] R.A. Ferchault, d. Réaumur, Observations sur les Mines de Turquoises du Royaume; sur la nature de la Matière qu'on y trouve; et sur la manière dont on lui donne la couleur, Mémoires de l' Académie Royale des Sciences, Académie Royale des Sciences, Paris, 1715, pp. 174–202.
[64] G.M. Fischer, Essai sur les turquoises, Ann. Mines VIII (1823) 326–327.
[65] L. Ginsburg, P. Tassy, Les fouilles paléontologiques dans la région de Simorre, Bull. Soc. Arch. Du Gers, Auch 4ème trimestre (1977) 443–466.
[66] I. Reiche, G. Morin, C. Brouder, A. Solé, P.E. Petit, C. Vignaud, T. Calligaro, M. Menu, Manganese accommodation in fossilised mastodon ivory and heat-induced colour transformation: evidence by EXAFS, Eur. J. Mineral. 14 (2002) 1069–1073.
[67] G.R. Summerhayes, J.R. Bird, R. Fullagar, C. Gosden, J. Pecht, R. Torrence, Application of PIXE-PIGME to archaeological analysis of changing patterns of obsidian uses, in M.S. Shackley (Ed.), Archaeological Obsidian Studies, Plenum Press, West New Britain, Papua, New Guinea, Chapter 6, 1998, pp. 129–158.
[68] K. Dardenne, D. Vivien, D. Huguenin, Color of Mn(V)-substituted apatites $A_{10}(B,Mn)O_4)_6F_2$, J. Solid State Chem. 146 (1999) 464–472.

This page intentionally left blank

SUBJECT INDEX